Deciphering the spatiotemporal dynamics of intestinal aging in vertebrates using the African turquoise killifish

Inaugural-Dissertation

zur

Erlangung des Doktorgrades
der Mathematisch-Naturwissenschaftlichen Fakultät
der Universität zu Köln

vorgelegt von
Miriam Lea Popkes
Aus Wiesbaden

Köln, Mai 2021

Gutachter: Dr. Dario R. Valenzano

Prof. Dr. Jan Riemer

Tag der letzten mündlichen Prüfung: 03.08.2021

Life has no limitations, except the ones you make.

Les Brown

Abstract

Aging is the major risk factor for many top-killing diseases and represents a problem for both the individual and the society. How the aging process is influenced and causally connected to microbiota is an emerging research area, with far-reaching findings obtained within the past few years. However, major underlying connections still remain elusive, in part hindered by a lack of suitable experimental model systems. The turquoise killifish is an ideal model to fill this gap and study microbiota in the context of aging, as it uniquely combines a very short lifespan with vertebrate features, such as a complex gut microbiota. However, knowledge about the killifish intestinal characteristics and gut microbiota is largely absent. Important key aspects I address include a detailed definition of aging dynamics, a characterization of gut compartmentalization and sex-specific intestinal traits, as well as the question whether non-invasive stool samples could be experimentally utilized for assessment of gut microbiota features.

I thus set out to characterize killifish spatiotemporal aging dynamics and sex-specific intestinal microbial and molecular patterns by performing multi-omics analyses on intestinal sections of young and old, male and female killifish. I found strong evidence for a compartmentalization of the killifish intestine on a molecular and morphological level, with specific functions that can also be found in the mammalian intestine. Surprisingly, I did not observe section-specific microbial communities in contrast to findings from other animals including fish. I detected compelling evidence for extracellular matrix restructuring in the aged killifish intestine, with an accumulation of collagen and an increase in muscle thickness, possibly impeding the intestinal function in old fish. For the first time, I showed that the killifish intestine exhibits sex-specific molecular traits, especially concerning the coagulation process.

Moreover, I asked whether non-invasive stool samples can be used as a proxy for gut microbiota by collecting microbiota samples of stool, intestinal and food samples. In addition, I set out to explore whether stool samples can be utilized to build models predicting fish age or remaining life by conducting a longitudinal collection of individual

stool samples along killifish life. Excitingly, I discovered shared microbial features between stool and gut microbiota and showed for the first time that a series of stool microbial samples in combination with a machine learning approach allows prediction of both age and lifespan. My studies not only set the ground for future research on killifish gut microbiota, but provide novel promising results highlighting the importance of gut microbiota research in the context of aging.

Acknowledgments

Although a journey full of scientific ups and downs, my last 5 years in Cologne have been a truly amazing and fulfilling time which I would not want to miss! All of this would have not been possible without many great people in my life - I am very lucky to work in a great lab environment and be surrounded by a wonderful husband, gorgeous friends and an amazing family.

First, I would like to thank Dario for giving me the opportunity to work and play around with fish poop for so many years – it has been an inspiring journey, and I really learned a lot from you! I also want to thank Jan Riemer and Kay Hofmann to agree to be part of my thesis committee and to participate in my defense – thanks for taking the time!

Thanks to Mum & Dad for always being there for me, supporting me in every detail of my life and always having my back. You are the best parents one could ever wish for – I would be honored if I could be a comparably good parent to Knirps one day ☺ Thanks to Lena & Flo, Oma Marlis & Oma Walli, Opa Herbert – and of course also Opa Johann. I know you are all so proud of me for achieving this life goal and care so much about me. You are a very big part in my life and I'm so glad you are all there for me! I'm also very lucky to have found a great second family with the van Oepens & Gahlens – I could have not wished for better parents-in-law! I'm looking forward to the many family celebrations and upcoming times we will share ☺

Next, I really want to thank all of my friends – what is all that hard work without great people to enjoy the free times? Julia & Hannah, you have been amazing besties for such a long time now, I am so glad that you are a part of my life! It's impossible to name all the people close to my heart, but especially Franzi & Tascha, Jan & Veni, the Bumsebrummel squad with Laura, Virigina, Kira, Isa – thanks for all your support in the past years and making my life so much fun!

Thanks to all the people making the MPI time so special – Raymondo for the Spanish-German-failed conversations & the dance lessons, Jens & David & Franzi for funny times in the lab, great discussions, the best carnival and Christmas parties! Dany, you are the BEST student coordinator one can think of (you should get & wear a crown!) and I had so much fun interacting with you throughout the PhD rep phase and all the years. Special thanks also to my amazing helpers in the lab, Joni & Quinn & Sam! I was always very lucky to have the best (!!) students around ☺ Also thanks to the great core facilities, especially Patrick & Ilian, for all your help, discussions and sweat you put into supporting my projects!

Last and most importantly: Thank you Till, for everything! Your never-ending help and support, scientific discussions, building me up in rough times – and of course for being the best hubby in the world. I cannot put into words how much you mean to me – and I'm so much looking forward to our new life chapter! We rock ☺

List of abbreviations

AMP	Antimicrobial peptide
ASV	Amplicon sequence variant
bp	Basepairs
BZ	Benzoyl chloride
C. elegans	*Caenorhabditis elegans*
CRISPR	Clustered Regularly Interspaced Short Palindromic Repeats
DAG	Diacylglyceride
D. melanogaster	*Drosophila melanogaster*
DNA	Deoxyribonucleic acid
ESI	Electrospray ionization
ESV	Exact sequence variant
EtOH	Ethanol
FA	Formic acid
FC	Fold-change
FFA	Free fatty acids
fw	Forward
G	Gram
GO	Gene ontology
h	Hour
H&E	Hematoxylin & Eosin
Hz	Hertz
IC	Ion Chromatography
ID	Identifier
IgA	Immunoglobulin A
IGF	Insulin growth factor
L	Liter
LC	Liquid chromatography
LC-MS	Liquid chromatography-mass spectrometry
LDL	Low density lipoprotein
LRE	Lysosome-enriched vacuolated enterocytes
lysoPC	Lysophosphatidylcholine
lysoPE	Lysophosphatidylethanolamine
M	Molar
min	Minute
mm	Millimeter
mM	Millimolar
NCT	National Clinical Trial
n.s.	Not significant
OD	Optical density
PFA	Paraformaldehyde
PG	Phosphatidylglycerol
pHILIC	Polymeric hydrophilic interaction liquid chromatography
ppm	Parts per million
PPP	Percent positive pixel

PBS	Phosphate buffered saline
PC	Phosphatidylcholine
PCA	Principal component analysis
PCoA	Principal coordinate analysis
PCR	Polymerase chain reaction
PE	Phosphatidylethanolamine
PFA	Paraformaldehyde
PLS-DA	Partial least-squares discriminant analysis
qPCR	Quantitative real-time PCR
RF	Random Forest
RNA	Ribonucleic acid
ROI	Region of interest
rRNA	Ribosomal Ribonucleic acid
RT	Room temperature
rv	Reverse
s	Seconds
SCFA	Short-chain fatty acids
SM	Sphingomyeline
SRFG	Sirius Red & Fast Green
TAG	Triacylglyceride
TCA	Tricarboxylic acid
TMT	Tandem mass tag
UPLC	Ultra Performance Liquid chromatography
V3V4	Variable region 3 & 4
V4	Variable region 4
x g	Times gravity
16S	16 Svedberg
µ	Micro
°C	Degree Celsius

Table of Contents

Chapter 1

Introduction

1.1 Aging

"Education is the best provision for old age". *Aristotle*

The desire to live forever has been deeply rooted in us since centuries. However, aging affects all of us – at least us humans – and nearly all living organisms on this planet. Biological aging is defined as the age-dependent decline of key homeostatic processes of the host, acting on several levels of complexity. Besides some manifest morphological aging-related changes, such as loss of hair pigmentation and increased spinal curvature, aging is the outcome of several processes that occur at the molecular level.

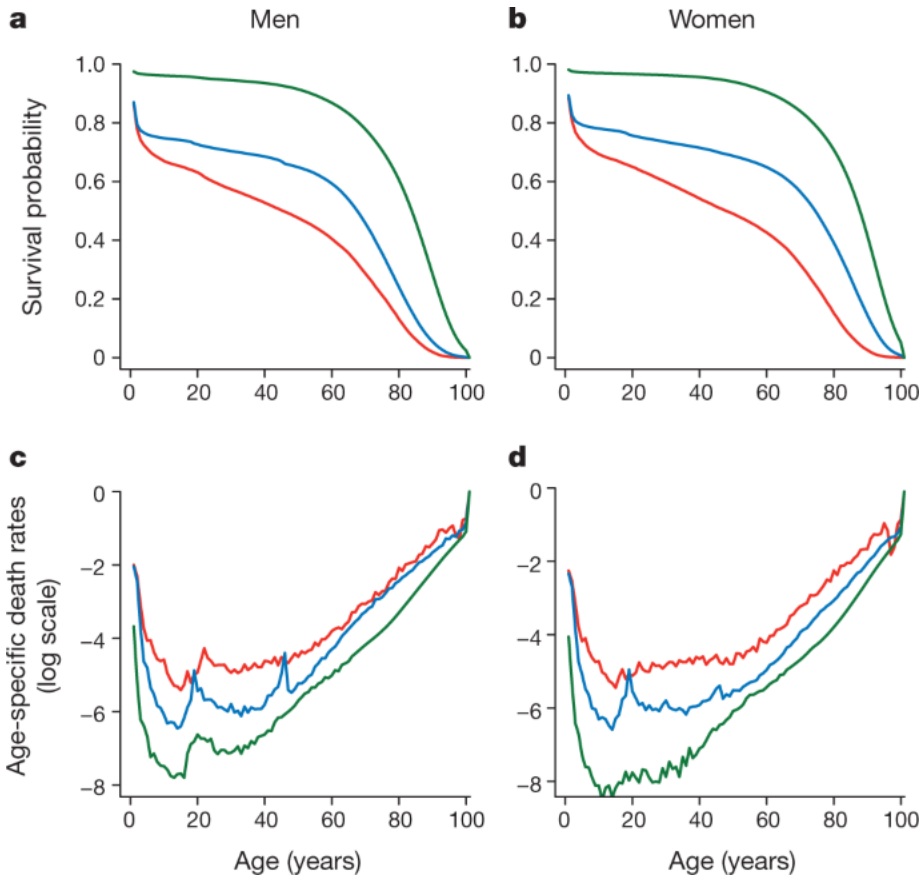

Figure 1: Sex-specific cumulative survival and death rates. Cumulative survival (A+B) and death rates (C+D) in males and females. Colors indicate the different years of data collection: 1850 (red), 1900 (blue) and 1950 (green). Based on life tables from the Netherlands. Figure taken from Partridge et al., 2018.

Functional aging is not only a problem of a single individual, but rather affects the whole population. Life-expectancy has been rising steadily in the past decades (Fig. 1), with an approximate rate of 3 months per year, resulting in a nearly doubled life-expectancy since 1840 (Oeppen & Vaupel, 2002). This increase in the average life expectancy is mainly driven by a reduction in infant/juvenile mortality (Wilmoth, 2000), and moreover owed to enhanced hygiene concepts, better quality of food and water plus an improvement and advances in medical care and therapies (Partridge et al., 2018). Although it is still debated whether human lifespan has a natural limit, future lifespan expectancy is projected to increase in the coming years (Kontis et al., 2017). However, while human lifespan has increased over the years, the years spent in good health condition (= healthspan) have not increased with the same pace (Crimmins, 2015).

Age is the main risk factor for the development of various diseases that increase the risk of individual mortality, including cancer, neurodegenerative diseases and cardiovascular diseases (Melzer et al., 2020; Niccoli & Partridge, 2012). Hence, extended lifespan may result in longer periods of frailty and a higher rate of age-related diseases. This is not only a burden for the suffering elderly patients, but also a major burden to society and health care systems – including a rapid increase for hospitalization costs (Alemayehu & Warner, 2004). Studying aging as the underlying contributor to the top mortality-causing diseases could be key for finding novel therapies and for a longer life in a healthy state.

The aging process has long been assumed as a random and general process and thus as inevitable. However, recent discoveries impressively show that aging is a complex and multi-factorial but fine-tuned molecular process, and that mutations in single genes allow to greatly extend lifespan in model organisms (Kenyon et al., 1993; Vijg & Campisi, 2008), and also lead to premature aging diseases (Ashapkin et al., 2019). Interestingly, how we age also seems to be evolutionarily conserved – the major known aging-associated pathways are conserved from yeast to worms and fruit flies, rodents and humans (Barbieri et al., 2003).

While aging research is still a very young field of investigation, discoveries over the past years have resulted in a number of characterized cellular and molecular hallmarks of aging (López-Otín et al., 2013). The nine identified hallmarks include: genomic instability, telomere attrition, epigenetic alterations, loss of proteostasis, deregulated nutrient sensing, mitochondrial dysfunction, cellular senescence, stem cell exhaustion and altered intracellular communication. The hallmarks of aging are interconnected, can co-occur in the aging process and are based on alterations in specific molecular pathways.

The first major breakthrough in the field was the discovery of a loss-of-function mutation in the *daf-2 gene*, which leads to exceptional long lifespan in *C. elegans* (Kenyon et al., 1993). The *daf-2* gene encodes for an insulin-like growth factor receptor and is evolutionary conserved up to humans. Over the years, many other components of the insulin signaling pathway have been associated with longevity. Importantly, several studies have shown that the insulin/IGF-1-like signaling pathway plays an intricate role in aging also for other animals, including flies and rodents (Holzenberger et al., 2003; Tatar et al., 2001). Moreover, sequence analysis of the IGF1/IGF1-receptor genes in female centenarians revealed an overrepresentation of partial loss-of-function mutations, indicating that IGF-signaling probably also has an influence for human lifespan (Suh et al., 2008).

Besides the insulin signaling pathway, other metabolic pathways are importantly involved in the aging process, most notably the mTOR pathway. mTOR is an enzyme with essential roles in the regulation of cell metabolism and acts as a nutrient, energy and oxygen level sensor (Tokunaga et al., 2004). Several studies have shown that decreased mTOR activity leads to lifespan extension in yeast, worms, flies and mice (Harrison et al., 2009; Kaeberlein et al., 2005; Kapahi et al., 2004; Vellai et al., 2003). Interestingly, mTOR pathway inhibitors are currently tested in medical trials in the context of aging (NCT number = NCT04488601).

One important aspect of aging on the physiological level is the overall decline in immune system function, leading to diminished immune responses to infections or

vaccines (Sambhara & McElhaney, 2009; Segre & Segre, 1977), impaired functionality of the adaptive immune system (Frasca & Blomberg, 2009; Nikolich-Žugich, 2018) and a chronic activation of the innate immune system. The latter is resulting in chronic low-grade inflammation, called inflammaging, another typical characteristic of aging (Franceschi et al., 2018).
Over the last years, the interest in microbiota studies has grown considerably. It was discovered that the intestinal microbiota plays an important role in integrating environmental stimulation and host metabolism. An emerging interest in the aging field is thus the connection between gut microbial communities and aging, as exciting findings propose a possible causal connection during the aging process (1.2.4).

To study aging and age-associated diseases, adequate model organisms for aging are essential, as controlled studies in humans are challenging and time-consuming due to human lifespan. There are several aging model organisms, each with specific advantages that make them ideal to study certain aspects of the aging process – and new model systems continue to be established, more or less suited to different experimental needs (Brunet, 2020). Invertebrates like *Drosophila melanogaster* and *C. elegans* were among the first aging model systems and enabled many of the first discoveries in the field of molecular biology of aging (Guarente & Kenyon, 2000; Piper & Partridge, 2018). Invertebrates have a very short lifespan, making them ideally suited for lifespan screening assays and are very low cost in maintenance. On the other hand, vertebrate model systems like mice and rats share a lot of key features with humans, for example a complex immune system and shared aging phenotypes, and provide a large number of disease-relevant models (Brunet, 2020). However, comparably long lifespan and maintenance costs impede high throughput experiments and lifespan assays. One promising model system to close the gap between short-lived invertebrates and long-lived vertebrates is the turquoise killifish (*Nothobranchius furzeri)*, which combines a very short lifespan with key aspects of aging phenotypes and vertebrate features (more in 1.3).

1.2 The intestine and gut microbiota in health & aging

1.2.1 The role of microbiota in host physiology

Microbiota play a key role in nature, and we are only beginning to understand and appreciate the impact of the microbiota surrounding and populating us on our human bodies. Microorganisms reside on our planet since more than 3 billion years (Baumgartner et al., 2019; Popkes & Valenzano, 2020) and can be found ubiquitously in nature. Eukaryotes, including vertebrates, mammals and humans, have thus evolved in the context of a rich and diverse microbial surrounding - leading to co-evolution of host and their associated microbial communities resulting in strong connections and symbiotic relationships (Popkes & Valenzano, 2020).

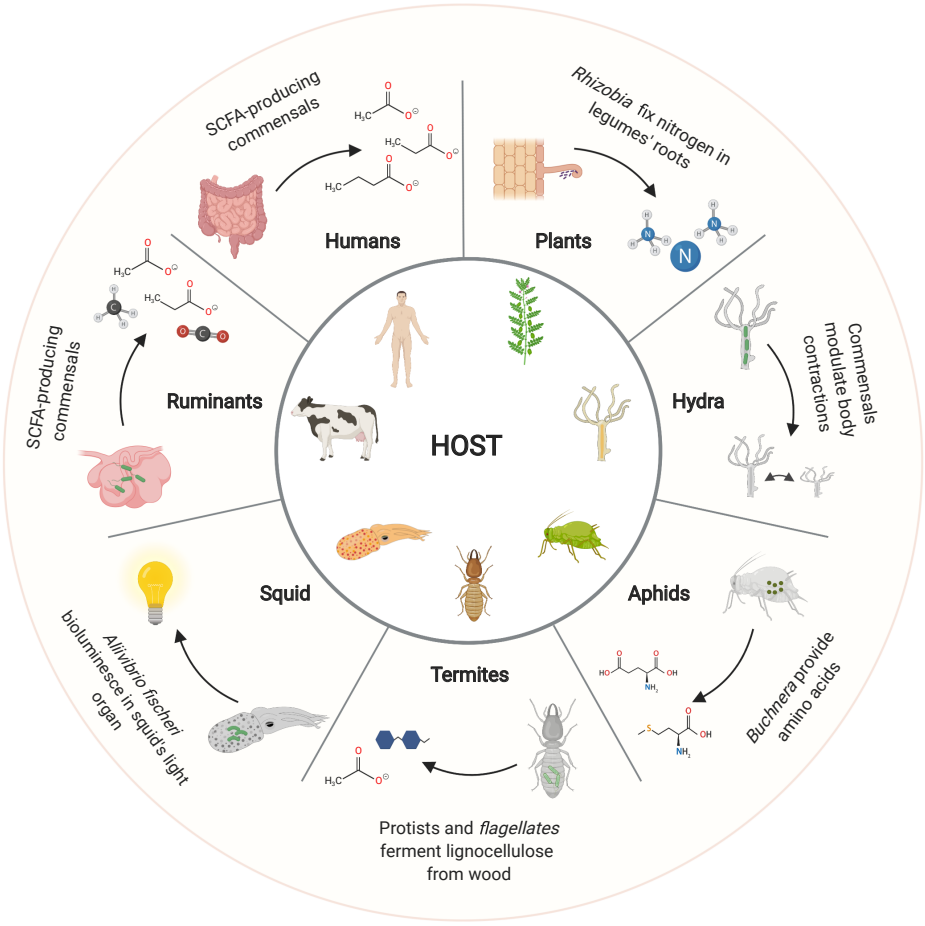

Figure 2: Mutualistic relationships between microbiota and their host. Clockwise, from top right: *Rhizobia* fix nitrogen in legumes roots to molecular forms accessible to the plants. Commensal bacteria in the hydra modulate spontaneous body contractions and prevent the

host from lethal fungal infections. *Buchnera* provide essential amino acids to sap-feeding aphids. Protists and *flagellates* ferment lignocellulose from wood in termite food digestion. *Aliivibrio fischeri* bioluminesce the light organ of bobtail squids. Commensal bacteria ferment cellulose to SCFA in ruminants, and complex carbohydrates to SCFA in humans. Figure taken from Popkes & Valenzano, 2020.

Specialized host-microbiota interactions are ubiquitous, providing mutual advantages (Fig. 2, Popkes & Valenzano, 2020). Microbiota in the hydra for example protect the animal from lethal fungal infections (Fraune et al., 2015). Microbial communities are also invaluable for nutrition in several animals – they ensure amino-acid supply in sap-feeding ants (Rouhbakhsh et al., 1996), ferment indigestible lignocellulose in termites (Benemann, 1973) and ferment fiber-rich cellulose in specialized fermentation chambers of ruminants (Nocek & Russell, 1988).

Microbial communities can be found in various host body sites – humans are for example inhabited by distinct communities on the skin (Grice et al., 2009), the mouth (Nasidze et al., 2009) and the vagina (Ravel et al., 2011). Especially the intestinal microbiota is of great interest, as the intestinal tract is the biggest reservoir of microbiota in the human body (Dieterich et al., 2018). The human intestine is dominated by Bacteroidetes, Firmicutes, Actinobacteria and Proteobacteria (The Human Microbiome Project Consortium, 2012). Gut microbes in the densely populated colon are roughly of equal number to all human cells (Sender et al., 2016), and the number of microbial genes outnumbers the human genome by roughly two order of magnitude (Tierney et al., 2019). Recent advances in microbiota research are constantly revealing the great importance of gut microbiota for human physiology.

Microbial colonization of the gastrointestinal tract likely starts with birth (de Goffau et al., 2019; Lauder et al., 2016) - even if some studies report microbiota existence beforehand (Aagaard et al., 2014; Collado et al., 2016), birth is definitely the major encounter of microbiota in human life. The infant microbial gut communities then develop over the first years of life, with an increase in diversity and a shift in composition, until an adult-like stage is reached at around 2-3 years (Bäckhed et al., 2015; Yatsunenko et al., 2012). Importantly, several studies have suggested that proper gut microbiota establishment in infants is a crucial process, with impairments

in the process leading to negative health consequences later in life (Dogra et al., 2015; Korpela & de Vos, 2016). In adulthood, microbial communities are relatively stable and resilient, and rapidly return to the initial composition after disturbances (Caporaso et al., 2011; Faith et al., 2013; Palleja et al., 2018). Important factors influencing microbial communities include mainly environmental parameters, such as antibiotic usage, diet and exercise, but also genetic parameters (Petriz et al., 2014; Rothschild et al., 2018; Willing et al., 2011; G. D. Wu et al., 2011).

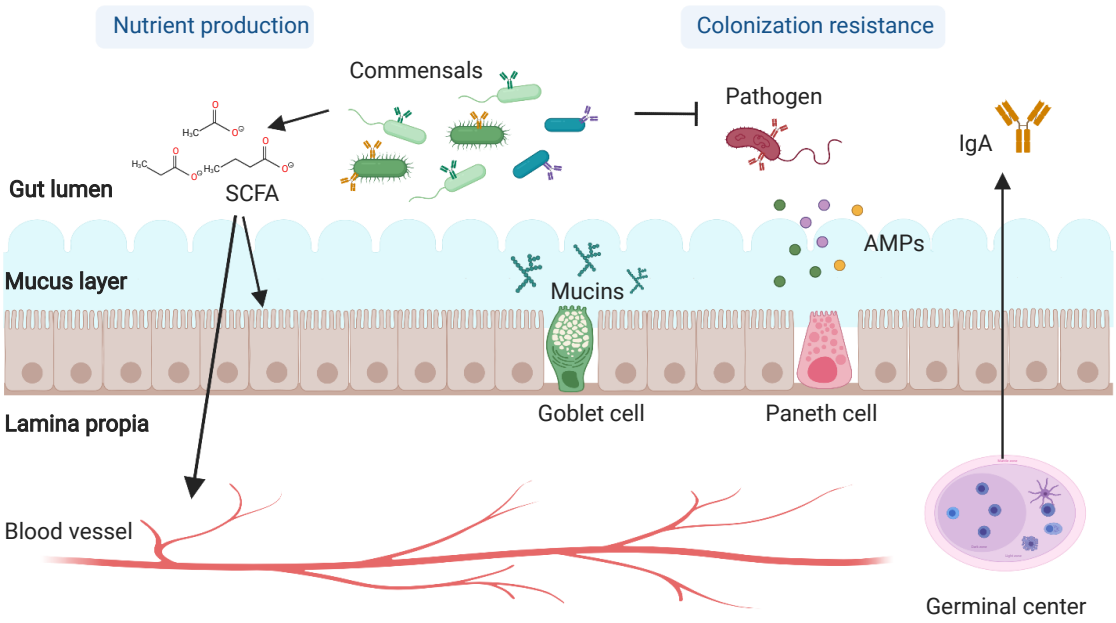

Figure 3: Host-microbiota interactions in homeostasis. The host establishes an intestinal barrier, including a thin layer of epithelial cells, a mucus layer consisting of mucins produced from goblet cells, antimicrobial peptides (AMPs) produced by Paneth cells and secreted immunoglobulins A (IgA) from the germinal center. Commensal microbes are involved in nutrient production, fermenting non-digestible complex carbohydrates to short-chain fatty acids (SCFA), and ensure colonization resistance by fighting pathogens directly and indirectly by stimulating immune system responses. This figure was generated with BioRender.

The intestinal microbiota plays a major role in physiology, not only for mammals but also for other vertebrate and even invertebrate species such as fish and flies (Butt & Volkoff, 2019; Ludington & Ja, 2020). In humans, gut microbiota is responsible for several main physiological processes (Fig. 3) (Clemente et al., 2012). Gut microbial communities are involved in metabolic functions and nutrient provision, as they ferment carbohydrates which are undigestible for the human host enzymes,

metabolize primary bile salts and produce essential vitamins (Gill et al., 2006a; Hill, 1997; Wahlström et al., 2016). The gut microbial communities moreover provide crucial signals for the development and function of the immune system, thanks to microbial surface antigens and produced metabolites (Bouskra et al., 2008; Chow et al., 2010; Lathrop et al., 2011; Rooks & Garrett, 2016). Gut microbiota are also communicating to the nervous system via the gut-brain axis and play an important role in neurodevelopment, host behavior such as stress, anxiety and social activity, and neuropsychiatric diseases (Chu et al., 2019; Sherwin et al., 2019; Vuong et al., 2017).

Bacterial metabolism generates several metabolites that have crucial functions for hosts, such as short-chain fatty acids (SCFA), secondary bile acids or tryptophane metabolites. The SCFAs acetate, propionate and butyrate have been in particular focus in the research community – since their action has been linked with roles in immune homeostasis and in the microbiota-brain-axis. SCFAs are a valuable energy source for the intestinal epithelial cells, enhance the intestinal barrier function and stimulate mucus production by goblet cell (Peng et al., 2009; Roediger, 1982). Moreover, SCFAs are importantly involved in intestinal immune homeostasis, establishing a tolerogenic response and boosting immune responses (Bachem et al., 2019; Kim et al., 2016; Smith et al., 2013), as well as in the gut-brain axis (De Vadder et al., 2014). SCFA levels have also been correlated with a growing list of diseases, including diabetes, obesity and atherosclerosis (Kasahara et al., 2018; Mariño et al., 2017; Ridaura et al., 2013).

Another important metabolite class are secondary bile acids. Primary bile salts are cholesterol-based compounds produced in the liver and stored in the gallbladder. Bile acids are secreted into the small intestine, where they are critically involved in the digestion of fatty acids (Hofmann, 1963). More than 95% of primary bile acids are reabsorbed in the ileum and circulate back to the liver (Krautkramer et al., 2021). The remaining primary bile acids are converted to secondary bile acids through microbiota via dehydroxylation or deconjugation (Wahlström et al., 2016). The implication of secondary bile acids in host physiology is still under investigation and probably depends on the specific bile acid molecule – studies showed important roles involving

the immune system (Tregs pools, Song et al., 2020), but also an implication in colorectal cancer and hepatic carcinomas (Jia et al., 2018; Yoshimoto et al., 2013).

The intestinal tract is not only home to commensal microbiota, but is a place of continuous contact with ingested microbes, including pathogenic bacteria. Interestingly, the commensal microbiota helps the host to protect the body against pathogen infection – a process called colonization resistance (Buffie & Pamer, 2013). Several mechanisms contribute to colonization resistance, including direct inhibition of pathogenic bacteria by intestinal commensals through antimicrobial substances (Ducluzeau et al., 1976; Honda et al., 2011). In addition, commensal microbiota can indirectly support and modulate pathogen defense by enhancing the intestinal immune system (Kobayashi et al., 2005; Zheng et al., 2008). One of the major roles of the intestinal immune system is to ensure a proper balance between a tolerogenic response against the commensal, useful microbes, while still ensuring an efficient and strong defense against pathogens.

The intestinal microbiota clearly is of utmost importance for host physiology. Accordingly, disturbance of the microbial communities (called “dysbiosis”) has been linked to several diseases, including obesity and severe cases of *Clostridioides difficile* infections. Dysbiotic microbial communities have been shown to directly contribute to disease course – for example, transfer of microbiota from obese individuals to germ-free mice led to weight gain (Turnbaugh et al., 2006). Vice versa, transplanting gut microbial communities from healthy donors to the dysbiotic intestine of patients severely infected with *Clostridioides difficile* led to significant improvements (Khoruts et al., 2010).

1.2.2 Spatial organization of the intestine

The digestive system plays a key role in organismal health – although hidden in our bowel, the gastrointestinal tract is along with our skin the largest area of environmental contact and essential for nutrient uptake and thus survival of the host. Over time, gastrointestinal tracts have evolved into a complex system with specialized subregions

– for example, the mouth, esophagus, stomach, small and large intestine in humans (Hartenstein & Martinez, 2019; Mowat & Agace, 2014). The compartmentalization of the intestine is key for a successful digestion and maximizes nutrient availability – compartments allow the controlled, highly coordinated sequence of successive digestive steps. The subregions are defined by distinct morphological and molecular features, equipped for highly specialized functions (Buchon et al., 2013; Gebert et al., 2020).

Compartmentalization of intestines is a conserved feature across both vertebrates and invertebrates, such as *Drosophila melanogaster*. The *Drosophila* intestine is structured into a food-storing foregut, a midgut characterized by digestion and absorption, and a hindgut (Buchon et al., 2013; Guo et al., 2016). The intestinal tracts of fish are very diverse in structure and shape, and around 20% of fish are even agastric, lacking a true stomach (Fig. 4) (Wilson & Castro, 2010). Fish intestines differ strongly in terms of length, also depending on the food-source, with herbivore fish possessing longer intestines, probably due to more epithelial surface needed for sufficient uptake of nutrients (German & Horn, 2006).

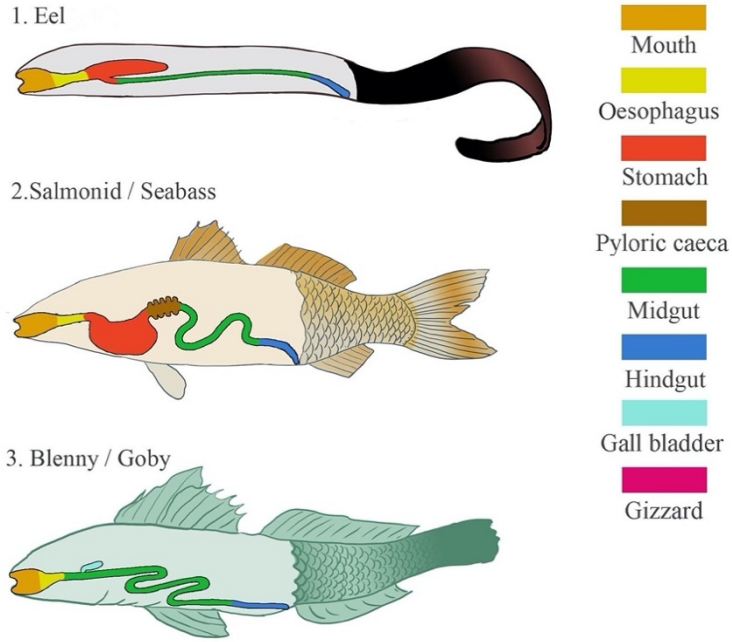

Figure 4: Overview of fish intestinal tracts. Representation of different types of intestinal tracts in different fish. Some fish are agastric, lacking a real stomach. Figure taken from Egerton et al., 2018.

The fish gut is normally classified into four sections – the head gut comprising mouth and pharynx, the foregut entailing esophagus and stomach, the midgut and a hindgut including the rectum (Egerton et al., 2018). Agastric fish may show an enlarged region in the anterior intestinal tract, also called intestinal bulb, for food storage (Kapoor et al., 1976). The midgut is characterized by digestive processes in carbohydrate and lipid metabolism, while water retention is one of the processes found particular in the hindgut (Z. Wang et al., 2010).

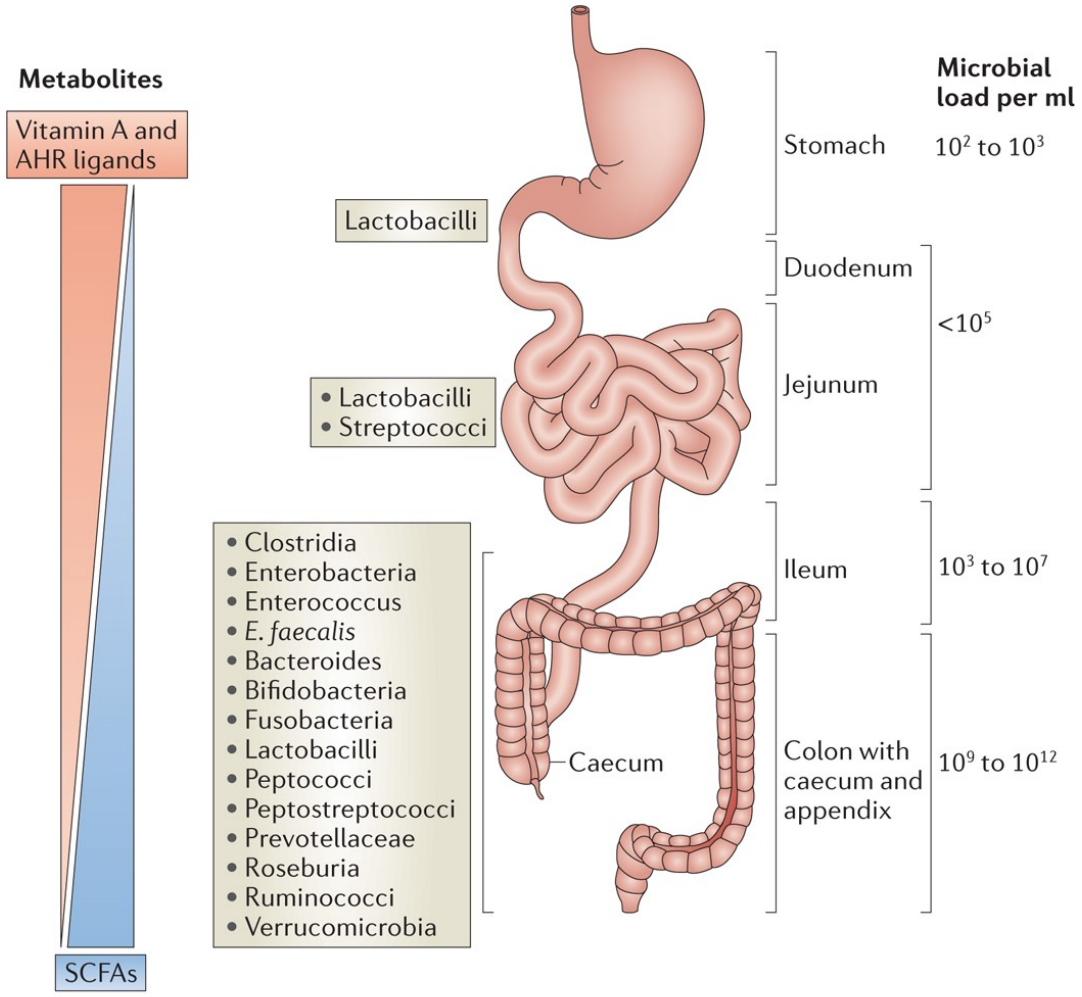

Figure 5: Overview of the human intestinal tract. Structure of the human intestinal tract indicating the microbial load, the enriched bacteria and distribution of some major bacterial metabolites in the different gut compartments. Figure taken from Mowat & Agace, 2014b.

Mammals, including humans, show an even finer distribution of specialized subregions with specific morphological and molecular signatures and functions (Fig. 5, Mowat &

Agace, 2014; Sheth et al., 2019). The small intestine is highly specialized for digestive processes, with a maximized surface area thanks to unique anatomical structures, such as villi and microvilli. It is further defined into the duodenum, the ileum and the jejunum. The duodenum is the place of chemical digestion, due to a high abundance of digestive enzymes – carbohydrates and proteins are broken down, fats are emulsified by bile components. The majority of nutrient absorption occurs in the adjacent jejunum, the longest intestinal segment with the largest surface area. The ileum is specialized in bile salt and vitamin B12 reabsorption. The large intestine is structured into the caecum with the appendix, the colon and the rectum. The surface area of the large intestine is a lot smaller due to villi being absent, reflecting that the key function is not nutrient absorption. The colon is in contrast home to the largest number of microbes in the body, important for key physiological processes, including the production of essential nutrients (1.2.1). In addition, the colon is specialized in water absorption and thus important for solidifying the fecal matter (Moran & Jackson, 1992).

Although the fine structure and morphology differs between fish and mammals, the molecular functions associated with the regions seem to overlap on a global level. For example, the posterior intestine of zebrafish is characterized by high expression levels of aquaporins indicating active water retention processes, similar to the colon of mammals (Lickwar et al., 2017). In addition, genes involved in lipid metabolism are enriched in the anterior intestinal sections of zebrafish, mirroring the characteristics of mammalian small intestines (Lickwar et al., 2017). Fish also have specialized epithelial cell types important in mammalian intestines, including mucus-producing goblet cells and enteroendocrine cells (Brugman, 2016), and proliferating intestinal stem cells (Rombout et al., 1984; Wallace et al., 2005).

As the intestinal tract is an important contact region to the environment, many foreign particles, microbes and antigens arrive in the intestine every day. Given the large area of possible pathogen entry points into the body, the immune system therefore plays a key role in the intestine – and indeed, around 80% of the immune cells reside in the gut-associated lymphatic tissue (Vighi et al., 2008). The main role of the intestinal

immune system is to keep the intricate balance between pathogen defense and the tolerance for commensal, important microbes. One important aspect in this regard is the intestinal barrier function, keeping the microbes at a safe distance and localized to the lumen (Turner, 2009). Several components contribute to the intestinal barrier, including a tight layer of intestinal epithelial cells, a protective mucus layer produced by goblet cells, and chemical defense molecules produced by immune cells, such as antimicrobial peptides (AMPs), defensins and secretory Immunoglobulins A (IgAs) (Fig. 3) (Johansson & Hansson, 2016; Muniz et al., 2012).

The specialized subregions provide highly specialized niches for microbes - intestinal tracts thus often show a spatial organization of microbial communities. Even in the invertebrate wood-feeding beetle *Odontotaenius disjunctus*, microbial communities differ in composition along the different gut compartments (Ceja-Navarro et al., 2014). Spatial organization of microbiota is also found in several fish species, including cod, seabass and salmon (Gajardo et al., 2016; Kokou et al., 2019; Ringø et al., 2016a). In mammals, bacterial communities differ largely between the small and the large intestine, both in terms of composition and bacterial load (Fig. 5). In addition to a bacterial gradient along the longitudinal intestinal axis, bacterial communities differ a lot along the lateral axis – with most bacteria residing in the lumen and some mucus-metabolizing bacteria closer to the mucosal surface. The small intestine microbiota is of lower complexity compared to the large intestine, and is enriched in microbes metabolizing various carbohydrates such as *Lactobacillus* and *Streptococcus* (Zoetendal et al., 2012). The large intestine shows a high microbial diversity and is home to complex carbohydrate-fermenting bacteria, which produce essential metabolites such as SCFAs (Cummings & Macfarlane, 1991).

1.2.3 The effect of sex on intestinal physiology and microbiota composition

Sexual dimorphism, the difference in characteristics between sex, is a very prevalent phenomenon in nature – including the very prominent coloration differences in several animals (Bell & Zamudio, 2012; Zi et al., 2003). Gastrointestinal tracts also show

sexually dimorphic features. In humans, the absorption rate of specific nutrients is sex-specific (Johnson et al., 1992). Women have a longer intestine (Saunders et al., 1996) and exhibit higher prevalence of certain intestine-specific diseases like inflammatory bowel diseases (Lovell & Ford, 2012). Sex is also a major influencing factor in terms of diseases and aging – several immune system features show sexual dimorphism (McCombe & Greer, 2013), the life expectancy of women exceeds that of men and the occurrence of age-related diseases also shows a sex-specific pattern (Austad & Fischer, 2016).

As sex hormones have a strong connection to microbiota, with mutual influences and reactions, sex-specific differences in intestinal microbiota composition also appear reasonable (Org et al., 2016; Sinha et al., 2019). However, up to now only very few studies have specifically investigated the effect of sex differences with regards to microbiota. Nevertheless, sexual dimorphic microbiota compositions were reported for some animals, such as mice (Org et al., 2016; Yurkovetskiy et al., 2013). Interestingly, a great part of the reported sex differences in microbiota composition are likely related to sex hormone levels, as castration of males or blockage of androgen receptors both prevent the reported sex-specific phenotypes (Markle et al., 2013; Org et al., 2016).
For fish, studies showed inconsistent results regarding sexual dimorphic microbiota patterns, depending on the investigated species. Most reports for zebrafish indicate no difference in microbiota composition or diversity (Liu et al., 2016; Stephens et al., 2016). In contrast, Wang *et al.* found sex differences in the intestinal flora of swamp eels, both in diversity and differentially abundant species (X. Wang et al., 2020).
Studies investigating human sex differences in microbiota composition have shown contradicting outcomes. In general, an overall trend for differences in microbiota composition and higher diversity levels for females seems likely. Several papers indicate differential abundance in specific bacterial species, including Lactobacillales, *Bateroides* and *Prevotella* (Borgo et al., 2018; Ding & Schloss, 2014). In addition, a study on two large cohorts identified sex as a significant effector of microbiota composition, with the 10th largest effect of 69 significant effect factors (Falony et al., 2016). In contrast, some studies did not find significant sex-differences for global

microbiota composition or diversity levels (Haro et al., 2016; Takagi et al., 2019) - although often slight differences in specific bacterial species were reported.
Taken together, sex differences in mammalian microbiota composition were reported in several studies and sex dimorphism is most probably also relevant for human microbiota composition – however, further research is necessary to support this hypothesis. As sex-specific differences in gut microbiota could affect major physiological processes, investigating sexual dimorphic microbiota and molecular expression patterns in the intestine remains a critical part of future studies.

1.2.4 Gut microbiota and aging

Although aging research is still a young field of investigation, important findings already shed light on key molecular and cellular processes underlying aging (1.1). However, aging research has so far mostly concentrated on the host side of age-related changes – but as shown in 1.2.1, microbiota and especially the intestinal microbial communities play an essential and intricate role in host physiology (Bana & Cabreiro, 2019). Aging is thus most probably influenced by the complex interactions between the host and its associated microbiota.

Indeed, several studies have reported not only age-related changes in microbiota composition and diversity, but moreover showed that disturbing the balance of microbial communities (a process known as “dysbiosis”) is strongly linked to aging, and might even be causally related to the aging process (Li et al., 2016; Smith, Willemsen, Popkes et al., 2017). During the aging process, profound alterations cannot only be found on the host side, but also involve the microbial communities, in particular the intestinal microbiota. Research in flies showed a marked alteration of gut microbiota composition upon aging, with an increased bacterial load and an expansion of Gammaproteobacteria (Clark et al., 2015; Ren et al., 2007). This dysbiosis precedes an intestinal barrier dysfunction, which results in loss of commensal control, a rapid health decline and presents a strong marker for death (Clark et al., 2015; Rera et al., 2012). Similarly in mice, aging is correlated with microbiota composition and results in significant community changes, with an increase

of the *Bacteriodaceae* family in old age and a decrease of *Prevotellaceae*, *Rikenellaceaea* and *Lachnospiraceae* families (Langille et al., 2013).

Studies on the aging gut microbiota in humans show varying results, but seem to be congruent on several aspects. Old age is accompanied with a loss of individual microbial diversity in the intestine (Biagi et al., 2010; Claesson, Jeffery, Conde, Power, O'Connor, et al., 2012), while a greater variability between individuals is observed (Claesson et al., 2011). Aging is clearly characterized with a shift in microbiota composition – an altered Bacteroidetes to Firmicutes ratio has been reported in several studies (Fransen et al., 2017; Mariat et al., 2009), and there are distinct changes to specific bacterial subgroups. This includes a decrease of "core" microbial communities such as *Lachnospiraeceae*, *Ruminococcaceae*, *Bacteroidaceae* (Biagi et al., 2016) and changes in *Clostridium* (Claesson et al., 2011). Functionally, gut microbial communities of aged humans are characterized by reduced SCFA-producing capacity and an increase in pro-inflammatory opportunistic pathogens (Rampelli et al., 2013). In contrast, microbial communities of especially long-lived individuals are characterized by an enrichment in health-associated bacteria (Biagi et al., 2016). It is important to note that microbiota composition correlates with health status and especially the frailty index instead of correlating with chronological age (Jackson et al., 2016).

Notably, gut microbiota changes do not just occur passively during the aging process – in fact, several studies suggest that microbiota-dependent mechanisms potentially also regulate aging processes (Bana & Cabreiro, 2019). Germ-free flies show an increased lifespan, and bacterial load is a strong influencing factor for lifespan (Lee et al., 2019). Moreover, germ-free mice do not show an age-related increase in pro-inflammatory cytokines like their counterparts raised under normal conditions. Interestingly, transfer of gut microbiota from old but not young animals to germ-free mice lead to an increase in pro-inflammatory markers and weakened the intestinal barrier function (Thevaranjan et al., 2017). In line with this, fecal microbiota transfer of old mice into germ-free mice contributed to systemic inflammaging (Fransen et al., 2017). Interestingly, Stebegg et al. showed in 2019 that transfer of young microbiota to aged mice rescues the age-related defective germinal center reaction. These

studies clearly indicate a strong interconnection between gut microbiota and the host immune system during the aging process.
Moreover, overall lifespan is directly affected by the gut microbiota. It was shown that metformin treatment, a well-known lifespan extending procedure in worms, relies on altering microbial folate and methionine metabolism (Cabreiro et al., 2013). Also in flies, modulation of gut microbiota has an effect on lifespan (Obata et al., 2018; Westfall et al., 2018). Ultimately, our group provided the first evidence that the gut microbiota changes upon aging causally connect to the aging process, by showing that transfer of young gut microbiota prolonged lifespan of middle-aged fish for more than 30% (Smith, Willemsen, Popkes et al., 2017). Supporting evidence from progeroid mice has later been published, where microbiota transfer of young mice resulted in extension of both lifespan and healthspan (Bárcena et al., 2019).

Interestingly, some gut microbiota aging aspects are sex- and region-specific. Steegenga et al. found in 2012 that aging-induced DNA hypomethylation was observed in the colon and distal small intestine, however not in the anterior section of the small intestine. Proteomic analysis of intestinal crypts from different intestinal regions further resulted in region-specific alterations in cell composition and metabolism upon aging (Gebert et al., 2020). Although only few studies investigated sex-specific aging phenotypes, one particularly interesting study found that the age-specific decline in intestinal stem cell barrier function is female-specific, and dietary restriction reduces the age-related gut pathologies in female flies more than in male flies (Regan et al., 2016).

Taken together, the intestinal microbiota is subject to profound changes upon aging, both influenced by host aging mechanisms but also affecting the host aging processes. Microbiota dysbiosis was thus proposed to be an additional hallmark and biomarker for aging (Bana & Cabreiro, 2019).

1.3 The African turquoise killifish as a model organism for microbiota research in the context of aging

The African turquoise killifish (*Nothobranchius furzeri)* is an annual teleost fish that belongs to the cyprinodont clade (Cellerino et al., 2016). It is adapted to live in extreme environmental conditions in the south-east of Africa, where it lives in ephemeral fresh-water ponds that only carry water for 4-6 months per year during the wet season (Blažek et al., 2013). Living under such harsh conditions led to evolving a very unique life cycle, including a special embryonic diapause state to survive the long dry season (Hu et al., 2020; Wourms, 1972). Once the ephemeral ponds are filled with water, killifish hatch and rapidly grow to sexual maturation, followed by rapid aging (Vrtílek et al., 2018). Turquoise killifish, especially the widely used, highly inbred laboratory GRZ strain, therefore show the shortest lifespan recorded for vertebrates kept in captivity, with a maximum lifespan of just 4-6 months (Fig. 6) (Reichwald et al., 2015).

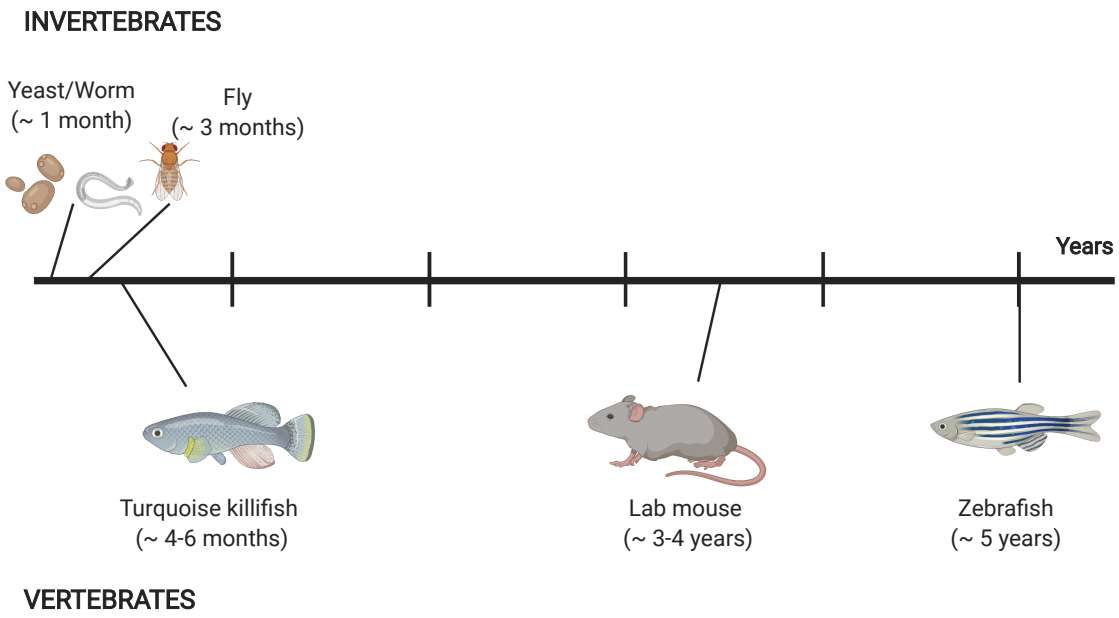

Figure 6: Maximum lifespan across experimental aging model systems. Figure was generated with BioRender.

Despite its short lifespan, the turquoise killifish shows a wide range of aging phenotypes comparable to those observed in other vertebrates, including humans.

Those age-related phenotypes comprise morphological, cellular and molecular changes. Old turquoise killifish show decreased fecundity (Blažek et al., 2013) and increased spinal curvature (Cellerino et al., 2016), and male turquoise killifish lose pigmentation during aging (Geyfman & Andersen, 2010). Aging in the turquoise killifish is moreover characterized by increased neurodegeneration and a decline in cognitive and behavioral capacity (Genade et al., 2005; Dario R. Valenzano et al., 2006). This decline is accompanied by an increase of histological aging biomarkers such as lipofuscin and senescence-associated β-galactosidase. Old turquoise killifish show an increased risk for the development of cancer (Di Cicco et al., 2011) and an accumulation of α-synuclein in the brain (Matsui et al., 2019).

Next to the well-established aging phenotypes, prominent anti-aging interventions such as resveratrol treatment or dietary restriction have been shown to extend lifespan in the turquoise killifish (Terzibasi et al., 2009; Dario R. Valenzano et al., 2006). Moreover, several state-of-the-art molecular tools, such as the establishment of CRISPR-Cas9 techniques (Harel et al., 2016), and a completely sequenced and assembled genome (Reichwald et al., 2015; Dario Riccardo Valenzano et al., 2015), have facilitated research in this model.

With regard to conducting aging research, the research community has so far mainly worked with short-lived invertebrate model systems or long-lived vertebrates. Classically used invertebrate aging models include *C. elegans* and *Drosophila melanogaster*, which are genetically tractable and display short lifespans. However, invertebrates cannot recapitulate important key aspects of human aging, including stem cell dynamics, cancer processes as well as an adaptive immune system (Poeschla & Valenzano, 2020). Common vertebrate model systems such as mice and rats however have comparably long lifespans of more than three years, posing hurdles for lifespan experiments. The turquoise killifish combines a very short lifespan with key vertebrate features and is thus an optimal model organism for aging research, closing the gap between the available short-lived invertebrates and long-lived vertebrate model systems (Fig. 6).

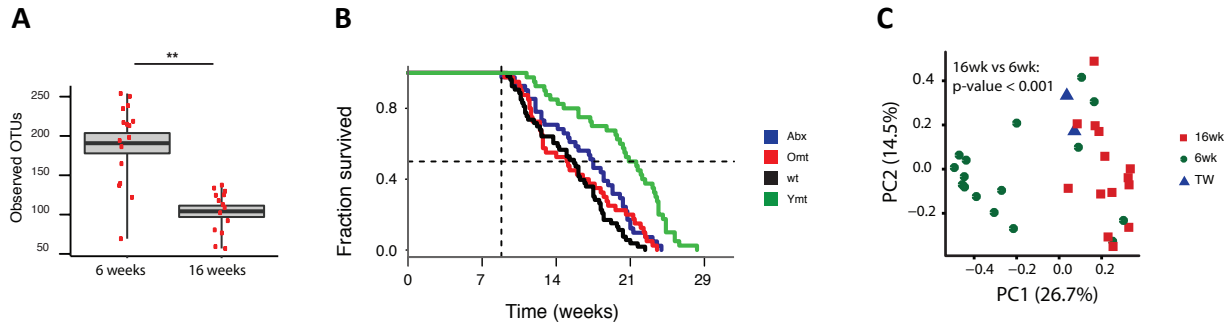

Figure 7: Killifish intestinal characteristics. (A) Alpha diversity levels of young (6 weeks) and old (16 weeks) killifish intestines. (B) Survival analysis of the young-microbiota transfer experiment. Different colors mark the experimental groups: Wildtype control (black), Fish receiving young gut microbiota (green), control fish receiving only antibiotic treatment (blue), control fish receiving old gut microbiota (red). (C) Beta diversity PCoA on intestinal samples from young (green) and old fish (red), including tank water controls (blue). Figures adapted from Smith, Willemsen, Popkes et al., 2017.

Next to the established aging phenotypes, our lab has recently characterized and established the turquoise killifish as a suitable model system for intestinal microbiota research. Turquoise killifish have a complex gut microbiota, comparable in diversity with those of other vertebrate model systems (Smith, Willemsen, Popkes et al., 2017). Moreover, killifish show common gut-related aging phenotypes, such as decline in alpha diversity (Fig. 7A) and an increased variability between individuals in old age, as previously reported for other animals (1.2.4). Our lab furthermore found that specific bacterial taxa can be associated with young and old killifish, with a shift towards more pathogenic bacterial taxa in old age. Next to characterizing the killifish aging gut microbiota features, we discovered that exposing middle-aged fish with microbial communities from young donor fish led to a lifespan extension of more than 30% (Fig. 7B), indicating that gut microbiota is causally involved in the killifish aging proves.

Although we identified important gut microbial changes upon aging, several aspects still remain unclear. In the PCoA of intestinal samples from young and old fish, clear clustering of the two groups was visible – however, some samples from young fish clustered preferentially with the old group (Fig. 7C). This could imply that those young fish, displaying “old-like” microbiota, could be naturally shorter-lived fish. However, we so far concentrated on whole intestinal samples, which requires sacrificing the fish. We thus did not have any chance of correlating microbiota composition with the

lifespan of individual fish, which might enable us in the future to predict host health or future lifespan. In addition, as we only characterized gut microbiota from young, middle-aged and old fish until now, it still remains elusive at what exact time point the particular age-related remodeling occurs.

1.4 Aims of this thesis

Aging is a major restructuring process in the body, negatively impacting both the aged individual and the society as a whole. While several age-related molecular and cellular pathways have been uncovered in the past years, reflecting the host side, recent findings revealed several connections between intestinal microbiota and aging, including age-related diseases. Interestingly, the intestine and its associated microbiota is highly specialized into compartments and moreover shows several sex-specific phenotypes - with some aspects also influencing the aging process.
While research on the aging intestine so far concentrated on global intestinal aging using single-omics approaches, combining several omics approaches including the host and microbial side could deepen the understanding of intestinal aging.

The turquoise killifish is a promising model to study gut microbiota in the context of aging, combining essential vertebrate features like a complex microbiota with a very short lifespan. Our previous work (Smith, Willemsen, Popkes et al., 2017) has already characterized the killifish aging microbiota to some extent and found first hints on a causal connection between gut microbiota and lifespan. However, a detailed understanding of the spatiotemporal aging dynamics of the killifish intestine and its associated microbiota is still lacking.
In addition, analyzing to what extent non-invasive stool samples resemble intestinal microbiota and their potential to serve as an intestinal proxy would enable repeated sampling of gut microbiota - thus allowing to answer the exciting question whether stool microbiota samples can be used to predict individual fish age or remaining fish lifespan.
Moreover, although turquoise killifish shows sexual dimorphism (Vrtílek et al., 2018), the majority of the studies conducted up to date investigated phenotypes exclusively in male turquoise fish. Given the important intestinal sex-differences reported on morphological and molecular level in other animals (1.2.3), also impacting aging processes, it is of utmost interest to characterize potential sex-specific differences in the killifish intestine.

Therefore, the three aims of my thesis are:

Aim 1: Analyzing the temporal dynamics of the killifish intestinal aging over lifespan in a longitudinal manner. I furthermore aim to elucidate whether the gut microbiota at a given stage is predictive for lifespan.

Aim 2: Characterizing the microbiota features of stool and intestinal killifish samples in the context of aging to evaluate whether stool samples can be used as a proxy for intestinal samples when the experimental setup requires a non-invasive sampling approach.

Aim 3: Detailed characterization of the killifish intestine on a morphological, molecular and microbial level. In this regard, I aim to identify potential intestinal sections, intestinal sex differences and to investigate the killifish intestinal aging process in a spatiotemporal manner.

Chapter 2

Results

2.1 Longitudinal characterization of individual killifish stool samples

Previous results on microbiota composition of the aging killifish intestine show differences in microbiota composition and diversity values between young and old individuals (Smith, Willemsen, Popkes et al., 2017). However, the temporal dynamics of age-related changes in microbiota composition are largely unknown. As time-dependent microbial changes may causally influence killifish aging, information about the temporal dynamics could be very useful for understanding killifish aging on a broader level. An important question is whether specific changes in microbiota composition could be predictive of remaining life or could be used as proxies for imminent death, possibly helping to identify the most suitable timepoints for microbiota-related anti-aging interventions.

To characterize individual dynamics of intestinal microbiota composition during aging and to build a predictive model of lifespan based on microbiota composition, I designed and performed a longitudinal collection of stool samples of individually housed male turquoise killifish throughout their adult life (Fig. 8A). After weekly collection of stool and food control samples, I simultaneously extracted the DNA of all samples after every fish died a natural death. I then established a library preparation protocol for 16S rRNA sequencing of the variable V4-region to obtain information about the weekly microbiota composition of each individual fish over its whole lifespan (Fig. 8A). To validate any age-related dynamics and enable the generation of predictive models, I sampled stool of two independent cohorts hatched two weeks apart – the first cohort comprising 42 male fish (= group 1), the second cohort 9 male fish (= group 2) (Fig. 8B).

The median lifespan of the first, experimental cohort was 18.5 weeks and comparable to that of the female control siblings from the same hatch date (19 weeks median lifespan, Fig. 8C). The obtained lifespan data is in line with previously generated data from our fish facility. The median lifespan of the second cohort was noticeably shorter than expected, with a median lifespan of 11 weeks (Fig. 8D). Possible underlying reasons for this difference in lifespan will be discussed later.

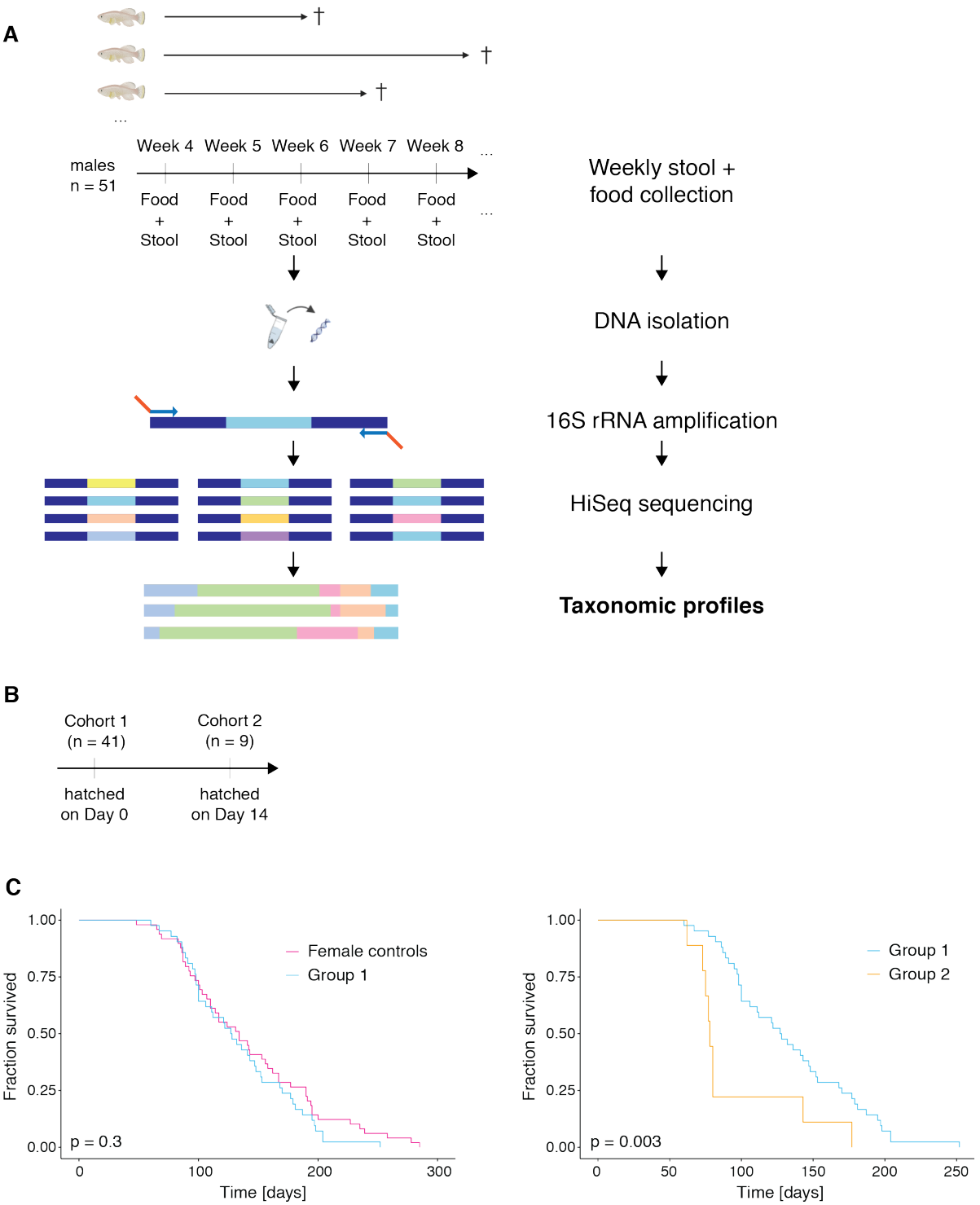

Figure 8: Experimental setup of the longitudinal fecal collection study. (A) Workflow of the longitudinal fecal collection study. Stool and food control samples were collected weekly from week 4 until natural fish death. DNA was isolated from the samples, followed by library preparation and V4 16S rRNA sequencing. (B) Overview of the hatching time points and fish numbers of the two cohorts included in the study. (C) Survival analysis of group 1 (blue) and the female siblings (pink). (D) Survival analysis of group 1 (blue) and group 2 (orange). Statistical significance was calculated by a Log-Rank test.

2.1.1 Killifish stool microbiota strongly correlates with food microbiota

Sequencing of the samples resulted in 115 million paired-end reads, with a median of 200.000 reads per sample after quality filtering.

To investigate the similarity between all the samples of the experimental group, I first performed principal coordinate analysis (PCoA) on Bray-Curtis diversity levels of the fish stool samples. The samples did not cluster by fish ID (Fig. 9A), but by week of sampling – following a trajectory alongside the first principal coordinate (PC1, Fig. 9B) (p-value < 0.001, PERMANOVA analysis). I observed a similar temporal trajectory in the sequences from group 2 (Fig. 9C) (p-value < 0.001, PERMANOVA analysis), implying that either aging drives the microbiota changes, or a time-dependent extrinsic environmental factor is contributing substantially to the microbiota profile of the stool samples. Food is acknowledged as a major contributing factor to the gut microbiota composition (Claesson, Jeffery, Conde, Power, O'Connor, et al., 2012; Ringø et al., 2016b). Hence, I analyzed the time-dependent changes in the microbiota of brine shrimp and bloodworm (i.e. the two constituents of killifish diet) compared to stool, via PCoA. The brine shrimp samples clustered more distantly from the fish samples (Fig. 9D), suggesting minor effects of this food type on microbiota composition. The bloodworm samples, in contrast, showed an overlapping trajectory with the stool samples, clustering together with the respective weekly fish samples (Fig. 9E). Based on this finding, I hypothesized that the microbiota composition of the stool samples is in large part dictated by the bloodworm microbiota. To test this hypothesis, I further dissected the microbiota composition of fish and food samples over the whole longitudinal experiment.

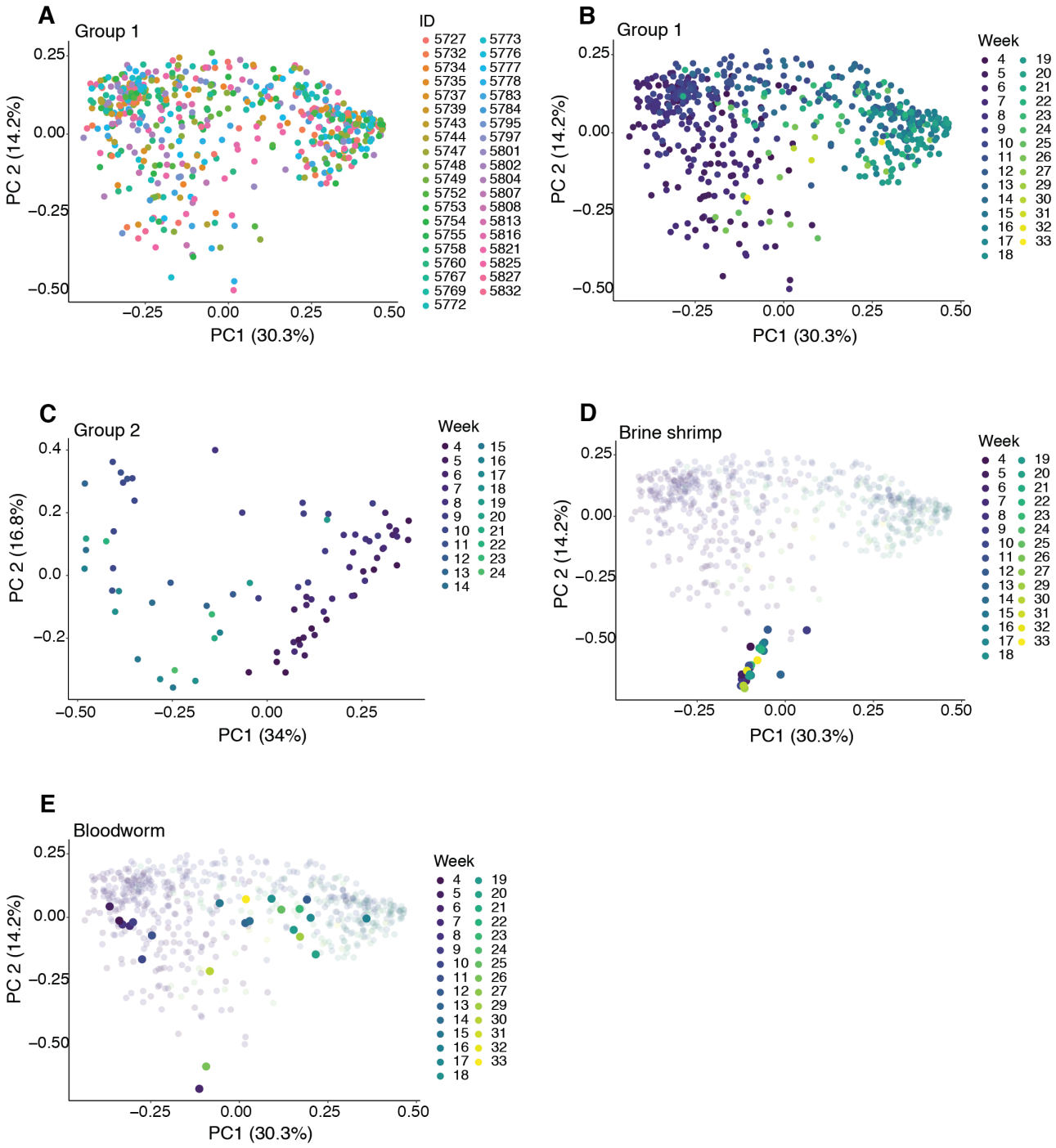

Figure 9: Bray-Curtis dissimilarity PCoAs. (A) PCoA of Bray-Curtis dissimilarity of the samples from group 1. Samples are colored by their individual fish ID. (B) PCoA of Bray-Curtis dissimilarity of the samples from group 1. Samples are colored by the week of collection. (C) PCoA of Bray-Curtis dissimilarity of the samples from group 2. Samples are colored by the week of collection. (D) PCoA of Bray-Curtis dissimilarity of the samples from group 1 (transparent) and the brine shrimp food samples (non-transparent). Samples are colored by the week of collection. (E) PCoA of Bray-Curtis dissimilarity of the samples from group 1 (transparent) and the bloodworm food samples (non-transparent). Samples are colored by the week of collection.

2.1.2 Taxonomic composition of stool and food samples over killifish lifespan

To gain insight into the contribution of the bloodworm microbiota across the killifish lifespan, I analyzed the taxonomic composition of the fish and food samples.

The fish samples comprised 3142 amplicon sequence variants (ASVs), with 70 ASVs of an abundance of >1%. On a higher taxonomic level, I identified 30 phyla, of which 6 phyla showed an abundance of >1%. The fish stool samples were dominated by Proteobacteria (82.8%), with Firmicutes (9.1%) and Fusobacteria (6.1%) as the next most abundant phyla. At the genus level, I identified 586 genera, with only 34 genera of an abundance >1%. The most abundant genera were *Vibrio* (42.8%), *Aeromonas* (14.9%), *Shewanella* (11.2%), *Plesiomonas* (4.9%) and *Cetobacterium* (3.6%).

The food samples comprised 1951 ASVs with 92 ASVs showing an abundance of >1%. I identified 28 phyla, of which 6 had an abundance of >1%. Similar to the fish samples, food samples also consisted of a major fraction of Proteobacteria (64.3%), followed by Bacteroidetes (14%), Firmicutes (8.2%), Fusobacteria (6.6%) and Epsilonbacteria (5.9%). The food samples contained 490 genera with 54 genera >1% abundance – the most enriched genera were *Vibrio* (24.3%), *Catenococcus* (9%), *Pseudoalteromonas* (8.8%), *Tenacibaculum* (8.6%) and *Arcobacter* (6%).

To describe the dynamics of microbiota composition over time, I plotted the taxonomic composition per week as mean relative abundances of the top contributing phyla (Fig. 10A). At the phylum level, fish samples showed a consistent taxonomic composition with Proteobacteria as predominant phylum, confirming previous results from killifish gut microbiota (Smith, Willemsen, Popkes et al., 2017). Firmicutes showed a relatively stable abundance over time with a short but strong increase in abundance at week 28. While the taxonomic composition was highly similar in the first weeks of life, a shift became apparent after week 10, when Fusobacteria increased in relative abundance and Proteobacteria decreased their relative abundance. This pattern slowly reversed later in life after week 20.

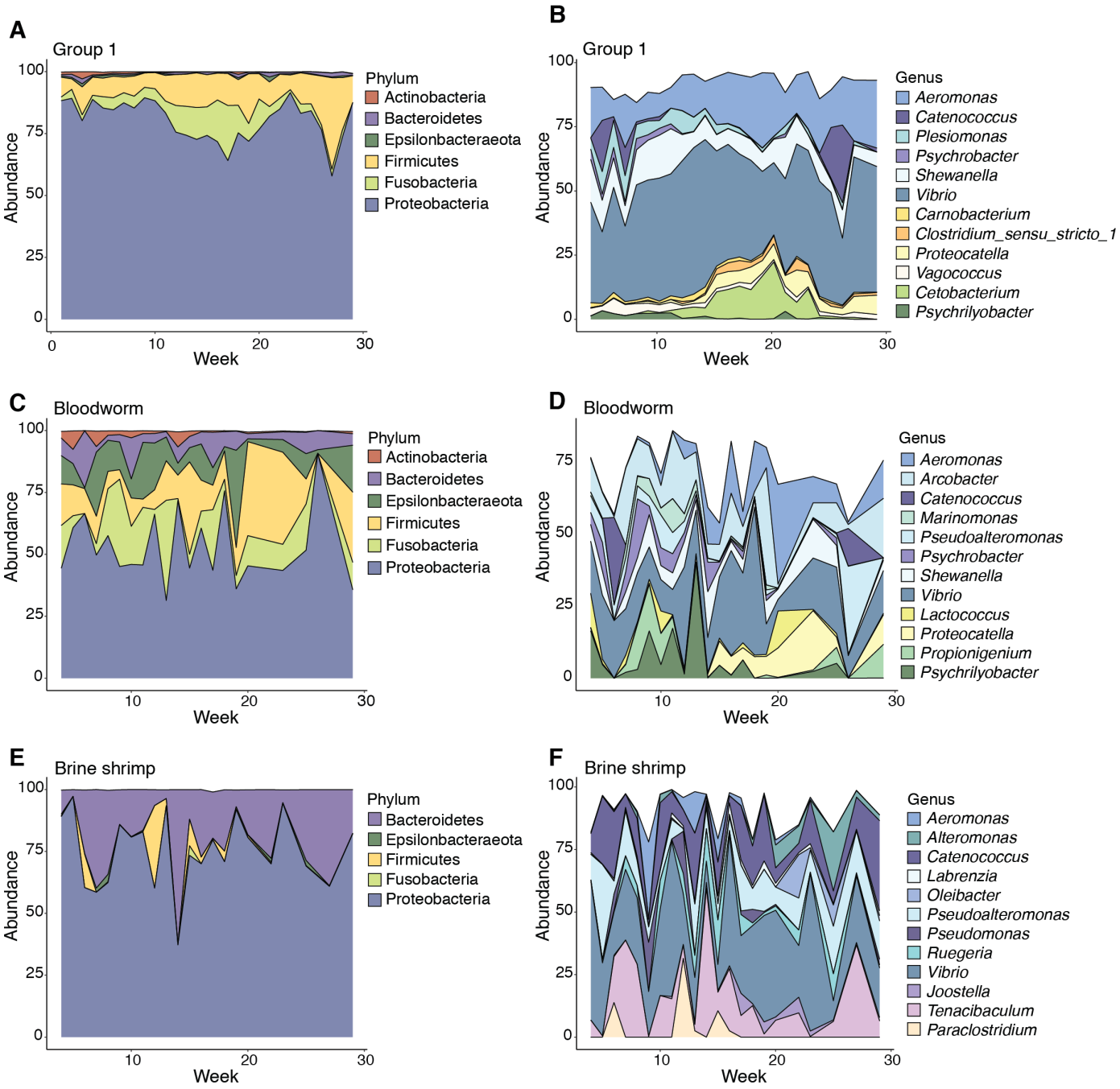

Figure 10: Taxonomic composition analyses. Relative abundance of the most prevalent phyla across the longitudinal experiment for (A) group 1, (C) bloodworm and (E) brine shrimp food samples. The chosen colors represent the different phyla. Relative abundance of the most prevalent genera over the collection time for (B) group 1, (D) bloodworm and (F) brine shrimp food samples. The chosen colors represent the different genera, the color shades represent the respective phylum.

To note, bloodworm samples remained largely dominated by Proteobacteria, but also showed significant levels of Bacteroidetes, Fusobacteria, Actinobacteria and

Firmicutes. Brine shrimp samples were mostly dominated by Proteobacteria and Bacteroidetes, with a minor contribution of Firmicutes. Contrary to the fish samples, the microbial composition of the food samples was fluctuating rather strongly between the weeks (Fig. 10A).

To identify specific bacteria contributing to the shifts in composition at a deeper taxonomic level, I next plotted the most abundant genera over time (Fig. 10B). While in the fish samples some genera, including *Shewanella*, remained rather stable over time, some genera were only detected at specific timepoints. The most striking example was *Cetobacterium*, whose abundance increased drastically after week 11, accompanied with an increase in *Proteocatella* and *Clostridium_sensu_stricto_1*. In contrast, I observed an inverse pattern for the abundance of *Vibrio,* which showed low levels in the weeks of high *Cetobacterium* abundance.

The most abundant genera present in young fish before week 12 were *Vagococcus*, *Psychrobacter*, *Psychrilyobacter* and *Catenococcus*, while *Catenococcus* showed a strong reappearance later in life around weeks 25-27. *Plesiomonas* were also more abundant in the first weeks, with a drop in abundance at around week 20. Such clear patterns were not detectable for the food samples. In line with the fluctuation of the different phyla, the abundance of single genera was highly variable over time.

The taxonomic analysis of the sample types showed clear differences, but also some similarities between the fish stool and the food samples. All sample types were dominated by Proteobacteria, while Epsilonbacteria and Bacteroidetes were enriched in food samples. The fish stool samples shared particular microbiota especially with the bloodworm food, mainly including Firmicutes and Fusobacteria, supporting the hypothesis that the bloodworm food has a stronger impact on fish stool microbiota composition compared to the brine shrimp food. The taxonomic composition of the most abundant genera remained largely stable for the fish samples, whereas food samples were characterized by high fluctuation.

Another important factor of microbiota community composition are measurements of diversity, as high diversity levels can hint on more resilient microbial communities with a wide array of functional responses (Lozupone et al., 2012). Since our previous results showed age-related changes in diversity, I next focused on the diversity measures along the time course of the longitudinal experiment.

2.1.3 Diversity measures over killifish lifespan

Diversity measurements provide important insights into the variety and structure of bacterial communities. Beta diversity is calculated to assess the diversity between single communities – this can be either within a specific group (e.g., from individuals of the same age), or also between specific groups (e.g., comparing individuals from group A to group B).

Previous work from our lab (Smith, Willemsen, Popkes et al., 2017) showed an increase in the intestinal beta diversity levels between week 6 (young) and week 16 (old) of killifish age, indicating that the fish intestinal microbiota composition becomes more dissimilar between individual fish at older age. As assessing the microbiota composition of fish intestines requires invasive sampling, sampling killifish stool provides an experimental non-invasive method to trace killifish microbiota. Importantly, this straightforward method shares similarities with sampling methods used in humans. I thus asked whether stool microbiota displayed beta diversity changes compatible to those previously observed in microbiota sampling from the gut. In this regard, I assessed the beta diversity levels within and between different weeks from the experimental cohort of the longitudinal collection study.

Contrary to our previous observations, I could not identify differences in the within-group beta diversity levels between week 6 and week 16 (Fig. 11A). Within-group diversity levels were slightly higher at weeks 4 and 5, followed by lower but rather stable diversity levels from week 6 to week 20. Finally, diversity levels tended to increase for the later weeks. As only one food control sample was collected per week, within-group beta diversity levels could not be determined for bloodworm and brine shrimp controls.

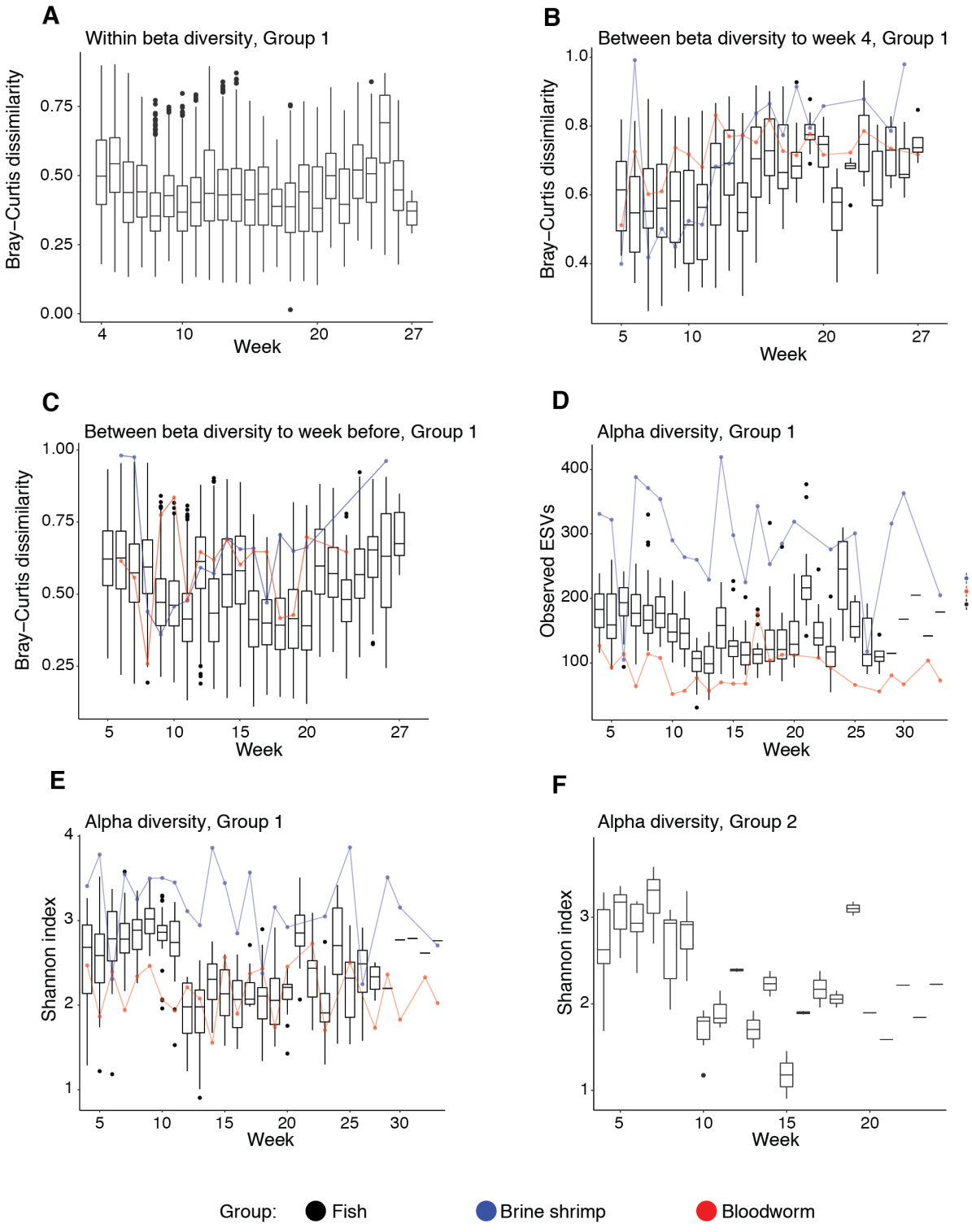

Figure 11: Alpha and beta diversity measures. (A) Bray-Curtis dissimilarity values comparing samples within the same collection weeks for group 1 across the longitudinal experiment. (B) Bray-Curtis dissimilarity values comparing samples of the different weeks to the first collection week 4 across the longitudinal experiment. Group 1 is shown in black, bloodworm food in blue, brine shrimp food in red. (C) Bray-Curtis dissimilarity values comparing samples of the different weeks to the preceding week across the longitudinal

experiment. Group 1 is shown in black, bloodworm food in blue, brine shrimp food in red. (D) Alpha diversity in observed ESVs across the longitudinal experiment. Group 1 is shown in black, bloodworm food in blue, brine shrimp food in red. (E) Shannon index alpha diversity across the longitudinal experiment. Group 1 is shown in black, bloodworm food in blue, brine shrimp food in red. (F) Shannon index alpha diversity across the longitudinal experiment for group 2.

I next assessed the between-group beta diversity levels. I first compared the samples of every week to the microbiota composition of the beginning of the longitudinal collection (week 4, Fig. 11B), which explores the drift in microbiota composition along the experiment. To uncover strong changes in microbiota compositions between weeks, I then also compared the samples of every week to the microbiota composition of the samples from the preceding week (e.g., week 6 to week 5, Fig. 11C).

The Bray-Curtis dissimilarity values generally increased over the time course, indicating that the microbiota composition over the weeks was steadily diverging from the starting microbiota composition (Fig. 11B). The same trend was apparent in both food types. When comparing the microbiota composition of each week to the preceding week, the dissimilarity values were fluctuating over time, with higher dissimilarity values at the first 4 weeks (week 4-8), at week 12, 14, 15 and then from week 21 onwards (Fig. 11C). This suggests that the microbiota composition changed more strongly between the single weeks in those periods, while the composition was rather stable at weeks 9-11 and 16-20.

In our previous work we observed a decrease in alpha diversity of intestinal samples upon aging (Smith, Willemsen, Popkes et al., 2017). To examine whether this phenomenon not only applies to intestinal but also to stool samples, I next assessed alpha diversity levels using two different approaches. The “Observed ESV” measure estimates the richness of the samples by counting the exact sequence variants (ESVs) present (i.e. the number of different species in the community), whereas Shannon diversity computes both richness and evenness (i.e. how evenly distributed are the species in the community). Both measures confirmed the previously reported reduction in alpha diversity between young fish (6 weeks) and old fish (16 weeks) (Fig. 11D+E) (p-value <0.001, Wilcox-test). However, diversity did not steadily decline,

but showed a strong drop from week 11 to week 12, especially for Shannon diversity. To further examine the potential of this age-related trend as a general aging phenotype, I analyzed the diversity levels also in the smaller cohort 2. Surprisingly, the second cohort showed a similar decrease in alpha diversity – however from week 9 to week 10 (Fig. 11F). As the cohorts were hatched with a time difference of two weeks, the change in alpha diversity appeared at the same chronological timepoint (i.e. calendar time) for both cohorts. This indicates that the observed drop in diversity was not influenced by intrinsic fish aging, but possibly by external factors. Since the PCoA representation suggests a strong influence of food microbiota on stool microbiota composition, one possible explanation could be a shift in microbiota composition of the food samples around that chronological time.
However, the alpha diversity of the food samples did not show comparable changes for either the bloodworm or brine shrimp food (blue and red lines in Fig. 11D+E). The observed shift in diversity in the fish samples therefore cannot be explained by any detectable variable present in the food at this stage. I moreover checked whether several fish room parameters, including water temperature, pH and conductivity, could have explained the compositional fluctuations observed in the fish stool microbiota. However, the parameter values did not show any apparent changes around the chronological time point where the shift in diversity was observed (data not shown).

Taken together, I found that the microbiota composition of stool samples is strongly associated with the bloodworm food microbiota. However, some patterns such as the strong drop in alpha diversity after week 11 could not be directly associated with bloodworm 16S microbial composition. This finding begs the question of whether we can use the stool samples to extract information about food-independent microbiota – which may reflect fish-intrinsic intestinal aging patterns. I therefore took a closer look at the most abundant genera and searched for food-independent abundance patterns over time.

2.1.4 Identifying food-independent bacterial taxa

To identify potential fish gut-intrinsic aging patterns, I more deeply investigated the abundance profiles of the most frequent genera. For most of the genera, the mean relative abundance in the fish stool samples (purple line) showed a similar pattern to the bloodworm samples (blue line) – the abundance levels in the stool samples were thus strongly correlated with the food microbiota levels (e.g., *Proteocatella* and *Enterococcus*, Fig. 12A+B).

However, the abundance of particular genera showed divergent patterns between fish stool and the food control samples. *Marinomonas* for example strongly increased in the bloodworm samples between week 7-13, which was not reflected in the fish stool samples (Fig. 12C) – therefore marking a bloodworm-specific behavior. Several microbial genera also displayed stool-specific patterns with relative abundances higher than expected, such as *Vibrio* and *Plesiomonas* in general or *Aeromonas* during the first weeks (Fig. 12D-F). Interestingly, the mentioned genera demonstrated a similar pattern in the smaller cohort 2, further supporting this observation (data not shown). These genera are potential candidates for fish-specific bacteria, where the stool samples might reflect the underlying intestinal microbiota changes.

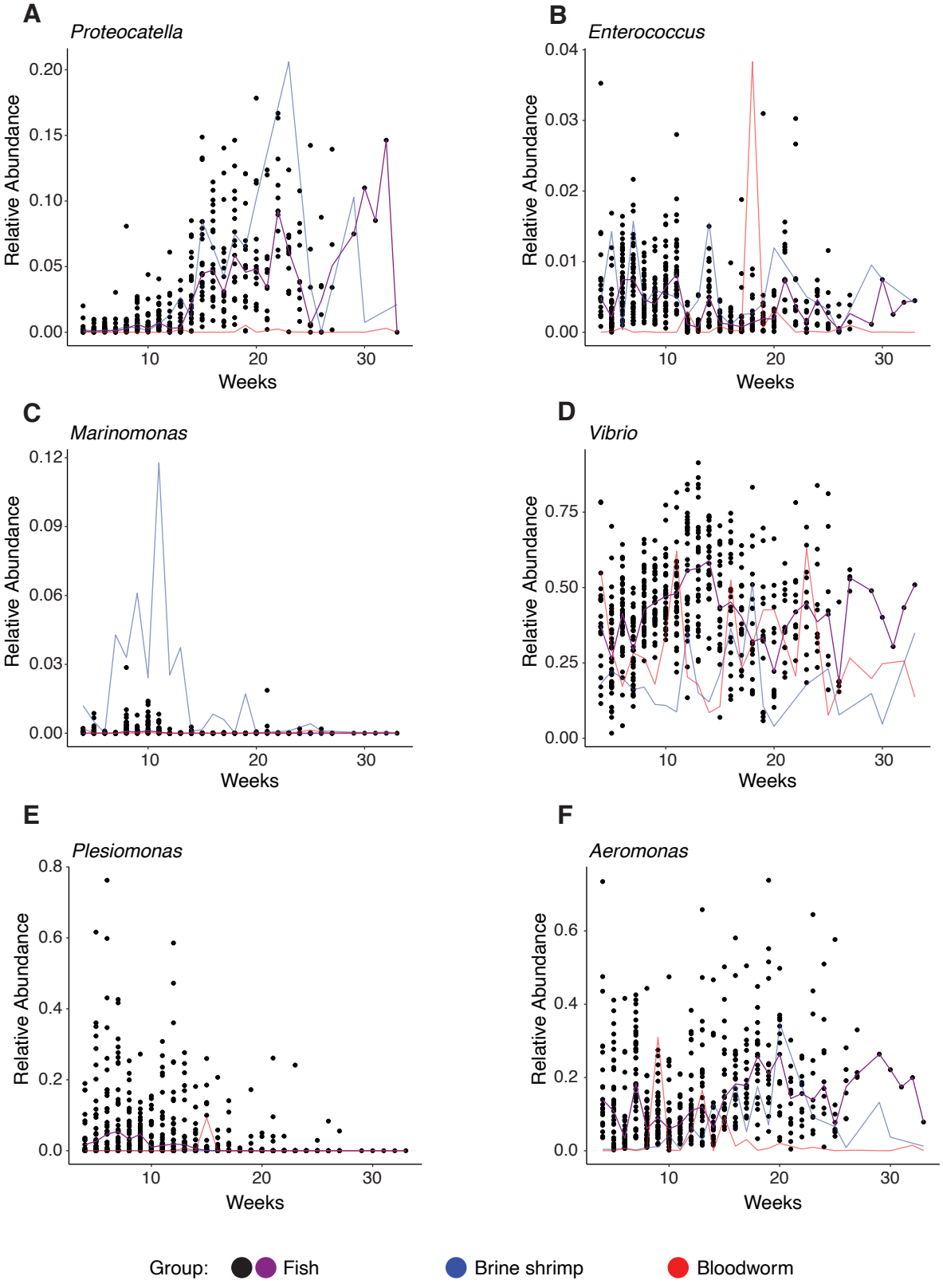

Figure 12: Relative abundances of food-dependent and food-independent genera. Relative abundance across the longitudinal experiment of (A) *Proteocatella,* (B) *Enterococcus*, (C) *Marinomonas*, (D) *Vibrio*, (E) *Plesiomonas* and (F) *Aeromonas*. Samples from group 1 are

shown in black, the mean relative abundance is represented in purple. Food control samples are shown in blue (bloodworm) and red (brine shrimp).

2.1.5 The overlap of food and stool microbiota over lifetime

I next sought to analyze the food-independent genera in more detail. Particularly, the analysis of the ratio between food-dependent and food-independent bacteria could deepen our understanding of the underlying fish-intrinsic intestinal aging patterns. Concrete changes in food-specific bacteria might provide insights into host-controlled selection for specific bacteria over time. I therefore calculated the overlapping ASVs between young fish and the corresponding bloodworm samples (weeks 4-11) or between old fish and the corresponding bloodworm samples (weeks 12-29) (Fig. 13). The number of shared ASVs significantly increased with age (p-value 0.011, Fisher's exact test), suggesting that old fish might lose the capability of selecting specific bacteria from the orally ingested microbiota in their intestine.

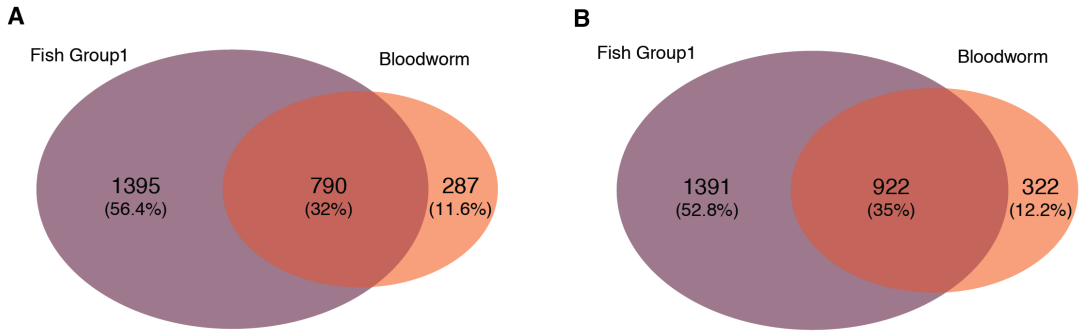

Figure 13: Venn diagrams illustrating the overlap of group 1 fish and bloodworm food ASVs. (A) Shared ASVs between young fish (week 4-11) and the corresponding bloodworm food samples (week 4-11). (B) Shared ASVs between old fish (week 12-29) and the corresponding bloodworm food samples (week 12-29). The number of shared ASVs increases with age (p-value = 0.011, Fisher's exact test).

2.1.6 Remaining lifespan can be predicted based on microbiota composition

The analyses of the longitudinal stool collection dataset revealed that the strong global changes, such as diversity and overall taxonomic composition, are mainly driven by

bloodworm food and by yet unknown environmental factors. While a descriptive approach that compares microbial communities between fish and food across time points did not lead to a straightforward identification of an age-specific component of the killifish stool microbiota, I decided to employ a machine learning strategy that takes into account stool-bloodworm interactions over the experimental setup. This approach, performed in collaboration with Sam Kean, a student in our lab, was aimed to build prediction models to identify microbial features associated with remaining killifish lifespan.

To build the prediction models, the samples were split into a large training dataset for training the model, and a test dataset, which is unseen by the model and is thus used for validation. For the training dataset, a subset of 80% fish from group 1 was randomly chosen. The corresponding longitudinal microbiota composition data was used for training of a Random Forest (RF) regressor model to predict the fish age in weeks. The remaining 20% of group 1 were then used as the test dataset to validate the prediction model. The prediction model was highly accurate with an r-value of 0.95, a p-value of <0.001 and a slope of 0.9 (Fig. 14A). However, as I previously observed a strong association between the microbiota composition of stool and bloodworm food samples, we sought to examine whether the age prediction is driven by the underlying longitudinal bloodworm food microbiota composition. Indeed, testing the stool-trained model on the bloodworm food controls also revealed a very accurate prediction, with an r-value of 0.86, a p-value of <0.001 and a slope of 0.54 (Fig. 14B), indicating that a large part of the prediction power arose from the food microbiota composition of the given week. At the same time, the slope was lower for the bloodworm samples and the prediction thus less accurate compared to the group 1 samples, suggesting that a fraction of the prediction power also came from either intrinsic fish compositional changes or non-bloodworm extrinsic influences.

We therefore next searched for a possibility to build a prediction model with less influence of the food controls. Using remaining life at a sampled timepoint (individual lifespan minus the days lived at collection time) instead of using weeks adds variability to the training dataset, as the remaining life values differ per individual at a given week. We thus again built the prediction models on 80% randomly chosen fish of group 1

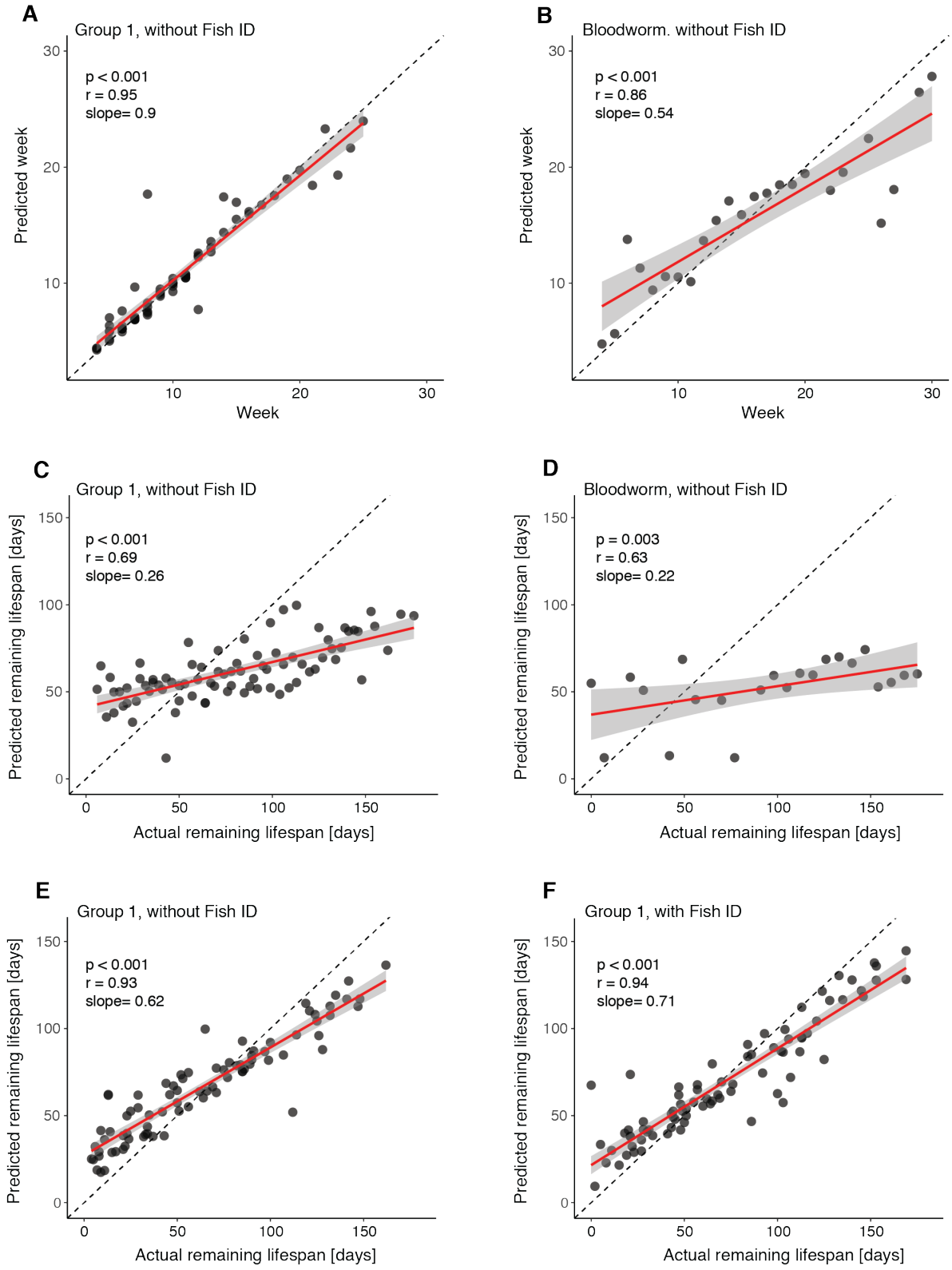

Figure 14: Prediction models based on microbiota composition. Random Forest regressor model trained on a random 80% subset of individual fish, to predict the age in weeks for (A) group 1 individuals and (B) the bloodworm food samples. (C-D) Random Forest regressor model trained on a random 80% subset of individual fish, to predict remaining life for (C) group 1 individuals and (D) the bloodworm food samples. (E-F) Random Forest

regressor models trained on a random 80% subset of all sample datapoints, to predict remaining life of group 1 individuals (E) not including the individual fish ID and (F) including the individual fish ID.

and trained a Random Forest regressor model to predict the remaining fish life in days. Validation of this model resulted in a prediction with an r-value of 0.69, a p-value of <0.001 and a slope of 0.26 (Fig. 14C). The new model retained some predictive accuracy, but the accuracy was considerably lower when compared to the model predicting week. When we tested the trained model on the bloodworm control samples, the prediction accuracy was still comparable to group 1 accuracy, although with slightly lower values (r-value of 0.63, p-value of 0.003, slope of 0.22) (Fig. 14D). This difference in accuracy again indicates that a part of the predictive power arose from the underlying bloodworm microbiota - however, also a part was explained by a fish-intrinsic or extrinsic non-bloodworm-related variable.

To determine the proportion of predictive power explained by the fish-intrinsic microbiome, we trained a model with encoded host information by including the fish ID into the model. For this, the selection process of the training and test datasets was amended, as the model needed samples with each fish ID in both the training and the test dataset. We thus chose a random 80% of all the sample data instead of using 80% of individual fish. Considering a random 80% subset of all samples alone, without adding the ID information, already improved the prediction model greatly, with an r-value of 0.93, a p-value of <0.001 and a slope of 0.62 (Fig. 14E). Notably though, additionally including the fish IDs into the prediction model increased the accuracy even further, and the slope increased from 0.62 to 0.71 (Fig. 14F).

Taken together, the results from the prediction models suggest that we can predict week and remaining life based on longitudinal stool microbiota data. Although a large portion of the predictive power arose from the underlying bloodworm microbiota composition, including the individual fish IDs into the prediction model improved the prediction accuracy. The difference in prediction accuracy strongly suggests that host features also contribute to the prediction model.

2.2 Characterization of the microbiota profile of gut, stool and food samples

The longitudinal collection of stool samples provided clear insights into the strong connection between stool microbiota composition, environmental factors and in particular the bloodworm food. It is therefore of great interest to study how stool and food microbiota correlate with one another throughout fish aging. In addition, it is of critical importance to analyze to what extent stool microbiota samples resemble the intestinal microbiota composition and whether they are a suitable proxy for intestinal samples. I therefore sampled stool and intestinal samples of young (8-week-old) and old male (20-week-old) killifish and old female (20-week-old) killifish, together with food control samples and performed V3/V4 16S rRNA sequencing on the extracted DNA (Fig. 15).

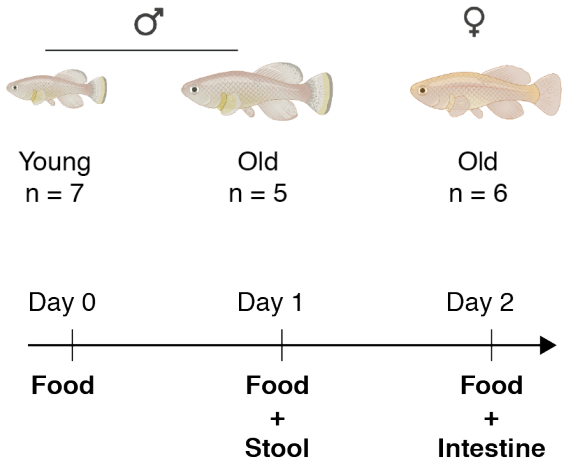

Figure 15: Experimental setup for the comparative stool-gut-food microbiota study. Young and old male fish, and old female fish were included in the study. Food samples were collected on day 0, 1, 2 (young fish = 8 weeks, old fish = 20 weeks). Stool samples were collected on day 1, followed by collection of the intestines on day 2.

2.2.1 Stool, food and gut samples show clear differences in microbiota profiles

The sequencing of the samples resulted in 850.000 paired-end reads, with a median of 23.500 reads per sample after quality filtering.

To investigate the similarity between the different sample types, I conducted PCoA based on Bray-Curtis beta diversity levels (Fig. 16). The samples from the different tissues clearly clustered together, with a strong separation of the gut and the stool samples. The three food samples clustered together with the stool samples, confirming the observed strong relationship between stool and food from the previously described longitudinal experiment. Moreover, the clustering pattern suggests a higher similarity between the microbiota composition of stool and food samples compared to stool and intestinal samples.

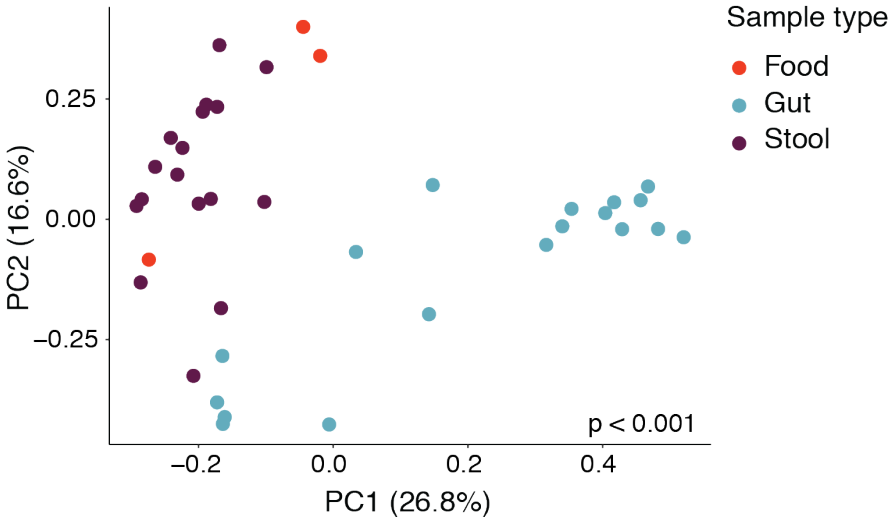

Figure 16: Bray-Curtis dissimilarity PCoA. PCoA of Bray-Curtis dissimilarity of the collected samples from the stool-gut-food microbiota study. Intestinal samples are marked in blue, stool samples are marked in purple, food samples are marked in red. Statistical significance was calculated by PERMANOVA analysis.

I next checked the detailed microbiota composition to define which bacteria were enriched per sample type. Gut samples showed the highest number of ASVs (869 ASVs), followed by stool samples (523 ASVs) and food samples (332 ASVs).

However, the majority of the observed ASVs were rare in all sample types, with an abundance of <0.1%. This is especially interesting for the intestinal samples – despite overall having the highest number of ASVs, gut samples showed a lower number of ASVs with an abundance higher than 0.1% (81 ASVs) compared to food (97 ASVs) and stool samples (103 ASVs).

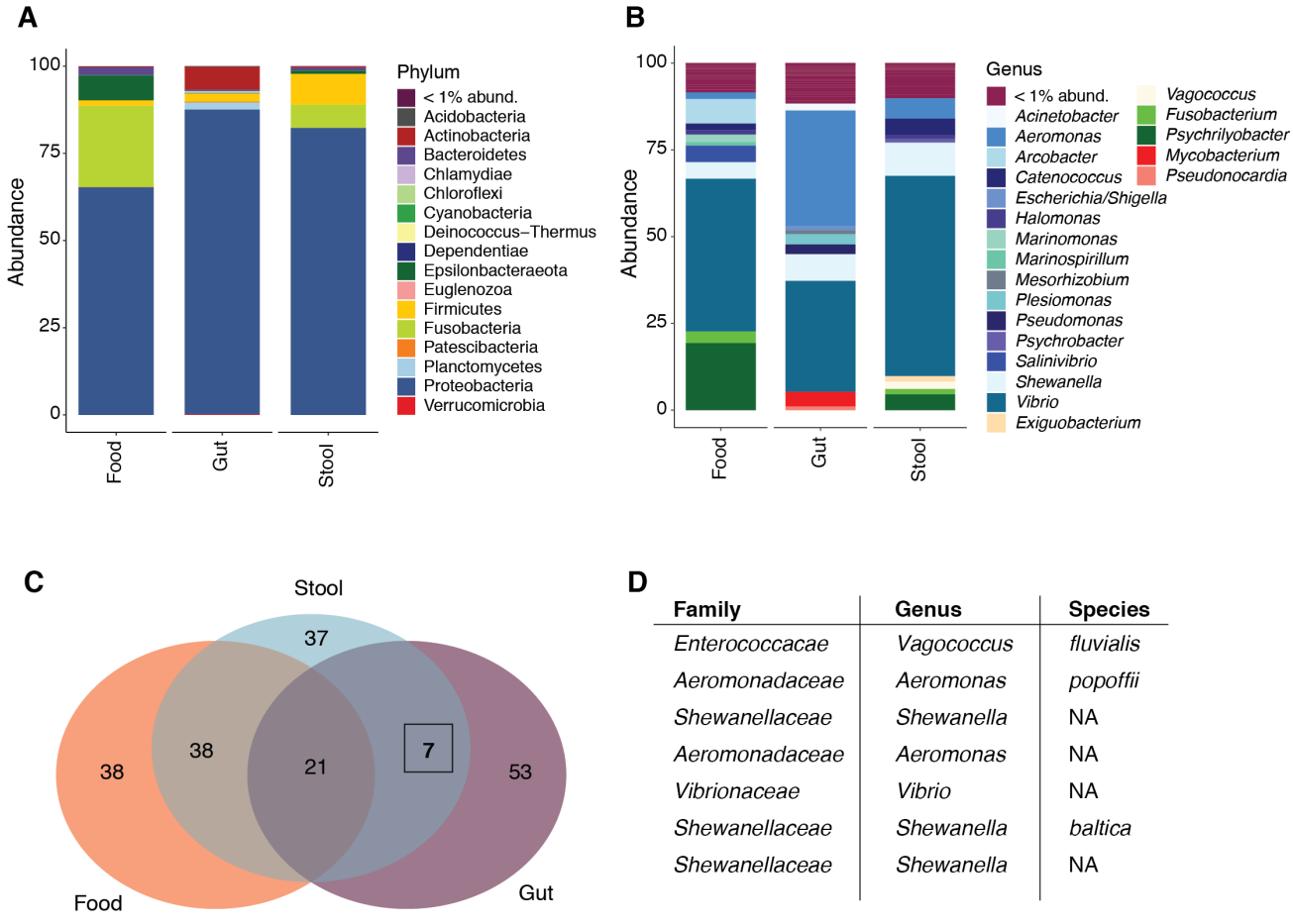

Family	Genus	Species
Enterococcacae	*Vagococcus*	*fluvialis*
Aeromonadaceae	*Aeromonas*	*popoffii*
Shewanellaceae	*Shewanella*	NA
Aeromonadaceae	*Aeromonas*	NA
Vibrionaceae	*Vibrio*	NA
Shewanellaceae	*Shewanella*	*baltica*
Shewanellaceae	*Shewanella*	NA

Figure 17: Taxonomic composition of the tissue samples. (A) Relative abundance of the most prevalent phyla for food, gut and stool samples. The chosen colors represent the different phyla. (B) Relative abundance of the most prevalent genera for food, gut and stool samples. The chosen colors represent the different genera, the color shades represent the respective phylum. (C) Venn diagram illustrating the overlap of gut, stool and food ASVs with a minimal abundance of >0.1%. (D) Taxonomic assignment of the 7 ASVs shared between stool and gut samples.

With regards to the composition, I found clear patterns for each sample type (Fig. 17A). Gut samples were mostly driven by Proteobacteria (90.8%), followed by Actinobacteria (4.6%), Firmicutes (1.8%) and Planctomycetes (1.6%). Proteobacteria were also the most abundant phyla in food samples, although only to an extent of 66%, followed by Fusobacteria (22.7%), Epsilonbacteria (7.5%), Bacteroidetes (2.5%) and Firmicutes (1.4%). Stool samples also displayed high levels of Proteobacteria (82.6%), followed by Firmicutes (9%), Fusobacteria (6%) and Bacteroidetes (1%).

At the genus level, gut samples showed high relative abundance of *Aeromonas*, *Vibrio*, *Shewanella*, *Plesiomonas* and *Mycobacterium* (Fig. 17B). The most abundant genera of the food samples were *Vibrio* and *Psychrilyobacter*, followed by *Arcobacter*, *Shewanella* and *Salinivibrio*. As expected from the PCoA, stool samples shared some characteristics with the food samples, for example the appearance of *Psychrilyobacter* and *Fusobacterium*. However, also some gut properties were present in the stool samples – including a higher fraction of *Aeromonas*.

I therefore asked which particular bacteria were shared between the different sample types, and which were sample-type specific. For this analysis I only considered the most frequent taxa, using ASVs with a minimal abundance of 0.1%, and visualized the results in a Venn diagram (Fig. 17C). The gut samples showed the highest percentage of sample type-specific ASVs, with 53 of 81 ASVs only occurring in the intestinal samples. These ASVs mostly belonged to the genera *Aeromonas*, *Shewanella*, *Mycobacterium*, *Acinetobacter* and *Plesiomonas*.

Stool and food samples had less tissue-specific ASVs, with some *Vibrio*, *Arcobacter* and *Marimonas* species only detected in food samples and other *Vibrio*, *Flavobacterium*, *Shewanella* and *Psychrobacter* being specific for stool samples. In line with the PCoA results, stool samples seemed to be more similar to food samples than to intestinal samples, as 38 ASVs were shared between stool and food samples while only seven ASVs were shared between gut and stool samples. ASVs which were shared between stool and food belonged to the genera *Psychrilyobacter*, *Vibrio*, *Catenococcus* and *Fusobacterium*, among others.

Of particular interest were the seven ASVs shared between the stool and gut samples, which were not present in the food controls (Fig. 17D). Such ASVs have a great potential to serve as intestinal biomarkers for studies including only stool samples. This would be of great importance especially for lifespan studies, where the invasive sampling of intestines is not an option. The seven ASVs comprised unknown species of *Shewanella*, *Vibrio* and *Aeromonas*, plus *Vagococcus fluvialis* and *Aeromonas popoffii*.

Taken together, clear taxonomic patterns were visible per sample type. While all sample types were dominated by Proteobacteria, food samples were enriched for Fusobacteria and Epsilonbacteria. Intestinal samples in contrast showed a particular fraction of Actinobacteria, including the gut-specific genus *Mycobacterium.* The stool samples had a higher similarity with the food samples. However, stool samples were combining features of both the intestinal and the food samples - with an enrichment in food-related Fusobacteria but also a significant fraction of *Aeromonas*, comparable to the intestinal sample composition. In particular, seven ASVs were shared only between intestinal and stool samples, suggesting those as potential intestinal biomarkers.

2.2.2 Diversity measures of food, gut and stool samples

To test whether diversity differs between the sample types, I next calculated alpha diversity levels. Interestingly, food samples showed the highest levels of alpha diversity considering observed ASVs and Shannon diversity (Fig. 18A) and gut samples showed the lowest levels. However, when taking phylogeny into account, gut samples had significant higher levels of diversity (Fig. 18B). These results suggest that individual gut samples contain lower numbers of ASVs which are less evenly distributed, but that those ASVs are phylogenetically far away from each other.

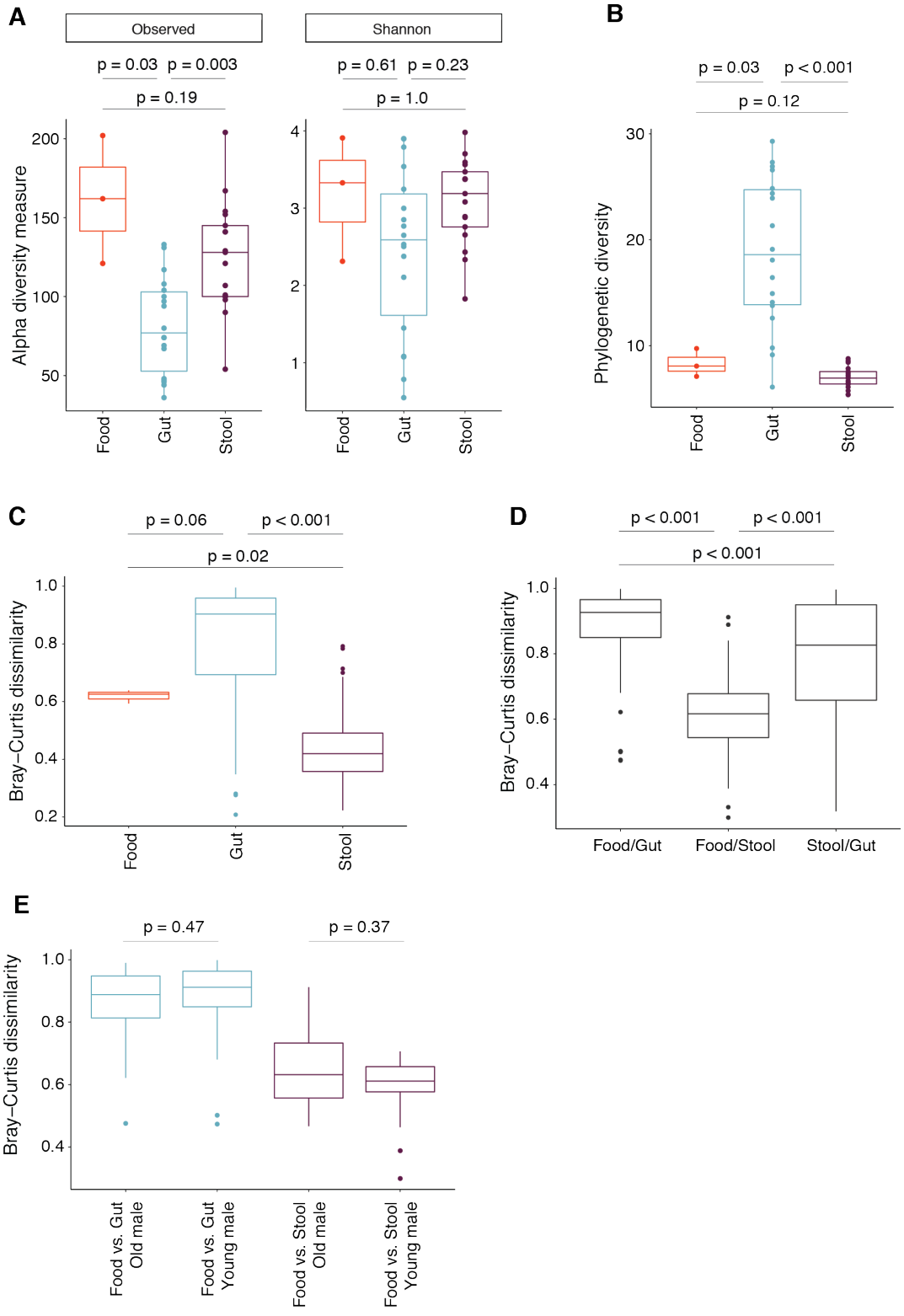

Figure 18: Alpha and beta diversity measures of the different sample types. (A) Observed ESV and Shannon index alpha diversity for gut, stool and food samples. (B) Phylogenetic alpha diversity for gut, stool and food samples. (C) Bray-Curtis dissimilarity values comparing samples within the same sample type for gut, stool and food samples. (D) Bray-Curtis dissimilarity values comparing samples between the sample types for gut, stool and food. For example, Food/Gut shows the dissimilarity values between all food samples

compared to all gut samples. (E) Bray-Curtis dissimilarity values comparing food samples to gut or stool samples, for young and old male fish separately. Gut samples are marked in blue, stool samples are marked in purple and food samples are marked in red. Statistical significance was calculated by a Wilcox-test (Holm-adjusted).

I then assessed beta diversity levels to gain insight into the similarity between the sample types. The diversity within a sample type provides insights into the heterogeneity of the samples, i.e. how similar the samples are to each other within a sample type. As expected from the taxonomic composition, the within diversity levels were higher for gut samples compared to stool and food samples, indicating that intestinal samples are particularly heterogenous in terms of microbiota composition (Fig. 18C).

The “between diversity” estimates the differences between sample types. In this regard, the high values of the food-gut and the stool-gut comparison clearly showed that gut samples are distinct and different in composition compared to food and stool samples (Fig. 18D) (p-values < 0.001, BH-corrected, Dunn Kruskal-Wallis test). The difference in the dissimilarity values was lower between the gut samples and the stool samples compared to the gut samples and the food samples, which indicates that stool samples are more similar to the fish intestinal microbiota than the food. At the same time, food samples were still more similar to the food samples than to the gut samples (Fig. 18D).

As the results from the longitudinal experiment suggested an increasing overlap between food and stool ASVs throughout aging, I next examined the beta diversity levels between food and either stool or gut samples, separately for both the young and the old fish samples. In contrast to my previous findings, beta diversity levels remained stable with advancing age for both stool and gut samples (Fig. 18E, p-values n.s., BH-corrected, Dunn Kruskal-Wallis test), indicating an unchanged similarity to food samples with old age, possibly implying that fish may not lose the capability of selecting specific bacteria from the input microbiota with old age.

2.2.3 Differences in microbiota composition between young and old samples

Previous data from our lab (Smith, Willemsen, Popkes et al., 2017) has shown that the microbiota composition is subject to drastic changes upon aging. Moreover, the results from the longitudinal experiment revealed aging-specific microbiota patterns. I therefore next focused on analyzing the microbiota composition in young and old male killifish gut and stool samples.

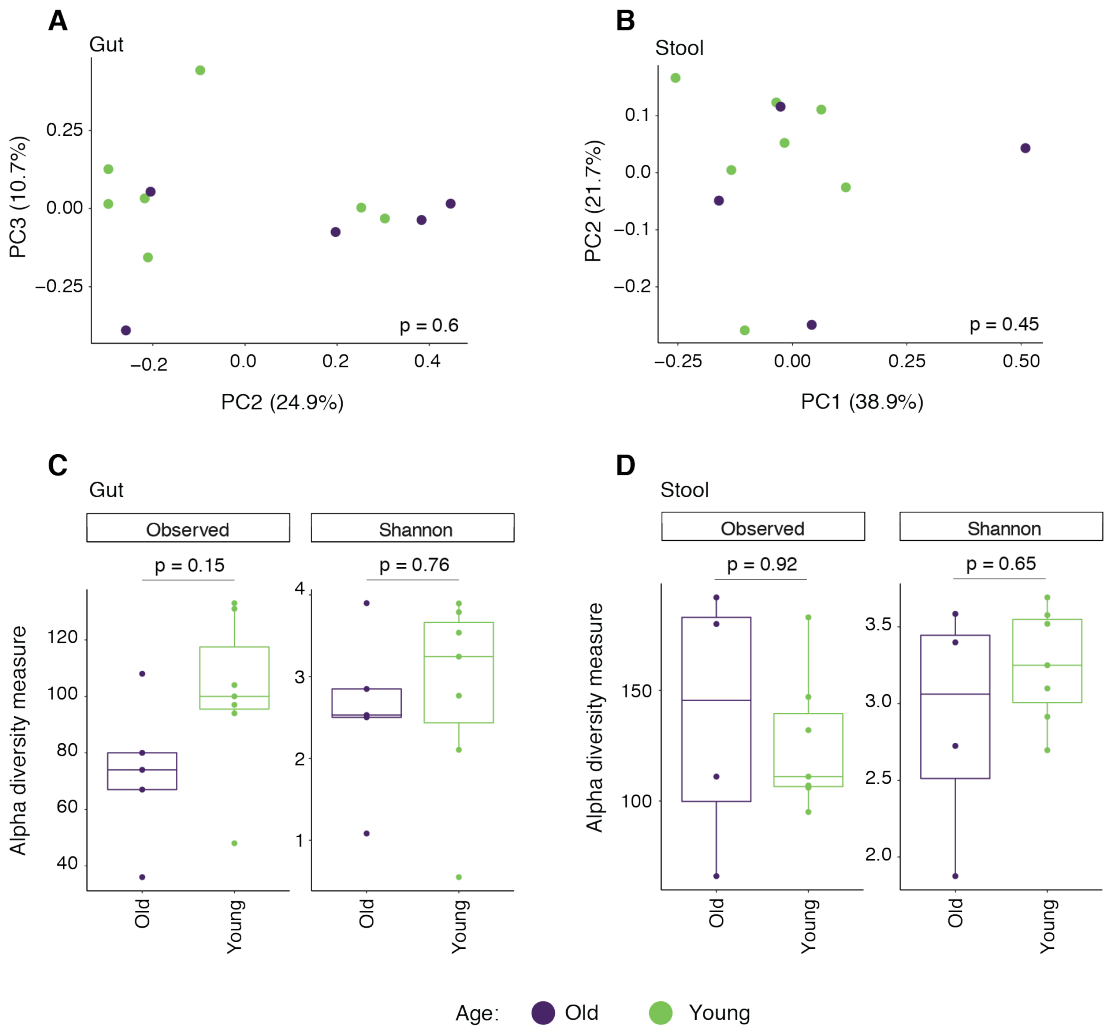

Figure 19: Alpha and beta diversity measures for stool and gut samples during aging. PCoA of Bray-Curtis dissimilarity of (A) young and old gut samples and (B) young and old stool samples. (C) Observed ESV and Shannon index alpha diversity for young and old gut samples and (D) young and old stool samples. Old samples are shown in purple, young samples are shown in green. Statistical significance was calculated by PERMANOVA-analysis (PCoAs) or a Wilcox-test (Holm-adjusted).

I first conducted PCoA based on Bray-Curtis beta diversity to explore the similarity between samples from old and young fish on a global level. Neither stool samples nor intestinal samples showed a clear clustering (Fig. 19A+B). I then assessed alpha diversity levels, as we previously found that diversity in the killifish intestine decreases with age. However, neither the gut nor the stool samples showed a significant decrease in diversity levels for observed ASVs and Shannon diversity measures at these time points (Fig. 19C+D) (p-values n.s., Dunn Kruskal-Wallis test). In addition, also beta diversity levels were equal between samples from young and old fish (data not shown).

I next checked the taxonomic composition of young and old gut and stool samples (Fig. 20A-D). As slight differences were visible between young and old samples, I conducted DESeq2 differential abundance testing to determine the significantly differential abundant bacteria (Fig. 20E). For the gut samples, two *Shewanella* and one *Aeromonas* species were enriched in the old samples, while *Acinetobacter*, two species of *Rhizobiales*, *Caldilineacea* and *Gemmatacea* were significantly more abundant in young intestinal samples. There was no significant difference in composition between young and old stool samples.

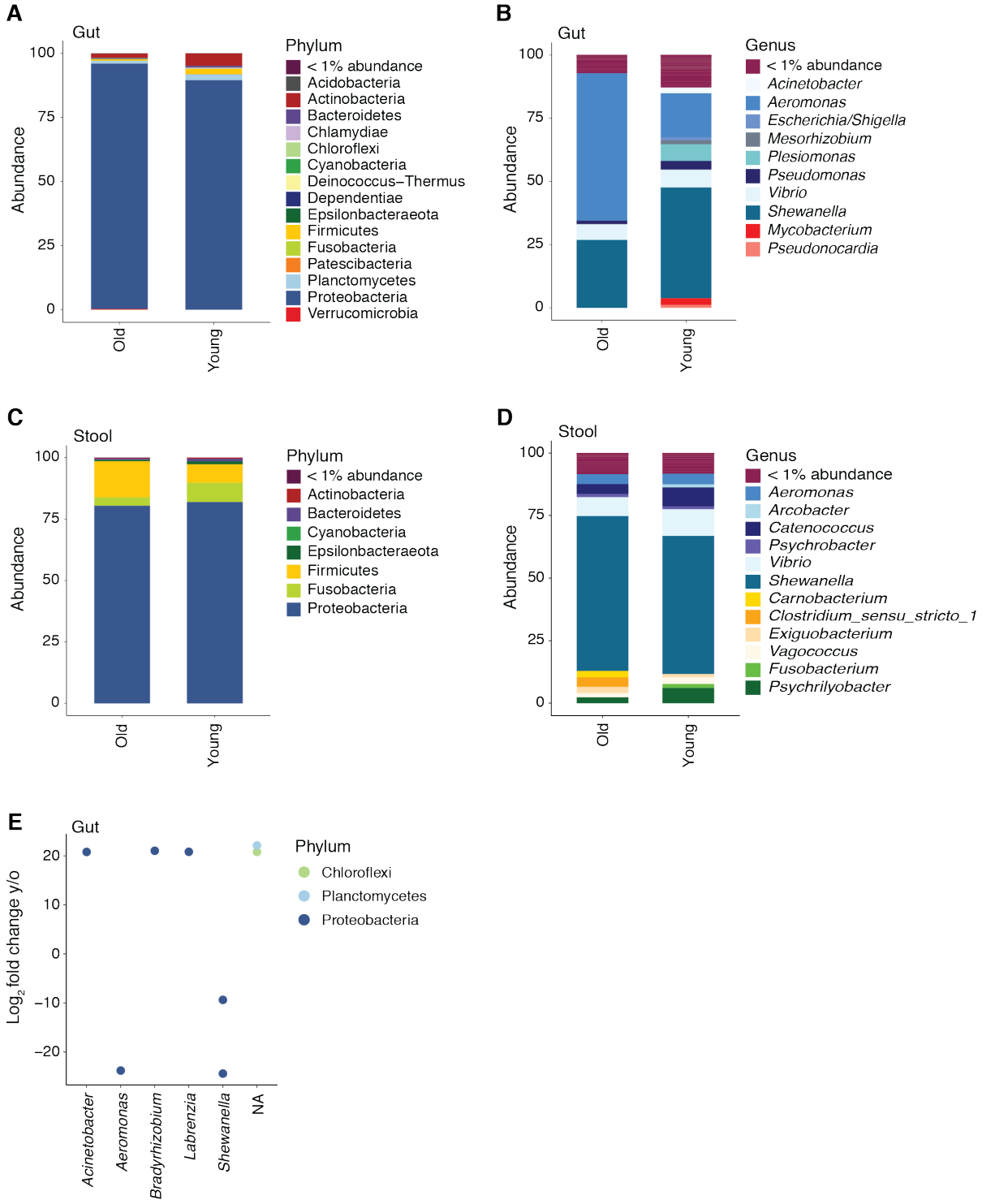

Figure 20: Taxonomic composition of stool and gut samples during aging. Relative abundance of the most prevalent (A) phyla for young and old gut samples, (B) genera for young and old gut samples, (C) phyla for young and old stool samples, (D) genera for young and old stool samples. (E) DESeq2 differential abundance analysis for young and old gut samples.

2.2.4 Microbiota differences between male and female samples

It is known from several other model organisms that sex has a strong influence on the intestinal microbiota composition, thus affecting major physiological processes, including host aging. However, until now it remains an open question whether the killifish intestine shows any sex-specific characteristics. Gaining deeper knowledge on sex-specific microbiota differences in killifish could help to increase our understanding on the physiological relevance of the microbiota in this model organism.

Hence, to gain insight into possible sex-specific microbiota traits, I compared the stool and gut samples in old male and female killifish.

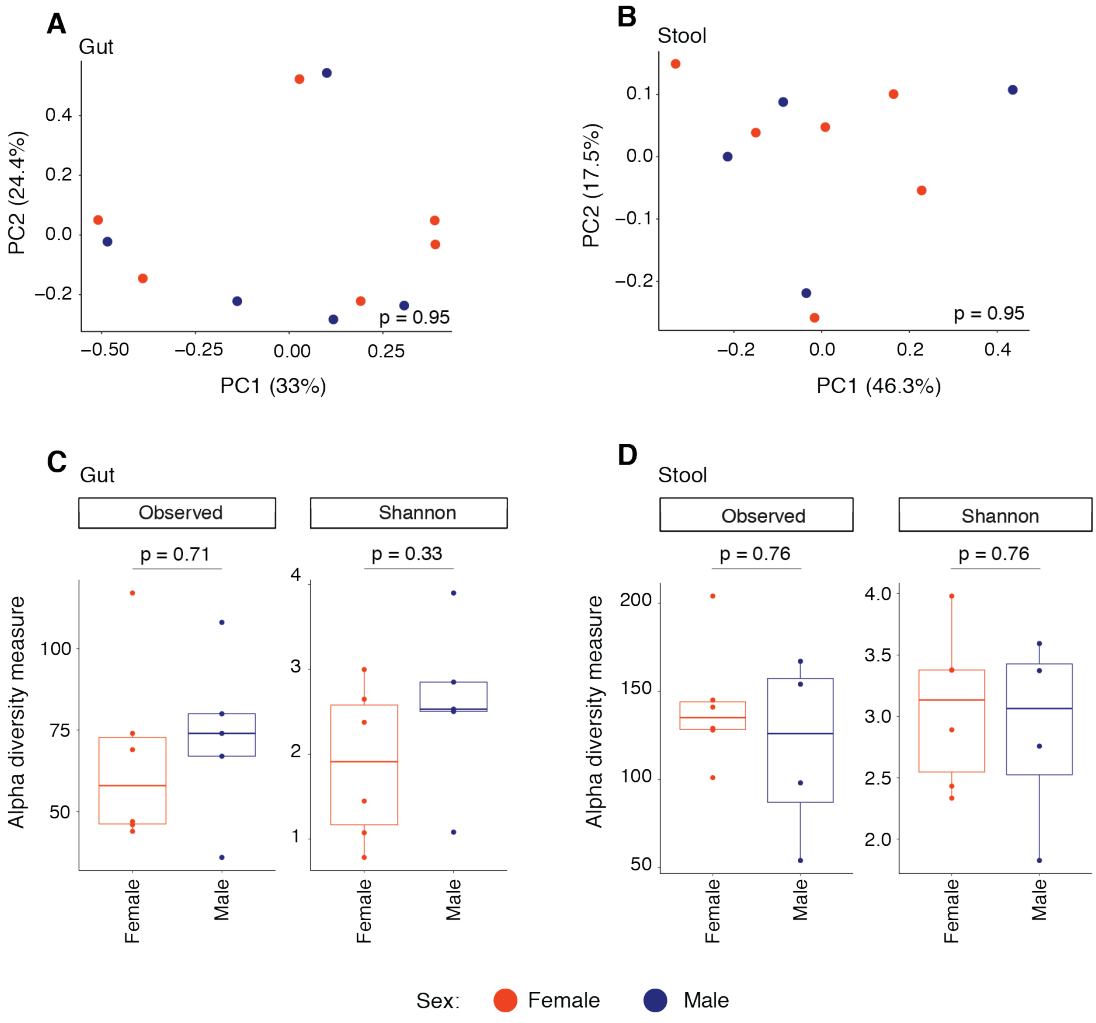

Figure 21: Alpha and beta diversity measures for stool and gut samples between sex. PCoA of Bray-Curtis dissimilarity of (A) male and female gut samples and (B) male and female stool samples. (C) Observed ESV and Shannon index alpha diversity for male and female gut samples and (D) male and female stool samples. Male samples are shown in blue, female samples are shown in red. Statistical significance was calculated by PERMANOVA-analysis (PCoAs) or a Wilcox-test (Holm-adjusted).

To investigate sex-specific changes in killifish, I conducted PCoA based on Bray-Curtis beta diversity levels. No significant clustering was visible for the intestinal or stool samples (Fig. 21A+B). In line with this, also alpha diversity levels were not different between male and female samples for both tissues (Fig. 21C+D), neither were beta diversity levels (data not shown).

Although the samples did not show significant differences on the global level, the analysis of the taxonomic composition suggested specific changes in microbiota composition between male and female gut and stool samples (Fig. 22A-D). Subsequent DESeq2 differential abundance testing revealed small but significant differences in taxonomic composition between males and females (Fig. 22E+F). Female intestinal samples were enriched in a particular *Chloroflexi* and *Shewanella* species, while 2 *Vibrio* and one *Aeromonas* species were highly abundant in male intestines. With regards to the stool samples, females had higher levels of *Chitinibacter* and *Psychrilyobacter*, while male samples were again enriched in two *Aeromonas* species.

In summary, the conducted analyses revealed that killifish stool, intestinal and food samples show clear sample type-specific properties. Intestinal samples showed a high variability between the samples and low diversity levels in terms of species richness and evenness - however, the ASVs present were phylogenetically far away from each other. In terms of microbiota composition, gut samples showed higher levels of Actinobacteria as well as *Aeromonas* and *Mycobacterium*. Stool samples resembled the food microbiota to a great extent – they shared for example Fusobacteria and Epsilonbacteria such as *Psychrilyobacter.* However, stool samples also shared properties with the intestinal samples, such as a large fraction of *Aeromonas* or also specific *Shewanella, Aeromonas* and *Vibrio* species. Stool samples thus have the potential to serve as a proxy for intestinal microbiota composition, at least to some extent. This information is of crucial importance for future experiments when a non-invasive sampling of the microbiota is necessary, such as in lifespan experiments.

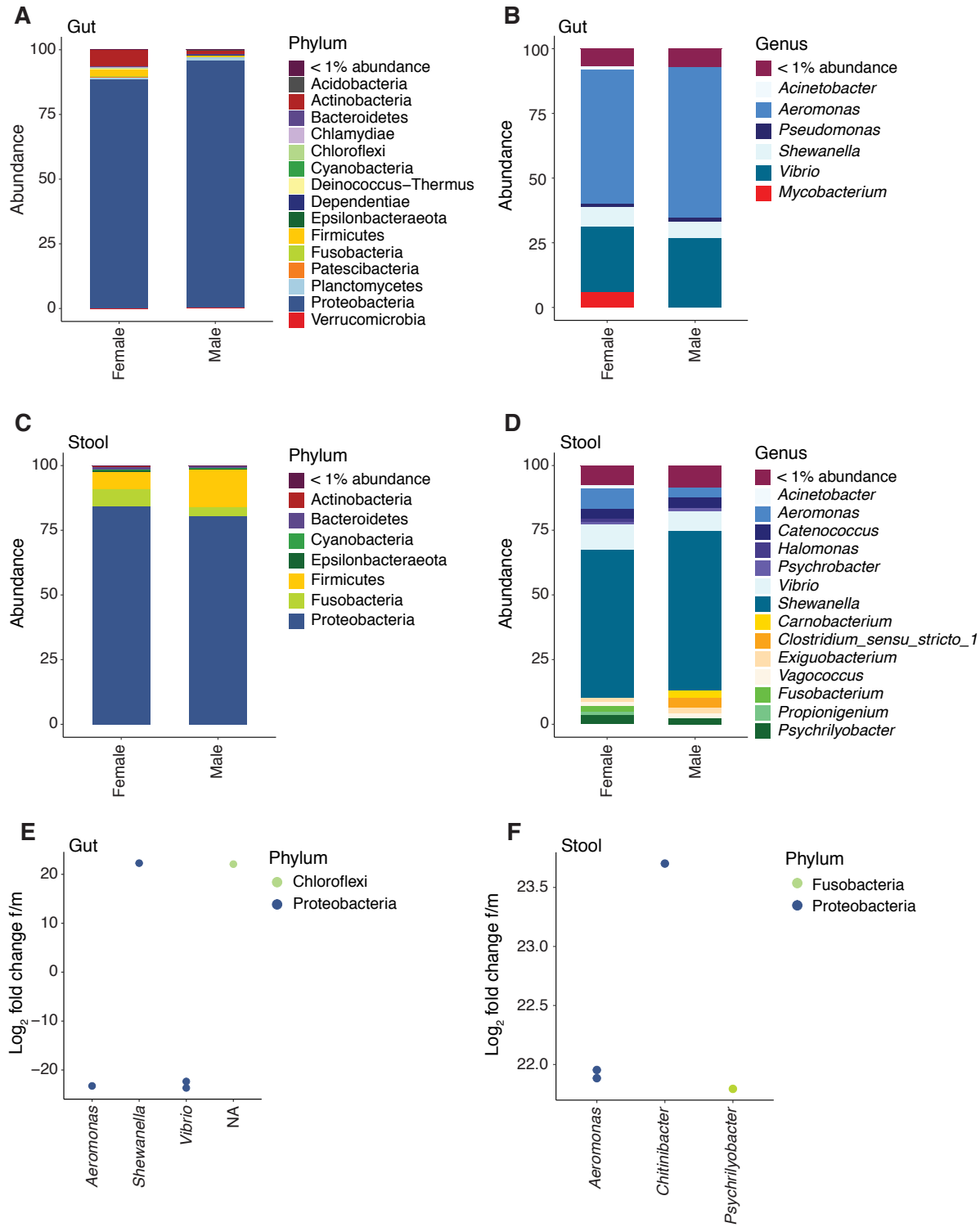

Figure 22: Taxonomic composition of stool and gut samples between sex. Relative abundance of the most prevalent (A) phyla for male and female gut samples, (B) genera for male and female gut samples, (C) phyla for male and female stool samples, (D) genera for male and female stool samples. (E) DESeq2 differential abundance analysis for male and female gut samples and (F) for male and female stool samples.

Although I did not observe sex- and age-differences on a global level, I was able to detect slight changes in microbiota composition between young and old, or male and female samples. It would thus be interesting to evaluate sex- or age-differences with an increased number of samples and to also consider aging phenotypes on the host side.

2.3 Deep multi-omics characterization of killifish intestinal sections

My previous results from part 1 and 2 and previous studies from our group (Smith, Willemsen, Popkes et al., 2017) clearly showed that the microbiota of the killifish intestine is subject to strong changes upon aging. However, a deep understanding of the host side during aging is still lacking. Performing aging experiments on host intestinal tissue and intestinal microbiota could shed light on the question how the intestine ages on both a molecular and microbial level – and could provide first insights into host-microbiota interactions in intestinal killifish aging.

In addition, microbiota-associated anatomical and molecular differences on host side are a well-known phenomenon in organisms of different sex. In line with this, I found slight differences in microbiota composition with regards to different killifish sex (part 2.4). However, it remains unclear whether those sex differences can be found not only on microbiota level, but also on the broader host tissue level. Deepening our knowledge of whether and how the killifish intestinal structure and function is sex-specific – during young and old age – provides pivotal information for designing future experiments and to further strengthen the killifish as an aging model system.

Finally, studies on the killifish intestine so far have been limited to the whole intestine. However, the intestinal tract of most animals is structured into different compartments with unique biological functions. It is therefore of great importance to first investigate whether the expected compartmentalization of the killifish gut is reflected on the molecular and on the microbial level, and second to characterize the intestinal changes in a sex- and age-dependent manner on a molecular and anatomical level.

To address these three open questions, I designed and performed two experiments – on the one hand a proteomics study to identify the killifish sections on a molecular level, and on the other hand a multi-omics experiment comprising proteomic analysis, metabolomic analysis, 16S-sequencing and histological analysis to characterize the age- and sex-differences of the killifish intestinal sections on a deep molecular and micro-anatomical level.

2.3.1 Proteomic analyses to identify intestinal sections in killifish

To determine whether the killifish gut shows differences on the molecular level from anterior to posterior regions, I opted for an unbiased approach and sampled a young killifish intestine for performing proteomic analysis on ten intestinal slices (Fig. 23A). The cutting sites for the slices were chosen based on observable anatomical differences under the binocular stereoscope. The TMT-labelled proteomics analysis was performed by the proteomics facility of the MPI-AGE and resulted in a total amount of 5559 annotated proteins.

I first conducted Principal Component analysis (PCA) on the proteomics data of the ten intestinal slices to analyze the similarity in protein expression. The PCA revealed a clear separation between the posterior slices 9/10 and the anterior slices 1-8 (Fig. 23B). The anterior slices lined up in the expected order along principal component 2, from slice 3 to slice 8. Hierarchical clustering of the ten slices revealed four distinct clusters, suggesting that the killifish intestine is structured into four sections: Section 1 comprised intestinal slice 1 (yellow), section 2 consisted of intestinal slices 2, 3, 4 and 5 (red), section 3 of intestinal slices 6, 7 and 8 (green) and section 4 with intestinal slices 9 and 10 (brown) (Fig. 23C+D). As indicated in the cluster dendrogram, section 1 and 2 were most similar in their protein expression patterns, followed by section 3. The posterior section 4 is the most distinct section with regards to expressed proteins.

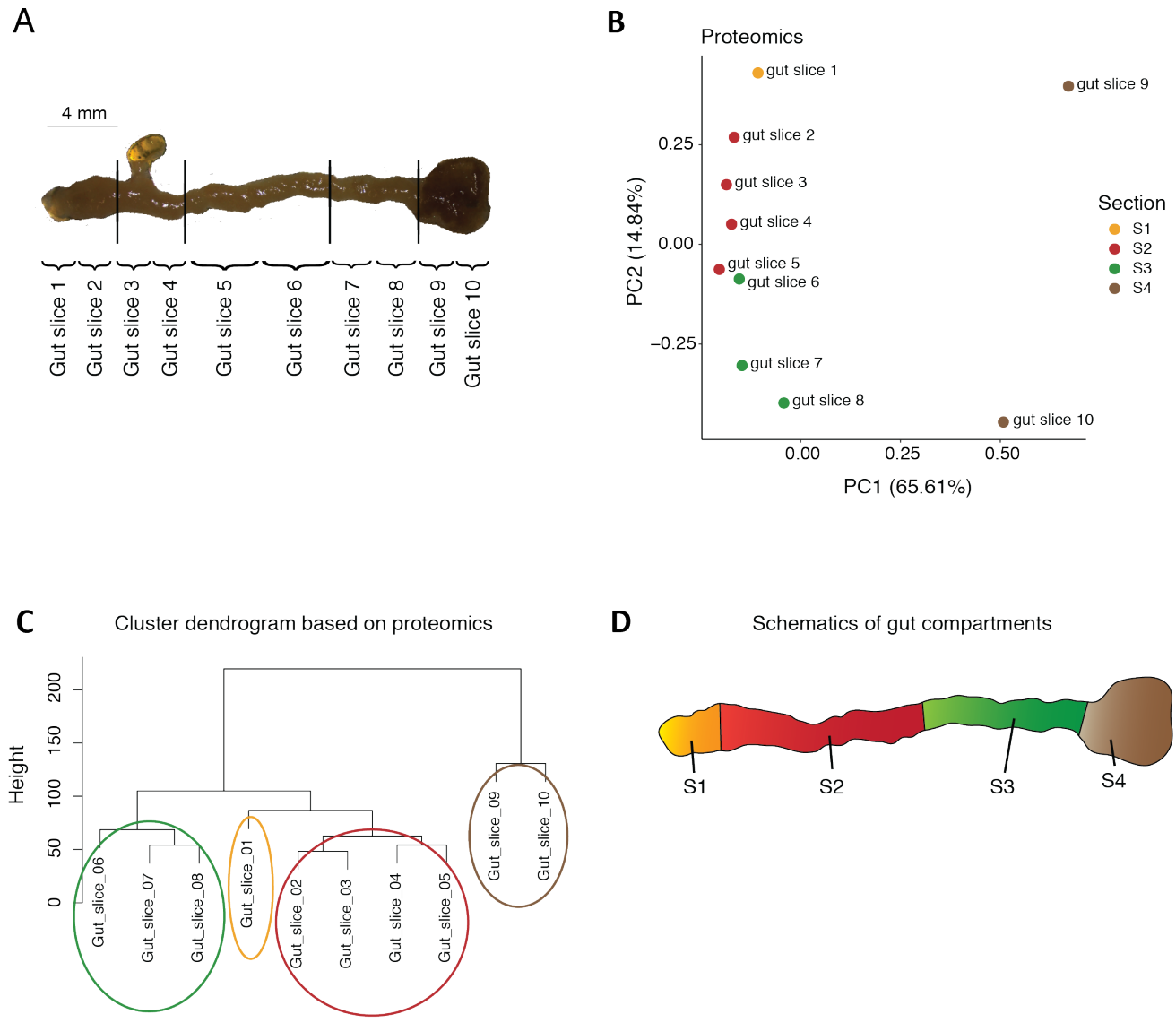

Figure 23: Proteomic analysis of 10 intestinal slices. (A) Overview about the 10 killifish gut slices. The black lines indicate strong anatomical structural differences. (B) PCA of the proteomics run of the 10 gut slices. Samples are colored for the resulting sections. (C) Dendrogram based on similarity of protein expression patterns. The four resulting clusters are marked with colored circles. (D) Schematic of the killifish intestine with the resulting four intestinal sections (S1-S4).

2.3.2 Setup and experimental approach of the multi-omics intestinal experiment

To characterize the resulting four intestinal sections on a deeper molecular level, to identify sex differences in intestinal killifish aging and to furthermore identify

correlations between microbiota and host intestinal aging, I collected intestinal sections of young (8-week-old) and old (16-week-old), male and female turquoise killifish along with respective stool and food control samples (Fig. 24). I then extracted DNA, protein and both polar and non-polar metabolites of the same, individual section samples to generate a multi-omics dataset. Distinct subgroups of metabolites were measured on different columns. The pHILIC column binds hydrophilic (polar) metabolites, while the C18 column retains lipophilic (non-polar) metabolites. Ion chromatography (IC) allows for measurement of specific ions like metabolites from glycolysis, the TCA cycle or the pentose phosphate pathway. Derivatization of metabolites with benzoyl chloride (BZ) allows detection of amines, like amino acids. The polar metabolites were processed and run in both targeted (BZ and IC datasets) and untargeted mode (pHILIC, BZ and IC datasets) while the non-polar metabolites were run in an untargeted mode (C18 dataset). The untargeted runs were further analyzed in both a positive and negative mode, allowing to analyze positively and negatively charged metabolites separately.
Targeted datasets include a previously defined library of labeled metabolites and thus allow for confident annotation of those metabolites. The untargeted metabolomics analysis allows for the quantification of a large number of metabolites. However, the major fraction of the metabolites remains unidentified. The section, food and stool DNA was used for V3/V4 16S rRNA amplicon sequencing to obtain information about the microbiota composition of the intestinal and the control samples. Due to limitations in the number of possibly measured samples, a subset of samples was split in two separately measured groups for the proteomics analysis.

To evaluate possible differences on the micro-anatomical level, I moreover cut a tissue piece adjacent to each section and stored it in PFA for histological experiments.

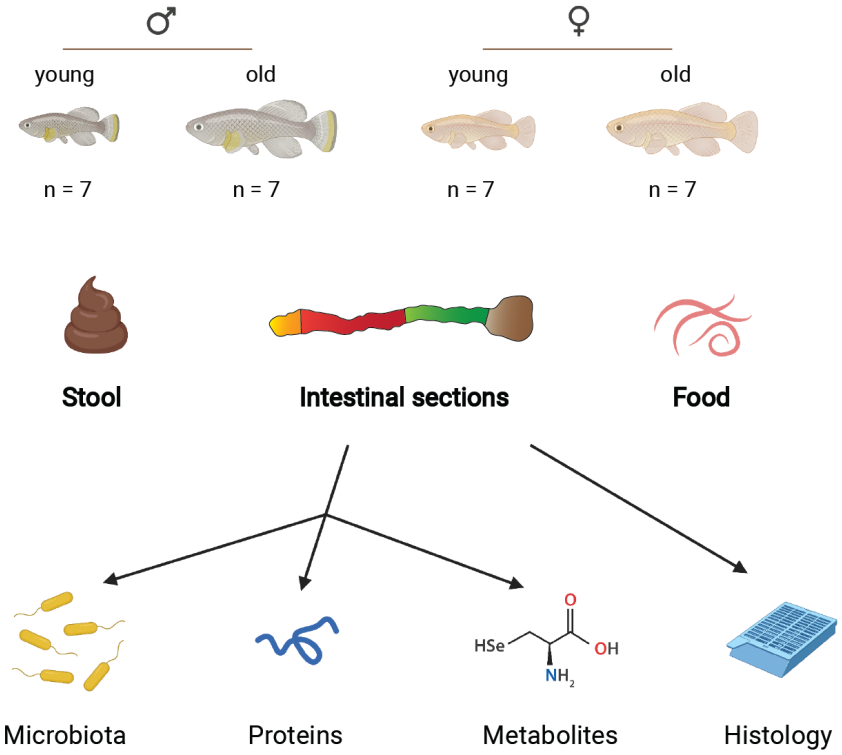

Figure 24: Experimental setup of the multi-omics experiment. Intestinal sections were collected for young and old, male and female killifish. The sections were subject to a multi-omics extraction protocol designed to analyze microbiota, protein and metabolite levels. Metabolite levels were assessed in a targeted and untargeted manner. A part of the intestinal sections was stored for histology experiments. Food and corresponding stool samples were collected as controls.

2.3.3 Intestinal sections of the killifish

2.3.3.1 Molecular characteristics

To gain a clear picture about the molecular profiles of the different sections, I first simultaneously extracted proteins and metabolites from the intestinal sections and performed metabolomics and proteomics measurements.

The 2 proteomic runs resulted in 4496 and 6723 annotated proteins.

The targeted and untargeted metabolomic runs resulted in the number of metabolites presented in Table 1.

Table 1: Metabolites detected in the metabolomic analysis

Metabolomics method	Total metabolites detected	Identified metabolites
C18, positive mode	5350 metabolites	157 metabolites
C18, negative mode	2054 metabolites	28 metabolites
BZ	420 metabolites	44 metabolites
IC	538 metabolites	27 metabolites
pHILIC, positive mode	1003 metabolites	-
pHILIC, negative mode	1321 metabolites	-

The PCA on all the untargeted metabolomic datasets revealed a clear clustering of the four different sections, with a strong separation between the anterior sections 1, 2, 3 and the posterior section 4 (Fig. 25A–E). I next investigated the subsets of annotated, known metabolites as this could give insight into which metabolites are driving the detected section-specific pattern. PCA on the annotated metabolites from the C18 datasets resulted in two contrasting results: While the annotated lipids from the positive-mode C18 dataset (Fig. 25F) showed a highly similar pattern to the respective untargeted C18 dataset (Fig. 25A), the negative annotated lipids (Fig. 25G) were not clustering in a section-specific manner. This suggests that the known positively charged lipids (including DAGs, TAGs, PCs, PEs and SMs) contribute strongly to the section differences, while the known negatively charged lipids (FFAs and PGs) play a minor role.

On the side of the polar metabolites, PCA on the targeted BZ dataset (which includes mainly amino acids) showed a similar but weaker clustering pattern as the untargeted BZ dataset (Fig. 25H). This indicates that amino acids levels are indeed different between the sections; however, unknown polar metabolites play a main role in driving the differences between the sections.

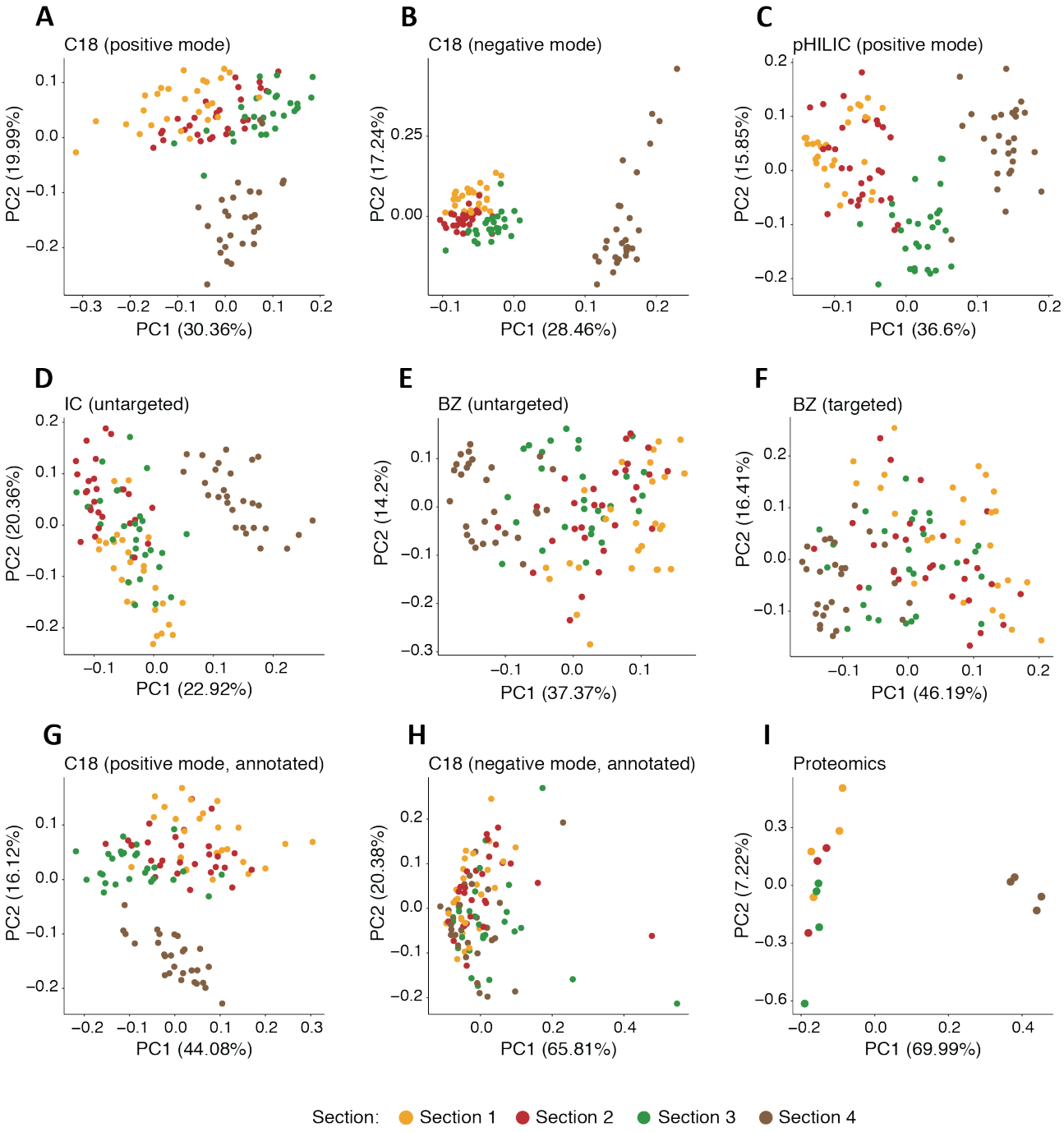

Figure 25: PCA of metabolomic and proteomic datasets. PCA on the metabolomic datasets for (A) positive lipids, (B) negative lipids, (C) positive polar metabolites, (D) untargeted IC run, (E) untargeted BZ run, (F) targeted BZ run, (G) annotated positive lipids and (H) annotated negative lipids. (I) PCA of the proteomic dataset. Samples are colored by section, with section 1 marked in yellow, section 2 marked in red, section 3 marked in green and section 4 marked in brown.

In line with the previously observed section differences on proteomic level (2.3.1), the four sections also revealed distinct clustering profiles in the second proteomic dataset (Fig. 25I). A particular strong separation was observed between the anterior part (sections 1, 2 and 3) and the posterior part (section 4). It is important to note that only samples from old fish were used in this analysis due to the small size of the young fish intestines.

After this initial clustering analysis, I sought to identify the main driver metabolites responsible for the separation of the different sections. To this end, I performed supervised methods (PLS-DA and RF classification) on all the metabolomic datasets (Fig. 26A+B, displaying the positive C18 data as an example) and screened the main metabolites contributing to the models (Top 10%). The RF classification resulted in an overall error rate of 0.08, (error rate for the single sections: section 1 = 0.15; section 2 = 0.07; section 3 = 0.1; section 4 = 0.0). Such a low overall error rate implies a good classification of the single sections, while especially section 4 is classified correctly in all cases.
The most important metabolites included mainly uncharacterized metabolites, but also some annotated, known metabolites. Betaine levels increased along the intestinal tract (Fig. 26C), whereas Glutamine levels were particularly high in the posterior section 4 (Fig. 26D). In contrast, both primary and secondary bile acids showed a decrease in abundance from the anterior to the posterior intestinal sections (Fig. 26E+F).

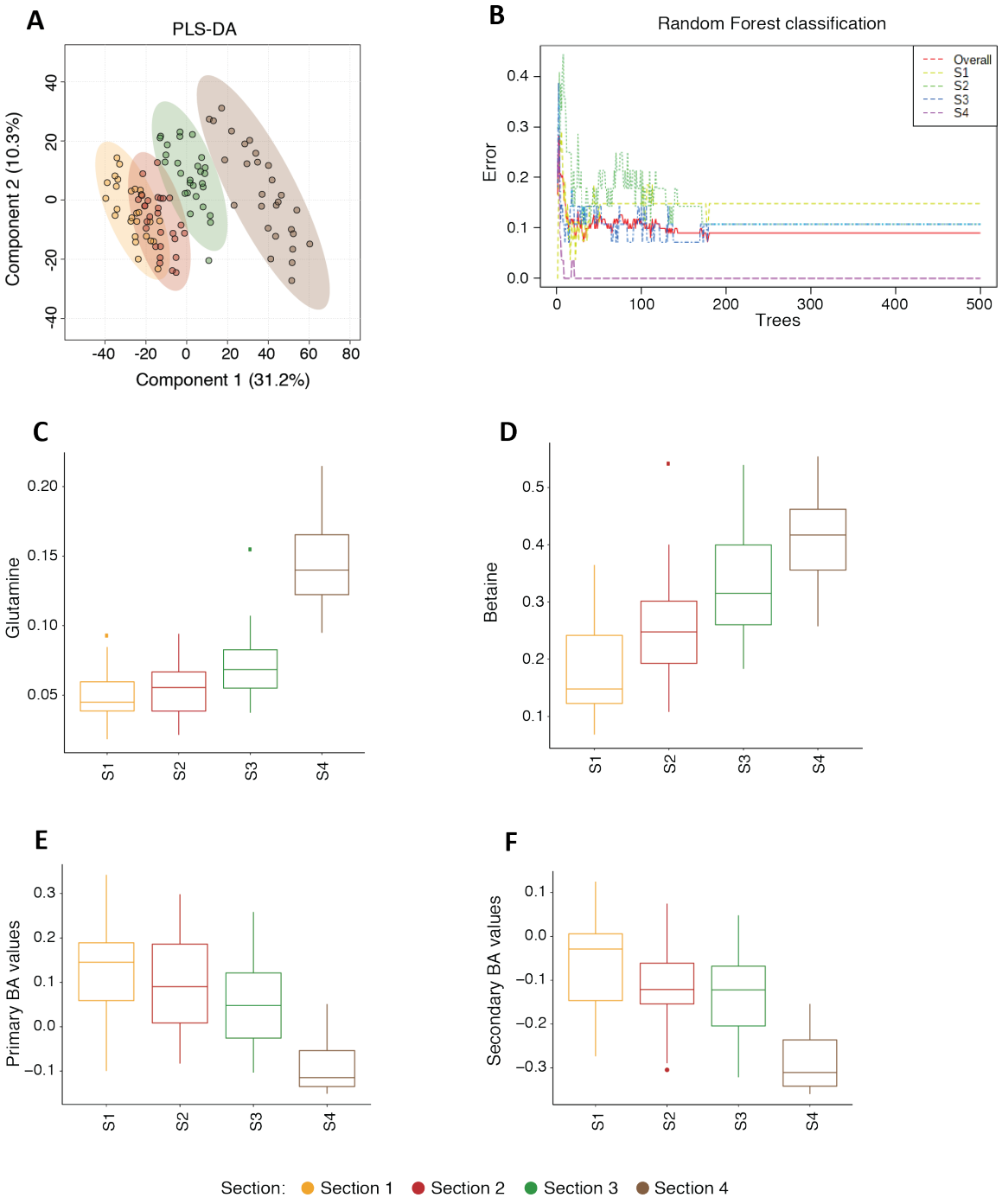

Figure 26: Section-specific metabolites. (A) PLS-DA on the positive lipids metabolomic dataset. (B) Error rates of the Random Forest classification on the positive lipids metabolomic dataset. (C) Annotated metabolites contributing to the top 10% of the section-specific classification models. Samples are grouped and colored by the respective section, with section 1 marked in yellow, section 2 marked in red, section 3 marked in green and section 4 marked in brown.

I next set out to determine the proteins characterizing the anterior or posterior sections. For this, I grouped sections 1, 2 and 3 and had a closer look at the differentially expressed proteins between the anterior and posterior sections (Fig. 27A). It is again important to note that this proteomics dataset is based on section samples from old fish. Proteins with high abundance in the anterior section included PCK2 and FABP2, while CUBN, DPEP1 and FABP6 were present in high levels for the posterior section samples.

As region-specific differential protein expression is well known in the intestines of many model organisms, I furthermore checked whether the significantly changing proteins have been reported in other animal models. To this end, I screened the literature and collected a list of section-specific genes from zebrafish and mouse intestines (Lickwar et al., 2017; Z. Wang et al., 2010). Noteworthy, several of the most significant changing proteins overlap with this list, indicating a conservation of intestinal gene expression patterns (Fig. 27B).

So far, I focused on individual metabolites and proteins. To further assess which biological processes characterize the different sections, I performed gene ontology and pathway enrichment analysis of the significant proteins for the anterior and the posterior sections (adj. p-value <0.05). The anterior sections were characterized by translation-related terms as well as metabolic and catabolic processes, such as *ribosomal subunit, peptide biosynthetic process* or *RNA catabolic process* (Fig. 28A+B). In comparison, the posterior part was characterized by terms associated with uptake, transport and lytic processes, such as *lysosomal membrane*, *vacuolar transport* and *vesicle-mediated transport* (Fig. 28C+D).

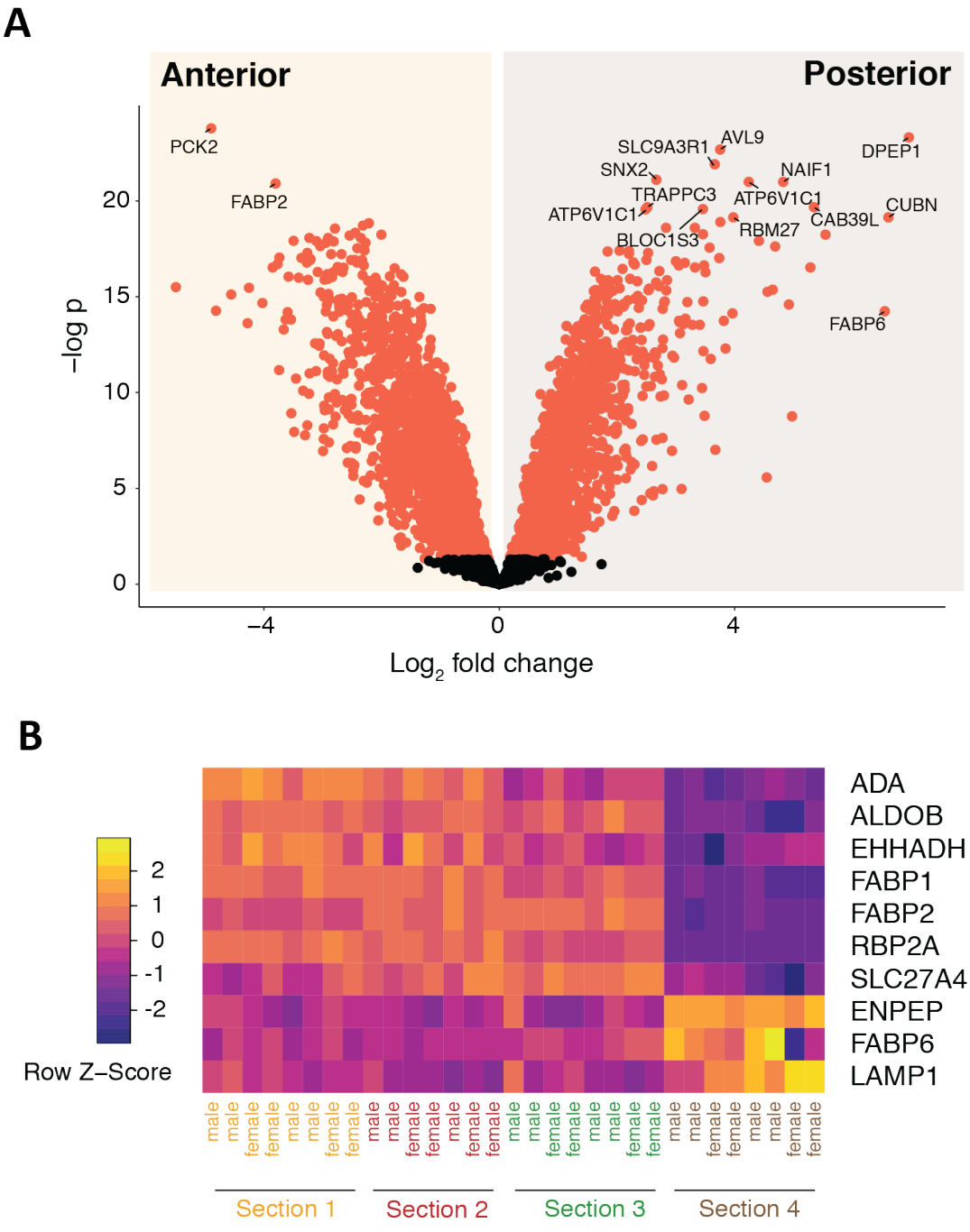

Figure 27: Section-specific proteins. (A) Volcano plot showing differences on protein level between anterior (S1/2/3) and posterior (S4) sections. Red color indicates proteins with a BH-adjusted p-value <0.01 (moderated t-test). (B) Heatmap of conserved section-specific proteins. Yellow color indicates high expression levels, purple color indicates low expression levels.

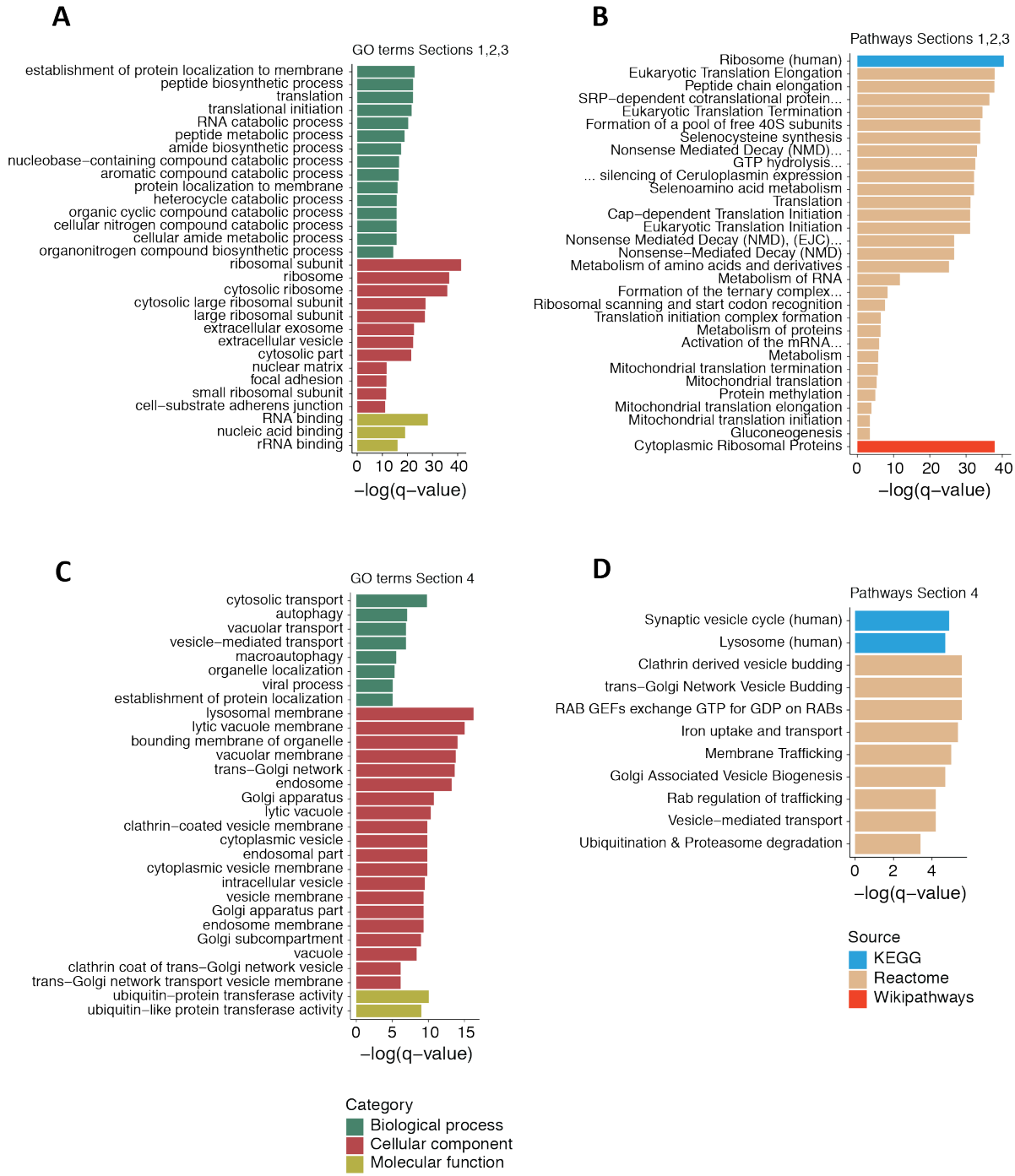

Figure 28: GO term and pathway enrichment analysis of the sections. (A) Top gene ontology terms (Top 30) of proteins highly expressed in the anterior sections (S1/2/3). (B) Top pathway enrichment terms (q-value <= 0.1) of proteins highly expressed in the anterior sections (S1/2/3). (C) Top gene ontology terms (Top 30) of proteins highly expressed in the posterior (S4) section. (D) Top pathway enrichment terms (q-value <= 0.1) of proteins highly expressed in the posterior (S4) section. The negative natural logarithm of the q-values is shown. Statistical significance was calculated by a hypergeometric test.

2.3.3.2 Histological analyses

I next investigated whether the clear molecular differences I detected between the sections also reflect on a micro-anatomical scale. For this, Quinn Quesenberry (a bachelor student I supervised) conducted two histological staining experiments on a subset of the intestinal sections – a qualitative Hematoxylin-Eosin (H&E) staining and a quantitative Sirius Red – Fast Green staining (SRFG).

The H&E staining allowed for detailed insights into the micro-anatomy of the intestinal sections. As there were no apparent differences between the anterior sections 1, 2 and 3, those sections were grouped together and the statistical analysis was conducted for the comparison between the anterior (S1, S2, S3 – Fig. 29A) and posterior (S4 – Fig. 29B) sections.

We first analyzed the overall structure of the killifish intestine. Like many other teleost fish, the intestine of *N. furzeri* did not show crypt- and villi-like structures - in contrast, several “primary folds” were visible in all four sections (Figure 29A+B). The gut epithelial layer consisted of several different cell types, including enterocytes and goblet cells. The *lamina propria* separated the epithelial layer from the *submucosa* and the adjacent *muscularis propria,* which consisted of both circular and longitudinal muscle fibers. Due to the sampling procedure, the posterior sections 4 were not cut as a cross-section, resulting in the intestinal folds projecting to the outside. All parameters (except for total diameter) could still be assessed in this orientation of the posterior section.

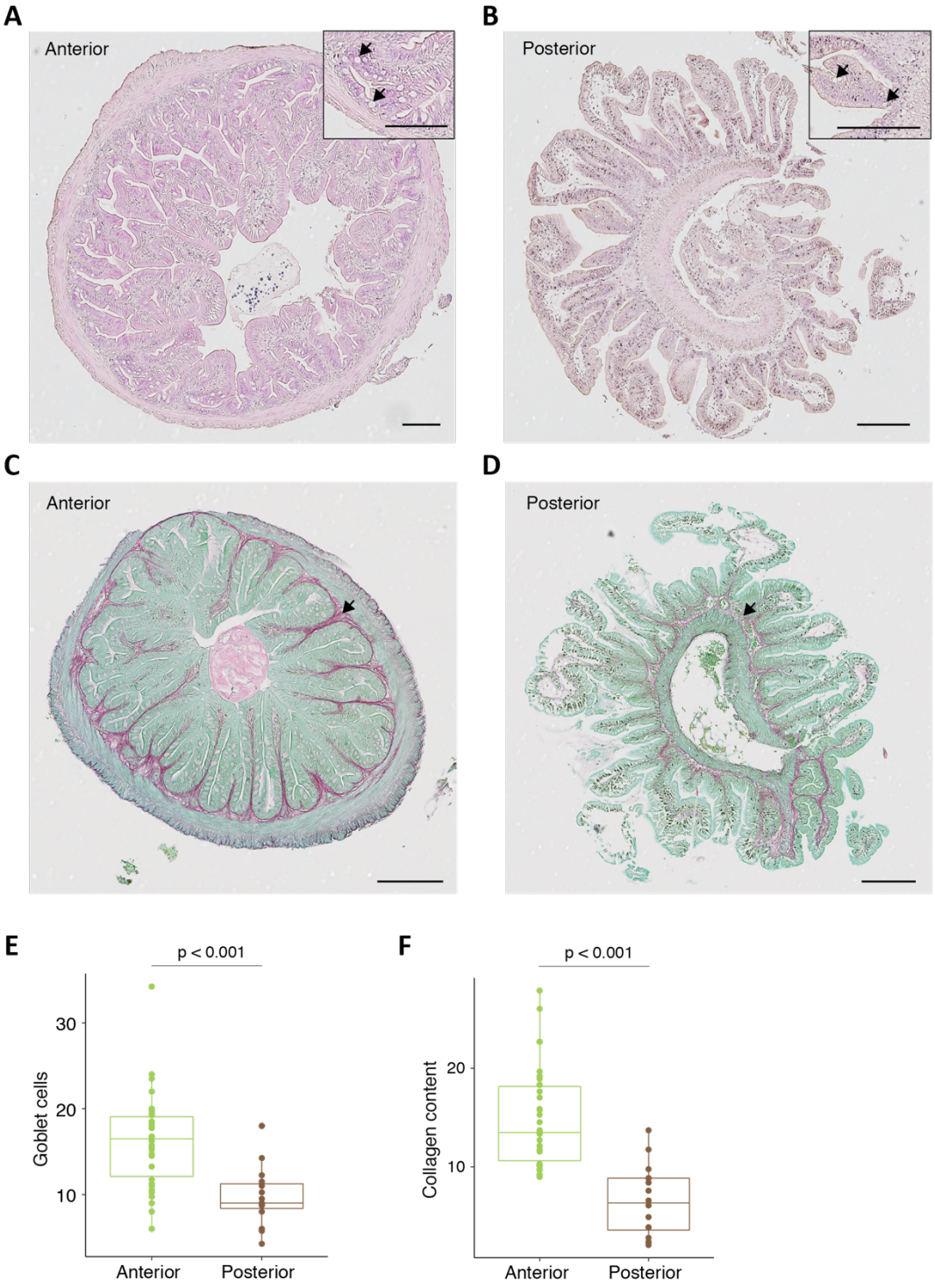

Figure 29: Histological staining of anterior and posterior sections. (A) H&E staining of the anterior and (B) posterior section of the killifish intestine. Cell nuclei are stained in blue, other structures including the cytoplasm are stained in pink. The arrows mark goblet cells. (C) SRFG staining of the anterior and (D) posterior section. Collagen fibers are stained in red, non-collagenous proteins are stained in green. The arrows mark collagen. (E) Quantification of the intestinal goblet cells. (F) Quantification of the intestinal collagen content. Samples are colored by sections, with light green marking the anterior sections (S1/S2/S3) and brown

marking the posterior section (S4). The scale bars mark 100μm. Statistical significance was calculated by a Wilcox-test (Holm-adjusted).

The H&E staining enables to measure the thickness of the *muscularis propria* layer. No difference in muscular thickness was detectable between the anterior and posterior sections (data not shown). A histological staining with H&E moreover allows the discrimination between specific cell subtypes. Quinn analyzed the histological slides for the occurrence of goblet cells and infiltration of leukocytes. The mucus produced by goblet cells plays a key role in the function of the intestinal barrier, protecting the epithelial layer from microbes and digestive enzymes. Leukocyte infiltration is analyzed as an inflammation marker. While both the extent and the severity of leukocyte infiltration did not obviously differ among sections (data not shown), the number of goblet cells was significantly higher in the anterior sections compared to the posterior section (Fig. 29E) (p-value <0.001, Wilcox-test). This suggests that the anterior sections are in higher demand of protective mucus, possibly related to a high level of digestion.

Fibrotic changes in the extracellular matrix are a common feature of aged tissues (Murtha et al., 2019). Quinn therefore used the SRFG staining to quantify the collagen content in the extracellular matrix (Fig. 29C+D) to investigate the matrix structure and potential fibrotic changes. Interestingly, the anterior sections showed a significantly higher amount of collagen compared to the posterior section 4 (Fig. 29F) (p-value <0.001, Wilcox-test), indicating a difference in tissue structure (strength & elasticity).

2.3.3.3 Microbiota composition along the intestinal sections

The metabolomic, proteomic and histological data clearly revealed that the four intestinal sections display differences at the molecular and micro-anatomical level. However, the killifish intestine is home to a complex gut microbiota and host-microbiota interactions are important for various physiological processes. I therefore investigated whether the killifish intestine has section-specific microbial communities.

To assess the microbiota composition of the intestinal sections, I extracted DNA from the intestinal sections in a multi-omics manner, e.g., the same tissue pieces that were used for the metabolomics and proteomics dataset, and performed V3/V4 16S rRNA amplicon sequencing. In addition, DNA from stool and food samples was isolated and sequenced as controls. The sequencing of the samples resulted in 2.75 million paired-end reads, with an average of 20.000 reads per sample after quality filtering.

I first focused on the microbiota profiles of the different sample types (stool, intestinal sections and the food samples). The distribution of the most important phyla was similar to the sample-type specific patterns observed in my previous results of thesis part 2: The sample types showed a distinct pattern with food samples enriched in Epsilonbacteria and Fusobacteria, while Actinobacteria were specific for intestinal samples (Fig. 30). The stool samples showed features of both the intestinal and the food samples, with an enrichment in Fusobacteria but also the presence of a major fraction of Firmicutes, comparable to the intestinal sample composition.
As the major aim of the multi-omics datasets lies in the deep analysis of the killifish intestinal sections, I will from now on focus the microbiota analysis only on the intestinal sections.

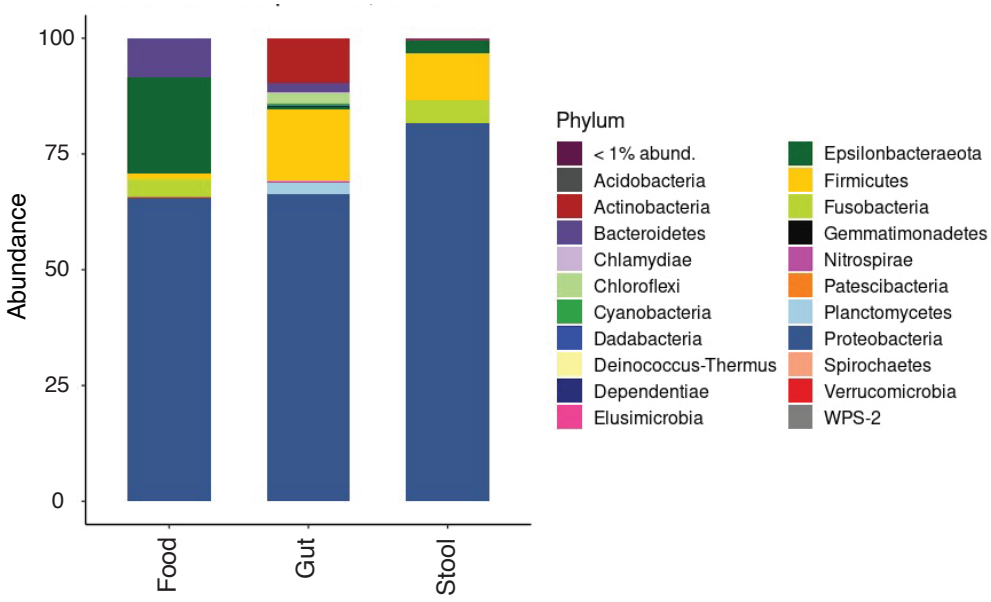

Figure 30: Taxonomic composition of different sample types. Relative abundance of the most prevalent phyla for food, section and stool samples.

I identified 26 phyla in the intestinal sections, of which 13 had an abundance of >0.1%. The 5 most abundant phyla were Proteobacteria, Firmicutes, Actinobacteria, Planctomycetes and Chloroflexi. I identified 466 genera, with 79 genera showing an abundance of >0.1%. The 5 most abundant genera were *Aeromonas*, *Vibrio*, *Catenococcus*, *Vagococcus* and *Pseudomonas*. On the lowest taxonomic level, 2703 ASVs were identified, with 159 ASVs of >0.1% abundance.

To investigate the similarities between all the section samples, I first conducted PCoA based on Bray-Curtis beta diversity levels. Interestingly, the samples did not cluster by section (Fig. 31A). In addition, alpha and beta diversity measures showed no difference between the different sections (Fig. 31B and data not shown).

To further explore potential microbiota differences between the sections, Sam Kean performed a Random Forest classification for the intestinal sections. The classification resulted in an overall accuracy rate of 0.375, which indicates low predictive power (Fig. 31C). Interestingly, the prediction accuracy was differing between the specific sections – while section 1 and 2 had very low classification rates (0.16 and 0), section 3 showed better prediction rates (0.5) and section 4 was classified with high accuracy (0.83). This might indicate that the microbiota composition of section 4 is more section-specific compared to the anterior sections – confirming the strong separation between the anterior and posterior intestine in the metabolomics and proteomics data.

Although the Random Forest classification suggested section-specific microbial patterns for the anterior-posterior sections, I asked to which extent the individuality aspect plays a role for microbiota composition. To this end, I performed PERMANOVA analysis on the Bray-Curtis dissimilarity PCoA and found significant clustering by individual fish ID (p-value < 0.001, Fig. 31D). I observed a similar clustering in a hierarchical clustering approach (Fig. 31E).

Overall, these results indicate that each fish has a unique microbial signature that persists across gut sections, and individuality is a stronger contributor compared to section-specific microbiota patterns.

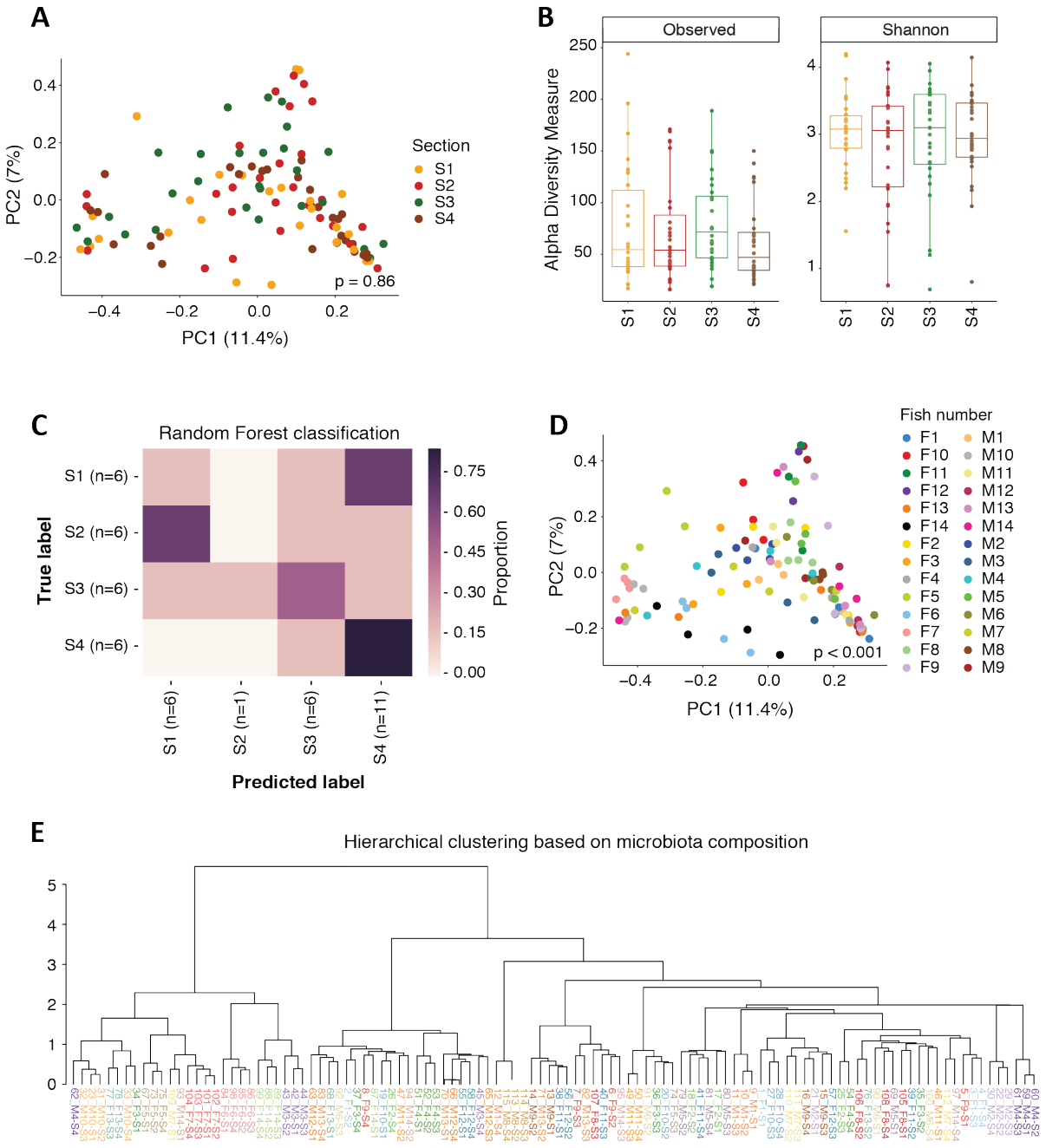

Figure 31: Analysis of microbiota composition of intestinal sections. (A) PCoA of Bray-Curtis dissimilarity of the samples from the intestinal sections. Samples are colored by section, with S1 marked in yellow, S2 marked in red, S3 marked in green and S4 marked in brown. P-value = 0.86, PERMANOVA analysis. (B) Observed ESV and Shannon index alpha diversity for intestinal sections. Samples are colored by section, with S1 marked in yellow, S2 marked in red, S3 marked in green and S4 marked in brown. All p-values > 0.5, Wilcox-test (Holm-adjusted). (C) Random Forest classification accuracy for intestinal sections. (D) PCoA of Bray-Curtis dissimilarity of the samples from the intestinal sections. Samples are colored by individual fish ID. P-value <0.001, PERMANOVA analysis. (E) Hierarchical clustering of the intestinal sections based on microbiota composition. Samples are colored by individual fish ID.

In summary, the four sections of the killifish intestine displayed clear differences on the molecular and microanatomical level, with strongest differences between the three anterior sections (S1-3) and the posterior section (S4). The anterior sections were characterized by processes such as translation, metabolism and catabolism, while the posterior section was characterized by transport, uptake und lytic processes. Bile acid levels decreased along the intestinal tract, suggestion constant reabsorption along the sections. On the microanatomical level, anterior sections were characterized by an increased collagen content and a higher number of mucus-producing goblet cells. Unexpectedly, these molecular differences were not mirrored on microbiota level – slight changes were present between the anterior sections (S1/2/3) and the posterior section (S4), but the microbiota composition was mainly individual-specific, indicating that the individuality of each fish's gut microbiome is the strongest factor.

2.3.4 Intestinal age differences on multi-omics level

My previous results showed age-specific changes in the killifish intestinal microbiota, including a shift in microbiota composition (Smith, Willemsen, Popkes et al., 2017; paragraph 2.2.3). However, understanding the intestinal age-related changes on the host side could provide valuable insight into host-microbiota interactions upon aging. I therefore next sought to analyze the killifish intestinal sections on a deeper level, combining molecular and micro-anatomical analyses on the fish host with an analysis of the microbiota composition during aging.

2.3.4.1 Molecular characteristics

After analyzing the metabolomic and proteomic datasets for section-specific signatures, I next grouped the samples by age and checked for molecular signatures between intestines from young and old individuals.

PCA on all the untargeted metabolomics datasets revealed a clear clustering for age, suggesting differences between young and old age in all metabolite classes including polar and non-polar metabolites (Fig. 32A-E). The clustering was in most cases apparent on lower principal components - one exception was the untargeted IC dataset, where the age clustering was apparent on principal component 2. While most

of the metabolites were uncharacterized, the analysis of the identified metabolite subset could provide insights into the underlying aging processes. Interestingly, the annotated positive lipids clustered strongly in the PCA, comparable to the clustering of the whole C18 dataset in positive mode (Fig. 32F). This indicates that the known positive lipids (TAGs, DAGs, SMs, PCs, PEs) have a substantial influence on the age differences in metabolomic composition. The annotated BZ metabolites, which include mainly amino acids, also clustered for age in the PCA (Fig. 32G), implying that intestinal amino acid levels change upon aging. No comparable strong clustering for age was visible for the other annotated metabolomics datasets (Fig. 32H, negative C18 data as an example).

Similar to the metabolomics data, PCA of the proteomics data clearly distinguished between samples according to age. It is important to note that the analyzed proteomics dataset only contained samples from section 2, as only this section had sufficient tissue material in young fish. As with the metabolomics datasets, the clustering was apparent on lower levels (principal component 2 and 3), indicating that age has an important but less strong effect than section identity (Fig. 32I).

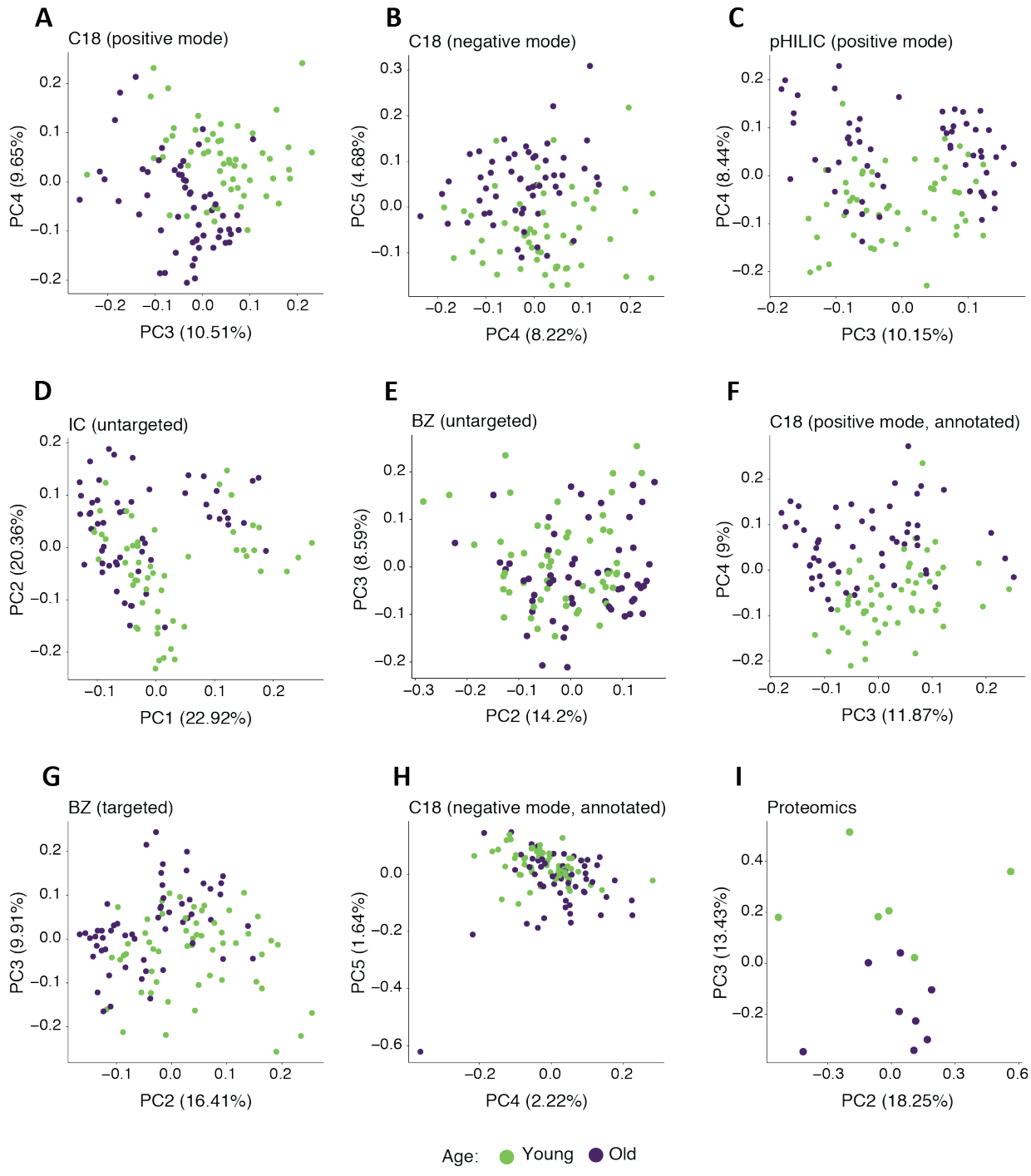

Figure 32: PCA of metabolomic and proteomic datasets for age differences. PCA on the metabolomic datasets for (A) positive lipids, (B) negative lipids, (C) positive polar metabolites, (D) untargeted IC run, (E) untargeted BZ run, (F) annotated positive lipids, (G) targeted BZ run and (H) annotated negative lipids. (I) PCA of the proteomic dataset. Samples are colored by age, with old samples colored in purple and young samples colored in green.

To identify metabolites that mainly drive the differences detected between age groups, I performed PLS-DA and a RF classification on all the metabolomics datasets (Fig. 33A+B, untargeted BZ as an example) and checked the main metabolites contributing to the models (Top 10%). The RF classification resulted in an overall error rate of 0.06 (error rate old = 0.05; young = 0.07). Such a low error rate implies a very good classification of young and old samples.

Again, only a minor number of key metabolites were annotated, especially in the BZ and the IC dataset. Annotated metabolites which were significantly enriched in young samples include Pyruvic acid, Histidine and Putrescine. The most significant known metabolites with a high abundance in the old samples included 4-Hydroxyproline, Dimethylglycine, Seduheptulose-7-Phosphate, Pantothenic acid and Fructose-6-Phosphate (Fig. 33C). The PCA result of the annotated positive lipid suggested that known positive lipids were key contributors for the age changes. I was therefore particularly interested in the PLS-DA and RF results from this dataset. Indeed, several sphingomyelins were among the top metabolites, and the overall levels of sphingomyelins were higher in old samples (Fig. 33C).

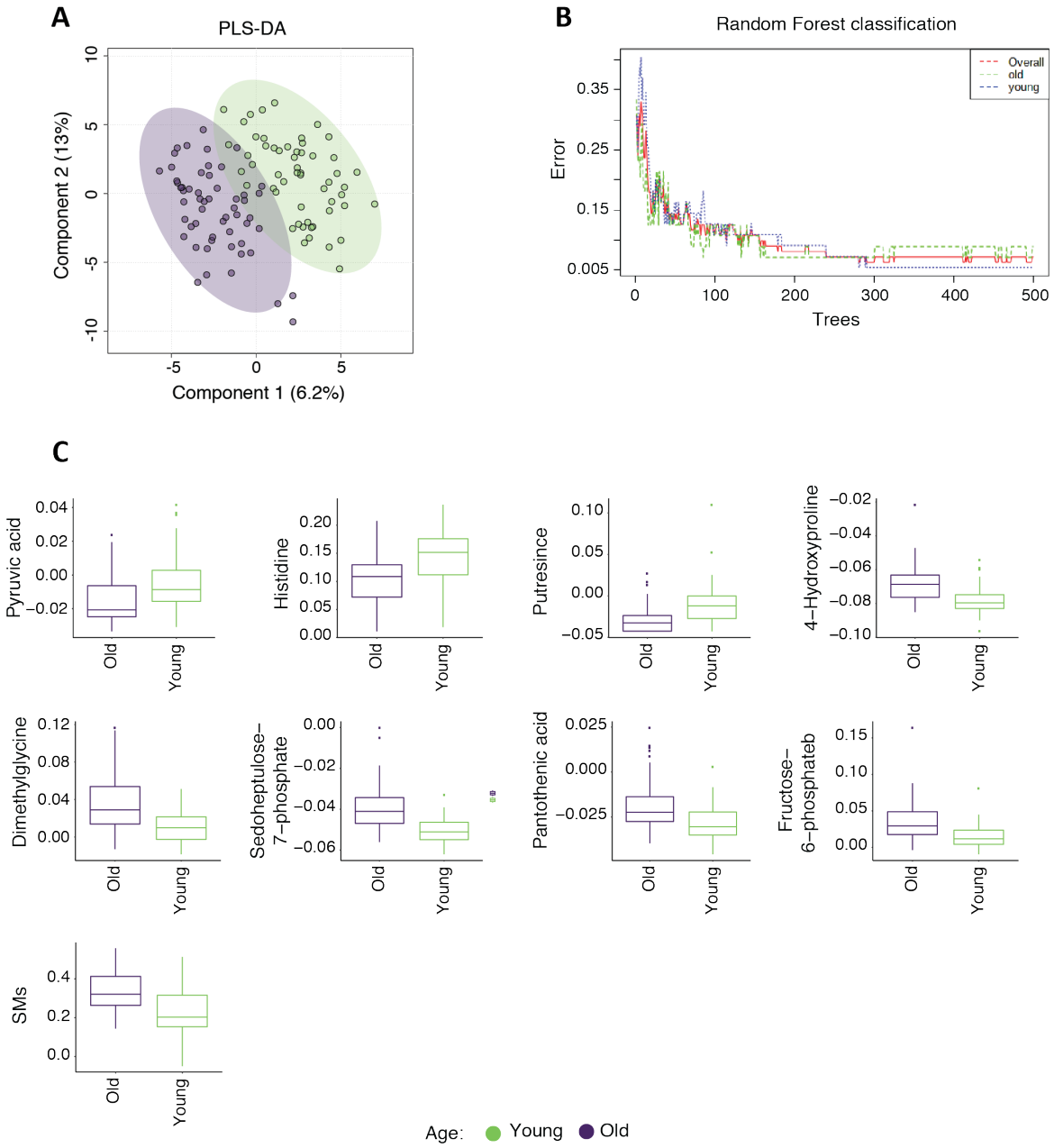

Figure 33: Age-specific metabolites. (A) PLS-DA on the untargeted BZ metabolomic dataset. (B) Error rates of the Random Forest classification on the untargeted BZ metabolomic dataset. (C) Annotated metabolites contributing to the top 10% of the section-specific classification models. Samples are colored by age, with old samples colored in purple and young samples colored in green. All p-values < 0.001, Wilcox-test (Holm-adjusted).

Next to analyzing the global age-changes with the methods mentioned above, I asked which of the detected aging patterns are shared between sexes and which are sex-specific. While most metabolites (including all the metabolites mentioned above)

showed similar age-specific trends for male and female fish, I made a striking observation in the lipid datasets. The lipid metabolites changing between young and old samples (Fig. 34A+B, marked in orange) were significantly enriched for male fish compared to female fish (p-value <0.001, Fisher's exact test). This held true for both the negative and the positive lipid metabolites. It thus appears that both negative and positive lipid levels change more drastically during age in male fish intestines, indicating a sex-specific aging pattern.

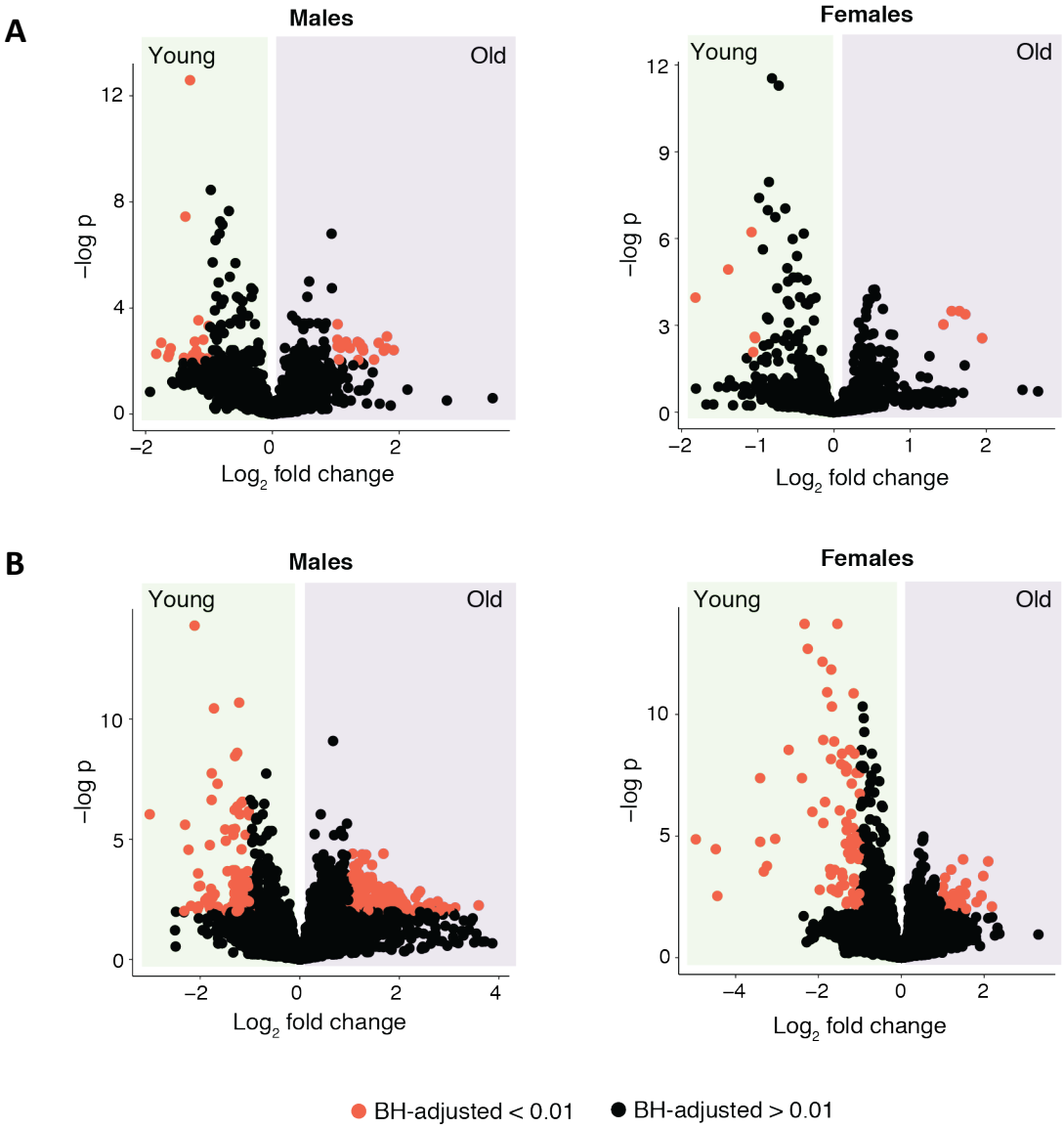

Figure 34: Sex-specific age differences. Volcano plots showing differences on metabolite level between young and old samples in females or in males, for (A) the negative lipid metabolomic dataset and (B) the positive lipid metabolomic dataset. Red color indicates metabolites with a BH-adjusted p-value <0.01 (Students t-test).

To gain insight into the protein expression patterns characterizing intestines from young and old individuals, I visualized the differentially expressed proteins in a Volcano plot (Fig. 35). Again, only samples from section 2 were included in the analysis due to size limitations. Proteins with high abundance in old samples included CLU, C4A4, HSPB1 and COL6A3, while IGF2BP3, GB-BETA4 and GATM were present in high levels in the young samples.

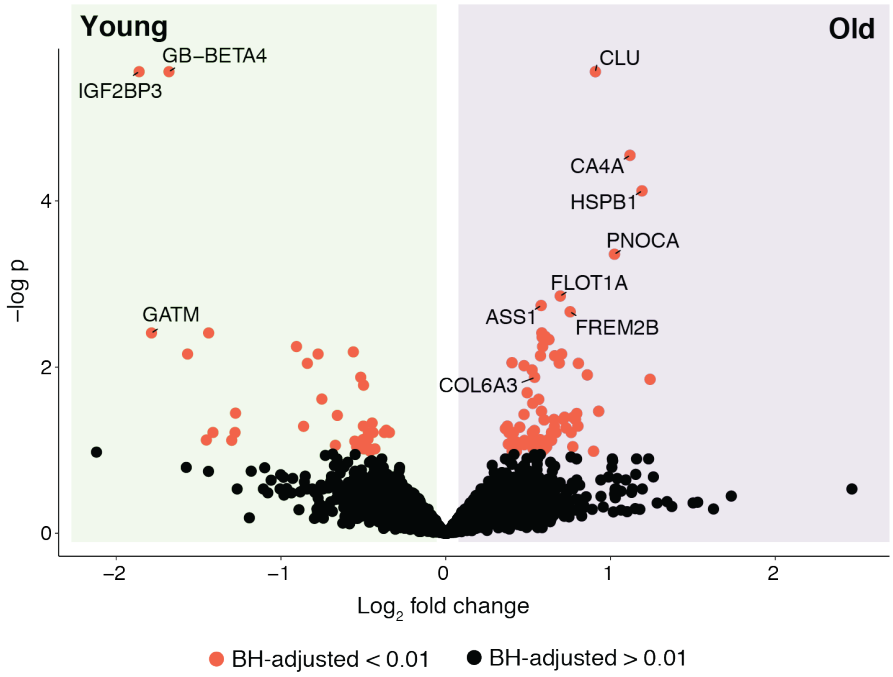

Figure 35: Age-specific proteins. (A) Volcano plot showing differences on protein level between young and old sections. Red color indicates proteins with a BH-adjusted p-value <0.01 (moderated t-test).

To assess which biological processes characterize the aging intestine, I performed gene ontology (GO) and pathway enrichment analysis of the significant proteins between young and old samples (adj. p-value <0.05). The young intestines were characterized by translation terms, for example *translation initiation* and *ribosome* (Fig. 36A+B), indicating high metabolic activity. In contrast, old intestines were characterized by terms such as *collagen-containing ECM*, and several transport and muscle-related terms including *sarcolemma* and *chemotaxis* (Fig. 36C+D).

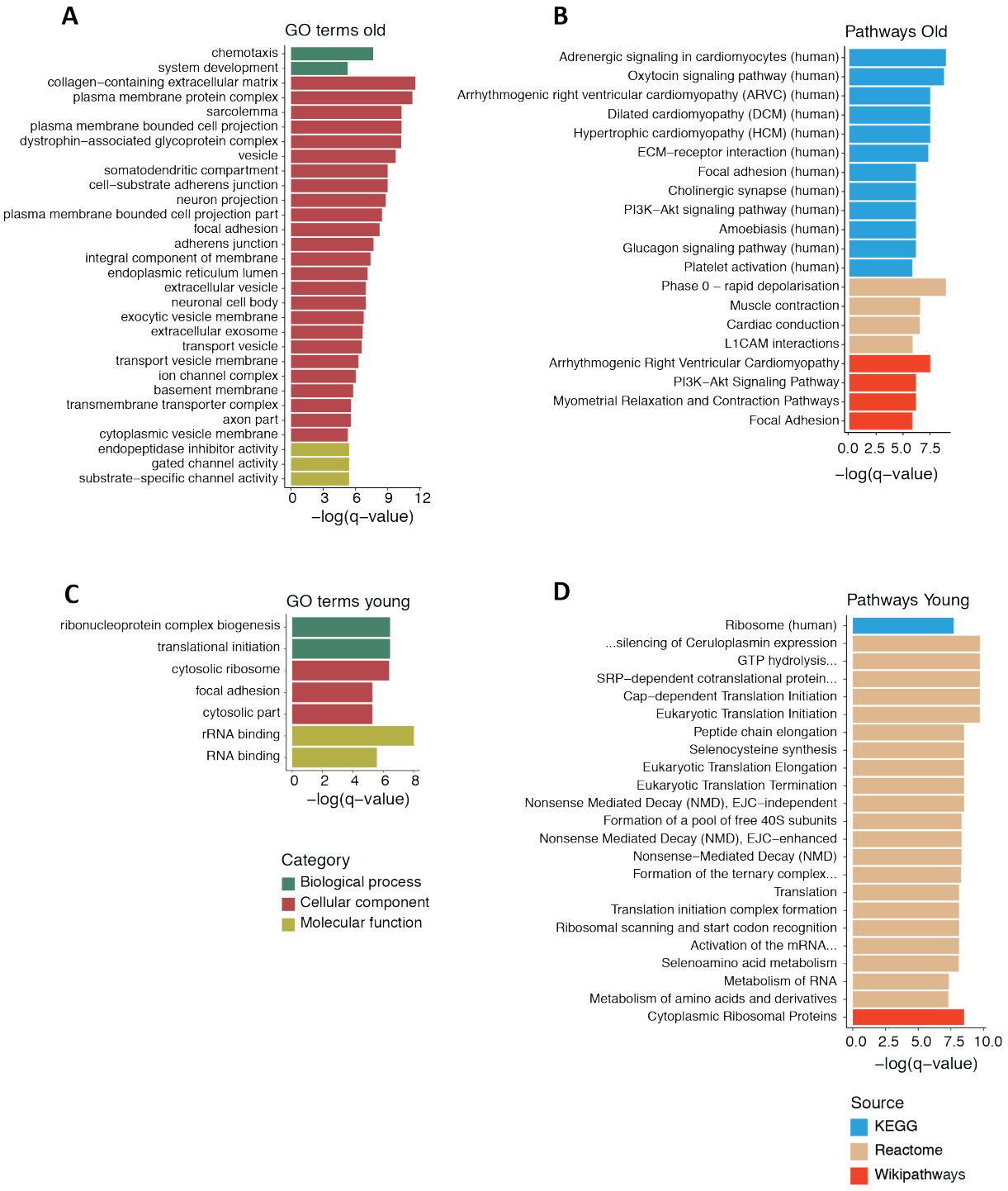

Figure 36: GO term and pathway enrichment analysis of young and old samples. (A) Top gene ontology terms (q-value <= 0.03) of proteins highly expressed in sections of young fish. (B) Top pathway enrichment terms (q-value <= 0.1) of proteins highly expressed in sections of young fish. (C) Top gene ontology terms (Top 30) of proteins highly expressed in sections of old fish. (D) Top pathway enrichment terms (q-value <= 0.1) of proteins highly expressed in sections of old fish. The negative natural logarithm of the q-values is shown. Statistical significance was calculated by a hypergeometric test.

2.3.4.2 Histological analyses

To test whether the intestinal age-differences I detected on the molecular level were also reflected on micro-anatomical level, Quinn Quesenberry analyzed the H&E and SRFG-stained section slices of young and old sections (Fig. 37A-D).

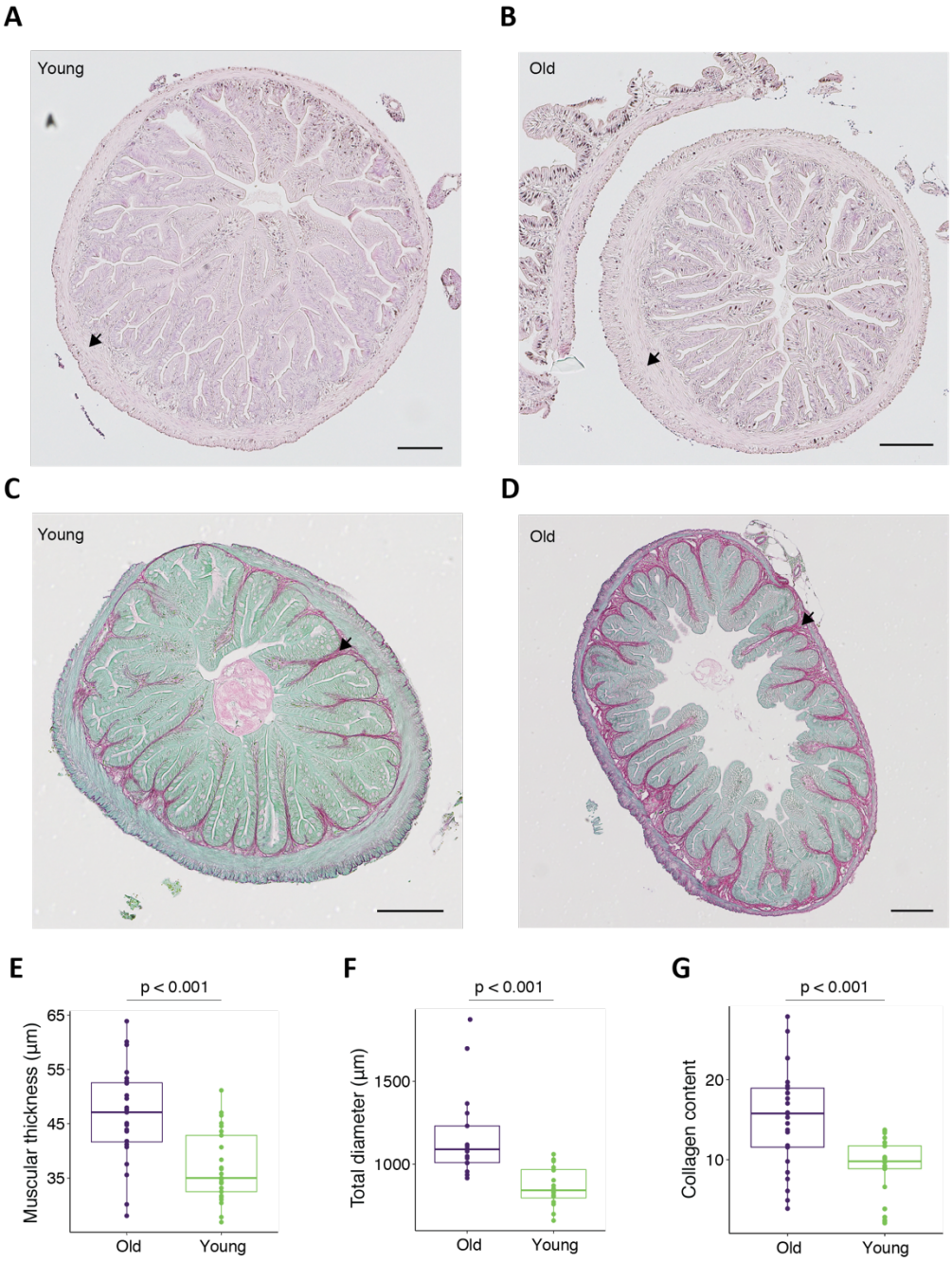

Figure 37: Histological staining of the young and old intestinal samples. (A) H&E staining of the intestine from young and (B) old killifish. Cell nuclei are stained in blue, other structures including the cytoplasm are stained in pink. The arrows mark the muscular layer. (C) SRFG staining of the intestine from young and (D) old killifish. Collagen fibers are stained in red, non-collagenous proteins are stained in green. The arrows mark collagen. (E) Quantification of the muscular thickness. (F) Quantification of the total intestinal diameter. (G) Quantification of the

intestinal collagen content. Samples are colored by age, with old samples colored in purple and young samples colored in green. The scale bars mark 100μm. Statistical significance was calculated by a Wilcox-test (Holm-adjusted).

We first analyzed the H&E-stained intestinal samples to identify changes in the overall structure and the cell type composition of the aging killifish intestine. No difference in global structures was visible – the goblet cell levels or the infiltration of leukocytes did not change between young and old samples (data not shown).
However, the thickness of the muscular layer increased with age (Fig. 37E, p-value <0.001, Wilcox-test) – as well as the total diameter (of the anterior sections, as diameter could only be measured for these samples) (Fig. 37F, p-value <0.001, Wilcox test). Moreover, quantification of the collagen content revealed that the collagen levels are significantly higher in old fish intestines (Fig. 37G, p-value <0.001, Wilcox-test).

2.3.4.3 Microbiota composition of young and old intestines

I have shown in this and previous work (Smith, Willemsen, Popkes et al., 2017) that the intestinal microbiota of the killifish underlies compositional age-related changes. However, all previous analyses were based on data obtained from whole intestinal samples. To characterize the intestinal microbiota on a more detailed level, I assessed whether also the intestinal sections show age-specific microbial profiles based on the 16S rRNA amplicon sequencing results.

I first performed PCoA based on Bray-Curtis dissimilarity to visualize a potential separation by age. Although the grouping was not strikingly obvious using the first two principal coordinates (cumulatively explaining 18.3% of the whole variance) (Fig. 38A), young and old samples still clustered significantly (p-value = 0.003, PERMANOVA analysis). As a second line of evidence, Sam Kean performed a RF classification for age, which resulted in an overall prediction accuracy of 0.82 (Fig. 38B).

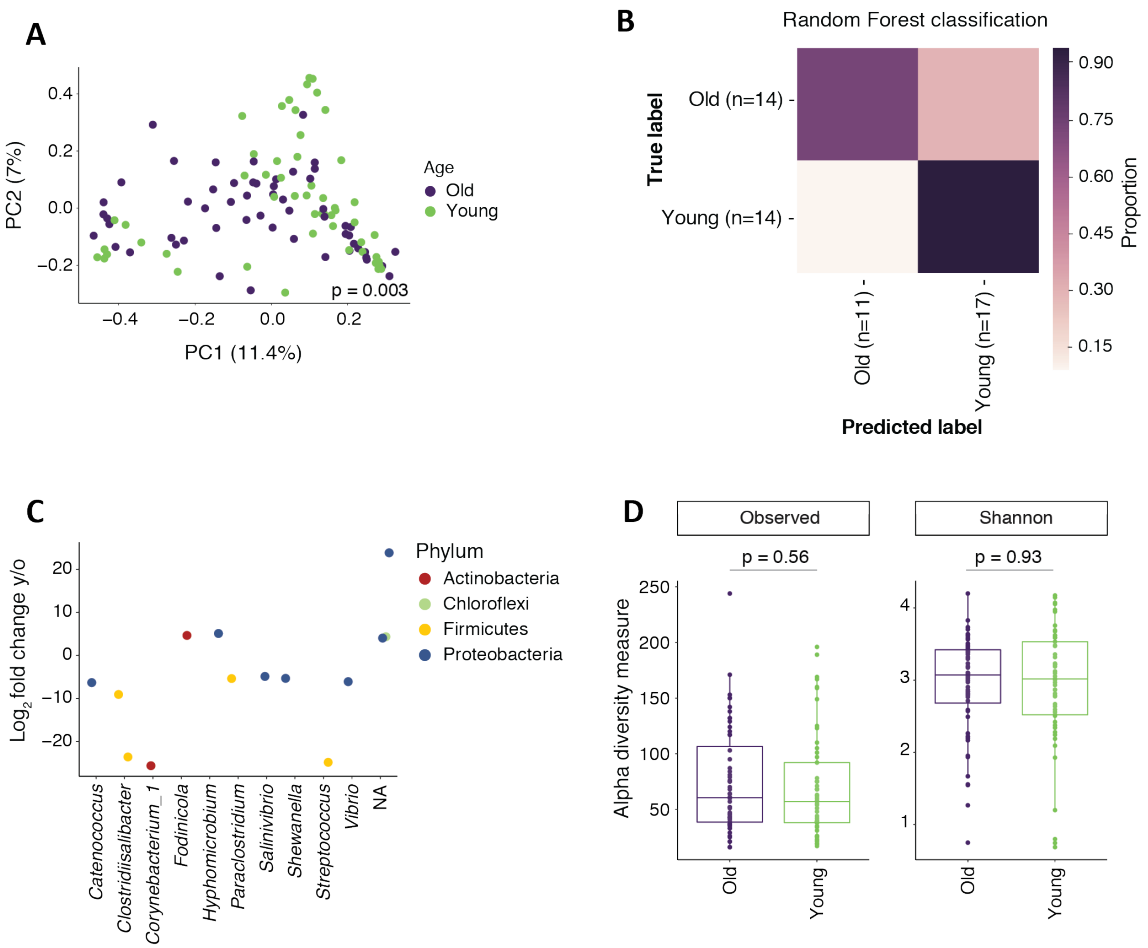

Figure 38: Analysis of microbiota composition of young and old samples. (A) PCoA of Bray-Curtis dissimilarity of samples from young and old fish. Samples are colored by age, with old samples colored in purple and young samples colored in green. P-value = 0.003, PERMANOVA-analysis. (B) Random Forest classification accuracy for young and old killifish intestinal samples. (C) DESeq2 differential abundance analysis for young and old intestinal sections. (D) Observed ESV and Shannon index alpha diversity for young and old killifish sections. Statistical significance was calculated by a Wilcox-test (Holm-adjusted). Samples are colored by age, with old samples colored in purple and young samples colored in green.

To further identify the age-specific bacteria, I performed DESeq2 differential abundance testing. ASVs enriched in young fish belonged to the genera *Fodinicola* and *Hyphomicrobiom*, while old fish were enriched for *Corynebacterium*, *Clostridisalibacter*, *Streptococcus* and *Vibrio* (Fig. 38C).

Previous data from our lab showed lower alpha diversity levels for old intestines (Smith, Willemsen, Popkes et al., 2017). In contrast to our expectations, alpha diversity levels remained unchanged between section samples from young (8 weeks) and old

(16 weeks) fish in this dataset (Fig. 38D). The same was true for beta diversity levels (data not shown).

Taken together, the killifish intestinal sections showed clear age differences on molecular and microanatomical level, as well as small but significant changes with regards to microbiota composition. Based on gene ontology enrichment analysis, young intestines seemed to have a higher protein biogenesis and metabolism rate, while old intestines showed an enrichment in muscle-related terms and in particular collagen, which goes in line with the increase in collagen on histological level. Interestingly, male intestines showed a significantly higher number of lipid metabolites changing upon aging, compared to female intestines. This indicates that an age-related change in lipid composition and abundance might be a sex-specific aging pattern in the killifish intestine.

2.3.5 Intestinal sex differences on multi-omics level

Several animal models show sex-specific structures and functional differences in the intestine, both in young and old age. My comparative approach considering intestinal, food and stool samples already revealed first evidence for sex differences in the killifish intestines with regard to microbiota composition (2.2.4). Moreover, my untargeted metabolomics data suggested that intestinal aging is, at least to some extent, sex-specific. However, a detailed characterization of sex-specific differences on metabolic, protein and microbial level is still absent. I therefore investigated the potential differences between male and female intestines based on my multi-omics dataset on a deeper level.

2.3.5.1 Molecular characteristics

I first focused on the metabolomic and proteomic datasets by grouping the samples by sex to examine potential sex-specific molecular signatures.

PCA of the untargeted metabolomic datasets demonstrated a clear clustering of male and female samples (Fig. 39A-E), indicating distinct molecular patterns for fish of different sex. The clustering was apparent on lower levels, mostly on principal component 3. To draw first functional conclusions, I next focused on the annotated subsets of the metabolomics datasets. The degree of clustering differs in a subset-dependent manner, suggesting particular metabolite groups as main drivers. For instance, the annotated metabolites from the BZ dataset, mainly including amino acids, showed a comparable clustering to the untargeted BZ dataset, indicating the importance of those amino acids regarding sex-specificity (Fig. 39F). I observed a similar trend for the annotated positive lipids (TAGs, DAGs, SMs, PCs, PEs) compared to the respective untargeted dataset (Fig. 39G). In contrast, a clear clustering was absent in case of the annotated negative lipids (PGs and FFAs) (Fig. 39H), supporting the notion that annotated positive, but not negative lipids explain large parts of the sex-specific variation in PCA.

To test whether this sex-specific separation is also reflected on protein levels, I next performed PCA on the proteomic dataset. The analysis was based on data from section 2 of young and old, male and female killifish. Remarkably, the samples showed a very strong clustering already on principal component 2 (Fig. 39I), suggesting that intestinal protein expression is highly sex-specific. A second proteomic analysis considering data from all sections, taken from old male and female fish, confirmed those findings (data not shown).

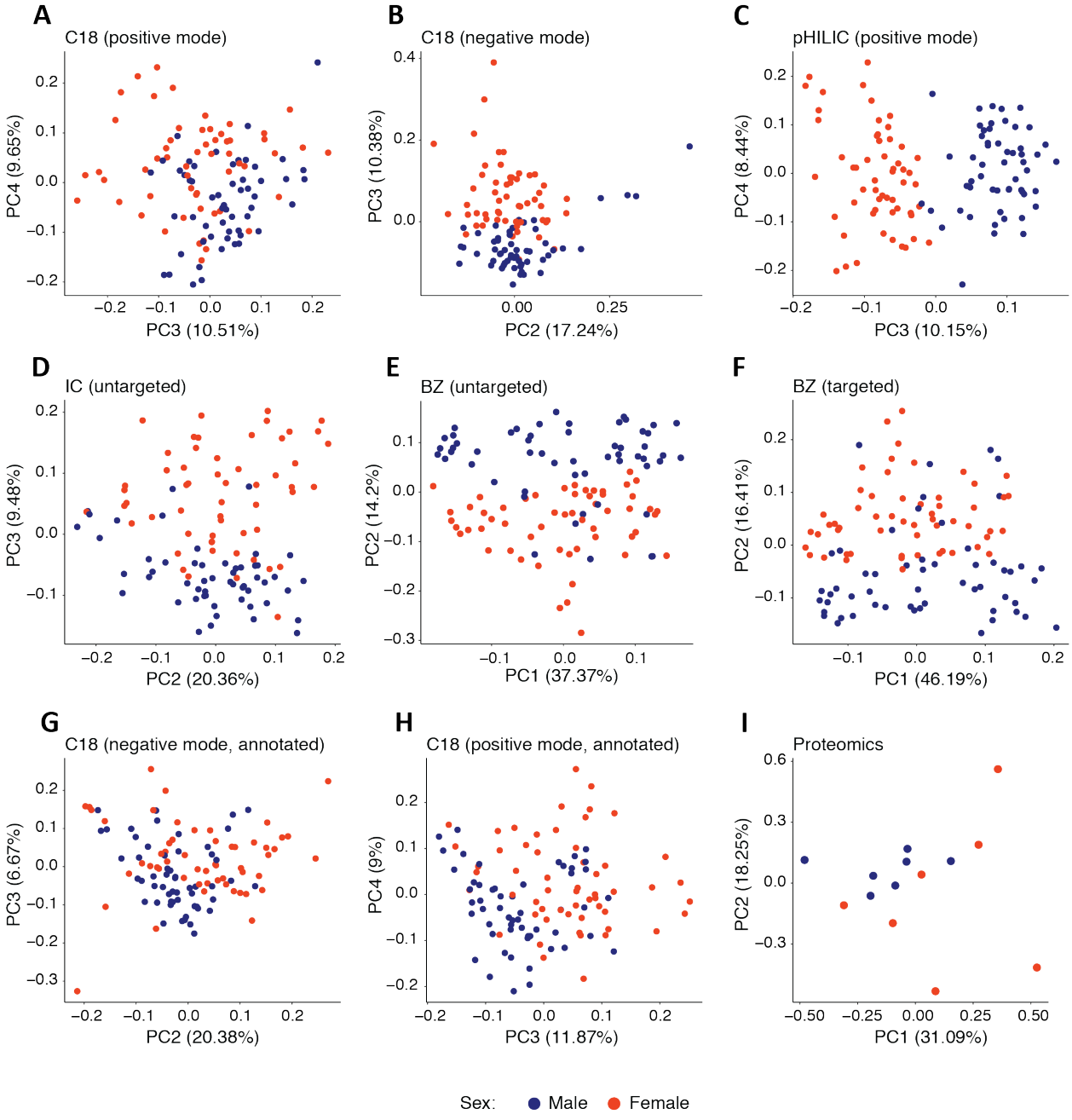

Figure 39: PCA of metabolomic and proteomic datasets for sex differences. PCA on the metabolomic datasets for (A) positive lipids, (B) negative lipids, (C) positive polar metabolites, (D) untargeted IC run, (E) untargeted BZ run, (F) annotated positive lipids, (G) targeted BZ run and (H) annotated negative lipids. (I) PCA of the proteomic dataset. Samples are colored by sex, with female samples colored in red and male samples colored in blue.

To identify characteristic metabolites for female and male intestines, I performed PLS-DA and RF classification on all the metabolomics datasets (Fig. 40A+B, untargeted BZ as an example) and checked the main metabolites based on contribution to the models (Top 10%). The RF classification resulted in an overall error rate of 0.009 (error rate old = 0; young = 0.018). Such a low error rate implies an extremely good classification of male and female samples. Again, only a minor fraction of the key metabolites was annotated.

I was especially interested in the levels of annotated positive lipids and amino acids given the strong clustering pattern in the PCA. Indeed, Taurine and 7-alpha-27-dihydroxycholesterol were among the annotated metabolites enriched in male intestines. In addition, I found higher overall levels of sphingomyelins in male compared to female fish. The most significant metabolites with a high abundance in female fish included Cystathionine and Proline, as well as higher levels of overall DAGs, lysoPCs and FFAs (Fig. 40C).

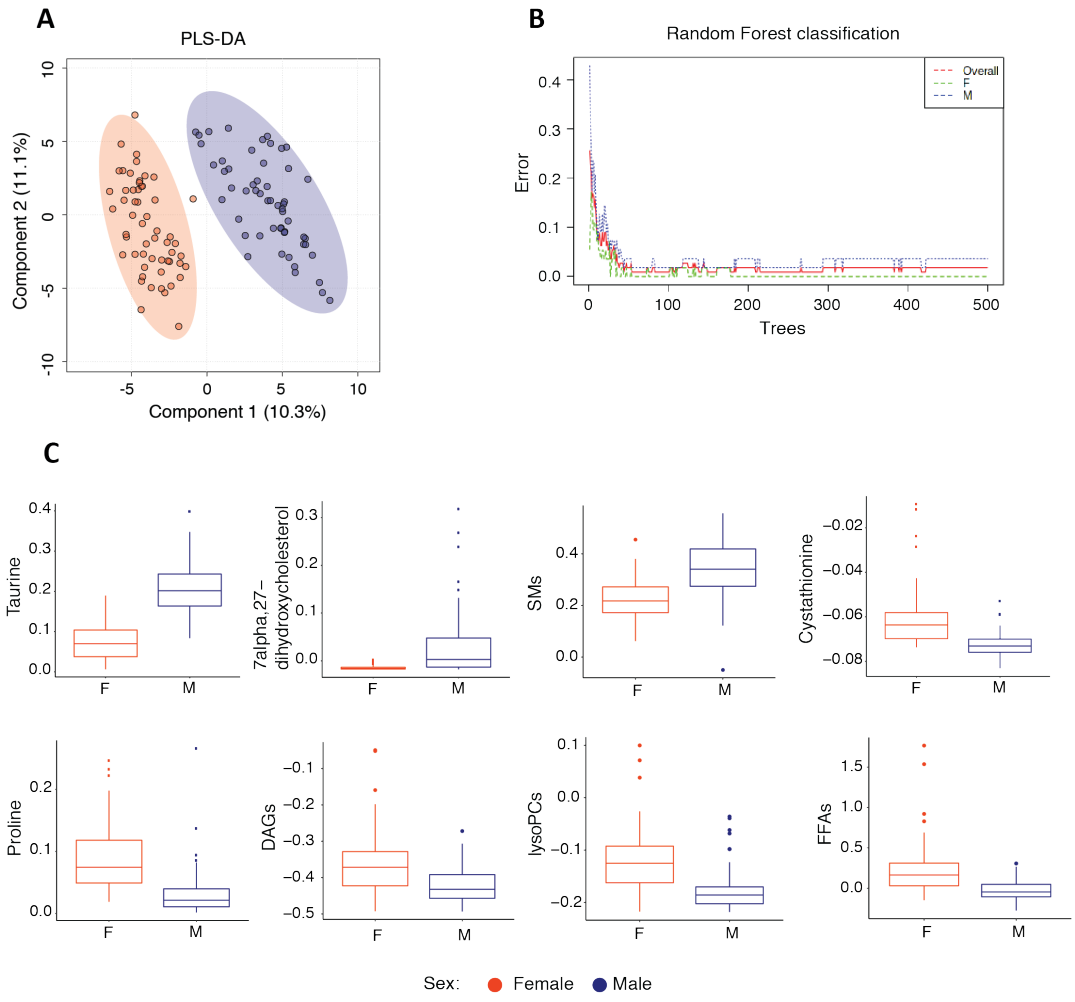

Figure 40: Sex-specific metabolites. (A) PLS-DA on the untargeted BZ metabolite dataset. (B) Error rates of the Random Forest classification on the untargeted BZ metabolite dataset. (C) Annotated metabolites contributing to the top 10% of the section-specific classification models. Samples are colored by sex, with female samples (F) colored in red and male samples (M) colored in blue. All p-values < 0.001, Wilcox-test (Holm-adjusted).

To gain insight into the proteins characterizing male and female intestines, I visualized the differentially expressed proteins in a Volcano plot (Fig. 41). It is important to note that the analyzed proteomics dataset only contained samples from section 2. Proteins with high abundance in male intestines included HPX, APOH, SCGN and APOB, while OL-VIT1, COX20 and ECM1 were presented in high levels in female samples. A second proteomic analysis considering data from all sections, taken from old male and female fish, confirmed those findings (data not shown).

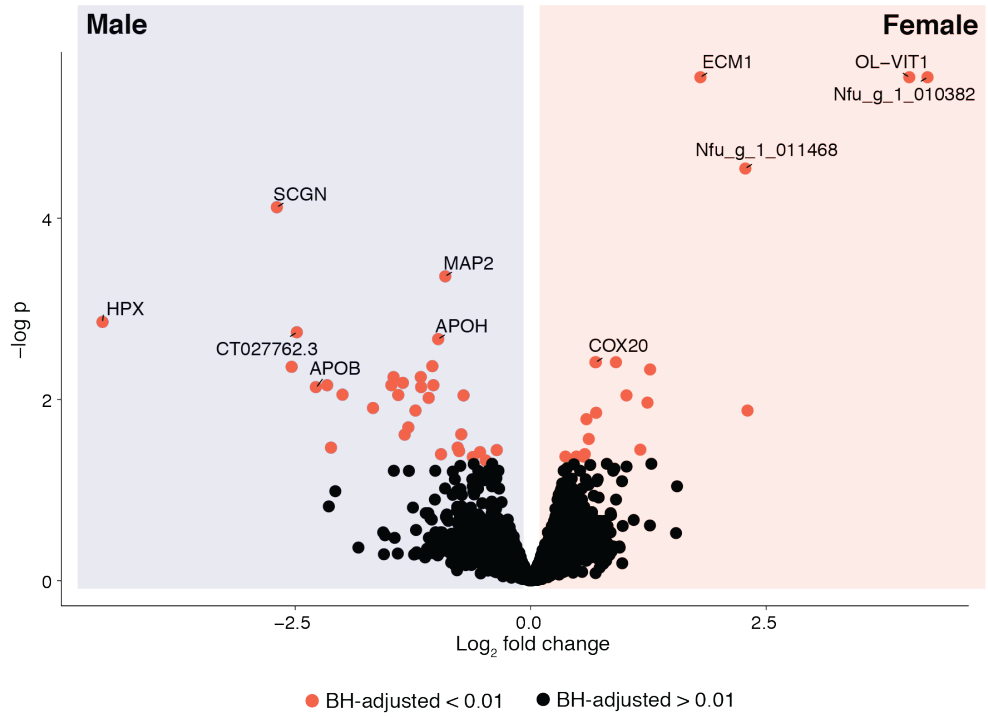

Figure 41: Sex-specific proteins. (A) Volcano plot showing differences on protein level between female and male sections. Red color indicates proteins with a BH-adjusted p-value <0.01 (moderated t-test).

To draw functional conclusions from the proteomic analysis comparing male and female intestines, I performed gene ontology and pathway enrichment analysis of the significantly different proteins (adj. p-value <0.05). While the female intestines did not show a strong enrichment in terms other than *peptidase activity* and *secretory granule lumen* (Fig. 42A), male intestines were characterized by terms related to blood clotting (e.g. *fibrinogen*, *coagulation*, *platelets*), to lipids (e.g. *lipid transport, lipoprotein*

particle) and to the immune system (e.g. *regulation of TLR*, *regulation of defense response*) (Fig. 42B+C).

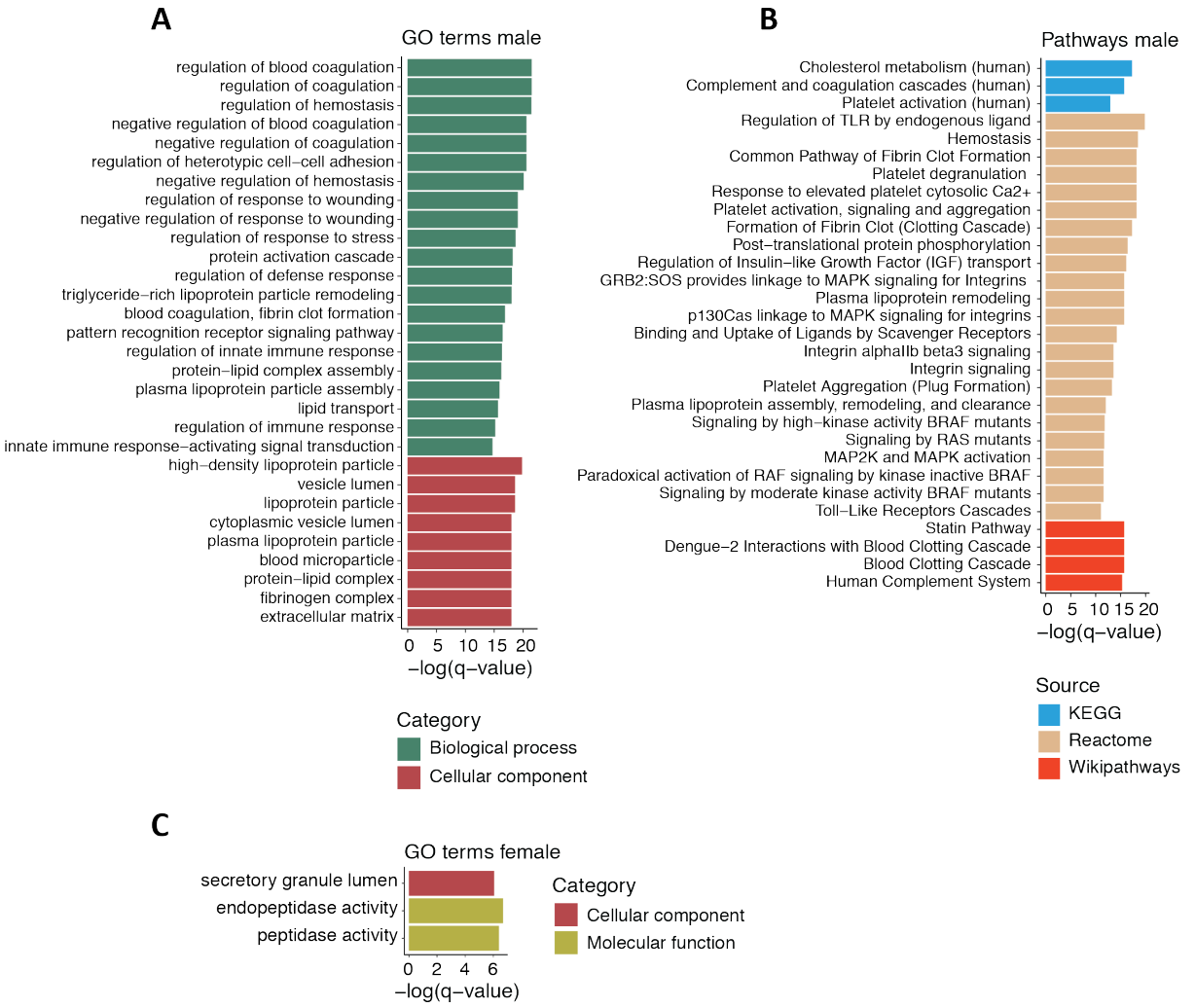

Figure 42: GO term and pathway enrichment analysis of female and male samples. (A) Top gene ontology terms (q-value <= 0.03) of proteins highly expressed in sections of female fish. (B) Top gene ontology terms (Top 30) of proteins highly expressed in sections of male fish. (C) Top pathway enrichment terms (Top 30) of proteins highly expressed in sections of male fish. The negative natural logarithm of the q-values is shown. Statistical significance was calculated by a hypergeometric test.

The metabolomic and proteomic data clearly support the notion of strong sex-differences. Next, I asked whether age contributes to sex differences. To this end, I subset the metabolomic data into young and old samples and assessed the

significantly changing metabolites between males and females (Fig. 43). Remarkably, all datasets except for the untargeted BZ dataset showed significantly more sex-specific metabolites in old age (p-values <0.001, Fisher's exact test). Notably, this trend was also confirmed in the proteomic dataset – the number of differently expressed proteins between males and females was significantly higher in the subset of old fish (p-value <0.001, Fisher's exact test). This suggests that sex differences increase with age on a molecular level.

2.3.5.2 Histological analysis

After this detailed analysis on molecular level, I asked whether the sex-related changes I detected on metabolomic and proteomic levels were reflected on micro-anatomical level. However, we did not find any statistical differences in the quantitative and qualitative histological analysis (data not shown).

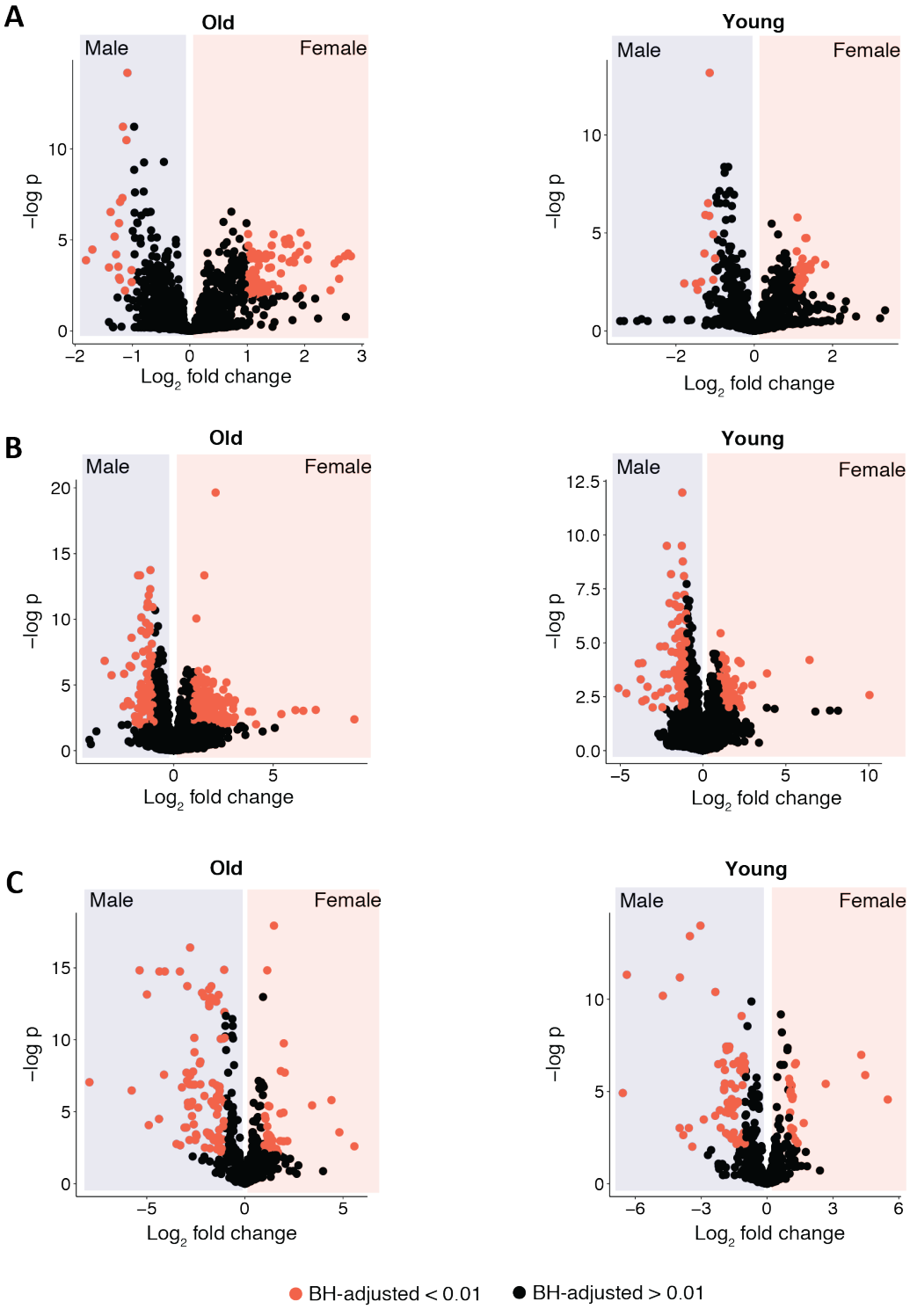

Figure 43: Age-specific sex differences. Volcano plots showing differences on metabolite level between male and female samples in young or old age, for (A) the negative lipid metabolomic dataset, (B) the positive lipid metabolomic dataset, (C) the positive pHILIC metabolomic dataset. Red color indicates metabolites with a BH-adjusted p-value <0.01 (Student's t-test).

2.3.5.3 Microbiota composition of male and female intestines

I demonstrated that the killifish intestine shows strong sex-differences on a molecular level. Furthermore, it is well known for other animal models that also microbiota composition shows sex-specific attributes, at least to some extent (Org et al., 2016). As the previous results of my thesis pointed towards small sex differences in whole killifish intestines on microbiota level (2.4), I sought to confirm these findings on the sections data. I therefore analyzed the sex-specific microbiota profiles based on the 16S rRNA amplicon sequencing results.

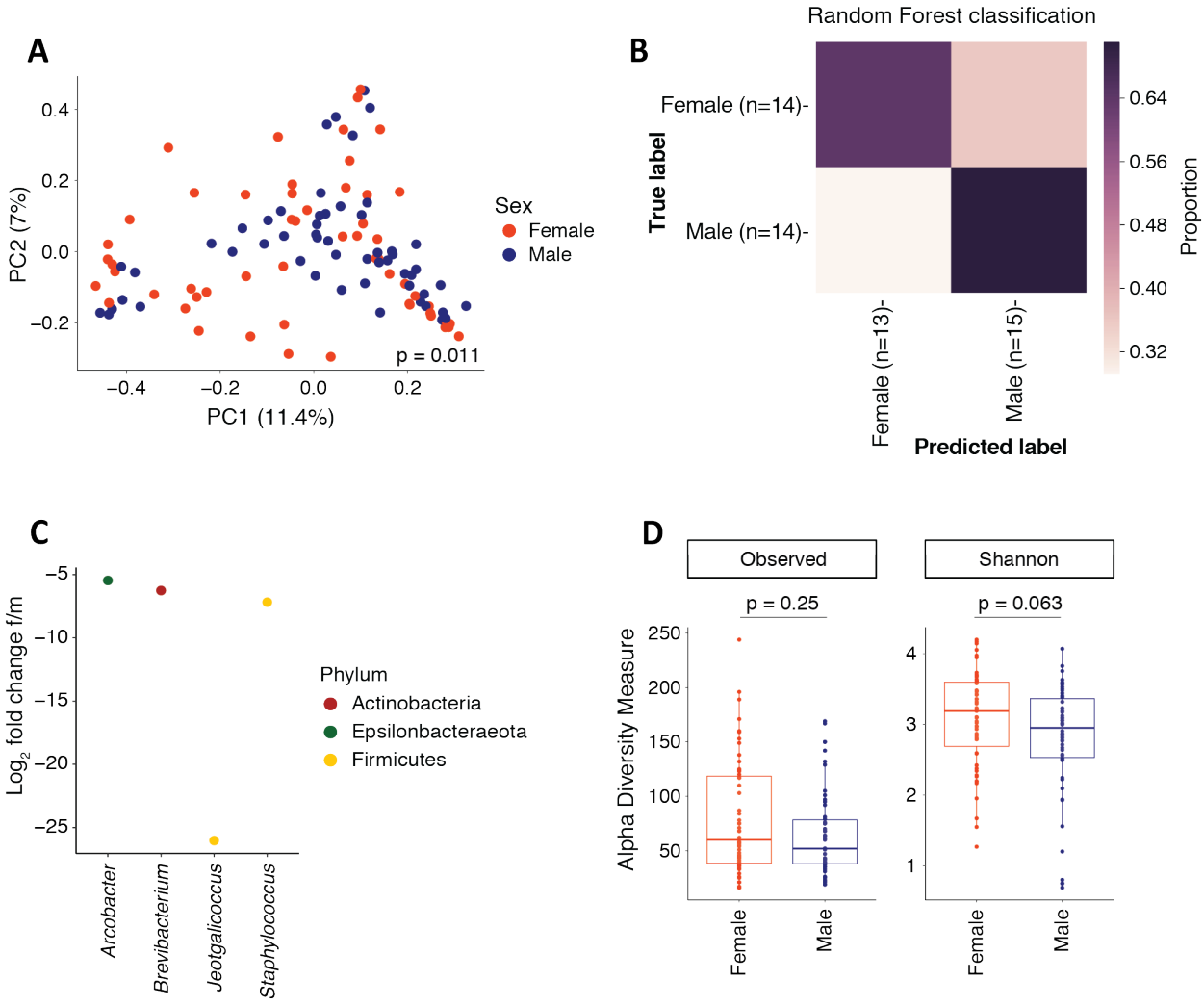

Figure 44: Analysis of microbiota composition of female and male samples. (A) PCoA of Bray-Curtis dissimilarity of samples from female and male fish. Samples are colored by sex, with female samples colored in red and male samples colored in blue. P-value = 0.011, PERMANOVA-analysis. (B) Random Forest classification accuracy for female and male killifish intestinal samples. (C) DESeq2 differential abundance analysis for female and male intestinal sections. (D) Observed ESV and Shannon index alpha diversity for female and male killifish sections. Statistical significance was calculated by a Wilcox-test (Holm-adjusted).

Samples are colored by sex, with female samples colored in red and male samples colored in blue.

I first performed PCoA based on Bray-Curtis dissimilarity to see whether the samples were separated by sex. Although the grouping was not strikingly obvious using the first two principal coordinates (Fig. 44A), male and female samples still clustered significantly (p-value = 0.011). As a second line of evidence, RF classification resulted in an overall prediction accuracy for age of 0.68 (Fig. 44B), indicating that slight changes in microbiota composition must be present between male and female samples. I thus performed DESeq2 differential abundance testing to identify the enriched sex-specific bacteria. ASVs enriched in female fish belonged to the genera *Arcobacter*, *Brevibacterium and Staphylococcus*, while male fish were enriched for *Jeotgalicoccus* (Fig. 44C).
With regards to diversity however, no significant differences in either alpha diversity (Fig. 44D) or beta diversity levels could be detected (data not shown).

Taken together, the killifish intestinal sections show clear sex differences on the molecular and microanatomical levels, as well as small but significant changes with regards to microbiota composition. Female intestines were characterized by higher levels of positive lipids, including DAGs, FFAs and lysoPCs. Male intestinal sections showed an enrichment in muscle-related terms and collagen, as well as high levels of sphingomyelins and Taurine. Remarkably, overall sex differences seemed to increase with aging.

2.3.6 Correlation between metabolites and microbiota composition

The multi-omics approach resulted in a multi-level dataset for the same sections, including information about the molecular patterns on metabolomic and proteomic level, information about the microanatomical structures as well as information about the microbiota composition. This special dataset provided the unique opportunity to draw correlations between the different subsets, allowing to gain first insights into the connection between the killifish host side and the residing intestinal microbiota.

To identify correlations between single bacteria and host metabolites, I performed a linear regression analysis on the relative abundance levels of the most prevalent and widespread genera and all the annotated metabolites.

The correlation analyses resulted in 28 significant correlations between single genera and single metabolites (adj. p-value <0.1). Among the strongest correlations was the negative correlation between *Hyphomicrobium* and 4-Hydroxyproline (Fig. 45A), and the positive correlations between an unknown genus from the *Rhizobiaceae* family and two bile acids, namely Taurocholic acid (Fig. 45B) and 7-Oxotaurodeoxycholic acid.

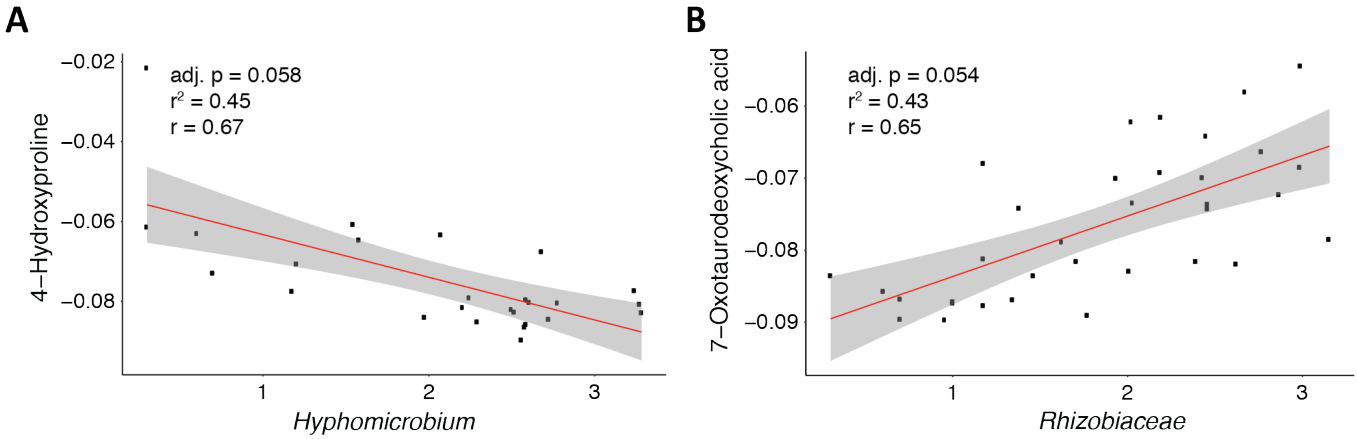

Figure 45: Correlation analysis between ASVs and metabolites. (A) Linear regression model between *Hyphomicrobiom* and 4-Hydroxyproline. (B) Linear regression model between *Rhizobiaceae* and 7-Oxotaurodeoxycholic acid.

Chapter 3

Discussion

Research on the aging gut microbiota has sparked strong interest in recent years, with exciting findings pointing to a causal connection between gut microbes and the aging process. To study gut microbiota in the context of aging, we need to know about spatiotemporal dynamics of the aging intestine and its associated microbial communities, as research has found gut section-specific microbial communities, which play integral roles in host physiology and thus could essentially affect the aging process (Bana & Cabreiro, 2019; Rooks & Garrett, 2016; Smith, Willemsen, Popkes et al., 2017). Moreover, it is important to study intestinal host–microbiota interactions especially with regards to sex differences, as several studies have shown sex-specific patterns in intestinal morphology and microbiota composition, influencing major host processes such as nutrient absorption and even playing a role in susceptibility to diseases and aging (Markle et al., 2013; Regan et al., 2016).

The killifish is an intriguing model system to study microbial dynamics and intestinal features during aging, as it uniquely combines vertebrate properties such as a complex gut microbiota with an extremely short lifespan for aging studies. While we previously profiled killifish intestinal age-related changes, the question of intestinal sections, temporal aging dynamics and sex-specific intestinal aspects still remains elusive.

I thus set out to characterize killifish spatiotemporal aging dynamics and sex-specific intestinal morphological, microbial and molecular patterns by performing multi-omics analyses on intestinal sections of young and old, male and female killifish. I furthermore asked whether non-invasive stool samples can serve as a proxy for gut microbiota by microbiota analysis of stool, intestinal and food samples. Last, I set out to explore whether it is possible to build models predicting fish age or remaining life based on stool microbiota composition, by conducting a longitudinal collection of individual killifish stool samples across the whole life.

Notably, I observed a clear compartmentalization of the killifish intestine on a morphological and molecular level, partially reflecting the mammalian intestine on a functional level. In contrast to findings from other animals, including fish, I did not find strong microbiota patterns specific for the distinct sections. Moreover, analysis of aged

fish revealed strong evidence for a restructuring of the intestinal extracellular matrix, including collagen accumulation and muscle thickening, potentially adversely affecting the intestinal function in old age. For the first time, I demonstrate clear sex-specific molecular features involving differences in the coagulation process. In addition, I found first evidence that the killifish intestinal molecular differences increase between sex upon aging. Excitingly, I discovered shared microbial features between stool and gut microbiota and could, for the first time, combine data of a longitudinal collection of stool samples with individual killifish lifespan to build prediction models for not only age, but also remaining life.

My results set the important foundation for future killifish research focusing on gut microbiota in the context of aging. Beyond this, I provide novel insights into sex- and age-specific pathways – and show promising results which lay the ground for predicting remaining life based on stool microbiota samples.

3.1 The intestinal microbiota composition in the killifish

The earth is home to a myriad of microorganisms, predicted to be as many as 1 trillion microbial species (Locey & Lennon, 2016). Microbes are extremely diverse in genetic constitution resulting in an enormous amount of specialized functional potential, suited to fit into completely different environmental niches (Fahimipour & Gross, 2019). The microbiota present in different environments, animals, individuals or even different tissues and body sites within an individual is thus varying substantially (The Human Microbiome Project Consortium, 2012).

In line with the strong niche-specific microbiota communities for different environments and tissues, I found that the microbiota composition of stool, intestinal and food samples are very different between the sample types (Fig. 17A+B). While Proteobacteria are the dominating phylum in all sample types, similar to what has been reported for other aquatic animals (Sullam et al., 2012) and what we also previously

found for the killifish intestine (Smith, Willemsen, Popkes et al., 2017), differences between the sample types become apparent in other phyla and genera. Intestinal samples were for example enriched for Actinobacteria and Aeromonas, while food and stool samples showed a major fraction of Fusobacteria and Epsilonbacteria/Psychrilyobacter. Aquatic Actinobacteria are a very rich source of bioactive compounds and secondary metabolites (Jami et al., 2015; Manivasagan et al., 2013) and probably play an important role in the nutrient production of the killifish intestine. The genus Aeromonas contains several known pathogens, both for humans and for fish (Janda & Abbott, 2010; Parker & Shaw, 2011), however also one species (*Aeromonas media*) has been reported to function as a potential probiotic in fish (Lategan & Gibson, 2003). As the 16S sequencing approach does not allow discrimination to the species or strain level, it is not possible to assess whether the large fraction of intestine-specific Aeromonas is an opportunistic pathogen or rather a beneficial killifish commensal. Fusobacteria are commonly found in fish microbiota, especially in carnivores, and interestingly have been reported to be enriched in bloodworm-fed juvenile sturgeons (Q. Hao et al., 2021). Fusobacteria might be involved in with fatty acid metabolism in fish (Mekuchi et al., 2018), but clear evidence for functional importance is still missing.

In addition to the sample-type specific microbiota composition, I found interesting differences in diversity comparing the intestinal, stool and food samples. Intestinal samples, analyzed together, showed the highest number of reported ASVs, but the lowest number of ASVs with an abundance of >0.1%, pointing to a large fraction of rare ASVs present in the killifish intestine. Interestingly, intestinal samples showed the lowest values for diversity measures accounting for richness and evenness when samples were analyzed individually (Fig. 18A). This is congruent with the observed beta diversity: Intestinal samples had the highest rate of within beta diversity (Fig. 18C), thus the variation and differences in microbiota composition are very high between individual fish intestines. Notably, while food and stool samples showed higher values for diversity measures accounting for richness and evenness, intestinal samples had a higher phylogenetic diversity (Fig. 18B). Intestinal samples are thus dominated by a few highly abundant ASVs and show a lot of additional, rare ASVs

with a very low abundance, resulting in low richness and evenness measures. The high beta diversity levels moreover could suggest that the intestine builds individual-specific niches and selects particular, individual-specific bacteria which can also be phylogenetically diverse.

In general, the global sample-type specific observations, such as diversity measures or overall phyla composition, were congruent between all my datasets generated in this thesis – supporting the reproducibility and importance of my findings. Some specific observations, such as the detailed microbiota composition, were however specific for individual datasets. As environmental factors can largely impact the intestinal microbiota (Rothschild et al., 2018), differences between the datasets might be explained by different collection timepoints and associated environmental changes in the fish facility.

While sampling microbiota from intestines is usually an invasive procedure, sampling stool is a non-invasive procedure, and is therefore frequently adopted to gain information about the intestinal microbiota. However, stool reflects only parts of the intestinal microbiota (Momozawa et al., 2011), mostly the colon microbiota (Gierse et al., 2020). It has been shown that while most intestinal taxa could be identified in feces, the microbial community structure between intestine and feces is not equivalent (Yan et al., 2019).

In addition, it is known that the intestinal microbiota composition is influenced by various factors, of which diet plays a key role (David et al., 2014; De Filippo et al., 2010; G. D. Wu et al., 2011). Dietary components also have a major impact on intestinal microbiota features in aquatic animals (Hartviksen et al., 2014; Mansfield et al., 2010; Ringo & Olsen, 1999).

In line with this, I discovered that killifish stool samples share a lot of microbial properties with the food samples and are highly similar to the killifish bloodworm food in terms of composition and diversity. However, stool samples also shared some ASVs with the intestinal samples which were not present in the food samples, including bacteria from the genera *Aeromonas* and *Vagococcus* (Fig. 17C). Similar to *Aeromonas,* the *Vagococcus* genus includes potential fish pathogens (*Vagococcus*

salmoninarum, Schmidtke & Carson, 1994). Nevertheless, *Vagococcus fluvialis* has also been studied as a potential fish probiotic (Sorroza et al., 2012). The species assigned for one of the seven shared ASVs was indeed *Vagococcus fluvialis*, pointing to a potential fish commensal shared between stool and gut. However, due to the detection limit of the 16S sequencing, I could not reliably assess whether the microbes classified as *Aeromonas* and *Vagococcus* have a pathogenic or commensal role in the killifish intestine.

Where do microbes emerge from that are present in the gut and stool, but not in the food? One possibility is that stool- and gut-specific bacteria were either present in earlier food samples and the intestine specifically selected for those microbes, or they were present in the killifish environment such as the tank water. Another possibility is that those bacteria were vertically transmitted by the parents, although studies for several fish indicate that horizontal bacterial transfer is the dominant factor for transmission (Llewellyn et al., 2014; Stephens et al., 2016).

The conducted analysis of shared stool-gut microbiota takes into account the occurrence of specific bacterial strains, but not their relative abundance. Therefore, a better resolution could be achieved by implementing advanced statistical models, such as modified available batch effect normalization methods, to infer intestinal-specific information from the detected stool microbiota composition. With this, the model would not only focus on single genera known to be intestine-specific, but on the microbiota composition and its structure as a whole.

Several studies have presented sexual dimorphic patterns for the intestinal morphology and also the associated microbial community. Sex-specific differences in microbiota composition or diversity have been reported for various animals (Markle et al., 2013; Org et al., 2016; Yurkovetskiy et al., 2013). For humans, few studies have evaluated gut microbiota sex differences with contradicting outcomes (Ding & Schloss, 2014; Haro et al., 2016; Sinha et al., 2019), leaving human sex-specific microbiota patterns an interesting topic for deeper investigation.

I found no global differences for sex in terms of microbiota composition or diversity measures. At the same time, I was able to identify specific ASVs enriched in male and female samples, both for intestinal and stool samples. Interestingly, also some human studies suggest that microbial sex-differences are rather found in specific bacteria, but less often on global measures such as diversity or overall composition (Haro et al., 2016; Takagi et al., 2019). My studies suggest an enrichment in *Aeromonas* and *Vibrio* in male fish, and *Shewanella* in female fish. While the former two genera are known to include many fish pathogens, *Shewanella* species are often investigated as potential fish probiotics (García de La Banda et al., 2010; Sáenz de Rodrigáñez et al., 2009). However, the potential sex-specific bacteria I identified are not overlapping in both generated datasets and therefore need further investigation in additional studies. There might not be any global differences in microbiota composition between sex, or the lack of sex-specific differences in microbiota might be rooted in different sampling timepoints, again associated with environmental changes in the fish facility. Another reason could be the limited detection depth of the applied 16S sequencing method.

Taken together, the intestinal microbiome of male and female fish largely overlaps except for some specific bacterial strains. However, which strains are of particular importance need to be examined in additional studies.

3.2 The intestinal microbiota during killifish aging

Intestinal microbial communities undergo extensive changes during aging, both for model systems and also for humans, including a shift in composition and a decrease in alpha diversity (Biagi et al., 2016; Claesson, Jeffery, Conde, Power, O'connor, et al., 2012; Langille et al., 2013). In my work, I assessed the aging gut microbiota of the killifish from several angles – I profiled the temporal dynamics of stool microbiota, investigated the gut microbiota profiles from young and old male intestines and furthermore the intestinal sections of young and old, male and female killifish.

3.2.1 Stability aspects of killifish stool microbiota composition

The longitudinal collection of stool samples revealed that the microbiota composition of killifish stool remains largely stable over time, in contrast to the control food samples, indicating that the food samples are more prone to environmental changes (Fig. 10). One possible reason for the variability of the food samples might include changing influences in the production process. This is most probably the case for the bloodworm food, as it is delivered by an external vendor - brine shrimp are produced inhouse and are therefore raised under very controlled conditions, although also here quality differences have been noted in the past. Another explanation could be that both the bloodworm food and the brine shrimp are still at very juvenile stages when being fed to the fish. It is well known for humans that the microbiota communities are fluctuating widely in the first developmental stages (Rodríguez et al., 2015), and juvenile zebrafish gut microbiota are more similar to the surrounding microbiota compared to adult zebrafish (Stephens et al., 2016). The large fluctuations between consecutive weeks could be explained by juvenile bloodworm and brine shrimp being less capable of selecting specific surrounding microbes, and therefore more directly mirroring environmental changes.

The high variability of the food microbiota could potentially pose difficulties for fish gut microbiota experiments, as stable environmental conditions may not be guaranteed and food has a strong influence on the fish microbiome. While controlled conditions have their clear benefits in separating causal factors contributing to killifish gut microbiota, our specific setup provides an opportunity, as it reflects the actual real-life situation much better, both of non-laboratory wild animals and also humans, which do not adhere to strict diets but have highly changing and varying food input.

Despite the overall stability of the microbiota composition, some genera showed a shift in abundance in the killifish stool samples over time – this was especially seen for Fusobacteria, foremost *Cetobacterium*, which increased in abundance after week 11. This bloom of *Cetobacterium* coincided with the timepoint of a strong decrease in alpha diversity levels from week 11 to week 12 (Fig. 11E). Notably, this was the case for both fish cohorts at the same chronological timepoint, indicating that an external

factor and not intrinsic aging contributed to the diversity drop. Surprisingly, the drop in diversity was not reflected in the food control samples, although I detected a very strong influence of bloodworm microbiota on the killifish stool samples. The time-dependent shift in diversity might therefore be dependent on an unknown environmental factor other than the fish food, including the water microbiota. Another possibility is that other microbes than bacteria such as fungi or viruses, not detected by the chosen 16S amplicon sequencing approach, were emerging in the food samples – which in turn then could have influenced the stool microbiota composition. *Cetobacterium* is a known fish commensal which has been found in several marine and freshwater species (Egerton et al., 2018; Ramírez et al., 2018). It likely plays a role in Vitamin B12 production in fish (H. Sugita et al., 1991) and *Cetobacterium* abundance was shown to correlate with a shift in fish diet (Y. T. Hao et al., 2017). The selective bloom of *Cetobacterium* may have been caused due to low levels of Vitamin B12 in the fish food, resulting in fish specifically selecting for a Vitamin B12-producing bacterial species.

With regards to the longitudinal stool collection study, it is important to note that the lifespan of the second cohort was considerably shorter than expected and observed in the first cohort (Fig. 8D). One possible reason could be that the observed drop in alpha diversity and subsequent shift in composition happened during a critical timeframe in fish life, resulting in several animals not surviving a sudden environmental change. On the other hand, the second cohort only comprised nine individuals and the lifespan data should not be overinterpreted.

3.2.2 Diversity measures remain constant across killifish lifespan

With regards to microbial diversity, I indeed observed lower alpha diversity levels for stool samples from 16-week-old fish compared to 6-week-old fish (Fig. 11D+E), comparable to the observations from our previously published data (Smith, Willemsen, Popkes et al., 2017). However, as the drop in diversity was observed across all samples between week 11 and week 12, comparing data before and after the diversity shift needs to be seen with caution. In addition, I did not observe lower alpha diversity levels in the other datasets I generated, neither in the stool samples nor in the whole

intestines or intestinal sections. The higher beta diversity levels we reported in 2017, which indicated higher inter-individual variability upon age, were not reflected in my new data. In contrast to our previous findings, I thus did not find any changed diversity measures between young and old intestinal or stool samples, at least not for the investigated timepoints and circumstances. Possible reasons for the incongruence might include environmental shifts influencing the microbiota composition, including the water and the food sources. In addition, the investigated timepoints for young and old fish samples do not entirely overlap between the published dataset from 2017 – the published data took 6-week-old and 16-week-old fish into consideration, while my intestinal datasets comprise fish of 8 weeks, 16 weeks or 20 weeks. It might be that there is a strong difference between 6-week-old and 8-week-old fish and thus no strong decrease in diversity to older fish is visible. Such a differences could not be observed in my longitudinal stool collection data – however as previously discussed, stool samples are not directly comparable to intestinal samples. Last, the underlying lifespans of the cohorts could have been different between the dataset from 2017 and my recent datasets, leading to potential differences in the aging process affecting microbiota composition. In support of this, I observed a trend for decreased alpha diversity levels in the dataset comparing young and old male whole intestines, where I analyzed 8-week-old and 20-week-old fish (Fig. 19C). As sampling intestines is an invasive procedure, statements about the underlying cohort lifespans are however not possible.

3.2.3 Specific bacterial taxa are enriched in young and old intestines

Although I did not detect differences in alpha or beta diversity in stool and gut samples between young and old fish, young and old samples clustered separately in the intestinal section dataset, indicating age-specific patterns in microbiota composition. In addition, a subsequent Random Forest classification resulted in an age prediction with an overall accuracy of 0.82. In line with this, DESeq2 differential abundance testing revealed several genera enriched in intestinal samples of young and old fish. Young intestines showed high levels of *Acinetobacter*, *Bradyrhizobium* and *Hyphomicrobium*, while old intestines were enriched for *Vibrio*, *Shewanella*,

Aeromonas and *Streptococcus*. As discussed before, the genera *Aeromonas*, *Vibrio* and *Streptococcus* contain potential pathogenic species, possibly indicating that killifish intestinal aging is accompanied with a shift in microbial composition towards more pathogenic species. The genus *Shewanella* in contrast comprises potential fish probiotic strains, however the exact strains could not be determined with the chosen 16S amplicon sequencing method thus not allowing final statements. Young-associated *Bradyrhizobium* are widespread in the environment and possess the ability to fix nitrogen and aromatic compounds (VanInsberghe et al., 2015). They are often found associated with fish (Khurana et al., 2020) and have been positively correlated with carbon metabolism in fish adipose tissue (Dvergedal et al., 2020).
Hyphomicrobium are one-carbon compound utilizer with the ability to oxidize iron (Martineau et al., 2015). Residing in soils and water sources, they have also been frequently found associated with fish – in the filter microbiota, aquarium water, foregut or skin microbiota of aquarium-reared fish (McDonald et al., 2012; Mudarris & Austin, 1988; Haruo Sugita et al., 2005). This might hint that *Hyphomicrobium* in the killifish derives from the circulating tank water system.
Acinetobacter are also frequently found in fish intestines (Banerjee & Ray, 2017) – the genus comprises several opportunistic pathogens, however one study also found a potential probiotic strain that helped against a known fish pathogen (Bunnoy et al., 2019). Again, 16S sequencing does not provide the necessary resolution to determine the exact strain in the killifish intestine.

Taken together, the longitudinal stool collection study revealed that stool microbiota composition is fairly stable over time, with some timepoints of expansion of specific taxa. In terms of microbiota diversity, no differences could be detected between young and old killifish stool or gut microbiota, in contrast to our previous findings. Nevertheless, I found an enrichment in specific bacterial taxa in young and old age in killifish intestines. As the chosen 16S sequencing method has limited resolution, a final interpretation of the potential function of the young- and old-associated genera in the killifish intestine remains however unknown. One possibility to address this question would be conducting shotgun metagenomics on the samples, as this would allow both

to determine the species and also would provide insight into the function potential of the enriched bacteria.

3.3 Prediction of remaining life based on microbiota composition

The longitudinal collection of stool samples provides not only the possibility to track individual dynamics in microbiota composition over life, but moreover to build predictive models for both age and remaining life. That was only possible because stool sampling is a non-invasive procedure and thus the actual lifespan of each individual fish could be assessed. Indeed, a recent study has shown that application of neural networks on the microbiota composition of human stool samples can be used to predict host age. Based on the data the authors were able to construct a human microbiome clock with a mean absolute error of 5.91 years (Galkin et al., 2020).

In our hands, the Random Forest regressor model could predict fish age, e.g. the collection week of the individual sample (r-value = 0.95, p-value < 0.001, slope = 0.9). However, testing the model on the bloodworm control samples revealed that most predictive power resulted from the underlying bloodworm microbial composition – meaning that age prediction was mainly reflecting the bloodworm food. However, not all predictive power could be explained by bloodworm controls, indicating a key role of either intrinsic fish compositional changes or non-bloodworm extrinsic influences in the prediction models. In the future, we will thus correct for the bloodworm component changes in microbiota composition and will explore the predictability from bloodworm-independent microbial features (work in progress).

Besides fish age, we decided to investigate prediction of remaining life. We thus built a Random Forest regressor model to predict remaining life based on the longitudinal microbiota data. The predictive power for remaining life was weaker, but still present (r-value = 0.69, p-value < 0.001, slope = 0.26).
Interestingly, we found that although the majority of predictive power again was driven by bloodworm food, some predictive power probably originated from different intrinsic

or extrinsic factors. To assess whether the non-bloodworm-originating predictive power stemmed from fish-intrinsic factors, we added individual fish IDs into the model. Notably, including individual fish IDs improved the predictive model, indicating that indeed fish-intrinsic microbial features played a role in the quality of the prediction models. Future work is needed to answer the question whether individual trajectories contribute more to predicting remaining life than global microbiome trajectories. The greater the individuality factor, the harder it will be to build broadly applicable prediction models. On the other hand, it might be that building the prediction models on several instead of single timepoints is a solution to address the individuality problem – possibly not the microbiota composition at a certain time per se is predictive for lifespan, but rather the variability over time or specific patterns of individuality. In the future, we will thus extend our models to incorporate several collection dates into training of the model.

I showed that the data from my longitudinal collection of stool samples can be used to build prediction models of remaining fish life. At the same time some challenges still need to be addressed. First of all, most of the predictive power still arose from the underlying bloodworm microbiota composition, leaving the predictive models to not reveal fish-specific, but mainly food-related patterns.

One possibility to approach this problem would be to include only microbial features that do not appear in food samples – this however leaves only a handful of microbes, too little for training of prediction models. Implementing advanced statistical models such as machine learning to infer intestinal-specific information from the stool microbiota composition, perhaps trained on the gut-stool-food sample types dataset, could be a future way to take into account the relative distribution of bacterial strains. Another option would be to repeat the longitudinal stool collection with a different feeding protocol, using autoclaved food pellets instead of live fish food with intrinsic microbial communities (Žák et al., 2020). This method would reduce the environmental microbiota factors and thus probably yield in stool samples more closely mirroring fish gut microbiota features and not food microbiota. Studies in this direction are ongoing in the lab.

An additional important fact to consider is the retrodictive nature of the built models for remaining life - even if several samples are collected in a longitudinal manner, the lifespan remains unknown until the individual fish dies. The goal of a transferable lifespan prediction model though would of course be to reliably forecast remaining life while the individuals are still alive. With respect to applicability and transferability, retrodiction and the food-dependency of the data are important factors that need to be addressed in the future.

So far, we focused on using microbiota composition as the determining variables to build our predictive models. However, also including diversity measures or individual variability over time could be interesting microbiota-related aspects to train the models, as diversity measures and variability are frequently reported to change upon aging (Claesson et al., 2011; Claesson et al., 2012).

3.4 Compartmentalization of the killifish intestine

The digestive tract plays a key role for organismal health, ensuring nutrient supply and being involved in immune system homeostasis (Chow et al., 2010; Clemente et al., 2012; Gill et al., 2006b). The intestinal tracts of most animals show clear compartmentalization into subregions with unique biological functions, optimizing the digestive process (Karasov et al., 2011; Mowat & Agace, 2014).
As expected from the literature, I found that also the killifish intestine is structured into compartments with different morphological and molecular features. The strongest differences were detected between the anterior sections (S1, S2, S3) and the posterior section (S4), which is in line with the macro-anatomical differences.
As mentioned before, 20% of fish species do not possess a real stomach and are thus agastric (Wilson & Castro, 2010), including zebrafish (Z. Wang et al., 2010). Until now, there is no clear evidence to which of those groups the turquoise killifish can be assigned. Based on my section dataset, I was therefore wondering whether I could find stomach-specific expression patterns for different sections. Unfortunately, I could not make a final statement based on my findings, as no stomach-specific proteins such

as pepsin-like proteins, gastrin or H^+-ATPases were annotated in the proteomics datasets. One possibility to address this still open question would be to measure the pH of the killifish intestinal sections *in vivo*, as gastric proton pumps ensure a low pH. This could however be experimentally challenging given the small size of the killifish intestine. Another possibility would include immunostainings on transverse sections of the killifish gut, targeting stomach-specific proteins such as gastrins, or the generation of transgenic killifish reporter lines.

Considering the global section differences, the functional analysis on molecular level showed an enrichment for metabolic processes and suggested a higher protein biosynthesis in the anterior killifish sections. The high metabolic activity might indicate that several digestive processes take place, which is in line with previous studies showing that the majority of digestion occurs in the anterior intestine in stomachless fish (Le et al., 2019). Proteins enriched in the killifish anterior sections include FABP1 and FABP2, both key proteins involved in the lipid digestion and absorption process. This would be congruent with the lipid metabolism of the mammalian intestine, where lipids are reabsorbed mainly in the small intestine (Ko et al., 2020). I further found an enrichment of goblet cells in the anterior sections on histological level, indicating elevated mucus production. Mucin-producing goblet cells play a key role in intestinal barrier function including the protection of the epithelial intestinal layer from digestive enzymes (Birchenough et al., 2015), supporting the hypothesis that the majority of digestive processes occur in the anterior killifish intestine. It is important to note however that mammals show an inverse pattern in mucus density with a thicker mucus layer in the colon tissue, serving as a protection layer for the high-density microbiota.

The posterior section in contrast was characterized by transport processes, including vesicular transport and lysosomal activity. This is in line with previous studies hypothesizing that specialized, lysosome-enriched vacuolated enterocytes (LREs) can aid in protein uptake and enhance protein digestion, which is often impaired in stomachless fish due to low protease activity (Rombout et al., 1985). Interestingly, one of the key components for the endocytotic machinery essential for LRE-function is Cubilin (CUBN), a protein that is highly enriched for the posterior section in my

proteomics data. The posterior killifish intestine could thus be an important region specialized in protein uptake.
Other proteins with increased expression in the posterior killifish section include FABP6 and ENPEP, proteins enriched in the midgut of zebrafish or the distal small intestine in mice (Lickwar et al., 2017). I moreover found LAMP1 to be significantly enriched in the posterior killifish section - LAMP-genes, in particular LAMP2, have been associated with mammalian colon tissue and the zebrafish hindgut (Lickwar et al., 2017). Other specialized functions of the mammalian colon or the zebrafish hindgut include water retention, shown by a high expression of aquaporins. However, no aquaporins were annotated in the proteomics datasets – it was thus not possible to check the spatial expression patterns of potential water retention molecules. A different analysis approach, also considering proteins that were not measured in all samples, could shed light on the question whether these proteins are expressed only in the posterior killifish intestine.

Taken together, I found that the killifish intestine shows clear compartmentalization on the molecular level. The detected protein signature of the killifish posterior section interestingly combined features of both the mammalian distal small intestine and colon, while the anterior killifish sections showed a clear small intestine-like signature. The killifish intestine thus shares important elements with mammals, implying that the killifish is a well-suited model for intestinal research, at least to some extent.

The different intestinal compartments provide highly specialized niches for microbes, resulting in spatial organization of microbial communities for several animals including humans (Sheth et al., 2019; Zoetendal et al., 2012). In contrast to observations in other fish (Gajardo et al., 2016; Kokou et al., 2019), I did not find strong differences in microbiota composition along the killifish intestinal tract (Fig. 31A). One possible explanation is that the killifish intestine is very short compared to the fish where microbiota differences have been reported, hence microbiota can quickly move between the different killifish intestinal sections. Another explanation could be that the resolution level of the chosen 16S sequencing approach is not high enough – shotgun

metagenomics could here be a better approach, enabling the detection of bacterial species and strains and moreover also other microorganisms such as viruses.

I lastly found that both primary and secondary bile acid levels decreased along the intestinal tract. This could suggest a constant uptake of bile acids along the intestinal tract, in contrast to mammals where the majority of bile salt reabsorption occurs in the distal small intestine (De Aguiar Vallim et al., 2013), or just be a result of diffusion processes as bile is secreted to the gut lumen in the anterior part of the intestine. Based on measurements of bile acid uptake in a killifish species, Honkanen & Patton already hypothesized in 1987 that passive reabsorption of bile salts along the whole intestinal tract is the main factor of bile salt resorption in fish. Moreover, similar levels of primary and secondary bile acids also imply that bacterial conversion from primary to secondary bile salts take place everywhere in the killifish intestine and is not "overrepresented" in specific regions, like in the mammalian colon (Ridlon et al., 2006). This is further supported by the fact that I did not find any global difference in microbiota composition in the four sections.

3.5 The killifish intestine during age and sex

I already discussed the age- and sex-specific patterns with regards to microbiota composition. However, several studies reported strong differences with regards to sex and age effects on the host side (Austad & Fischer, 2016; López-Otín et al., 2013; Regan et al., 2016).

3.5.1 The killifish intestine shows age-specific morphological and molecular features

In line with previously reported age differences, I found several striking phenotypes with regards to killifish intestinal aging, both on a morphological and a molecular level. Interestingly, IGF2BP3 was highly abundant in the intestinal samples from young fish. IGF2BP3 binds to the insulin-like growth factor and is implicated in several functions

within cellular metabolism, such as cell migration, proliferation and differentiation (Bell & Zamudio, 2012). IGF2BP3 levels were also shown to decline during zebrafish aging (Arslan-Ergul & Adams, 2014). Another protein enriched in the young fish samples was glycine amidinotransferase (GATM), an enzyme producing the direct precursor of creatine. Creatine has important roles in muscle energy metabolism, and several studies have reported decreased levels of muscle creatine in aged individuals (McCully et al., 1991; S. A. Smith et al., 1998). Interestingly, several studies suggest that creatine-supplementation in aged individuals may ameliorate common age-related features such as decreased muscle strength and lower fatigue resistance (Rawson et al., 1999; Stout et al., 2007). Both the enrichment of IGF2BP3 and GATM indicate active cell metabolism in the young killifish intestine. In line with this, I found pyruvic acid as a key intermediate metabolite from metabolic pathways being enriched in young samples – and GO-term enrichment analysis resulted in several terms related to active cell processes, including translation and metabolism terms.

Proteins enriched in old fish intestines included Clusterin (CLU), a protein potentially involved in apoptosis. Interestingly, clusterin has been reported as a senescence biomarker (Gonos et al., 1998) and is involved in many age-related pathologies such as neurodegenerative diseases and cancer (Foster et al., 2019; Koltai, 2014). The elevated CLU levels in the old gut sections thus might indicate increased senescence in the old killifish intestine. Moreover, the metabolomic analysis revealed elevated levels of sphingomyelins upon killifish aging. Sphingomyelins belong to the class of sphingolipids, which are complex lipids ensuring cell membrane fluidity and which are involved in cell signaling processes (MacEyka & Spiegel, 2014). Notably, accumulation of sphingomyelins in later life has also been shown in *C. elegans* (Gao et al., 2017) and human plasma and serum metabolomics (Jové et al., 2017; Mielke et al., 2015; Yu et al., 2012). Other studies in humans did not report a difference in sphingomyelin levels upon aging (Kawanishi et al., 2018) and observed an increased risk for diabetes and neurological diseases for low sphingomyelin levels (Gonzalez-Covarrubias et al., 2013; Han et al., 2011). Increased incorporation of sphingomyelins into cell membranes upon aging might also indicate changed sphingomyelin metabolism as an adaptation to oxidative stress (Clement et al., 2009; Yu et al., 2012).

In addition, I observed elevated levels of 4-Hydroxyproline in intestinal samples of old fish. 4-Hydroxyproline is a major component of collagen and is responsible for the stability of the collagen fibers. An increased level of 4-Hydroxyproline upon aging could indicate either a higher collagen abundance in old intestinal tissue, or a change in collagen substructure with an increased proportion of proline hydroxylation. Remarkably, quantification of the SRFG histological staining revealed an increase in extracellular matrix collagen levels for all the intestinal sections upon old age, confirming the hypothesis that the intestinal extracellular matrix is restructured during the aging process. In addition, enrichment analysis of the proteins differentially expressed in old intestines resulted in the term *collagen-containing ECM*.

With regards to structural changes in the aging intestine, I moreover found an increase in muscle thickness in samples from old fish. Several studies reported an increase in cell wall thickening upon aging in the vascular system (Lacolley et al., 2018) or in diseases (X. Wang et al., 2020; Zwingenberger et al., 2010). It has moreover been shown that the signaling and contractibility of intestinal smooth muscles is impaired in aging (Saffrey, 2014).

It is important to note that also the intestinal diameter increased with age – which makes sense, as the killifish continues to grow along its life. One might speculate that the increase in muscle thickness is thus a direct, passive consequence of the increase in intestinal diameter. However, correlation analysis between muscle thickness and total section diameter did not show a significant correlation (Pearson correlation, $r = 0.264$, p-value = 0.138), indicating that other factors play a role in the increased muscular layer thickness in old age. Based on the results, it is not possible to make a final conclusion about the extent of passive, age-related intestinal growth on muscular thickness – to address this question, one would have to investigate young and old fish with a size-matched intestine. Notably however, the GO-term and pathway enrichment analyses resulted in terms associated with muscular function and metabolism. Together with the increase in extracellular matrix collagen upon aging, I hypothesize that the increase in muscle thickness contributes to a higher stiffness of the aging killifish intestine, impeding normal intestinal functions.

Taken together, I found evidence that the killifish intestine shows classical aging phenotypes such as increased senescence and higher sphingomyelin levels – and moreover restructuring of the extracellular matrix upon aging, especially concerning increased collagen levels in old age, potentially impeding the normal intestinal function.

3.5.2 The killifish intestine shows sex-specific molecular patterns

Next to biological age, sex is a major influencing factor for host physiology - and interestingly, several studies have shown sex-specific aging phenotypes (Austad & Fischer, 2016; Regan et al., 2016). Structural sex differences in the human gastrointestinal tract include the intestinal length (Saunders et al., 1996), prevalence of gut-associated diseases (Lovell & Ford, 2012) and also the absorption of specific nutrients (Johnson et al., 1992). In line with this, my results show clear differences between male and female intestinal samples on a molecular level.

The female intestinal samples were highly enriched for Vitellogenin 1 (OL-VIT1), which is an egg-yolk protein precursor only produced by female individuals and can therefore serve as a proof of concept. Other proteins with high abundance levels in female fish intestines include Nfu_g_1_011468 and ECM1. Nfu_g_1_011468 is predicted to be a lipocalin-like protein. Lipocalin proteins have various functions, including an important role in innate immunity, tumorigenesis and iron homeostasis (Lu et al., 2019). Interestingly, Lipocalin-2 was shown to act in a highly sex-specific manner (Chella Krishnan et al., 2019). It moreover has been connected with adipocytes and obesity – one study showed that Lipocalin-2 has an anti-inflammatory effect on adipocytes resulting in browning of the fat tissue, and thus proposed Lipocalin-2 as a potential anti-obesogenic molecule (Meyers et al., 2020). The high levels of Lipocalin-like proteins in female intestines might be linked to the increased levels of lipids observed in the metabolomics datasets - compared to males, female intestines showed a higher abundance of FFAs, lysoPCs and DAGs. Gender differences in lipid metabolism are indeed well-known (Baars et al., 2018; Mittendorfer, 2005).

ECM1 is an extracellular matrix protein which is involved in several important physiological processes, including macrophage polarization, cancer biology and bone formation (Deckers et al., 2001; Zhang et al., 2020). It also interacts with several structural proteins, influencing skin homeostasis. Interestingly, high levels of ECM1 have been found to prevent fibrogenesis in liver tissue (Fan et al., 2019).

This is in line with the findings for the intestinal sections of male fish, where the GO-term and pathway enrichment analyses resulted in several fibrinogen- and coagulation-related terms. In addition, male intestines show high levels of Hemopexin (HPX). HPX is a glycoprotein with a very high binding affinity to heme, and thus functions as a heme scavenger and protects against oxidative stress and heme toxicity (Takagi et al., 2012; Tolosano & Altruda, 2002). As excessive heme in the blood contributes to coagulation (Sparkenbaugh et al., 2015), the high HPX levels in male intestines might be an approach to limit male-specific increased coagulation. In total, the data suggests that the fibrinogen-coagulation-cascade shows sex-specific patterns in the killifish intestine.

Among the proteins with the highest enrichment in males are two apolipoproteins, apolipoprotein B (APOB) and apolipoprotein H (APOH). Apolipoproteins bind lipids and form lipoproteins to transport lipids in the vascular system and other body fluids (Von Zychlinski et al., 2014). APOB is a primary constituent of chylomicrons and LDL-particles and has been correlated with an increased risk for vascular diseases such as atherosclerosis (Sniderman et al., 2010). Although named to be an apolipoprotein, APOH in contrast is not a major component of lipoproteins but involved in the agglutination of platelets, where it has anti-coagulation effects (Nimpf et al., 1987) – again supporting the hypothesis of sex-specific coagulation phenotypes. The high levels of APOH in male intestines could therefore also act as a compensatory mechanism to the high fibrinogen levels in the male intestines. In line with the male-specific upregulation of apolipoproteins, GO-term and pathway enrichment analyses resulted in several lipoprotein and lipid-related terms enriched in male intestines.
Another interesting connection to lipoproteins are the high male-specific Taurine levels I found in the metabolomic datasets. Taurine is an amino sulfonic acid which is

distributed widely among different tissues. It is important for bile acid metabolism, as it is conjugated to bile acids in the liver to form bile salts (Russell, 2003). Taurine moreover plays an essential role in cardiovascular function, the muscular system and has an antioxidant function (Jong et al., 2012; Warskulat et al., 2004; Xu et al., 2008). Interestingly, Taurine has also been reported to decrease secretion of APOB-100 (Yanagita et al., 2008) – the high Taurine levels might therefore be another compensatory mechanism for the high APOB levels observed in the male intestines.

I moreover found increased levels of secretagogin (SCGN) and 27-Dihydroxycholesterol in the male samples. SCGN is a protein highly expressed in the brain, pancreas and the gastrointestinal tract. It is involved in exocytotic processes and has been connected to secretion of several hormones in different tissues (Qin et al., 2020). The high levels of SCGN in killifish male intestines might thus be related to sex hormone levels. 27-Dihydroxycholesterol is a cholesterol oxidation product with pro-inflammatory properties. It is reported to be involved in gastrointestinal and neurodegenerative diseases, as well as in cancer biology (Willinger, 2019). One intriguing study found that 27-Dihydroxycholesterol induced gut microbiota perturbations, which negatively impacted SCFA levels and promoted inflammation and intestinal barrier failure (Y. Wang et al., 2020). Male intestines could therefore show more inflammation or a weaker gut barrier – indeed, GO-term and pathway enrichment indicated immunological alterations in the male killifish intestine.

One last interesting aspect are the increased sex differences I observed upon aging, both on metabolite as well as protein level (Fig. 43). This might appear counterintuitive, as aging in humans is associated with a loss of sex hormones (Horstman et al., 2012) and thus converging of male and female molecular signatures could be assumed. In contrast, studies in flies suggest a female-specific aging phenotype (Regan et al., 2016) and also intestine-related diseases show sex-specific prevalence (Lovell & Ford, 2012), indicating that intestinal aging might have sex-specific patterns. However, there are no convincing studies specifically addressing molecular sex differences with age and thus a final conclusion is still pending.

Taken together, my data suggest that the fibrinogen-coagulation-cascade and lipid/lipoprotein metabolism show sex-specific patterns in the killifish intestine – and that the molecular differences in sex increase upon aging.

3.6 Correlations between metabolites and microbiota

The multi-omics datasets I generated are based on the same individual samples, including information about the morphological and molecular host side as well as on the microbial side, opening the unique opportunity to draw correlations between single features of the datasets. As a starting point, I focused on using linear regression analysis between the annotated metabolites and the most prevalent genera, which enabled me to find several strong correlations.

Of particular interest was the negative correlation between 4-Hydroxyproline and *Hyphomicrobium*, implying that high levels of 4-Hydroxyproline correlate with low levels of *Hyphomicrobium*. As discussed before, 4-Hydroxyproline is a major component of collagen structures, and I found strong evidence for a changed collagen metabolism upon killifish intestinal aging. Notably, this goes in line with the DESeq2 differential abundance testing, which resulted in *Hyphomicrobium* as a young-associated genus. As discussed earlier, *Hyphomicrobium* are one-compound carbon utilizer with the ability to oxidize iron (Martineau et al., 2015). A connection between *Hyphomicrobium* and collagen metabolism has so far not been reported - *Hyphomicrobium* could be an interesting candidate for further studies related to investigating changed collagen metabolism upon aging.

In addition, I found a positive correlation between an unknown genus from the *Rhizobiaceae* family and two bile acids, the primary acid Taurocholic acid and the secondary bile acid 7-oxo-Taurodeoxycholic. The data thus indicated that the unknown genus might be involved in bile acid metabolism processes. Members of the *Rhizobiaceae* family are particularly known for their association with plants, where

they can promote plant growth but also act as plant pathogens (Poole et al., 2018), and have been found several times in fish intestines (Sullam et al., 2012; Wei et al., 2018). Interestingly, a zebrafish study investigating a gluten-rich, plant-based diet found increased levels of *Rhizobiacea*, among others, and a functional enrichment in bile acid metabolism (Koo et al., 2017). However, a convincing direct connection between bile acid metabolism and *Rhizobiacea* has so far not been reported to my knowledge.

Future work will be needed to expand the preliminary correlation analyses to the other multi-omics datasets, including proteomics data and also the non-annotated metabolites. As one important aspect we will improve the statistical approach by implementing Bayesian statistics, allowing us to better test hypotheses generated from the multi-omics dataset.

Lastly, vast parts of the generated metabolomic data consists of non-identified metabolites. As an encompassing manual annotation of all metabolites is a big effort, we might use correlation analyses to limit the metabolites to a manageable number.

Annotation of more metabolites would open the possibility to integrate metabolites and proteins in metabolic networks, to gain even more functional insight into the data and potentially detect novel aging- or sex-related pathways.

3.7 Future perspectives

While I have uncovered exciting molecular and morphological changes and profiled the spatiotemporal dynamics in the killifish intestine, further work is needed to confirm my findings and further improve the understanding of spatiotemporal changes in the killifish intestines.

The longitudinal stool collection provided first insights into the microbiota dynamics of individual fish over life and excitingly enabled building first prediction models for remaining fish lifespan. The analysis was impacted by the fact that bloodworm-derived food microbiota had a great contribution on fish stool microbial composition. Ongoing work in our lab is thus focused on repeating the longitudinal stool collection on fish raised with sterile food pellets, to possibly obtain stool microbiota profiles reflecting more the killifish intestinal microbiota. Such a dataset would not only allow to again profile the age-related intestinal microbiota changes without the interfering food microbiota, but moreover help with building the prediction models for age and remaining life. Once the new prediction models are set up, the models need to be tested on additional cohorts to validate the applicability of our findings. In the long term, the prediction models could result in bacterial biomarkers for aging. Bacterial candidates identified should also be extracted from the killifish gut, cultivated and then tested as potential lifespan-extending factors by providing them to the killifish at different life stages.
Importantly, we aim to take our findings to a higher level by also assessing longitudinal microbiota changes in mammals such as mice to build prediction models for age and remaining life. In the long term, we hope to find functional patterns that can deepen our understanding of the link between intestinal microbiota and human aging.

In this thesis, I further set out to explore whether stool samples reflect intestinal microbial features and thus can be used as a non-invasive proxy for gut microbiota. While I found shared features of stool and gut with regards to microbiota composition, it will be interesting to investigate not only the presence/absence of microbial species but expanding the analysis taking into consideration relative abundances. Including

relative abundances might result in a more detailed picture of shared microbial features, and moreover could improve the outcome of analyses which aim to identify gut-related features from stool samples.

In addition, applying shotgun metagenomics on stool and gut samples would allow a finer resolution with the determination of bacterial species and strains, and moreover would provide insight into the functional capacities of microbes shared between stool and intestinal samples. It would moreover be interesting to use shotgun metagenomics to challenge my finding of section-unspecific microbial communities along the killifish intestinal tract. Perhaps this could lead to detecting section-specific differences on species level and could moreover reveal changed functional capacities of possibly existing microbial niches. First insights into the functional profiles of the intestinal section microbiota and thus their interaction with the host environment could already be revealed by applying metaproteomic analysis on the already generated proteomic dataset by using the imetalab platform (Liao et al., 2018).

Utilizing shotgun metagenomics in the future holds another exciting advantage – as the whole genetic material is analyzed and no prior amplification of a specific bacterial gene is performed, shotgun metagenomics provides a unique picture of the interconnected microbial communities, including not only information about bacteria but also about fungi, viruses and protists.

In my thesis, I last focused on profiling age- and sex-specific aspects of the killifish intestine on a detailed level, with a particular focus on the host side. I found evidence on both molecular and morphological level for an age-associated accumulation of collagen in the intestine. To determine whether this collagen increase is associated with fibrotic phenotypes, we have to perform additional experiments. While mechanical testing of stiffness has been established for mammals (Stewart et al., 2018), this might be challenging in killifish due to the small intestine size. We will therefore check intestinal inflammation markers with qPCR, as fibrosis usually results from inflammation processes (Wynn, 2008). If we are able to confirm the intestinal age-related fibrosis, it will be interesting to explore whether we can find a way to eliminate or ameliorate with fibrotic aging phenotype, and whether lower intestinal fibrosis would extend killifish lifespan. Possibilities would include the use of anti-fibrotic drugs, for

example targeting TGF-β (Györfi et al., 2018), or genetic manipulation of key fibrosis-related pathways, as recently shown to be effective in lung fibrosis in mice (Rehan et al., 2021).

The multi-omics dataset already revealed potential age-related pathways in the intestine. Future analyses including the additional annotation of metabolites will most likely uncover even more intestinal processes linked to aging. To gain mechanistic insights and set the foundation for potential anti-aging and lifespan extending treatments, we would like to directly target those pathways by supplementation of specific compounds or genetic interventions targeting key components of identified pathways. Ultimately, we hope to extend our findings to mammals by extending our results to mice or even humans.

Chapter 4

Methods

4.1 Killifish husbandry and sample-preparation

4.1.1 Killifish husbandry and lifespan assessment

Turquoise killifish were individually housed from week 4 post-hatching in 2.8 L tanks. The tanks were connected to a water recirculation system with a light:dark cycle of 12h:12h. The water temperature was kept at 28°C. Fish were fed with bloodworm larvae and brine shrimp nauplii twice a day during the week, and once a day during the weekend. Feeding took place at the same time every day. For lifespan assessment, the fish tanks were checked daily for dead fish. Dead fish were stored in 95% ethanol. Lifespan analysis was carried out using the *survival* and *survminer* packages in R (Alboukadel Kassambara et al., 2020; Therneau, 2020).

4.1.2 Intestinal tissue extraction

Fish were sacrificed with 1.5 g/L Tricaine solution, the intestine was extracted and cut, shortly washed in 1x PBS-solution and then snap-frozen in liquid nitrogen. Young fish intestinal samples were taken at 8 weeks, old fish samples were taken at 16 or 20 weeks.

4.1.3 Collection of stool and food samples

For collection of stool samples, recently fed fish were shortly “washed” in autoclaved tank water and then transferred into single 0.8 L tanks containing 0.5 L autoclaved tank water. Stool was collected every hour and frozen in RNA*later* (Thermo Fisher) at –80°C. After 6 h, the fish were transferred back to the main system. For collection of food samples, brine shrimp and bloodworm were either sampled in separate tubes or mixed together in one tube (according to the feeding routine at the given timepoint) and stored in RNA*later* at –80°C.

4.2 Molecular methods

4.2.1 Simultaneous extraction of metabolites, proteins and DNA

To simultaneously extract DNA, protein and metabolites of intestinal fish sections, I adapted a protocol from Valledor et al. (2014). The frozen samples were pulverized by bead-beating with two steel beads for 1 min at 30 Hz. 800 µl extraction buffer (Methanol:Chloroform:H_2O in a ratio of 2.5:1:0.5, including standards: AA-mix (25 µL, MSK-A2-1.2, Eurisotop), 18:1-d7 LysoPC, 15:0-18:1-d7-PC, 15:0-18:1-d7-15:0 TG (3 µL each, SigmaAldrich)) was added and samples were vortexed shortly, followed by an incubation at 4°C and centrifugation at 800 rpm for 45 minutes. Afterwards, the beads were removed with a magnet and the appropriate volume for protein extraction was taken off into a new tube. Both tubes were then centrifuged for 1 h at 20.000 x g at 4°C. The supernatants were transferred and into a new tube, the pellets were dried in a SpeedVac for 20 mins and then stored at -80°C. 600 µl from the combined supernatant was pipetted into a new tube and 300 µl of each, H_2O and Chloroform, was added. The samples were shaken for 15 mins at 4°C, then centrifuged for 15 mins at 10.000 x g at 4°C. Next, the aqueous upper phase was carefully transferred into a new tube, the interphase generously discarded and the lower lipid phase was pipetted into a fresh tube. The aqueous phase was dried in a SpeedVac for 3h and both phases were stored at -20°C.

4.2.2 DNA isolation after multi-omics extraction

To isolate DNA from the pellet after metabolite extraction, 0.1 g of 0.1 mm zirconia/silica beads (Carl Roth) and 300 µl of DNA extraction buffer (80 mM EDTA, 200 mM Tris (pH 8.0) and 0.1M NaCl in PBS) were added to the pellets. The samples were lysed for 2 x 3 min at 30 Hz in a TissueLyser (Qiagen) and then centrifuged at 8.000 x g for 5 minutes at 15°C. 78 µl of the supernatant was transferred into PCR tubes containing 2 µl of RNAse A (Qiagen), the rest of the supernatant was stored at -20°C. The PCR-tube was shortly vortexed and incubated for 30 mins at 55°C. Afterwards, 10 µl Proteinase K (Thermo Fischer) and 10 µl 20% SDS were added, the

samples again shortly vortexed and then incubated for 1 h at 56°C. Next, 40 µl of C2 solution (Qiagen) were added to the samples and the samples were shortly mixed and incubated for 5 min at 4°C. 100 µl of supernatant was then transferred to a new PCR tube containing 35 µl of C3 (Qiagen) solution. Again, the samples were shortly mixed and incubated for 5 min at 4°C. 100 µl of the supernatant was transferred to a new PCR tube containing 100 µl pre-warmed SeraMag beads, with short mixing. The samples were incubated for 10 min at RT and then put on a magnet. After 5 min, the beads were drawn to the magnet and the supernatant was discarded. The beads were washed 2x with 150 µl of fresh 80% Ethanol and then air-dried for 5-10 min. The dried bead pellet was finally resuspended in 20 µl of nuclease free water.

4.2.3 DNA isolation from fresh stool, intestinal and food samples

To isolate DNA from fresh tissue samples, the protocol from 4.2.2 was followed except that 15-20 1.4 mm steel beads (Carl Roth) were added next to the zirconia/silica beads. Elution volumes also differed, with 17 µl (stool samples), 20 µl (food samples) and 30 µl (intestinal samples).

4.2.4 Library preparation for 16S-sequencing

Isolated DNA was used in a two-step PCR designed to target either the variable V3/V4 region of the 16S rRNA (intestinal, stool and food samples of result part 2 and 3) or to target the variable V4 region (intestinal and food samples of result part 1). In the first PCR, the primers consisted of V3/V4 or V4 gene-specific sequences plus Illumina overhang adaptor sequences to amplify the 16S V3V4 or V4 gene region. In the second PCR, individual barcodes and Illumina sequencing adapters were attached to the amplicons. PCR reactions were run in triplicate reactions to reduce PCR bias. All PCR reactions were prepared with KAPA HiFi Hotstart ReadyMix according to Table 2 and Table 5.

The first PCR reaction was carried out as stated in the Table 3 below, with 30/26 cycles of denaturation, annealing and elongation (30 cycles for intestinal samples, 26 cycles for food and stool samples). The used DNA input was varying between sample type, with 1 ng for stool samples, 5 ng for food samples and 30 ng for intestinal samples.

Triplicate reactions were pooled and cleaned using a bead-based approach as described before. The second PCR reaction was carried out with the same cycling conditions as stated above, but annealing cycles were reduced from 30/26 cycles to 8 cycles (Table 6). The PCR products of the second step PCR were cleaned as before and ran on a 2% agarose gel to confirm specific products. Cleaned DNA was quantified with the Qubit 2.0 fluorometer (Thermo Fisher, DNA HS assay kit) and pooled in equimolar ratios. The quality of the libraries was assessed via TapeStation analysis (Agilent, D1000 tape).

Table 2: PCR reaction composition for 16S rRNA library preparation - Step 1

Reagent	**Volume (µl)**	**Final concentration**
KAPA HiFi Hotstart ReadyMix	12.5	1x
Template DNA	1-10.5	
Primer fw + rv (Table 4)	2	5 µM
ddH_2O	up to 25	

Table 3: PCR program for 16S rRNA library preparation - Step 1

Temperature [°C]	**Time [min:sec]**	**Action**	**Cycle number**
98	3:00	Denaturation	1
98	0:30	Denaturation	26/30
61	0:30	Annealing	
72	0:30	Elongation	
72	5:00	Final elongation	1

Table 4: Primers used for 16S rRNA library preparation – Step 1

Primer	Primer sequence 5' to 3'
V3V4_341_fw	ACACTCTTTCCCTACACGACGCTCTTCCGATCTCCTACGGGNGGCWGCAG
V3V4_805_rv	GTGACTGGAGTTCAGACGTGTGCTCTTCCGATCTGACTACHVGGGTATCTAATCC
V4_515_fw	ACACTCTTTCCCTACACGACGCTCTTCCGATCTGTGYCAGCMGCCGCGGTAA
V4_806_rv	GTGACTGGAGTTCAGACGTGTGCTCTTCCGATCTGGACTACNVGGGTWTCTAAT

Table 5: PCR reaction composition for 16S rRNA library preparation - Step 2

Reagent	Volume (μl)	Stock concentration
KAPA HiFi Hotstart ReadyMix	12.5	2x
PCR 1 elution	7.5	
Primer fw +rv (Supplementary Table 1)	5	2 μM

Table 6: PCR program for 16S rRNA library preparation - Step 2

Temperature [°C]	Time [min:sec]	Action	Cycle number
98	3:00	Denaturation	1
98	0:30	Denaturation	8
61	0:30	Annealing	
72	0:30	Elongation	
72	5:00	Final elongation	1

2.2.5 Illumina sequencing

The combined libraries were sequenced on the Illumina HiSeq platform with 2 x 250bp paired-end reads (part 1) or on the Illumina MiSeq platform with 2 x 300bp paired-end reads (part 2 and 3). Sequencing was conducted by Admera Health, LLC.

4.2.6 Protein extraction and peptide preparation for proteomics

Proteins from frozen pellets were extracted with a guanidine chloride protocol. 20 µl of lysis buffer (6M Guanidinium chloride, 2.5 mM Tris(2-carboxyethyl)phosphin, 10 mM chloroacetamide, 100 mM Tris-HCl) was added to the pellet, depending on the pellet size. The samples were heated for 10 min at 95°C and then lysated with a Bioruptor for 10 cycles of 30 s sonication and 30 s break on high performance. The samples were then centrifuged at 20.000 x g for 20 minutes. The supernatant was transferred into a new tube and the protein concentration was measured via Nanodrop.

To prepare peptides, 300 µg of protein per sample was digested with 1:200 Trypsin (w/w) at 37°C overnight. The digest was then acidified with formic acid (FA) to a final concentration of 1% to stop tryptic digest. The samples were then centrifuged at 20.000 x g for 10 minutes to pellet any remaining debris.

The peptides were then cleaned with a StageTip protocol (C18-SD tips), including a series of wetting, equilibrating, washing and eluting steps. The C18-SD tips were first washed with 200 µl methanol by centrifugation for 1 minute, followed by a wash with 200 µl 40% acetonitrile (ACN)/0.1% FA by centrifugation for 1 minute. The tips were then equilibrated with 200 µl 0.1% FA by centrifuging for 1 minute. The digests were then loaded onto the tips and centrifuged for 2 minutes to ensure proper loading. The tips were washed twice with 200 µl 0.1% FA, followed by elution of the peptides with 100 µl 40% ACN/0.1% FA by centrifuging for 4 minutes at 1500 x g. The eluates were dried in a Speed-Vac at 45°C for 45 minutes, then resuspended in 0.1% FA and quantified with NanoDrop.

4.2.7 Proteomics

Proteomics was conducted by the MPI Proteomics core facility:

Four micro grams of the eluted peptides were dried and reconstituted in 9 µL of 0.1 M TEAB. Labeling with Tandem Mass Tags (TMTpro™ 16plex, Thermo Fisher Scientific) was carried out according to manufacturer's instruction with the following changes: 0.5

mg of TMTpro™ 16plex reagent was re-suspended with 33 μL of anhydrous ACN. Seven micro liters of TMT reagent in ACN were added to 9 μL of peptide resuspended in 0.1 M TEAB. The final ACN concentration was 43.75% and the ratio of peptides to TMT reagent was 1:20. After 60 min of incubation, the reaction was quenched with 2 μL of 5% hydroxylamine. Labelled peptides were pooled, dried, re-suspended in 200 μL of 0.1% formic acid (FA), split into two equal parts, and desalted using home-made STAGE tips (Rappsilber et al., 2003).

One of the two parts was fractionated on a 1 mm x 150 mm ACQUITY column, packed with 130 Å, 1.7 μm C18 particles (Waters cat. no SKU: 186006935), using an Ultimate 3000 UHPLC (Thermo Fisher Scientific). Peptides were separated using a 96 min segmented gradient from 1% to 50% buffer B for 85 min and from 50% to 95% buffer B for 11 min, at a flow of 30 μL/min with a; buffer A was 5% ACN, 10 mM ammonium bicarbonate (ABC), buffer B was 80% ACN, 10 mM ABC. Fractions were collected every three minutes, and fractions were pooled in two passes (1 + 17, 2 + 18 … etc.) and dried in a vacuum centrifuge (Eppendorf). Dried fractions were re-suspended in 0.1% formic acid (FA) and separated on a 50 cm, 75 μm Acclaim PepMap column (Product No. 164942 Thermo Fisher Scientific) using an EASY-nLC1200 (Thermo Fisher Scientific). The analytical column was operated at 50°C. The separation was performed using a using a 90 min linear gradient from 6% to 31% buffer; buffer A was 0.1% FA, buffer B was 0.1% FA, 80% ACN. Eluting peptides were analyzed on am Orbitrap Lumos Tribrid mass spectrometer (Thermo Fisher Scientific) equipped with a FAIMS device (Thermo Fisher Scientific). The FAIMS device was operated at two compensation voltages: -50V and -70V. Mass spectrometric data were acquired in a data-dependent manner with a top speed method. For MS1, the mass range was set to 350–1500m/z and resolution to 60K. Maximum injection time was 50 ms and the AGC target to 4e5. Peptides were fragmented using collision-induced dissociation; collision energy was to 35%. Peptide fragment MS2 spectra were acquired in the ion trap with a maximum injection time of 50 ms and “Turbo” scan rate, using an AGC target of 1e4. The ten most abundant peaks were subjected to Synchronous Precursor Selection and fragmented using higher-energy collisional dissociation; collusion energy was set to 65%. The resulting MS3 spectra were acquired in the Orbitrap at a resolution of 50K.

4.2.8 Metabolite preparation and metabolomics

Metabolomics was conducted by the MPI Metabolomics core facility:

BZ dataset:

The LC-HRMS analysis of amine-containing compounds was performed using an adopted benzoylchlorid-based derivatisation method (Wong et al., 2016).

In brief: The polar fraction of the metabolite extract was re-suspended in 150 µL of LC-MS-grade water (Optima-Grade, Thermo Fisher Scientific). 30 µL of the cleared supernatant were mixed in a critical clean autosampler vial equipped with a 200 µL glass insert (Chromatography Accessories Trott, Germany). The extract was mixed with 15 µl of 100 mM sodium carbonate (Sigma) followed by the addition of 15 µl 2% [v/v] benzoylchloride (Sigma) in acetonitrile (Optima-Grade, Thermo Fisher Scientific). Samples were vortexed and kept at 20°C until analysis.

For the analysis, 1 µl of the derivatized sample was injected onto a 100 x 2.1 mm HSS T3 UPLC column (Waters). The flow rate was set to 400 µl/min using a buffer system consisted of buffer A (10 mM ammonium formate (Sigma), 0.15% formic acid (Sigma) in Milli-Q water (Millipore)) and buffer B (acetonitrile, Optima-grade, Fisher-Scientific). The column temperature was set to 40°C, while the LC gradient was: 0% B at 0 - 4.1min; 0-15% B 4.1 – 4.5 min; 15-17% B 4.5-11 min; 17-55% B 11 – 11.5 min, 55-70% B 11.5 - 13 min; 70-100% B 13 - 14 min; 100% B 14 -14.1 min; 100-0% B 14.1-19 min; 0% B. The mass spectrometer was operating in positive ionization mode recording the mass range m/z 100-1000. The heated ESI source settings of the mass spectrometer were: Spray voltage 3.5 kV, capillary temperature 300°C, sheath gas flow 60 AU and aux gas flow 20 AU at a temperature of 340°C. The S-lens was set to a value of 60 AU.

Untargeted and semi-targeted data analysis for these samples was performed using the opensource software ElMaven (Agrawal et al., 2019), while targeted Peak annotation was performed using the TraceFinder software (Version 4.1, Thermo Fisher Scientific). The identity of each compound annotated by TraceFinder was validated by authentic reference compounds. Peak areas of $[M + nBz + H]^+$ ions were

extracted using a mass accuracy (<5 ppm) and a retention time tolerance of <0.05 min.

IC dataset:

Extracted metabolites were re-suspended in 150 µl of Optima UPLC/MS grade water (Thermo Fisher Scientific), of which 50 µl were transferred to p*olypropylene* autosampler vials (Chromatography Accessories Trott, Germany) before analysis.

The samples were analysed using a Dionex ionchromatography system (Integrion, Thermo Fisher Scientific) as described previously (Schwaiger et al., 2017). In brief, 5 µL of polar metabolite extract were injected in push partial mode using an overfill factor of 1, onto a Dionex IonPac AS11-HC column (2 mm × 250 mm, 4 µm particle size, Thermo Fisher Scientific) equipped with a Dionex IonPac AG11-HC guard column (2 mm × 50 mm, 4 µm, Thermo Fisher Scientific). The column temperature was held at 30°C, while the auto sampler was set to 6°C. A potassium hydroxide gradient was generated using a potassium hydroxide cartridge (Eluent Generator, Thermo Scientific), which was supplied with deionized water. The metabolite separation was carried at a flow rate of 380 µL/min, applying the following gradient conditions: 0-3 min, 10 mM KOH; 3-12 min, 10–50 mM KOH; 12-19 min, 50-100 mM KOH, 19-21 min, 100 mM KOH, 21-22 min, 100-10 mM KOH. The column was re-equilibrated at 10 mM for 8 min.

For the analysis of metabolic pool sizes the eluting compounds were detected in negative ion mode using full scan measurements in the mass range m/z 50 – 750 on a Q-Exactive HF high resolution MS (Thermo Fisher Scientific). The heated electrospray ionization (ESI) source settings of the mass spectrometer were: Spray voltage 3.2 kV, capillary temperature was set to 300°C, sheath gas flow 60 AU and aux gas flow 20 AU at a temperature of 300°C. The S-lens was set to a value of 60.

The untargeted and semi-targeted LC-MS data analysis was performed using the mzMine 2 opensource software (Du et al., 2020), while targeted Peak annotation was performed using the TraceFinder software (Version 4.1, Thermo Fisher Scientific). The identity of each compound was validated by authentic reference compounds.

For data analysis the area of the deprotonated $[M\text{-}H^+]^-$ monoisotopic [M0] mass peak of each compound was extracted and integrated using a mass accuracy <5 ppm and

a retention time (RT) tolerance of <0.05 min as compared to the independently measured reference compounds.

C18 dataset:

The dried lipid samples were re-suspended in 250 µL of UPLC-grade acetonitrile: isopropanol (70:30 [v:v]) mixture, followed by vortexing and 10 min incubation on a thermomixer at 10°C. Following 5 min centrifugation at 10.000 x g, the cleared supernatant was transferred to 2 ml glass vials with 200 µl glass inserts (Chromatography Zubehör Trott, Germany), which were placed in an Acquity iClass UPLC (Waters) sample manager at 6°C. The UPLC was connected to a Tribrid Orbitrap HRMS, equipped with a heated ESI (HESI) source (ID-X, Thermo Fischer Scientific).

Of each lipid sample 2 µl were injected onto a 100 x 2.1 mm BEH C8 UPLC column, packed with 1.7 µm particles (Waters). The flow rate of the UPLC was set to 400 µl/min and the buffer system consisted of buffer A (10 mM ammonium acetate, 0.1% acetic acid in UPLC-grade water) and buffer B (10 mM ammonium acetate, 0.1% acetic acid in UPLC-grade acetonitrile/isopropanol 7:3 [v/v]). The UPLC gradient was as follows: 0-1 min 45% A, 1-4 min 45-25% A, 4-12 min 25-11% A, 12-15 min 11-1% A, 15-18 min 1% A, 18-18.1 min 1-45% A and 18.1-22 min re-equilibrating at 45% A. This leads to a total runtime of 22 min per sample.

The ID-X mass spectrometer was operating either for the first injection in positive ionization mode or for the second injection in negative ionization mode. In both cases, the analyzed mass range was between m/z 150-1500. The resolution was set to 120.000, leading to approximately 4 scans per second. The RF lens was set to 60%, while the AGC target was set to 500% (~2E6 ions). The maximal ion time was set to 100 ms and the HESI source was operating with a spray voltage of 3.5 kV in positive ionization mode, while 3.2 kV were applied in negative ionization mode. The capillary temperature was 250°C, the sheath gas flow 60 arbitrary units (AU), the auxiliary gas flow 20 AU and the sweep gas flow was set to 2 AU at 350°C. All samples were analyzed in a randomized run-order and the untargeted data analysis was performed using QI for metabolomics (Version 2.3 Nonlinea Dynamics) according to the vendors manual.

Targeted data analysis was performed using the quan module of the TraceFinder 4.1 software (Thermo Fischer Scientific) in combination with a sample-specific in-house generated compound database.

pHILIC dataset:

Untargeted metabolic analysis was performed using a ZIC-pHILIC 2.1 × 150 mm (5-µm particle size column (Merck) coupled to a Q-Exactive HF mass spectrometer (Thermo Fisher Scientific), as described previously (Birsoy et al., 2015). In brief: Samples were re-suspended in 150 μL of ice-cold water, of which 25 μL were mixed with 75 μL of UPLC/MS Optima Grade (Fisher scientific) acetonitrile. 2.5 μL were injected onto the pHILIC column, using an Acquity iClass Ultra Performance Liquid Chromatography (UPLC) system. The metabolites were separated using Buffer A, which consisted of 20 mM ammonium carbonate, 0.1% ammonium hydroxide and buffer B that consisted of UPLC/MS Optima Grade (Fisher scientific) acetonitrile. The chromatographic gradient was operated at a flow rate of 0.150 ul/min as follows: 0–20 min.: linear gradient from 80% to 20% B; 20–20.5 min.: linear gradient from 20% to 80% B; 20.5–28 min.: hold at 80% B. The Q-Exactive HF mass spectrometer was operated in full-scan mode, polarity-switching mode. The spray voltage was set to 3.2 kV, the heated capillary and the HESI probe was held at 320°C. The sheath gas flow was set to 60 arbitrary units, the auxiliary gas flow was set to 20 units, and the sweep gas flow was set to 1 unit. The MS data acquisition was performed using a m/z range 60–900, with the resolution set to 70.000. The Acquired Gain Control (AGC) was set to a target value of 10E6, with a maximum injection time fixed at to 80 msec. The untargeted analysis of metabolites from the positive ionization, as well as the negative ionization mode was performed using the opensource software ElMaven. The targeted metabolite analysis was performed using the quan module of the TraceFinder software (Version 4.1, Thermo Fisher Scientific) by matching the measured spectra against a library of authentic reference standards.

4.2.9 Histology

Histology experiments were performed by Quinn Quesenberry.

Samples stored in PFA were transferred to micromesh embedding cassettes and drop-fixed in a solution of 10% neutral buffered formalin for 4 hours. After the fixation period, the tissues were infiltrated with liquid paraffin wax using the Thermo scientific Excelsior AS Tissue Processor. After tissue infiltration, the processed samples were embedded with paraffin. Cooled paraffin blocks were then cut into 5 μM sections using a microbiome and transferred onto glass slides. Slides were incubated overnight at 37°C and then stored at room temperature until further staining protocols.

For the H&E staining, the slides were first deparaffinized and rehydrated. The staining was conducted using the Scientific Gemini Automated Slide Stainer. The slides were stained in 300 ml of Mayer's Hematoxylin solution for 10 minutes at 30ºC and then rinsed under running tap water for 15 minutes, followed by a 2-minute counterstain in Eosin-Y Solution. The slides were transferred to a final graded ethanol dehydration series. Afterwards, slides were transferred into two xylene wash baths for 5 minutes each. Lastly, slides were removed from the xylene and excess xylene was allowed to air dry from the slide. The slides were then positioned flat and 1-3 drops of Cytoseal XYL were placed carefully onto the slide. The slides were promptly covered with coverslips and left overnight in the fume hood to cure.

For the SRFG staining, the slides were first deparaffinized and rehydrated. The staining was conducted using the Scientific Gemini Automated Slide Stainer. Firstly, the samples were stained in Weigert's Iron Hematoxylin for 5 minutes and then dipped in running tap water 3 times. The samples were then differentiated in a 1% HCl-Alcohol (70% ethanol) solution for 5 seconds and subsequently dipped in running tap water three times. The samples were then stained in 0.1% Direct Red 80 and 0.1% Fast Green FCF in 1.3% saturated aqueous picric acid in H_2O for one hour. Following the staining step, the slides were then dipped into a 0.5% acetic acid in H_2O wash 5 times and shaken dry. The slides were then dehydrated in two separate isopropanol baths for 2 minutes each. Finally, the slides were transferred into two xylene wash baths,

each for 5 minutes. Slides were removed from the xylene bath and excess xylene was allowed to air dry from the slide before 1-3 drops of Cytoseal XYL were placed carefully onto the slide. The slides were directly covered with coverslips and left overnight in the fume hood to cure.

All the samples were imaged on the Leica Biosystems SCN400 Brightfield Slide Scanner with a 20x objective. The images were viewed and quantitatively analyzed with QuPath (Bankhead et al., 2017). 4 samples representative of each experimental group (male/female, young/old) were selected for the analysis, yielding 16 animals in total. To prevent any scoring bias, every image was assigned a random identification number to blind the sample type during analysis.

For analysis of the H&E data, each sample was comparatively scored according to the following three criteria:

1. Epithelial Characteristics: Each image was overlayed with an adjusted grid with window-size 250 μm^2. The positive goblet cells within a given window were manually counted, tracked, and recorded. 4 windows in total were counted per section and the average was evaluated in the analysis.
2. Microanatomy: The thickness of the muscularis propria layer of each section was measured at four distinct locations and the average was evaluated in the analysis.
3. Inflammatory Markers: The extent and severity of leukocyte infiltration was scored based on an adapted intestinal scoring model outlined by Erben et al., 2014. To assess the severity of leukocyte infiltration, the percentage of leukocyte infiltration in a given window was estimated and assigned one of the following four grades:
    - Minimal: <10% = 1
    - Mild: 10-25% = 2
    - Moderate: 26-50% = 3
    - Severe: >51% = 4

Similarly, the extent of infiltration was scored by focal leukocyte localization and assigned one of the following four grades:

- Mucosal localization only = 1
- Mucosal and submucosal localization = 2
- Mucosal, submucosal and transmural localization = 3

The infiltration extent and severity were recorded for 4 windows per tissue section (the same windows which were used for counting of goblet cells) and the average was evaluated in the analysis.

Sirius Red Fast Green stained slides were viewed with QuPath (Bankhead et al., 2017). For consistent evaluation of both data sets, the same 16 samples as in the H&E analysis were evaluated. Again, every image was assigned a random identification number to blind the sample type during analysis. The whole tissue slice for every section (n=50) for each sample animal (n=16) was analyzed and evaluated in QuPath (Bankhead et al., 2017). Quantitative estimation of total collagen fibers in proportion to all other non-collagen proteins was performed according to previously defined protocols (Ippolito et al., 2015). The positive areas of the sample (red-stained collagen fibers) were expressed as a percentage of the total tissue area. To establish the appropriate stain vectors for each channel and effectively train the pixel classifier for the stain, a single channel deconvolution was performed. Here, the stain vector optical density (OD) for each single channel was created by defining a small, rectangular region of interest (ROI) that best represented the positive vector and assigning this ROI as the OD for the stain channel. This process was repeated for the negative channel. The pixel classifier was subsequently trained for the specific stain conditions for positive/negative pixel identification. The vector deconvolution was repeated for each sample to allow for appropriate identification. However, to ensure a fair comparison between the samples, down-sample factor (4.0), Gaussian sigma (2 μm), as well as positive (0.3 OD units) and negative (0.1 OD units) threshold values were kept consistent throughout the analysis. For whole sample pixel classification, an entire ROI was drawn around the sample perimeter and luminal obtrusions were excluded. Following pixel classification, percent positive pixel (PPP) as a function of

total pixel detection was recorded for each sample. Complete data was expressed as PPP, analogous to positive collagen fibers per total sample area.

Pearson correlation analyses were conducted with the *scipy* package from Python (Virtanen et al., 2020).

4.3 Computational analyses

RStudio version 1.2.5033 was used for most of the computational analysis, with R version 3.6.3. Parts of the microbiota analyses were conducted with Qiime2 (version 2018.11, Bolyen et al., 2019). Metaboanalyst 5.0 (Xia et al., 2009) was used for PLS-DA and RF analysis for the metabolite datasets, Microbiomeanalyst (Dhariwal et al., 2017) was used for the hierarchical clustering of the microbiota samples.

4.3.1 Microbiota community analysis

The fastq files of the sequencing facility were demultiplexed with *idemp* (Wu, 2020). Barcodes and adapters were trimmed with a custom script written by Dr. Rongfeng Cui. Further filtering, trimming and sample inference to amplicon sequence variants (ASVs) were conducted with the *dada2* package in R (Callahan et al., 2016). Taxonomy assignment was also conducted with *dada2*, using the RDP classifier (Q. Wang et al., 2007) and the SILVA 16S database, version 132 (Quast et al., 2013).
Further analyses were conducted using the *phyloseq* package in R (McMurdie & Holmes, 2013). Samples with less than 1000 sequences were filtered out. Relative abundance was calculated on individual ASV level or on merged samples for genus or phylum level.

For diversity analyses, samples were rarefied to a depth of 40000 sequences (samples sequenced with 2 x 250 bp paired-end HiSeq) or 4000 sequences per sample (samples sequenced with 2 x 300 bp paired-end MiSeq). Alpha and beta diversity levels were assessed using the *phyloseq* and the *vegan* R package (Oksanen et al.,

2020). Hierarchical clustering and dendrogram analysis based on Bray-Curtis dissimilarity values was performed with Microbiomeanalyst (Dhariwal et al., 2017) using the Ward algorithm and Bray-Curtis dissimilarity as distance measure. Significant changes in relative abundance were calculated using *DESeq2* package in R (Love et al., 2014), after filtering the ASVs for a minimal occurrence in 30% of the samples. Venn diagrams were built with the *VennDiagram* R package (Chen & Boutros, 2011).

4.3.2 Metabolomics analysis

Raw spectrum assignment was conducted at the Metabolomics core facility as described above. The metabolite values were first normalized to the internal standards which was added to the extraction buffer. Afterwards, metabolites were filtered for an occurrence in 88% of the samples and the 40% metabolites with the lowest variability were excluded as proposed in Hackstadt & Hess, 2009. Metabolites were then normalized based on their total ion count, followed by logarithmic transformation and pareto transformation. One sample was excluded in the C18 dataset in negative mode due to the strongly deviating internal standard. Principal component analysis was conducted using the *stats* R package (R Core Team, 2020). Differential metabolite levels were assessed using a t-test, followed by BH-multiple comparison correction (*stats* package). Venn diagrams were constructed using the *Venn.Diagram* R package. PLS-DA and RF-analysis was conducted with MetaboAnalyst 5.0.

4.3.3 Proteomic analysis

Parts performed by the proteomics core facility:

Raw data were analyzed using ProteomeDiscoverer version 2.4 (Thermo Fisher Scientific). Peptide fragmentation spectra were searched against Uniprot's canonical sequences for *Nothobranchius furzeri*, downloaded in September 2019. Methionine oxidation was set as variable modifications, cysteine carbamidomethylation and TMTPro as static modification. The digestion parameters were set to "Trypsin (Full)".

Protein identification was performed at a peptide spectrum matches and protein strict false discovery rate of 0.01. Reported quantification was based on intensity. The value for “Co-isolation Threshold”, “Average Reporter S/N Threshold”, and “SPS Mass Matches [%] Threshold” was set to 0. The isotope purity correction factors, provided by the manufacturer, were included in the analysis. Data wrangling and exploratory data analysis were performed using the *tidyverse* package (Wickham et al., 2019) in R (R Core Team, 2020). Differential expression analysis was performed using limma (Ritchie et al., 2015).

Parts performed by me:

Heatmaps were generated with the *heatmaps2* function from the *gplots* package (Warnes et al., 2020). GO term and pathway enrichment analysis was conducted with ConsensusPathDB (Kamburov et al., 2009). Only GO terms and pathways with more than two genes were considered. Depending on the dataset, the cut-off significance values were chosen at a minimum q-value of <0.1 or <0.03, and a maximum of the top 30 significant terms were shown.

4.3.4 Random Forest analyses

Parts performed by Sam Kean:

Section Age/Sex Classification

To preprocess the data, the ASV table was collapsed by genus level and ASVs with zero values in >=90% of samples were removed. The data was then split into a training group (~80%) and a testing group (~20%) by random selection of Sample IDs, so that all IDs contained in the test group were not in the train group, and vice versa. Scikit-learn’s MinMax scaler (Pedregosa et al., 2011) was fit to the training group, and used to transform both the training group and test group. The data was then converted to BIOM format for use with QIIME 2.

Classification analyses were performed with QIIME 2 (version 2019.7) (Bolyen et al., 2019) and the training data was used as input for the classify-samples pipeline (parameters: estimator=RandomForestClassifier, n-estimator=250, random-state=123). The testing data was used as input for the predict-classification function and plotted with the confusion-matrix function.

Longitudinal Prediction

To preprocess the data, the ASV table was collapsed by genus level and ASVs with zero values in >=90% of samples were removed. The data was then split into a training group (~80%) and a testing group (~20%) by random selection of Sample IDs, so that all IDs contained in the test group were not in the train group, and vice versa. Scikit-learn's MinMax scaler (Pedregosa et al., 2011) was fit to the training group, and used to transform both the training group and test group. The data was then converted to BIOM format for use with QIIME 2.

For the predictions with sample IDs included, scikit-learn's OneHotEncoder function (Pedregosa et al., 2011) was used to encode sample IDs into binary columns, prior to the splitting into testing and training groups. The ASV table was split into a training group (80%) and a test group (20%), absolutely, with no selection of sample IDs, i.e. a mix of all sample IDs in each group.

Classification analyses were performed with QIIME 2 (version 2019.7) and the training data was used as input for the regress-samples pipeline (parameters: estimator = RandomForestClassifier, n-estimators = 100, random-state = 123). The testing data was used as input for the predict-regression function and plotted with the scatterplot function.

For the predictions of remaining life from food, food data were given a remaining life equal to (final week minus current week) - e.g., food data from week 6 would have a 'remaining life' of 27 (33 (the final week measured) - 6 = 27).

Parts performed by me:

MetaboAnalyst 5.0 was used for Random Forest classifications of metabolite samples with following parameters: number of trees = 500, number of predictors = 7, randomness = on.

4.3.5 Correlation analysis

For the correlation analysis, the ASV tables were first merged on genus level. Only genera with a minimum count of 50 and appearance in 3 samples were taken into consideration. The count data of both the genus tables and the metabolite tables was log-transformed. Each genus was correlated with each metabolite using the *lm* function of the *stats* R package. Correlations with a minimum r-value of 0.45 and a BH-adjusted p-value of <0.1 were taken into consideration.

Appendix

References

Aagaard, K., Ma, J., Antony, K. M., Ganu, R., Petrosino, J., & Versalovic, J. (2014). The placenta harbors a unique microbiome. *Science Translational Medicine*, *6*(237), 237ra65-237ra65. https://doi.org/10.1126/scitranslmed.3008599

Agrawal, S., Kumar, S., Sehgal, R., George, S., Gupta, R., Poddar, S., Jha, A., & Pathak, S. (2019). EL-MAVEN: A fast, robust, and user-friendly mass spectrometry data processing engine for metabolomics. In *Methods in Molecular Biology* (Vol. 1978, pp. 301–321). Humana Press Inc. https://doi.org/10.1007/978-1-4939-9236-2_19

Alboukadel Kassambara, Marcin Kosinski, & Przemyslaw Biecek. (2020). *Drawing Survival Curves using "ggplot2" [R package survminer]* (R package version 0.4.8.). https://cran.r-project.org/package=survminer

Alemayehu, B., & Warner, K. E. (2004). The Lifetime Distribution of Health Care Costs. *Health Services Research*, *39*(3), 627–642. https://doi.org/10.1111/j.1475-6773.2004.00248.x

Arslan-Ergul, A., & Adams, M. M. (2014). Gene expression changes in aging Zebrafish (Danio rerio) brains are sexually dimorphic. *BMC Neuroscience*, *15*(1), 1–11. https://doi.org/10.1186/1471-2202-15-29

Ashapkin, V. V., Kutueva, L. I., Kurchashova, S. Y., & Kireev, I. I. (2019). Are there common mechanisms between the Hutchinson-Gilford progeria syndrome and natural aging? In *Frontiers in Genetics* (Vol. 10, Issue MAY, p. 455). Frontiers Media S.A. https://doi.org/10.3389/fgene.2019.00455

Austad, S. N., & Fischer, K. E. (2016). Sex Differences in Lifespan. In *Cell Metabolism* (Vol. 23, Issue 6, pp. 1022–1033). Cell Press. https://doi.org/10.1016/j.cmet.2016.05.019

Baars, A., Oosting, A., Lohuis, M., Koehorst, M., El Aidy, S., Hugenholtz, F., Smidt, H., Mischke, M., Boekschoten, M. V., Verkade, H. J., Garssen, J., van der Beek, E. M., Knol, J., de Vos, P., van Bergenhenegouwen, J., & Fransen, F. (2018). Sex differences in lipid metabolism are affected by presence of the gut microbiota. *Scientific Reports*, *8*(1), 1–11. https://doi.org/10.1038/s41598-018-31695-w

Bachem, A., Makhlouf, C., Binger, K. J., de Souza, D. P., Tull, D., Hochheiser, K., Whitney, P. G., Fernandez-Ruiz, D., Dähling, S., Kastenmüller, W., Jönsson, J., Gressier, E., Lew, A. M., Perdomo, C., Kupz, A., Figgett, W., Mackay, F., Oleshansky, M., Russ, B. E., … Bedoui, S. (2019). Microbiota-Derived Short-Chain Fatty Acids Promote the Memory Potential of Antigen-Activated CD8+ T Cells. *Immunity*, *51*(2), 285-297.e5. https://doi.org/10.1016/j.immuni.2019.06.002

Bäckhed, F., Roswall, J., Peng, Y., Feng, Q., Jia, H., Kovatcheva-Datchary, P., Li, Y., Xia, Y., Xie, H., Zhong, H., Khan, M. T., Zhang, J., Li, J., Xiao, L., Al-Aama, J., Zhang, D., Lee, Y. S., Kotowska, D., Colding, C., … Jun, W. (2015). Dynamics and stabilization of the human gut microbiome during the first year of life. *Cell Host and Microbe*, *17*(5), 690–703. https://doi.org/10.1016/j.chom.2015.04.004

Bana, B., & Cabreiro, F. (2019). The Microbiome and Aging. In *Annual Review of Genetics* (Vol. 53, pp. 239–261). Annual Reviews Inc. https://doi.org/10.1146/annurev-genet-112618-043650

Banerjee, G., & Ray, A. K. (2017). Bacterial symbiosis in the fish gut and its role in health and metabolism. In *Symbiosis* (Vol. 72, Issue 1, pp. 1–11). Springer Netherlands. https://doi.org/10.1007/s13199-016-0441-8

Bankhead, P., Loughrey, M. B., Fernández, J. A., Dombrowski, Y., McArt, D. G., Dunne, P. D., McQuaid, S., Gray, R. T., Murray, L. J., Coleman, H. G., James, J. A., Salto-Tellez, M., & Hamilton, P. W. (2017). QuPath: Open source software for digital pathology image analysis. *Scientific Reports*, *7*(1), 1–7. https://doi.org/10.1038/s41598-017-17204-5

Barbieri, M., Bonafè, M., Franceschi, C., & Paolisso, G. (2003). Insulin/IGF-I-signaling pathway: An evolutionarily conserved mechanism of longevity from yeast to humans. *American Journal of Physiology - Endocrinology and Metabolism*, *285*(5 48-5). https://doi.org/10.1152/ajpendo.00296.2003

Bárcena, C., Valdés-Mas, R., Mayoral, P., Garabaya, C., Durand, S., Rodríguez, F., Fernández-García, M. T., Salazar, N., Nogacka, A. M., Garatachea, N., Bossut, N., Aprahamian, F., Lucia, A., Kroemer, G., Freije, J. M. P., Quirós, P. M., & López-Otín, C. (2019). Healthspan and lifespan extension by fecal microbiota transplantation into progeroid mice. *Nature Medicine*, *25*(8), 1234–1242. https://doi.org/10.1038/s41591-019-0504-5

Baumgartner, R. J., Van Kranendonk, M. J., Wacey, D., Fiorentini, M. L., Saunders, M., Caruso, S., Pages, A., Homann, M., & Guagliardo, P. (2019). Nano-porous pyrite and organic matter in 3.5-billion-year-old stromatolites record primordial life. *Geology*, *47*(11), 1039–1043. https://doi.org/10.1130/G46365.1

Bell, R. C., & Zamudio, K. R. (2012). Sexual dichromatism in frogs: Natural selection, sexual selection and unexpected diversity. In *Proceedings of the Royal Society B: Biological Sciences* (Vol. 279, Issue 1748, pp. 4687–4693). Royal Society. https://doi.org/10.1098/rspb.2012.1609

Benemann, J. R. (1973). Nitrogen fixation in termites. *Science*, *181*(4095), 164–165. https://doi.org/10.1126/science.181.4095.164

Biagi, E., Franceschi, C., Rampelli, S., Capri, M., Brigidi, P., & Candela Correspondence, M. (2016). Gut Microbiota and Extreme Longevity. *Current Biology*, *26*. https://doi.org/10.1016/j.cub.2016.04.016

Biagi, E., Nylund, L., Candela, M., Ostan, R., Bucci, L., Pini, E., Nikkïla, J., Monti, D., Satokari, R., Franceschi, C., Brigidi, P., & De Vos, W. (2010). Through Ageing, and Beyond: Gut Microbiota and Inflammatory Status in Seniors and Centenarians. *PLoS ONE*, *5*(5), e10667. https://doi.org/10.1371/journal.pone.0010667

Birchenough, G. M. H., Johansson, M. E. V., Gustafsson, J. K., Bergström, J. H., & Hansson, G. C. (2015). New developments in goblet cell mucus secretion and function. In *Mucosal Immunology* (Vol. 8, Issue 4, pp. 712–719). Nature Publishing Group. https://doi.org/10.1038/mi.2015.32

Birsoy, K., Wang, T., Chen, W. W., Freinkman, E., Abu-Remaileh, M., & Sabatini, D. M. (2015). An Essential Role of the Mitochondrial Electron Transport Chain in Cell Proliferation Is to Enable Aspartate Synthesis. *Cell*, *162*(3), 540–551. https://doi.org/10.1016/j.cell.2015.07.016

Blažek, R., Polačik, M., & Reichard, M. (2013). Rapid growth, early maturation and short generation time in African annual fishes. *EvoDevo*, *4*(1), 24. https://doi.org/10.1186/2041-9139-4-24

Bolyen, E., Rideout, J. R., Dillon, M. R., Bokulich, N. A., Abnet, C. C., Al-Ghalith, G.

A., Alexander, H., Alm, E. J., Arumugam, M., Asnicar, F., Bai, Y., Bisanz, J. E., Bittinger, K., Brejnrod, A., Brislawn, C. J., Brown, C. T., Callahan, B. J., Caraballo-Rodríguez, A. M., Chase, J., … Caporaso, J. G. (2019). Reproducible, interactive, scalable and extensible microbiome data science using QIIME 2. In *Nature Biotechnology* (Vol. 37, Issue 8, pp. 852–857). Nature Publishing Group. https://doi.org/10.1038/s41587-019-0209-9

Borgo, F., Garbossa, S., Riva, A., Severgnini, M., Luigiano, C., Benetti, A., Pontiroli, A. E., Morace, G., & Borghi, E. (2018). Body Mass Index and Sex Affect Diverse Microbial Niches within the Gut. *Frontiers in Microbiology*, *9*(FEB), 213. https://doi.org/10.3389/fmicb.2018.00213

Bouskra, D., Brézillon, C., Bérard, M., Werts, C., Varona, R., Boneca, I. G., & Eberl, G. (2008). Lymphoid tissue genesis induced by commensals through NOD1 regulates intestinal homeostasis. *Nature*, *456*(7221), 507–510. https://doi.org/10.1038/nature07450

Brugman, S. (2016). The zebrafish as a model to study intestinal inflammation. *Developmental and Comparative Immunology*, *64*, 82–92. https://doi.org/10.1016/j.dci.2016.02.020

Brunet, A. (2020). Old and new models for the study of human ageing. In *Nature Reviews Molecular Cell Biology* (Vol. 21, Issue 9, pp. 491–493). Nature Research. https://doi.org/10.1038/s41580-020-0266-4

Buchon, N., Osman, D., David, F. P. A., Yu Fang, H., Boquete, J. P., Deplancke, B., & Lemaitre, B. (2013). Morphological and Molecular Characterization of Adult Midgut Compartmentalization in Drosophila. *Cell Reports*, *3*(5), 1725–1738. https://doi.org/10.1016/j.celrep.2013.04.001

Buffie, C. G., & Pamer, E. G. (2013). *Microbiota-mediated colonization resistance against intestinal pathogens*. https://doi.org/10.1038/nri3535

Bunnoy, A., Na-Nakorn, U., Kayansamruaj, P., & Srisapoome, P. (2019). Acinetobacter strain KUO11TH, a unique organism related to Acinetobacter pittii and isolated from the skin mucus of healthy bighead catfish and its efficacy against several fish pathogens. *Microorganisms*, *7*(11). https://doi.org/10.3390/microorganisms7110549

Butt, R. L., & Volkoff, H. (2019). Gut microbiota and energy homeostasis in fish. In *Frontiers in Endocrinology* (Vol. 10, Issue JAN, p. 9). Frontiers Media S.A. https://doi.org/10.3389/fendo.2019.00009

Cabreiro, F., Au, C., Leung, K. Y., Vergara-Irigaray, N., Cochemé, H. M., Noori, T., Weinkove, D., Schuster, E., Greene, N. D. E., & Gems, D. (2013). Metformin retards aging in C. elegans by altering microbial folate and methionine metabolism. *Cell*, *153*(1), 228–239. https://doi.org/10.1016/j.cell.2013.02.035

Callahan, B. J., McMurdie, P. J., Rosen, M. J., Han, A. W., Johnson, A. J. A., & Holmes, S. P. (2016). DADA2: High-resolution sample inference from Illumina amplicon data. *Nature Methods*, *13*(7), 581–583. https://doi.org/10.1038/nmeth.3869

Caporaso, J. G., Lauber, C. L., Costello, E. K., Berg-Lyons, D., Gonzalez, A., Stombaugh, J., Knights, D., Gajer, P., Ravel, J., Fierer, N., Gordon, J. I., & Knight, R. (2011). Moving pictures of the human microbiome. *Genome Biology*, *12*(5), R50. https://doi.org/10.1186/gb-2011-12-5-r50

Ceja-Navarro, J. A., Nguyen, N. H., Karaoz, U., Gross, S. R., Herman, D. J., Andersen, G. L., Bruns, T. D., Pett-Ridge, J., Blackwell, M., & Brodie, E. L.

(2014). Compartmentalized microbial composition, oxygen gradients and nitrogen fixation in the gut of Odontotaenius disjunctus. *ISME Journal*, *8*(1), 6–18. https://doi.org/10.1038/ismej.2013.134

Cellerino, A., Valenzano, D. R., & Reichard, M. (2016). From the bush to the bench: the annual *Nothobranchius* fishes as a new model system in biology. *Biological Reviews*, *91*(2), 511–533. https://doi.org/10.1111/brv.12183

Chella Krishnan, K., Sabir, S., Shum, M., Meng, Y., Acín-Pérez, R., Lang, J. M., Floyd, R. R., Vergnes, L., Seldin, M. M., Fuqua, B. K., Jayasekera, D. W., Nand, S. K., Anum, D. C., Pan, C., Stiles, L., Péterfy, M., Reue, K., Liesa, M., & Lusis, A. J. (2019). Sex-specific metabolic functions of adipose Lipocalin-2. *Molecular Metabolism*, *30*, 30–47. https://doi.org/10.1016/j.molmet.2019.09.009

Chen, H., & Boutros, P. C. (2011). VennDiagram: A package for the generation of highly-customizable Venn and Euler diagrams in R. *BMC Bioinformatics*, *12*(1), 35. https://doi.org/10.1186/1471-2105-12-35

Chow, J., Lee, S. M., Shen, Y., Khosravi, A., & Mazmanian, S. K. (2010). Host-bacterial symbiosis in health and disease. In *Advances in Immunology* (Vol. 107, Issue C, pp. 243–274). Academic Press Inc. https://doi.org/10.1016/B978-0-12-381300-8.00008-3

Chu, C., Murdock, M. H., Jing, D., Won, T. H., Chung, H., Kressel, A. M., Tsaava, T., Addorisio, M. E., Putzel, G. G., Zhou, L., Bessman, N. J., Yang, R., Moriyama, S., Parkhurst, C. N., Li, A., Meyer, H. C., Teng, F., Chavan, S. S., Tracey, K. J., … Artis, D. (2019). The microbiota regulate neuronal function and fear extinction learning. *Nature*, *574*(7779), 543–548. https://doi.org/10.1038/s41586-019-1644-y

Claesson, M. J., Cusack, S., O'Sullivan, O., Greene-Diniz, R., De Weerd, H., Flannery, E., Marchesi, J. R., Falush, D., Dinan, T., Fitzgerald, G., Stanton, C., Van Sinderen, D., O'Connor, M., Harnedy, N., O'Connor, K., Henry, C., O'Mahony, D., Fitzgerald, A. P., Shanahan, F., … O'Toole, P. W. (2011). Composition, variability, and temporal stability of the intestinal microbiota of the elderly. *Proceedings of the National Academy of Sciences of the United States of America*, *108*(SUPPL. 1), 4586–4591. https://doi.org/10.1073/pnas.1000097107

Claesson, M. J., Jeffery, I. B., Conde, S., Power, S. E., O'connor, E. M., Cusack, S., Harris, H. M. B., Coakley, M., Lakshminarayanan, B., O'sullivan, O., Fitzgerald, G. F., Deane, J., O'connor, M., Harnedy, N., O'connor, K., O'mahony, D., Van Sinderen, D., Wallace, M., Brennan, L., … O'toole, P. W. (2012). Gut microbiota composition correlates with diet and health in the elderly. *Nature*, *488*(7410), 178–184. https://doi.org/10.1038/nature11319

Claesson, M. J., Jeffery, I. B., Conde, S., Power, S. E., O'Connor, E. M., Cusack, S., Harris, H. M. B., Coakley, M., Lakshminarayanan, B., O'Sullivan, O., Fitzgerald, G. F., Deane, J., O'Connor, M., Harnedy, N., O'Connor, K., O'Mahony, D., van Sinderen, D., Wallace, M., Brennan, L., … O'Toole, P. W. (2012). Gut microbiota composition correlates with diet and health in the elderly. *Nature*, *488*(7410), 178–184. https://doi.org/10.1038/nature11319

Clark, R. I., Salazar, A., Yamada, R., Fitz-Gibbon, S., Morselli, M., Alcaraz, J., Rana, A., Rera, M., Pellegrini, M., Ja, W. W., & Walker, D. W. (2015). Distinct Shifts in Microbiota Composition during Drosophila Aging Impair Intestinal Function and Drive Mortality. *Cell Reports*, *12*(10), 1656–1667.

https://doi.org/10.1016/J.CELREP.2015.08.004
Clement, A. B., Gamerdinger, M., Tamboli, I. Y., Lütjohann, D., Walter, J., Greeve, I., Gimpl, G., & Behl, C. (2009). Adaptation of neuronal cells to chronic oxidative stress is associated with altered cholesterol and sphingolipid homeostasis and lysosomal function. *Journal of Neurochemistry*, *111*(3), 669–682. https://doi.org/10.1111/j.1471-4159.2009.06360.x
Clemente, J. C., Ursell, L. K., Parfrey, L. W., & Knight, R. (2012). The impact of the gut microbiota on human health: An integrative view. In *Cell* (Vol. 148, Issue 6, pp. 1258–1270). Elsevier B.V. https://doi.org/10.1016/j.cell.2012.01.035
Collado, M. C., Rautava, S., Aakko, J., Isolauri, E., & Salminen, S. (2016). Human gut colonisation may be initiated in utero by distinct microbial communities in the placenta and amniotic fluid. *Scientific Reports*, *6*(1), 1–13. https://doi.org/10.1038/srep23129
Crimmins, E. M. (2015). Lifespan and Healthspan: Past, Present, and Promise. *The Gerontologist*, *55*(6), 901–911. https://doi.org/10.1093/geront/gnv130
Cummings, J. H., & Macfarlane, G. T. (1991). The control and consequences of bacterial fermentation in the human colon. *Journal of Applied Bacteriology*, *70*(6), 443–459. https://doi.org/10.1111/j.1365-2672.1991.tb02739.x
David, L. A., Maurice, C. F., Carmody, R. N., Gootenberg, D. B., Button, J. E., Wolfe, B. E., Ling, A. V., Devlin, A. S., Varma, Y., Fischbach, M. A., Biddinger, S. B., Dutton, R. J., & Turnbaugh, P. J. (2014). Diet rapidly and reproducibly alters the human gut microbiome. *Nature*, *505*(7484), 559–563. https://doi.org/10.1038/nature12820
De Aguiar Vallim, T. Q., Tarling, E. J., & Edwards, P. A. (2013). Pleiotropic roles of bile acids in metabolism. In *Cell Metabolism* (Vol. 17, Issue 5, pp. 657–669). Cell Press. https://doi.org/10.1016/j.cmet.2013.03.013
De Filippo, C., Cavalieri, D., Di Paola, M., Ramazzotti, M., Poullet, J. B., Massart, S., Collini, S., Pieraccini, G., & Lionetti, P. (2010). Impact of diet in shaping gut microbiota revealed by a comparative study in children from Europe and rural Africa. *Proceedings of the National Academy of Sciences of the United States of America*, *107*(33), 14691–14696. https://doi.org/10.1073/pnas.1005963107
de Goffau, M. C., Lager, S., Sovio, U., Gaccioli, F., Cook, E., Peacock, S. J., Parkhill, J., Charnock-Jones, D. S., & Smith, G. C. S. (2019). Human placenta has no microbiome but can contain potential pathogens. *Nature*, *572*(7769), 329–334. https://doi.org/10.1038/s41586-019-1451-5
De Vadder, F., Kovatcheva-Datchary, P., Goncalves, D., Vinera, J., Zitoun, C., Duchampt, A., Bäckhed, F., & Mithieux, G. (2014). Microbiota-generated metabolites promote metabolic benefits via gut-brain neural circuits. *Cell*, *156*(1–2), 84–96. https://doi.org/10.1016/j.cell.2013.12.016
Deckers, M. M. L., Smits, P., Karperien, M., Ni, J., Tylzanowski, P., Feng, P., Parmelee, D., Zhang, J., Bouffard, E., Gentz, R., Löwik, C. W. G. M., & Merregaert, J. (2001). Recombinant human extracellular matrix protein 1 inhibits alkaline phosphatase activity and mineralization of mouse embryonic metatarsals in vitro. *Bone*, *28*(1), 14–20. https://doi.org/10.1016/S8756-3282(00)00428-2
Dhariwal, A., Chong, J., Habib, S., King, I. L., Agellon, L. B., & Xia, J. (2017). MicrobiomeAnalyst: A web-based tool for comprehensive statistical, visual and meta-analysis of microbiome data. *Nucleic Acids Research*, *45*(W1), W180–

W188. https://doi.org/10.1093/nar/gkx295
Di Cicco, E., Tozzini, E. T., Rossi, G., & Cellerino, A. (2011). The short-lived annual fish Nothobranchius furzeri shows a typical teleost aging process reinforced by high incidence of age-dependent neoplasias. *Experimental Gerontology*, *46*(4), 249–256. https://doi.org/10.1016/j.exger.2010.10.011
Dieterich, W., Schink, M., & Zopf, Y. (2018). Microbiota in the Gastrointestinal Tract. *Medical Sciences*, *6*(4), 116. https://doi.org/10.3390/medsci6040116
Ding, T., & Schloss, P. D. (2014). Dynamics and associations of microbial community types across the human body. *Nature*, *509*(7500), 357–360. https://doi.org/10.1038/nature13178
Dogra, S., Sakwinska, O., Soh, S.-E., Ngom-Bru, C., Brück, W. M., Berger, B., Brüssow, H., Karnani, N., Lee, Y. S., Yap, F., Chong, Y.-S., Godfrey, K. M., & Holbrook, J. D. (2015). Rate of establishing the gut microbiota in infancy has consequences for future health. *Gut Microbes*, *6*(5), 321–325. https://doi.org/10.1080/19490976.2015.1078051
Du, X., Smirnov, A., Pluskal, T., Jia, W., & Sumner, S. (2020). Metabolomics Data Preprocessing Using ADAP and MZmine 2. In *Methods in Molecular Biology* (Vol. 2104, pp. 25–48). Humana Press Inc. https://doi.org/10.1007/978-1-0716-0239-3_3
Ducluzeau, R., Dubos, F., & Raibaud andAbrams, P. G. D. (1976). Inhibition of Clostridium perfringens by an antibiotic substance produced by Bacillus licheniformis in the digestive tract of gnotobiotic mice: effect on other bacteria from the digestive tract. *Antimicrobial Agents and Chemotherapy*, *9*(1), 20–25. https://doi.org/10.1128/AAC.9.1.20
Dvergedal, H., Sandve, S. R., Angell, I. L., Klemetsdal, G., & Rudi, K. (2020). Association of gut microbiota with metabolism in juvenile Atlantic salmon. *Microbiome*, *8*(1), 160. https://doi.org/10.1186/s40168-020-00938-2
Egerton, S., Culloty, S., Whooley, J., Stanton, C., & Ross, R. P. (2018). The Gut Microbiota of Marine Fish. *Frontiers in Microbiology*, *9*, 873. https://doi.org/10.3389/fmicb.2018.00873
Erben, U., Loddenkemper, C., Doerfel, K., Spieckermann, S., Haller, D., Heimesaat, M. M., Zeitz, M., Siegmund, B., & Ku¨hl, A. A. (2014). A guide to histomorphological evaluation of intestinal inflammation in mouse models. *International Journal of Clinical and Experimental Pathology*, *7*(8), 4557–4576. /pmc/articles/PMC4152019/
Fahimipour, A. K., & Gross, T. (2019). Mapping the bacterial ways of life. In *arXiv* (Vol. 11, Issue 1, pp. 1–8). arXiv. https://doi.org/10.1038/s41467-020-18695-z
Faith, J. J., Guruge, J. L., Charbonneau, M., Subramanian, S., Seedorf, H., Goodman, A. L., Clemente, J. C., Knight, R., Heath, A. C., Leibel, R. L., Rosenbaum, M., & Gordon, J. I. (2013). The Long-Term Stability of the Human Gut Microbiota. *Science*, *341*(6141), 1237439. https://doi.org/10.1126/science.1237439
Falony, G., Joossens, M., Vieira-Silva, S., Wang, J., Darzi, Y., Faust, K., Kurilshikov, A., Bonder, M. J., Valles-Colomer, M., Vandeputte, D., Tito, R. Y., Chaffron, S., Rymenans, L., Verspecht, C., Sutter, L. De, Lima-Mendez, G., D'hoe, K., Jonckheere, K., Homola, D., … Raes, J. (2016). Population-level analysis of gut microbiome variation. *Science*, *352*(6285), 560–564. https://doi.org/10.1126/science.aad3503

Fan, W., Liu, T., Chen, W., Hammad, S., Longerich, T., Hausser, I., Fu, Y., Li, N., He, Y., Liu, C., Zhang, Y., Lian, Q., Zhao, X., Yan, C., Li, L., Yi, C., Ling, Z., Ma, L., Zhao, X., … Sun, B. (2019). ECM1 Prevents Activation of Transforming Growth Factor β, Hepatic Stellate Cells, and Fibrogenesis in Mice. *Gastroenterology*, *157*(5), 1352-1367.e13. https://doi.org/10.1053/j.gastro.2019.07.036

Foster, E. M., Dangla-Valls, A., Lovestone, S., Ribe, E. M., & Buckley, N. J. (2019). Clusterin in Alzheimer's disease: Mechanisms, genetics, and lessons from other pathologies. In *Frontiers in Neuroscience* (Vol. 13, Issue FEB, p. 164). Frontiers Media S.A. https://doi.org/10.3389/fnins.2019.00164

Franceschi, C., Garagnani, P., Parini, P., Giuliani, C., & Santoro, A. (2018). Inflammaging: a new immune–metabolic viewpoint for age-related diseases. In *Nature Reviews Endocrinology* (Vol. 14, Issue 10, pp. 576–590). Nature Publishing Group. https://doi.org/10.1038/s41574-018-0059-4

Fransen, F., van Beek, A. A., Borghuis, T., El Aidy, S., Hugenholtz, F., van der Gaast - de Jongh, C., Savelkoul, H. F. J., de Jonge, M. I., Boekschoten, M. V., Smidt, H., Faas, M. M., & de Vos, P. (2017). Aged gut microbiota contributes to systemical inflammaging after transfer to germ-free mice. *Frontiers in Immunology*, *8*(NOV). https://doi.org/10.3389/fimmu.2017.01385

Frasca, D., & Blomberg, B. B. (2009). Effects of aging on B cell function. In *Current Opinion in Immunology* (Vol. 21, Issue 4, pp. 425–430). Curr Opin Immunol. https://doi.org/10.1016/j.coi.2009.06.001

Fraune, S., Anton-Erxleben, F., Augustin, R., Franzenburg, S., Knop, M., Schröder, K., Willoweit-Ohl, D., & Bosch, T. C. (2015). Bacteria–bacteria interactions within the microbiota of the ancestral metazoan Hydra contribute to fungal resistance. *The ISME Journal*, *9*(7), 1543–1556. https://doi.org/10.1038/ismej.2014.239

Gajardo, K., Rodiles, A., Kortner, T. M., Krogdahl, Å., Bakke, A. M., Merrifield, D. L., & Sørum, H. (2016). A high-resolution map of the gut microbiota in Atlantic salmon (Salmo salar): A basis for comparative gut microbial research. *Scientific Reports*, *6*(1), 1–10. https://doi.org/10.1038/srep30893

Galkin, F., Mamoshina, P., Aliper, A., Putin, E., Moskalev, V., Gladyshev, V. N., & Zhavoronkov, A. (2020). Human Gut Microbiome Aging Clock Based on Taxonomic Profiling and Deep Learning. *ISCIENCE*, *23*, 101199. https://doi.org/10.1016/j.isci.2020.101199

Gao, A. W., Chatzispyrou, I. A., Kamble, R., Liu, Y. J., Herzog, K., Smith, R. L., Van Lenthe, H., Vervaart, M. A. T., Van Cruchten, A., Luyf, A. C., Van Kampen, A., Pras-Raves, M. L., Vaz, F. M., & Houtkooper, R. H. (2017). A sensitive mass spectrometry platform identifies metabolic changes of life history traits in C. elegans. *Scientific Reports*, *7*(1), 1–14. https://doi.org/10.1038/s41598-017-02539-w

García de La Banda, I., Lobo, C., León-Rubio, J. M., Tapia-Paniagua, S., Balebona, M. C., Moriñigo, M. A., Moreno-Ventas, X., Lucas, L. M., Linares, F., Arce, F., & Arijo, S. (2010). Influence of two closely related probiotics on juvenile Senegalese sole (Solea senegalensis, Kaup 1858) performance and protection against Photobacterium damselae subsp. piscicida. *Aquaculture*, *306*(1–4), 281–288. https://doi.org/10.1016/j.aquaculture.2010.05.008

Gebert, N., Cheng, C.-W., Kirkpatrick, J. M., Jasper, H., Yilmaz, H.,

Correspondence, A. O., Fraia, D. Di, Yun, J., Schä, P., Pace, S., Garside, G. B., Werz, O., Rudolph, K. L., & Ori, A. (2020). Region-Specific Proteome Changes of the Intestinal Epithelium during Aging and Dietary Restriction. *CellReports*, *31*, 107565. https://doi.org/10.1016/j.celrep.2020.107565

Genade, T., Benedetti, M., Terzibasi, E., Roncaglia, P., Valenzano, D. R., Cattaneo, A., & Cellerino, A. (2005). Annual fishes of the genus Nothobranchius as a model system for aging research. *Aging Cell*, *4*(5), 223–233. https://doi.org/10.1111/j.1474-9726.2005.00165.x

German AE Michael H Horn, D. P. (n.d.). *Gut length and mass in herbivorous and carnivorous prickleback fishes (Teleostei: Stichaeidae): ontogenetic, dietary, and phylogenetic effects*. https://doi.org/10.1007/s00227-005-0149-4

Geyfman, M., & Andersen, B. (2010). Clock genes, hair growth and aging. In *Aging* (Vol. 2, Issue 3, pp. 122–128). Impact Journals LLC. https://doi.org/10.18632/aging.100130

Gierse, L. C., Meene, A., Schultz, D., Schwaiger, T., Karte, C., Schröder, C., Wang, H., Wünsche, C., Methling, K., Kreikemeyer, B., Fuchs, S., Bernhardt, J., Becher, D., Lalk, M., Urich, T., Riedel, K., Mettenleiter, T., Beer, M., Blohm, U., … Ulrich, R. (2020). A multi-omics protocol for swine feces to elucidate longitudinal dynamics in microbiome structure and function. *Microorganisms*, *8*(12), 1–20. https://doi.org/10.3390/microorganisms8121887

Gill, S. R., Pop, M., DeBoy, R. T., Eckburg, P. B., Turnbaugh, P. J., Samuel, B. S., Gordon, J. I., Relman, D. A., Fraser-Liggett, C. M., & Nelson, K. E. (2006a). Metagenomic analysis of the human distal gut microbiome. *Science*, *312*(5778), 1355–1359. https://doi.org/10.1126/science.1124234

Gill, S. R., Pop, M., DeBoy, R. T., Eckburg, P. B., Turnbaugh, P. J., Samuel, B. S., Gordon, J. I., Relman, D. A., Fraser-Liggett, C. M., & Nelson, K. E. (2006b). Metagenomic analysis of the human distal gut microbiome. *Science*, *312*(5778), 1355–1359. https://doi.org/10.1126/science.1124234

Gonos, E. S., Derventzi, A., Kveiborg, M., Agiostratidou, G., Kassem, M., Clark, B. F. C., Jat, P. S., & Rattan, S. I. S. (1998). Cloning and identification of genes that associate with mammalian replicative senescence. *Experimental Cell Research*, *240*(1), 66–74. https://doi.org/10.1006/excr.1998.3948

Gonzalez-Covarrubias, V., Beekman, M., Uh, H., Dane, A., Troost, J., Paliukhovich, I., Kloet, F. M., Houwing-Duistermaat, J., Vreeken, R. J., Hankemeier, T., & Slagboom, E. P. (2013). Lipidomics of familial longevity. *Aging Cell*, *12*(3), 426–434. https://doi.org/10.1111/acel.12064

Gregory R. Warnes, Ben Bolker, Lodewijk Bonebakker, Robert Gentleman, W. H., Andy Liaw, Thomas Lumley, Martin Maechler, Arni Magnusson, Steffen Moeller, M., & Venables, S. and B. (2020). *gplots: Various R Programming Tools for Plotting Data.* (R package version 3.1.1). https://cran.r-project.org/package=gplots

Grice, E. A., Kong, H. H., Conlan, S., Deming, C. B., Davis, J., Young, A. C., Bouffard, G. G., Blakesley, R. W., Murray, P. R., Green, E. D., Turner, M. L., & Segre, J. A. (2009). Topographical and temporal diversity of the human skin microbiome. *Science*, *324*(5931), 1190–1192. https://doi.org/10.1126/science.1171700

Guarente, L., & Kenyon, C. (2000). Genetic pathways that regulate ageing in model organisms. In *Nature* (Vol. 408, Issue 6809, pp. 255–262). Nature Publishing

Group. https://doi.org/10.1038/35041700
Guo, Z., Lucchetta, E., Rafel, N., & Ohlstein, B. (2016). Maintenance of the adult Drosophila intestine: all roads lead to homeostasis. In *Current Opinion in Genetics and Development* (Vol. 40, pp. 81–86). Elsevier Ltd. https://doi.org/10.1016/j.gde.2016.06.009
Györfi, A. H., Matei, A. E., & Distler, J. H. W. (2018). Targeting TGF-β signaling for the treatment of fibrosis. In *Matrix Biology* (Vols. 68–69, pp. 8–27). Elsevier B.V. https://doi.org/10.1016/j.matbio.2017.12.016
Hackstadt, A. J., & Hess, A. M. (2009). Filtering for increased power for microarray data analysis. *BMC Bioinformatics*, *10*. https://doi.org/10.1186/1471-2105-10-11
Han, X., Rozen, S., Boyle, S. H., Hellegers, C., Cheng, H., Burke, J. R., Welsh-Bohmer, K. A., Doraiswamy, P. M., & Kaddurah-Daouk, R. (2011). Metabolomics in Early Alzheimer's Disease: Identification of Altered Plasma Sphingolipidome Using Shotgun Lipidomics. *PLoS ONE*, *6*(7), e21643. https://doi.org/10.1371/journal.pone.0021643
Hao, Q., Teame, T., Wu, X., Ding, Q., Ran, C., Yang, Y., Xing, Y., Zhang, Z., & Zhou, Z. (2021). Influence of diet shift from bloodworm to formulated feed on growth performance, gut microbiota structure and function in early juvenile stages of hybrid sturgeon (Acipenser baerii × Acipenser schrenckii). *Aquaculture*, *533*, 736165. https://doi.org/10.1016/j.aquaculture.2020.736165
Hao, Y. T., Wu, S. G., Xiong, F., Tran, N. T., Jakovlić, I., Zou, H., Li, W. X., & Wang, G. T. (2017). Succession and fermentation products of grass carp (Ctenopharyngodon idellus) hindgut microbiota in response to an extreme dietary shift. *Frontiers in Microbiology*, *8*(AUG). https://doi.org/10.3389/fmicb.2017.01585
Harel, I., Valenzano, D. R., & Brunet, A. (2016). Efficient genome engineering approaches for the short-lived African turquoise killifish. *Nature Protocols*, *11*(10), 2010–2028. https://doi.org/10.1038/nprot.2016.103
Haro, C., Rangel-Zúñiga, O. A., Alcalá-Díaz, J. F., Gómez-Delgado, F., Pérez-Martínez, P., Delgado-Lista, J., Quintana-Navarro, G. M., Landa, B. B., Navas-Cortés, J. A., Tena-Sempere, M., Clemente, J. C., López-Miranda, J., Pérez-Jiménez, F., & Camargo, A. (2016). Intestinal Microbiota Is Influenced by Gender and Body Mass Index. *PLOS ONE*, *11*(5), e0154090. https://doi.org/10.1371/journal.pone.0154090
Harrison, D. E., Strong, R., Sharp, Z. D., Nelson, J. F., Astle, C. M., Flurkey, K., Nadon, N. L., Wilkinson, J. E., Frenkel, K., Carter, C. S., Pahor, M., Javors, M. A., Fernandez, E., & Miller, R. A. (2009). Rapamycin fed late in life extends lifespan in genetically heterogeneous mice. *Nature*, *460*(7253), 392–395. https://doi.org/10.1038/nature08221
Hartenstein, V., & Martinez, P. (2019). Structure, development and evolution of the digestive system. In *Cell and Tissue Research* (Vol. 377, Issue 3, pp. 289–292). Springer Verlag. https://doi.org/10.1007/s00441-019-03102-x
Hartviksen, M., Vecino, J. L. G., Ringø, E., Bakke, A.-M., Wadsworth, S., Krogdahl, Å., Ruohonen, K., & Kettunen, A. (2014). Alternative dietary protein sources for Atlantic salmon (*Salmo salar* L.) effect on intestinal microbiota, intestinal and liver histology and growth. *Aquaculture Nutrition*, *20*(4), 381–398. https://doi.org/10.1111/anu.12087
Hill, M. J. (1997). Intestinal flora and endogenous vitamin synthesis. *European*

Journal of Cancer Prevention, *6*(SUPPL. 1). https://doi.org/10.1097/00008469-199703001-00009
HOFMANN, A. F. (1963). THE FUNCTION OF BILE SALTS IN FAT ABSORPTION. THE SOLVENT PROPERTIES OF. *The Biochemical Journal*, *89*(1), 57–68. https://doi.org/10.1042/bj0890057
Holzenberger, M., Dupont, J., Ducos, B., Leneuve, P., Géloën, A., Even, P. C., Cervera, P., & Le Bouc, Y. (2003). IGF-1 receptor regulates lifespan and resistance to oxidative stress in mice. *Nature*, *421*(6919), 182–187. https://doi.org/10.1038/nature01298
Honda, H., Gibson, G. R., Farmer, S., Keller, D., & McCartney, A. L. (2011). Use of a continuous culture fermentation system to investigate the effect of GanedenBC30 (Bacillus coagulans GBI-30, 6086) supplementation on pathogen survival in the human gut microbiota. *Anaerobe*, *17*(1), 36–42. https://doi.org/10.1016/j.anaerobe.2010.12.006
Honkanen, R. E., & Patton, J. S. (1987). Bile salt absorption in killfish intestine. *American Journal of Physiology - Gastrointestinal and Liver Physiology*, *253*(6). https://doi.org/10.1152/ajpgi.1987.253.6.g730
Horstman, A. M., Dillon, E. L., Urban, R. J., & Sheffield-Moore, M. (2012). The role of androgens and estrogens on healthy aging and longevity. In *Journals of Gerontology - Series A Biological Sciences and Medical Sciences* (Vol. 67, Issue 11, pp. 1140–1152). J Gerontol A Biol Sci Med Sci. https://doi.org/10.1093/gerona/gls068
Hu, C. K., Wang, W., Brind'Amour, J., Singh, P. P., Adam Reeves, G., Lorincz, M. C., Alvarado, A. S., & Brunet, A. (2020). Vertebrate diapause preserves organisms long term through Polycomb complex members. *Science*, *367*(6480), 870–874. https://doi.org/10.1126/science.aaw2601
Huttenhower, C., Gevers, D., Knight, R., Abubucker, S., Badger, J. H., Chinwalla, A. T., Creasy, H. H., Earl, A. M., Fitzgerald, M. G., Fulton, R. S., Giglio, M. G., Hallsworth-Pepin, K., Lobos, E. A., Madupu, R., Magrini, V., Martin, J. C., Mitreva, M., Muzny, D. M., Sodergren, E. J., … White, O. (2012). Structure, function and diversity of the healthy human microbiome. *Nature*, *486*(7402), 207–214. https://doi.org/10.1038/nature11234
Ippolito, C., Segnani, C., Errede, M., Virgintino, D., Colucci, R., Fornai, M., Antonioli, L., Blandizzi, C., Dolfi, A., & Bernardini, N. (2015). An integrated assessment of histopathological changes of the enteric neuromuscular compartment in experimental colitis. *Journal of Cellular and Molecular Medicine*, *19*(2), 485–500. https://doi.org/10.1111/jcmm.12428
Jackson, M., Jeffery, I. B., Beaumont, M., Bell, J. T., Clark, A. G., Ley, R. E., O'Toole, P. W., Spector, T. D., & Steves, C. J. (2016). Signatures of early frailty in the gut microbiota. *Genome Medicine*, *8*(1). https://doi.org/10.1186/s13073-016-0262-7
Jami, M., Ghanbari, M., Kneifel, W., & Domig, K. J. (2015). Phylogenetic diversity and biological activity of culturable Actinobacteria isolated from freshwater fish gut microbiota. *Microbiological Research*, *175*, 6–15. https://doi.org/10.1016/j.micres.2015.01.009
Janda, J. M., & Abbott, S. L. (2010). The genus Aeromonas: Taxonomy, pathogenicity, and infection. In *Clinical Microbiology Reviews* (Vol. 23, Issue 1, pp. 35–73). American Society for Microbiology Journals.

https://doi.org/10.1128/CMR.00039-09
Jari Oksanen, F. Guillaume Blanchet, Michael Friendly, Roeland Kindt, P. L., Dan McGlinn, Peter R. Minchin, R. B. O'Hara, Gavin L. Simpson, Peter Solymos, M. H., & H. Stevens, E. S. and H. W. (2020). *vegan: Community Ecology Package.* (R package version 2.5-7). https://cran.r-project.org/package=vegan
Jia, W., Xie, G., & Jia, W. (2018). Bile acid–microbiota crosstalk in gastrointestinal inflammation and carcinogenesis. In *Nature Reviews Gastroenterology and Hepatology* (Vol. 15, Issue 2, pp. 111–128). Nature Publishing Group. https://doi.org/10.1038/nrgastro.2017.119
Johansson, M. E. V., & Hansson, G. C. (2016). Immunological aspects of intestinal mucus and mucins. In *Nature Reviews Immunology* (Vol. 16, Issue 10, pp. 639–649). Nature Publishing Group. https://doi.org/10.1038/nri.2016.88
Johnson, P. E., Milne, D. B., & Lykken, G. I. (1992). Effects of age and sex on copper absorption, biological half-life, and status in humans. *The American Journal of Clinical Nutrition*, *56*(5), 917–925. https://doi.org/10.1093/ajcn/56.5.917
Jong, C. J., Azuma, J., & Schaffer, S. (2012). Mechanism underlying the antioxidant activity of taurine: Prevention of mitochondrial oxidant production. *Amino Acids*, *42*(6), 2223–2232. https://doi.org/10.1007/s00726-011-0962-7
Jové, M., Naudí, A., Gambini, J., Borras, C., Cabré, R., Portero-Otín, M., Viña, J., & Pamplona, R. (2017). A Stress-Resistant Lipidomic Signature Confers Extreme Longevity to Humans. *The Journals of Gerontology Series A: Biological Sciences and Medical Sciences*, *72*(1), 30–37. https://doi.org/10.1093/gerona/glw048
Kaeberlein, M., Powers, R. W., Steffen, K. K., Westman, E. A., Hu, D., Dang, N., Kerr, E. O., Kirkland, K. T., Fields, S., & Kennedy, B. K. (2005). Cell biology: Regulation of yeast replicative life span by TOR and Sch9 response to nutrients. *Science*, *310*(5751), 1193–1196. https://doi.org/10.1126/science.1115535
Kamburov, A., Wierling, C., Lehrach, H., & Herwig, R. (2009). ConsensusPathDB - A database for integrating human functional interaction networks. *Nucleic Acids Research*, *37*(SUPPL. 1). https://doi.org/10.1093/nar/gkn698
Kapahi, P., Zid, B. M., Harper, T., Koslover, D., Sapin, V., & Benzer, S. (2004). Regulation of lifespan in Drosophila by modulation of genes in the TOR signaling pathway. *Current Biology*, *14*(10), 885–890. https://doi.org/10.1016/j.cub.2004.03.059
Kapoor, B. G., Smit, H., & Verighina, I. A. (1976). The Alimentary Canal and Digestion in Teleosts. *Advances in Marine Biology*, *13*(C), 109–239. https://doi.org/10.1016/S0065-2881(08)60281-3
Karasov, W. H., Martínez Del Rio, C., & Caviedes-Vidal, E. (2011). Ecological physiology of diet and digestive systems. *Annual Review of Physiology*, *73*, 69–93. https://doi.org/10.1146/annurev-physiol-012110-142152
Kasahara, K., Krautkramer, K. A., Org, E., Romano, K. A., Kerby, R. L., Vivas, E. I., Mehrabian, M., Denu, J. M., Bäckhed, F., Lusis, A. J., & Rey, F. E. (2018). Interactions between Roseburia intestinalis and diet modulate atherogenesis in a murine model. *Nature Microbiology*, *3*(12), 1461–1471. https://doi.org/10.1038/s41564-018-0272-x
Kawanishi, N., Kato, Y., Yokozeki, K., Sawada, S., Sakurai, R., Fujiwara, Y., Shinkai, S., Goda, N., & Suzuki, K. (2018). Effects of aging on serum levels of lipid

molecular species as determined by lipidomics analysis in Japanese men and women. *Lipids in Health and Disease*, *17*(1). https://doi.org/10.1186/s12944-018-0785-6

Kenyon, C., Chang, J., Gensch, E., Rudner, A., & Tabtiang, R. (1993). A C. elegans mutant that lives twice as long as wild type. *Nature*, *366*(6454), 461–464. https://doi.org/10.1038/366461a0

Khoruts, A., Dicksved, J., Jansson, J. K., & Sadowsky, M. J. (2010). Changes in the Composition of the Human Fecal Microbiome After Bacteriotherapy for Recurrent Clostridium difficile-associated Diarrhea. *Journal of Clinical Gastroenterology*, *44*(5), 354–360. https://doi.org/10.1097/MCG.0b013e3181c87e02

Khurana, H., Singh, D. N., Singh, A., Singh, Y., Lal, R., & Negi, R. K. (2020). Gut microbiome of endangered Tor putitora (Ham.) as a reservoir of antibiotic resistance genes and pathogens associated with fish health. *BMC Microbiology*, *20*(1). https://doi.org/10.1186/s12866-020-01911-7

Kim, M., Qie, Y., Park, J., & Kim, C. H. (2016). Gut Microbial Metabolites Fuel Host Antibody Responses. *Cell Host and Microbe*, *20*(2), 202–214. https://doi.org/10.1016/j.chom.2016.07.001

Ko, C. W., Qu, J., Black, D. D., & Tso, P. (2020). Regulation of intestinal lipid metabolism: current concepts and relevance to disease. In *Nature Reviews Gastroenterology and Hepatology* (Vol. 17, Issue 3, pp. 169–183). Nature Research. https://doi.org/10.1038/s41575-019-0250-7

Kobayashi, K. S., Chamaillard, M., Ogura, Y., Henegariu, O., Inohara, N., Nuñez, G., & Flavell, R. A. (2005). Nod2-dependent regulation of innate and adaptive immunity in the intestinal tract. *Science*, *307*(5710), 731–734. https://doi.org/10.1126/science.1104911

Kokou, F., Sasson, G., Friedman, J., Eyal, S., Ovadia, O., Harpaz, S., Cnaani, A., & Mizrahi, I. (2019). Core gut microbial communities are maintained by beneficial interactions and strain variability in fish. *Nature Microbiology*, *4*(12), 2456–2465. https://doi.org/10.1038/s41564-019-0560-0

Koltai, T. (2014). Clusterin: A key player in cancer chemoresistance and its inhibition. In *OncoTargets and Therapy* (Vol. 7, pp. 447–456). DOVE Medical Press Ltd. https://doi.org/10.2147/OTT.S58622

Kontis, V., Bennett, J. E., Mathers, C. D., Li, G., Foreman, K., & Ezzati, M. (2017). Future life expectancy in 35 industrialised countries: projections with a Bayesian model ensemble. *The Lancet*, *389*(10076), 1323–1335. https://doi.org/10.1016/S0140-6736(16)32381-9

Koo, H., Hakim, J. A., Powell, M. L., Kumar, R., Eipers, P. G., Morrow, C. D., Crowley, M., Lefkowitz, E. J., Watts, S. A., & Bej, A. K. (2017). Metagenomics approach to the study of the gut microbiome structure and function in zebrafish Danio rerio fed with gluten formulated diet. *Journal of Microbiological Methods*, *135*, 69–76. https://doi.org/10.1016/j.mimet.2017.01.016

Korpela, K., & de Vos, W. M. (2016). Antibiotic use in childhood alters the gut microbiota and predisposes to overweight. In *Microbial Cell* (Vol. 3, Issue 7, pp. 296–298). Shared Science Publishers OG. https://doi.org/10.15698/mic2016.07.514

Krautkramer, K. A., Fan, J., & Bäckhed, F. (2021). Gut microbial metabolites as multi-kingdom intermediates. In *Nature Reviews Microbiology* (Vol. 19, Issue 2,

pp. 77–94). Nature Research. https://doi.org/10.1038/s41579-020-0438-4
Lacolley, P., Regnault, V., & Avolio, A. P. (2018). Smooth muscle cell and arterial aging: Basic and clinical aspects. In *Cardiovascular Research* (Vol. 114, Issue 4, pp. 513–528). Oxford University Press. https://doi.org/10.1093/cvr/cvy009
Langille, M. G. I., Zaneveld, J., Caporaso, J. G., McDonald, D., Knights, D., Reyes, J. A., Clemente, J. C., Burkepile, D. E., Vega Thurber, R. L., Knight, R., Beiko, R. G., & Huttenhower, C. (2013). Predictive functional profiling of microbial communities using 16S rRNA marker gene sequences. *Nature Biotechnology*, *31*(9), 814–821. https://doi.org/10.1038/nbt.2676
Lategan, M. J., & Gibson, L. F. (2003). Antagonistic activity of Aeromonas media strain A199 against Saprolegnia sp., an opportunistic pathogen of the eel, Anguilla australis Richardson. *Journal of Fish Diseases*, *26*(3), 147–153. https://doi.org/10.1046/j.1365-2761.2003.00443.x
Lathrop, S. K., Bloom, S. M., Rao, S. M., Nutsch, K., Lio, C. W., Santacruz, N., Peterson, D. A., Stappenbeck, T. S., & Hsieh, C. S. (2011). Peripheral education of the immune system by colonic commensal microbiota. *Nature*, *478*(7368), 250–254. https://doi.org/10.1038/nature10434
Lauder, A. P., Roche, A. M., Sherrill-Mix, S., Bailey, A., Laughlin, A. L., Bittinger, K., Leite, R., Elovitz, M. A., Parry, S., & Bushman, F. D. (2016). Comparison of placenta samples with contamination controls does not provide evidence for a distinct placenta microbiota. *Microbiome*, *4*(1), 29. https://doi.org/10.1186/s40168-016-0172-3
Le, H. T. M. D., Shao, X., Krogdahl, Å., Kortner, T. M., Lein, I., Kousoulaki, K., Lie, K. K., & Sæle, Ø. (2019). Intestinal Function of the Stomachless Fish, Ballan Wrasse (Labrus bergylta). *Frontiers in Marine Science*, *6*(MAR), 140. https://doi.org/10.3389/fmars.2019.00140
Lee, H. Y., Lee, S. H., Lee, J. H., Lee, W. J., & Min, K. J. (2019). The role of commensal microbes in the lifespan of Drosophila melanogaster. *Aging*, *11*(13), 4611–4640. https://doi.org/10.18632/aging.102073
Li, H., Qi, Y., & Jasper, H. (2016). Preventing Age-Related Decline of Gut Compartmentalization Limits Microbiota Dysbiosis and Extends Lifespan. *Cell Host & Microbe*, *19*(2), 240–253. https://doi.org/10.1016/j.chom.2016.01.008
Liao, B., Ning, Z., Cheng, K., Zhang, X., Li, L., Mayne, J., & Figeys, D. (2018). IMetaLab 1.0: A web platform for metaproteomics data analysis. *Bioinformatics*, *34*(22), 3954–3956. https://doi.org/10.1093/bioinformatics/bty466
Lickwar, C. R., Camp, J. G., Weiser, M., Cocchiaro, J. L., Kingsley, D. M., Furey, T. S., Sheikh, S. Z., & Rawls, J. F. (2017). Genomic dissection of conserved transcriptional regulation in intestinal epithelial cells. *PLoS Biology*, *15*(8), e2002054. https://doi.org/10.1371/journal.pbio.2002054
Liu, H., Guo, X., Gooneratne, R., Lai, R., Zeng, C., Zhan, F., & Wang, W. (2016). The gut microbiome and degradation enzyme activity of wild freshwater fishes influenced by their trophic levels. *Scientific Reports*, *6*(1), 24340. https://doi.org/10.1038/srep24340
Llewellyn, M. S., Boutin, S., Hoseinifar, S. H., & Derome, N. (2014). Teleost microbiomes: The state of the art in their characterization, manipulation and importance in aquaculture and fisheries. In *Frontiers in Microbiology* (Vol. 5, Issue JUN, pp. 1–1). Frontiers Research Foundation. https://doi.org/10.3389/fmicb.2014.00207

Locey, K. J., & Lennon, J. T. (2016). Scaling laws predict global microbial diversity. *Proceedings of the National Academy of Sciences of the United States of America*, *113*(21), 5970–5975. https://doi.org/10.1073/pnas.1521291113

López-Otín, C., Blasco, M. A., Partridge, L., Serrano, M., & Kroemer, G. (2013). The Hallmarks of Aging. *Cell*, *153*(6), 1194–1217. https://doi.org/10.1016/J.CELL.2013.05.039

Love, M. I., Huber, W., & Anders, S. (2014). Moderated estimation of fold change and dispersion for RNA-seq data with DESeq2. *Genome Biology*, *15*(12), 550. https://doi.org/10.1186/s13059-014-0550-8

Lovell, R. M., & Ford, A. C. (2012). Global Prevalence of and Risk Factors for Irritable Bowel Syndrome: A Meta-analysis. In *Clinical Gastroenterology and Hepatology* (Vol. 10, Issue 7, pp. 712-721.e4). W.B. Saunders. https://doi.org/10.1016/j.cgh.2012.02.029

Lozupone, C. A., Stombaugh, J. I., Gordon, J. I., Jansson, J. K., & Knight, R. (2012). Diversity, stability and resilience of the human gut microbiota. In *Nature* (Vol. 489, Issue 7415, pp. 220–230). NIH Public Access. https://doi.org/10.1038/nature11550

Lu, F., Inoue, K., Kato, J., Minamishima, S., & Morisaki, H. (2019). Functions and regulation of lipocalin-2 in gut-origin sepsis: A narrative review. In *Critical Care* (Vol. 23, Issue 1). BioMed Central Ltd. https://doi.org/10.1186/s13054-019-2550-2

Ludington, W. B., & Ja, W. W. (2020). Drosophila as a model for the gut microbiome. *PLOS Pathogens*, *16*(4), e1008398. https://doi.org/10.1371/journal.ppat.1008398

MacEyka, M., & Spiegel, S. (2014). Sphingolipid metabolites in inflammatory disease. In *Nature* (Vol. 510, Issue 7503, pp. 58–67). Nature Publishing Group. https://doi.org/10.1038/nature13475

Manivasagan, P., Venkatesan, J., & Kim, S.-K. (2013). *Introduction to Marine Actinobacteria*.

Mansfield, G. S., Desai, A. R., Nilson, S. A., Van Kessel, A. G., Drew, M. D., & Hill, J. E. (2010). Characterization of rainbow trout (Oncorhynchus mykiss) intestinal microbiota and inflammatory marker gene expression in a recirculating aquaculture system. *Aquaculture*, *307*(1–2), 95–104. https://doi.org/10.1016/j.aquaculture.2010.07.014

Mariat, D., Firmesse, O., Levenez, F., Guimarăes, V. D., Sokol, H., Doré, J., Corthier, G., & Furet, J. P. (2009). The firmicutes/bacteroidetes ratio of the human microbiota changes with age. *BMC Microbiology*, *9*(1), 123. https://doi.org/10.1186/1471-2180-9-123

Mariño, E., Richards, J. L., McLeod, K. H., Stanley, D., Yap, Y. A., Knight, J., McKenzie, C., Kranich, J., Oliveira, A. C., Rossello, F. J., Krishnamurthy, B., Nefzger, C. M., Macia, L., Thorburn, A., Baxter, A. G., Morahan, G., Wong, L. H., Polo, J. M., Moore, R. J., … Mackay, C. R. (2017). Gut microbial metabolites limit the frequency of autoimmune T cells and protect against type 1 diabetes. *Nature Immunology*, *18*(5), 552–562. https://doi.org/10.1038/ni.3713

Markle, J. G. M., Frank, D. N., Mortin-Toth, S., Robertson, C. E., Feazel, L. M., Rolle-Kampczyk, U., von Bergen, M., McCoy, K. D., Macpherson, A. J., & Danska, J. S. (2013). Sex differences in the gut microbiome drive hormone-dependent regulation of autoimmunity. *Science (New York, N.Y.)*, *339*(6123),

1084–1088. https://doi.org/10.1126/science.1233521
Martineau, C., Mauffrey, F., & Villemur, R. (2015). Comparative analysis of denitrifying activities of Hyphomicrobium nitrativorans, Hyphomicrobium denitrificans, and Hyphomicrobium zavarzinii. *Applied and Environmental Microbiology*, *81*(15), 5003–5014. https://doi.org/10.1128/AEM.00848-15
Matsui, H., Kenmochi, N., & Namikawa, K. (2019). Age- and α-Synuclein-Dependent Degeneration of Dopamine and Noradrenaline Neurons in the Annual Killifish Nothobranchius furzeri. *Cell Reports*, *26*(7), 1727-1733.e6. https://doi.org/10.1016/j.celrep.2019.01.015
McCombe, P. A., & Greer, J. M. (2013). Sexual Dimorphism in the Immune System. In *The Autoimmune Diseases: Fifth Edition* (pp. 319–328). Elsevier Inc. https://doi.org/10.1016/B978-0-12-384929-8.00024-1
McCully, K. K., Forciea, M. A., Hack, L. M., Donlon, E., Wheatley, R. W., Oatis, C. A., Goldberg, T., & Chance, B. (1991). Muscle metabolism in older subjects using 31P magnetic resonance spectroscopy. *Canadian Journal of Physiology and Pharmacology*, *69*(5), 576–580. https://doi.org/10.1139/y91-084
McDonald, R., Schreier, H. J., & Watts, J. E. M. (2012). Phylogenetic Analysis of Microbial Communities in Different Regions of the Gastrointestinal Tract in Panaque nigrolineatus, a Wood-Eating Fish. *PLoS ONE*, *7*(10), e48018. https://doi.org/10.1371/journal.pone.0048018
McMurdie, P. J., & Holmes, S. (2013). Phyloseq: An R Package for Reproducible Interactive Analysis and Graphics of Microbiome Census Data. *PLoS ONE*, *8*(4), e61217. https://doi.org/10.1371/journal.pone.0061217
Mekuchi, M., Asakura, T., Sakata, K., Yamaguchi, T., Teruya, K., & Kikuchi, J. (2018). Intestinal microbiota composition is altered according to nutritional biorhythms in the leopard coral grouper (Plectropomus leopardus). *PLoS ONE*, *13*(6), e0197256. https://doi.org/10.1371/journal.pone.0197256
Melzer, D., Pilling, L. C., & Ferrucci, L. (2020). The genetics of human ageing. In *Nature Reviews Genetics* (Vol. 21, Issue 2, pp. 88–101). Nature Research. https://doi.org/10.1038/s41576-019-0183-6
Meyers, K., López, M., Ho, J., Wills, S., Rayalam, S., & Taval, S. (2020). Lipocalin-2 deficiency may predispose to the progression of spontaneous age-related adiposity in mice. *Scientific Reports*, *10*(1), 14589. https://doi.org/10.1038/s41598-020-71249-7
Mielke, M. M., Bandaru, V. V. R., Han, D., An, Y., Resnick, S. M., Ferrucci, L., & Haughey, N. J. (2015). Factors affecting longitudinal trajectories of plasma sphingomyelins: the Baltimore Longitudinal Study of Aging. *Aging Cell*, *14*(1), 112–121. https://doi.org/10.1111/acel.12275
Mittendorfer, B. (2005). Sexual dimorphism in human lipid metabolism. In *Journal of Nutrition* (Vol. 135, Issue 4, pp. 681–686). American Institute of Nutrition. https://doi.org/10.1093/jn/135.4.681
Momozawa, Y., Deffontaine, V., Louis, E., & Medrano, J. F. (2011). Characterization of Bacteria in Biopsies of Colon and Stools by High Throughput Sequencing of the V2 Region of Bacterial 16S rRNA Gene in Human. *PLoS ONE*, *6*(2), e16952. https://doi.org/10.1371/journal.pone.0016952
Moran, B. J., & Jackson, A. A. (1992). Function of the human colon. In *British Journal of Surgery* (Vol. 79, Issue 11, pp. 1132–1137). Br J Surg. https://doi.org/10.1002/bjs.1800791106

Mowat, A. M., & Agace, W. W. (2014a). Regional specialization within the intestinal immune system. In *Nature Reviews Immunology* (Vol. 14, Issue 10, pp. 667–685). Nature Publishing Group. https://doi.org/10.1038/nri3738

Mowat, A. M., & Agace, W. W. (2014b). Regional specialization within the intestinal immune system. *Nature Reviews Immunology*, *14*(10), 667–685. https://doi.org/10.1038/nri3738

Mudarris, M., & Austin, B. (1988). Quantitative and qualitative studies of the bacterial microflora of turbot, Scophthalmus maximus L., gills. *Journal of Fish Biology*, *32*(2), 223–229. https://doi.org/10.1111/j.1095-8649.1988.tb05355.x

Muniz, L. R., Knosp, C., & Yeretssian, G. (2012). Intestinal antimicrobial peptides during homeostasis, infection, and disease. In *Frontiers in Immunology* (Vol. 3, Issue OCT). Front Immunol. https://doi.org/10.3389/fimmu.2012.00310

Murtha, L. A., Morten, M., Schuliga, M. J., Mabotuwana, N. S., Hardy, S. A., Waters, D. W., Burgess, J. K., Ngo, D. T. M., Sverdlov, A. L., Knight, D. A., & Boyle, A. J. (2019). The role of pathological aging in cardiac and pulmonary fibrosis. In *Aging and Disease* (Vol. 10, Issue 2, pp. 419–428). International Society on Aging and Disease. https://doi.org/10.14336/AD.2018.0601

Nasidze, I., Li, J., Quinque, D., Tang, K., & Stoneking, M. (2009). Global diversity in the human salivary microbiome. *Genome Research*, *19*(4), 636–643. https://doi.org/10.1101/gr.084616.108

Niccoli, T., & Partridge, L. (2012). Ageing as a risk factor for disease. In *Current Biology* (Vol. 22, Issue 17, pp. R741–R752). Cell Press. https://doi.org/10.1016/j.cub.2012.07.024

Nikolich-Žugich, J. (2018). The twilight of immunity: Emerging concepts in aging of the immune system review-article. *Nature Immunology*, *19*(1), 10–19. https://doi.org/10.1038/s41590-017-0006-x

Nimpf, J., Wurm, H., & Kostner, G. M. (1987). β2-glycoprotein-I (apo-H) inhibits the release reaction of human platelets during ADP-induced aggregation. *Atherosclerosis*, *63*(2–3), 109–114. https://doi.org/10.1016/0021-9150(87)90110-9

Nocek, J. E., & Russell, J. B. (1988). Protein and Energy as an Integrated System. Relationship of Ruminal Protein and Carbohydrate Availability to Microbial Synthesis and Milk Production. *Journal of Dairy Science*, *71*(8), 2070–2107. https://doi.org/10.3168/JDS.S0022-0302(88)79782-9

Obata, F., Fons, C. O., & Gould, A. P. (2018). Early-life exposure to low-dose oxidants can increase longevity via microbiome remodelling in Drosophila. *Nature Communications*, *9*(1), 1–12. https://doi.org/10.1038/s41467-018-03070-w

Oeppen, J., & Vaupel, J. W. (2002). Demography: Broken limits to life expectancy. In *Science* (Vol. 296, Issue 5570, pp. 1029–1031). https://doi.org/10.1126/science.1069675

Org, E., Mehrabian, M., Parks, B. W., Shipkova, P., Liu, X., Drake, T. A., & Lusis, A. J. (2016). Sex differences and hormonal effects on gut microbiota composition in mice. *Gut Microbes*, *7*(4), 313–322. https://doi.org/10.1080/19490976.2016.1203502

Palleja, A., Mikkelsen, K. H., Forslund, S. K., Kashani, A., Allin, K. H., Nielsen, T., Hansen, T. H., Liang, S., Feng, Q., Zhang, C., Pyl, P. T., Coelho, L. P., Yang, H., Wang, J., Typas, A., Nielsen, M. F., Nielsen, H. B., Bork, P., Wang, J., …

Pedersen, O. (2018). Recovery of gut microbiota of healthy adults following antibiotic exposure. *Nature Microbiology*, *3*(11), 1255–1265. https://doi.org/10.1038/s41564-018-0257-9

Parker, J. L., & Shaw, J. G. (2011). Aeromonas spp. clinical microbiology and disease. In *Journal of Infection* (Vol. 62, Issue 2, pp. 109–118). W.B. Saunders. https://doi.org/10.1016/j.jinf.2010.12.003

Partridge, L., Deelen, J., & Slagboom, P. E. (2018). Facing up to the global challenges of ageing. In *Nature* (Vol. 561, Issue 7721, pp. 45–56). Nature Publishing Group. https://doi.org/10.1038/s41586-018-0457-8

Pedregosa FABIANPEDREGOSA, F., Michel, V., Grisel OLIVIERGRISEL, O., Blondel, M., Prettenhofer, P., Weiss, R., Vanderplas, J., Cournapeau, D., Pedregosa, F., Varoquaux, G., Gramfort, A., Thirion, B., Grisel, O., Dubourg, V., Passos, A., Brucher, M., Perrot andÉdouardand, M., Duchesnay, andÉdouard, & Duchesnay EDOUARDDUCHESNAY, Fré. (2011). Scikit-learn: Machine Learning in Python Gaël Varoquaux Bertrand Thirion Vincent Dubourg Alexandre Passos PEDREGOSA, VAROQUAUX, GRAMFORT ET AL. Matthieu Perrot. In *Journal of Machine Learning Research* (Vol. 12). http://scikit-learn.sourceforge.net.

Peng, L., Li, Z.-R., Green, R. S., Holzman, I. R., & Lin, J. (2009). Butyrate Enhances the Intestinal Barrier by Facilitating Tight Junction Assembly via Activation of AMP-Activated Protein Kinase in Caco-2 Cell Monolayers. *The Journal of Nutrition*, *139*(9), 1619–1625. https://doi.org/10.3945/jn.109.104638

Petriz, B. A., Castro, A. P., Almeida, J. A., Gomes, C. P. C., Fernandes, G. R., Kruger, R. H., Pereira, R. W., & Franco, O. L. (2014). Exercise induction of gut microbiota modifications in obese, non-obese and hypertensive rats. *BMC Genomics*, *15*(1), 511. https://doi.org/10.1186/1471-2164-15-511

Piper, M. D. W., & Partridge, L. (2018). Drosophila as a model for ageing. In *Biochimica et Biophysica Acta - Molecular Basis of Disease* (Vol. 1864, Issue 9, pp. 2707–2717). Elsevier B.V. https://doi.org/10.1016/j.bbadis.2017.09.016

Poeschla, M., & Valenzano, D. R. (2020). The turquoise killifish: A genetically tractable model for the study of aging. In *Journal of Experimental Biology* (Vol. 223, Issue Suppl_1). Company of Biologists Ltd. https://doi.org/10.1242/jeb.209296

Poole, P., Ramachandran, V., & Terpolilli, J. (2018). Rhizobia: From saprophytes to endosymbionts. *Nature Reviews Microbiology*, *16*(5), 291–303. https://doi.org/10.1038/nrmicro.2017.171

Popkes, M., & Valenzano, D. R. (2020). Microbiota–host interactions shape ageing dynamics. *Philosophical Transactions of the Royal Society B: Biological Sciences*, *375*(1808), 20190596. https://doi.org/10.1098/rstb.2019.0596

Qin, J., Liu, Q., Liu, Z., Pan, Y. Z., Sifuentes-Dominguez, L., Stepien, K. P., Wang, Y., Tu, Y., Tan, S., Wang, Y., Sun, Q., Mo, X., Rizo, J., Burstein, E., & Jia, D. (2020). Structural and mechanistic insights into secretagogin-mediated exocytosis. *Proceedings of the National Academy of Sciences of the United States of America*, *117*(12), 6559–6570. https://doi.org/10.1073/pnas.1919698117

Quast, C., Pruesse, E., Yilmaz, P., Gerken, J., Schweer, T., Yarza, P., Peplies, J., & Glöckner, F. O. (2013). The SILVA ribosomal RNA gene database project: Improved data processing and web-based tools. *Nucleic Acids Research*,

41(D1), D590. https://doi.org/10.1093/nar/gks1219
R Core Team. (2020). *R: A language and environment for statistical computing. R Foundation for Statistical Computing, Vienna, Austria.* https://www.r-project.org/
Ramírez, C., Coronado, J., Silva, A., & Romero, J. (2018). Cetobacterium is a major component of the microbiome of giant amazonian fish (Arapaima gigas) in Ecuador. *Animals*, *8*(11). https://doi.org/10.3390/ani8110189
Rampelli, S., Candela, M., Turroni, S., Collino, E. B., Franceschi, C., O'Toole, P. W., & Brigidi, P. (2013). Functional metagenomic profiling of intestinal microbiome in extreme ageing. *Aging*, *5*(12), 902–912. https://doi.org/10.18632/aging.100623
Rappsilber, J., Ishihama, Y., & Mann, M. (2003). Stop And Go Extraction tips for matrix-assisted laser desorption/ionization, nanoelectrospray, and LC/MS sample pretreatment in proteomics. *Analytical Chemistry*, *75*(3), 663–670. https://doi.org/10.1021/ac026117i
Ravel, J., Gajer, P., Abdo, Z., Schneider, G. M., Koenig, S. S. K., McCulle, S. L., Karlebach, S., Gorle, R., Russell, J., Tacket, C. O., Brotman, R. M., Davis, C. C., Ault, K., Peralta, L., & Forney, L. J. (2011). Vaginal microbiome of reproductive-age women. *Proceedings of the National Academy of Sciences of the United States of America*, *108*(SUPPL. 1), 4680–4687. https://doi.org/10.1073/pnas.1002611107
Rawson, E. S., Wehnert, M. L., & Clarkson, P. M. (1999). Effects of 30 days of creatine ingestion in older men. *European Journal of Applied Physiology and Occupational Physiology*, *80*(2), 139–144. https://doi.org/10.1007/s004210050570
Regan, J. C., Khericha, M., Dobson, A. J., Bolukbasi, E., Rattanavirotkul, N., & Partridge, L. (2016a). Sex difference in pathology of the ageing gut mediates the greater response of female lifespan to dietary restriction. *ELife*, *5*, e10956. https://doi.org/10.7554/eLife.10956
Regan, J. C., Khericha, M., Dobson, A. J., Bolukbasi, E., Rattanavirotkul, N., & Partridge, L. (2016b). Sex difference in pathology of the ageing gut mediates the greater response of female lifespan to dietary restriction. *ELife*, *5*, e10956. https://doi.org/10.7554/eLife.10956
Rehan, M., Kurundkar, D., Kurundkar, A. R., Logsdon, N. J., Smith, S. R., Chanda, D., Bernard, K., Sanders, Y. Y., Deshane, J. S., Dsouza, K. G., Rangarajan, S., Zmijewski, J. W., & Thannickal, V. J. (2021). Restoration of SIRT3 gene expression by airway delivery resolves age-associated persistent lung fibrosis in mice. *Nature Aging*, *1*(2), 205–217. https://doi.org/10.1038/s43587-021-00027-5
Reichwald, K., Petzold, A., Koch, P., Downie, B. R., Hartmann, N., Pietsch, S., Baumgart, M., Chalopin, D., Felder, M., Bens, M., Sahm, A., Szafranski, K., Taudien, S., Groth, M., Arisi, I., Weise, A., Bhatt, S. S., Sharma, V., Kraus, J. M., … Platzer, M. (2015). Insights into Sex Chromosome Evolution and Aging from the Genome of a Short-Lived Fish. *Cell*, *163*(6), 1527–1538. https://doi.org/10.1016/j.cell.2015.10.071
Ren, C., Webster, P., Finkel, S. E., & Tower, J. (2007). Increased Internal and External Bacterial Load during Drosophila Aging without Life-Span Trade-Off. *Cell Metabolism*, *6*(2), 144–152. https://doi.org/10.1016/j.cmet.2007.06.006
Rera, M., Clark, R. I., & Walker, D. W. (2012). Intestinal barrier dysfunction links metabolic and inflammatory markers of aging to death in Drosophila. *Proceedings of the National Academy of Sciences of the United States of*

America, *109*(52), 21528–21533. https://doi.org/10.1073/pnas.1215849110
Ridaura, V. K., Faith, J. J., Rey, F. E., Cheng, J., Duncan, A. E., Kau, A. L., Griffin, N. W., Lombard, V., Henrissat, B., Bain, J. R., Muehlbauer, M. J., Ilkayeva, O., Semenkovich, C. F., Funai, K., Hayashi, D. K., Lyle, B. J., Martini, M. C., Ursell, L. K., Clemente, J. C., … Gordon, J. I. (2013). Gut microbiota from twins discordant for obesity modulate metabolism in mice. *Science*, *341*(6150). https://doi.org/10.1126/science.1241214
Ridlon, J. M., Kang, D. J., & Hylemon, P. B. (2006). Bile salt biotransformations by human intestinal bacteria. In *Journal of Lipid Research* (Vol. 47, Issue 2, pp. 241–259). Elsevier. https://doi.org/10.1194/jlr.R500013-JLR200
Ringo, E., & Olsen, R. E. (1999). The effect of diet on aerobic bacterial flora associated with intestine of Arctic charr (Salvelinus alpinus L.). *Journal of Applied Microbiology*, *86*(1), 22–28. https://doi.org/10.1046/j.1365-2672.1999.00631.x
Ringø, E., Zhou, Z., Vecino, J. L. G., Wadsworth, S., Romero, J., Krogdahl, Olsen, R. E., Dimitroglou, A., Foey, A., Davies, S., Owen, M., Lauzon, H. L., Martinsen, L. L., De Schryver, P., Bossier, P., Sperstad, S., & Merrifield, D. L. (2016a). Effect of dietary components on the gut microbiota of aquatic animals. A never-ending story? *Aquaculture Nutrition*, *22*(2), 219–282. https://doi.org/10.1111/anu.12346
Ringø, E., Zhou, Z., Vecino, J. L. G., Wadsworth, S., Romero, J., Krogdahl, Olsen, R. E., Dimitroglou, A., Foey, A., Davies, S., Owen, M., Lauzon, H. L., Martinsen, L. L., De Schryver, P., Bossier, P., Sperstad, S., & Merrifield, D. L. (2016b). Effect of dietary components on the gut microbiota of aquatic animals. A never-ending story? *Aquaculture Nutrition*, *22*(2), 219–282. https://doi.org/10.1111/anu.12346
Ritchie, M. E., Phipson, B., Wu, D., Hu, Y., Law, C. W., Shi, W., & Smyth, G. K. (2015). Limma powers differential expression analyses for RNA-sequencing and microarray studies. *Nucleic Acids Research*, *43*(7), e47. https://doi.org/10.1093/nar/gkv007
Rodríguez, J. M., Murphy, K., Stanton, C., Ross, R. P., Kober, O. I., Juge, N., Avershina, E., Rudi, K., Narbad, A., Jenmalm, M. C., Marchesi, J. R., & Collado, M. C. (2015). The composition of the gut microbiota throughout life, with an emphasis on early life. *Microbial Ecology in Health & Disease*, *26*(0). https://doi.org/10.3402/mehd.v26.26050
Roediger, W. E. W. (1982). Utilization of Nutrients by Isolated Epithelial Cells of the Rat Colon. *Gastroenterology*, *83*(2), 424–429. https://doi.org/10.1016/S0016-5085(82)80339-9
Rombout, J. H. W. M., Lamers, C. H. J., Helfrich, M. H., Dekker, A., & Taverne-Thiele, J. J. (1985). Uptake and transport of intact macromolecules in the intestinal epithelium of carp (Cyprinus carpio L.) and the possible immunological implications. In *Cell Tissue Res* (Vol. 239). Springer-Verlag.
Rombout, J. H. W. M., Stroband, H. W. J., & Taverne-Thiele, J. J. (1984). Proliferation and differentiation of intestinal epithelial cells during development of Barbus conchonius (Teleostei, Cyprinidae). *Cell and Tissue Research*, *236*(1), 207–216. https://doi.org/10.1007/BF00216533
Rooks, M. G., & Garrett, W. S. (2016). Gut microbiota, metabolites and host immunity. *Nature Reviews Immunology*, *16*(6), 341–352.

https://doi.org/10.1038/nri.2016.42
Rothschild, D., Weissbrod, O., Barkan, E., Kurilshikov, A., Korem, T., Zeevi, D., Costea, P. I., Godneva, A., Kalka, I. N., Bar, N., Shilo, S., Lador, D., Vila, A. V., Zmora, N., Pevsner-Fischer, M., Israeli, D., Kosower, N., Malka, G., Wolf, B. C., … Segal, E. (2018). Environment dominates over host genetics in shaping human gut microbiota. *Nature*, *555*(7695), 210–215. https://doi.org/10.1038/nature25973
Rouhbakhsh, D., Lai, C. Y., Von Dohlen, C. D., Clark, M. A., Baumann, L., Baumann, P., Moran, N. A., & Voegtlin, D. J. (1996). The tryptophan biosynthetic pathway of aphid endosymbionts (Buchnera): Genetics and evolution of plasmid-associated anthranilate synthase (trpEG) within the aphididae. *Journal of Molecular Evolution*, *42*(4), 414–421. https://doi.org/10.1007/BF02498635
Russell, D. W. (2003). The enzymes, regulation, and genetics of bile acid synthesis. In *Annual Review of Biochemistry* (Vol. 72, pp. 137–174). Annual Reviews 4139 El Camino Way, P.O. Box 10139, Palo Alto, CA 94303-0139, USA . https://doi.org/10.1146/annurev.biochem.72.121801.161712
SÁenz De RodrigÁÑez, M. A., DÍaz-Rosales, P., ChabrillÓn, M., Smidt, H., Arijo, S., LeÓn-Rubio, J. M., AlarcÓn, F. J., Balebona, M. C., MoriÑigo, M. A., Cara, J. B., & Moyano, F. J. (2009). Effect of dietary administration of probiotics on growth and intestine functionality of juvenile Senegalese sole (Solea senegalensis, Kaup 1858). *Aquaculture Nutrition*, *15*(2), 177–185. https://doi.org/10.1111/j.1365-2095.2008.00581.x
Saffrey, M. J. (2014). Aging of the mammalian gastrointestinal tract: A complex organ system. In *Age* (Vol. 36, Issue 3, pp. 1019–1032). Kluwer Academic Publishers. https://doi.org/10.1007/s11357-013-9603-2
Sambhara, S., & McElhaney, J. E. (2009). Immunosenescence and influenza vaccine efficacy. In *Current Topics in Microbiology and Immunology* (Vol. 333, Issue 1, pp. 413–429). Springer Verlag. https://doi.org/10.1007/978-3-540-92165-3_20
Saunders, B. P., Fukumoto, M., Halligan, S., Jobling, C., Moussa, M. E., Bartram, C. I., & Williams, C. B. (1996). Why is colonoscopy more difficult in women? *Gastrointestinal Endoscopy*, *43*(2 PART 1), 124–126. https://doi.org/10.1016/S0016-5107(06)80113-6
Schmidtke, L. M., & Carson, J. (1994). Chararacteristics of Vagococcus salmoninarum isolated from diseased salmonid fish. *Journal of Applied Bacteriology*, *77*(2), 229–236. https://doi.org/10.1111/j.1365-2672.1994.tb03068.x
Schwaiger, M., Rampler, E., Hermann, G., Miklos, W., Berger, W., & Koellensperger, G. (2017). Anion-Exchange Chromatography Coupled to High-Resolution Mass Spectrometry: A Powerful Tool for Merging Targeted and Non-targeted Metabolomics. *Analytical Chemistry*, *89*(14), 7667–7674. https://doi.org/10.1021/acs.analchem.7b01624
Segre, D., & Segre, M. (1977). Age-related changes in B and T lymphocytes and decline of humoral immune responsiveness in aged mice. *Mechanisms of Ageing and Development*, *6*(C), 115–129. https://doi.org/10.1016/0047-6374(77)90013-6
Sender, R., Fuchs, S., & Milo, R. (2016). Revised Estimates for the Number of Human and Bacteria Cells in the Body. *PLoS Biology*, *14*(8), e1002533.

https://doi.org/10.1371/journal.pbio.1002533
Sherwin, E., Bordenstein, S. R., Quinn, J. L., Dinan, T. G., & Cryan, J. F. (2019). Microbiota and the social brain. *Science*, *366*(6465). https://doi.org/10.1126/SCIENCE.AAR2016
Sheth, R. U., Li, M., Jiang, W., Sims, P. A., Leong, K. W., & Wang, H. H. (2019). Spatial metagenomic characterization of microbial biogeography in the gut. *Nature Biotechnology*, *37*(8), 877–883. https://doi.org/10.1038/s41587-019-0183-2
Sinha, T., Vich Vila, A., Garmaeva, S., Jankipersadsing, S. A., Imhann, F., Collij, V., Bonder, M. J., Jiang, X., Gurry, T., Alm, E. J., D'Amato, M., Weersma, R. K., Scherjon, S., Wijmenga, C., Fu, J., Kurilshikov, A., & Zhernakova, A. (2019). Analysis of 1135 gut metagenomes identifies sex-specific resistome profiles. *Gut Microbes*, *10*(3), 358–366. https://doi.org/10.1080/19490976.2018.1528822
Smith, P. M., Howitt, M. R., Panikov, N., Michaud, M., Gallini, C. A., Bohlooly-Y, M., Glickman, J. N., & Garrett, W. S. (2013). The microbial metabolites, short-chain fatty acids, regulate colonic Treg cell homeostasis. *Science (New York, N.Y.)*, *341*(6145), 569–573. https://doi.org/10.1126/science.1241165
Smith, P., Willemsen, D., Popkes, M., Metge, F., Gandiwa, E., Reichard, M., & Valenzano, D. R. (2017). Regulation of life span by the gut microbiota in the short-lived African turquoise killifish. *ELife*, *6*. https://doi.org/10.7554/eLife.27014
Smith, S. A., Montain, S. J., Matott, R. P., Zientara, G. P., Jolesz, F. A., & Fielding, R. A. (1998). Creatine supplementation and age influence muscle metabolism during exercise. *Journal of Applied Physiology*, *85*(4), 1349–1356. https://doi.org/10.1152/jappl.1998.85.4.1349
Sniderman, A., Couture, P., & De Graaf, J. (2010). Diagnosis and treatment of apolipoprotein B dyslipoproteinemias. In *Nature Reviews Endocrinology* (Vol. 6, Issue 6, pp. 335–346). Nat Rev Endocrinol. https://doi.org/10.1038/nrendo.2010.50
Song, X., Sun, X., Oh, S. F., Wu, M., Zhang, Y., Zheng, W., Geva-Zatorsky, N., Jupp, R., Mathis, D., Benoist, C., & Kasper, D. L. (2020). Microbial bile acid metabolites modulate gut RORγ+ regulatory T cell homeostasis. *Nature*, *577*(7790), 410–415. https://doi.org/10.1038/s41586-019-1865-0
Sorroza, L., Padilla, D., Acosta, F., Román, L., Grasso, V., Vega, J., & Real, F. (2012). Characterization of the probiotic strain Vagococcus fluvialis in the protection of European sea bass (Dicentrarchus labrax) against vibriosis by Vibrio anguillarum. *Veterinary Microbiology*, *155*(2–4), 369–373. https://doi.org/10.1016/j.vetmic.2011.09.013
Sparkenbaugh, E. M., Chantrathammachart, P., Wang, S., Jonas, W., Kirchhofer, D., Gailani, D., Gruber, A., Kasthuri, R., Key, N. S., Mackman, N., & Pawlinski, R. (2015). Excess of heme induces tissue factor-dependent activation of coagulation in mice. *Haematologica*, *100*(3), 308–313. https://doi.org/10.3324/haematol.2014.114728
Stebegg, M., Silva-Cayetano, A., Innocentin, S., Jenkins, T. P., Cantacessi, C., Gilbert, C., & Linterman, M. A. (2019). Heterochronic faecal transplantation boosts gut germinal centres in aged mice. *Nature Communications*, *10*(1), 2443. https://doi.org/10.1038/s41467-019-10430-7
Steegenga, W. T., de Wit, N. J., Boekschoten, M. V, IJssennagger, N., Lute, C., Keshtkar, S., Bromhaar, M. M. G., Kampman, E., de Groot, L. C., & Muller, M.

(2012). Structural, functional and molecular analysis of the effects of aging in the small intestine and colon of C57BL/6J mice. *BMC Medical Genomics*, *5*(1), 38. https://doi.org/10.1186/1755-8794-5-38

Stephens, W. Z., Burns, A. R., Stagaman, K., Wong, S., Rawls, J. F., Guillemin, K., & Bohannan, B. J. M. (2016). The composition of the zebrafish intestinal microbial community varies across development. *ISME Journal*, *10*(3), 644–654. https://doi.org/10.1038/ismej.2015.140

Stewart, D. C., Berrie, D., Li, J., Liu, X., Rickerson, C., Mkoji, D., Iqbal, A., Tan, S., Doty, A. L., Glover, S. C., & Simmons, C. S. (2018). Quantitative assessment of intestinal stiffness and associations with fibrosis in human inflammatory bowel disease. *PLoS ONE*, *13*(7), e0200377. https://doi.org/10.1371/journal.pone.0200377

Stout, J. R., Graves, B. S., Cramer, J. T., Goldstein, E. R., Costa, P. B., Smith, A. E., Walter, A. A., & Stout, J. R. (2007). Introduction EFFECTS OF CREATINE SUPPLEMENTATION ON THE ONSET OF NEUROMUSCULAR FATIGUE THRESHOLD AND MUSCLE STRENGTH IN ELDERLY MEN AND WOMEN (64-86 YEARS). In *HEALTH & AGING© The Journal of Nutrition* (Vol. 11, Issue 6).

Sugita, H., Miyajima, C., & Deguchi, Y. (1991). The vitamin B12-producing ability of the intestinal microflora of freshwater fish. *Aquaculture*, *92*(C), 267–276. https://doi.org/10.1016/0044-8486(91)90028-6

Sugita, Haruo, Nakamura, H., & Shimada, T. (2005). Microbial communities associated with filter materials in recirculating aquaculture systems of freshwater fish. *Aquaculture*, *243*(1–4), 403–409. https://doi.org/10.1016/j.aquaculture.2004.09.028

Suh, Y., Atzmon, G., Cho, M. O., Hwang, D., Liu, B., Leahy, D. J., Barzilai, N., & Cohen, P. (2008). Functionally significant insulin-like growth factor I receptor mutations in centenarians. *Proceedings of the National Academy of Sciences of the United States of America*, *105*(9), 3438–3442. https://doi.org/10.1073/pnas.0705467105

SULLAM, K. E., ESSINGER, S. D., LOZUPONE, C. A., O'CONNOR, M. P., ROSEN, G. L., KNIGHT, R., KILHAM, S. S., & RUSSELL, J. A. (2012). Environmental and ecological factors that shape the gut bacterial communities of fish: a meta-analysis. *Molecular Ecology*, *21*(13), 3363–3378. https://doi.org/10.1111/j.1365-294X.2012.05552.x

T, T. (2020). *_A Package for Survival Analysis in R_*. (R package version 3.2-7). https://cran.r-project.org/package=survival

Takagi, T., Naito, Y., Inoue, R., Kashiwagi, S., Uchiyama, K., Mizushima, K., Tsuchiya, S., Dohi, O., Yoshida, N., Kamada, K., Ishikawa, T., Handa, O., Konishi, H., Okuda, K., Tsujimoto, Y., Ohnogi, H., & Itoh, Y. (2019). Differences in gut microbiota associated with age, sex, and stool consistency in healthy Japanese subjects. *Journal of Gastroenterology*, *54*(1), 53–63. https://doi.org/10.1007/s00535-018-1488-5

Takagi, T., Naito, Y., Okada, H., Takaoka, M., Oya-Ito, T., Yamada, S., Hirai, Y., Mizushima, K., Yoshida, N., Kamada, K., Katada, K., Uchiyama, K., Ishikawa, T., Handa, O., Yagi, N., Konishi, H., Kokura, S., Ichikawa, H., & Yoshikawa, T. (2012). Hemopexin is upregulated in rat intestinal mucosa injured by indomethacin. *Journal of Gastroenterology and Hepatology (Australia)*,

27(SUPPL.3), 70–75. https://doi.org/10.1111/j.1440-1746.2012.07076.x
Tatar, M., Kopelman, A., Epstein, D., Tu, M. P., Yin, C. M., & Garofalo, R. S. (2001). A mutant Drosophila insulin receptor homolog that extends life-span and impairs neuroendocrine function. *Science*, *292*(5514), 107–110. https://doi.org/10.1126/science.1057987
Terzibasi, E., Lefrançois, C., Domenici, P., Hartmann, N., Graf, M., & Cellerino, A. (2009). Effects of dietary restriction on mortality and age-related phenotypes in the short-lived fish Nothobranchius furzeri. *Aging Cell*, *8*(2), 88–99. https://doi.org/10.1111/j.1474-9726.2009.00455.x
Thevaranjan, N., Puchta, A., Schulz, C., Naidoo, A., Szamosi, J. C., Verschoor, C. P., Loukov, D., Schenck, L. P., Jury, J., Foley, K. P., Schertzer, J. D., Larché, M. J., Davidson, D. J., Verdú, E. F., Surette, M. G., & Bowdish, D. M. E. (2017). Age-Associated Microbial Dysbiosis Promotes Intestinal Permeability, Systemic Inflammation, and Macrophage Dysfunction. *Cell Host and Microbe*, *21*(4), 455-466.e4. https://doi.org/10.1016/j.chom.2017.03.002
Tierney, B. T., Yang, Z., Luber, J. M., Beaudin, M., Wibowo, M. C., Baek, C., Mehlenbacher, E., Patel, C. J., & Kostic, A. D. (2019). The Landscape of Genetic Content in the Gut and Oral Human Microbiome. *Cell Host and Microbe*, *26*(2), 283-295.e8. https://doi.org/10.1016/j.chom.2019.07.008
Tokunaga, C., Yoshino, K. I., & Yonezawa, K. (2004). mTOR integrates amino acid- and energy-sensing pathways. *Biochemical and Biophysical Research Communications*, *313*(2), 443–446. https://doi.org/10.1016/j.bbrc.2003.07.019
Tolosano, E., & Altruda, F. (2002). Hemopexin: Structure, function, and regulation. In *DNA and Cell Biology* (Vol. 21, Issue 4, pp. 297–306). Mary Ann Liebert, Inc. . https://doi.org/10.1089/104454902753759717
Turnbaugh, P. J., Ley, R. E., Mahowald, M. A., Magrini, V., Mardis, E. R., & Gordon, J. I. (2006). An obesity-associated gut microbiome with increased capacity for energy harvest. *Nature*, *444*(7122), 1027–1031. https://doi.org/10.1038/nature05414
Turner, J. R. (2009). Intestinal mucosal barrier function in health and disease. In *Nature Reviews Immunology* (Vol. 9, Issue 11, pp. 799–809). Nature Publishing Group. https://doi.org/10.1038/nri2653
Valenzano, Dario R., Terzibasi, E., Genade, T., Cattaneo, A., Domenici, L., & Cellerino, A. (2006). Resveratrol prolongs lifespan and retards the onset of age-related markers in a short-lived vertebrate. *Current Biology*, *16*(3), 296–300. https://doi.org/10.1016/j.cub.2005.12.038
Valenzano, Dario Riccardo, Benayoun, B. A., Singh, P. P., Zhang, E., Etter, P. D., Hu, C. K., Clément-Ziza, M., Willemsen, D., Cui, R., Harel, I., MacHado, B. E., Yee, M. C., Sharp, S. C., Bustamante, C. D., Beyer, A., Johnson, E. A., & Brunet, A. (2015). The African Turquoise Killifish Genome Provides Insights into Evolution and Genetic Architecture of Lifespan. *Cell*, *163*(6), 1539–1554. https://doi.org/10.1016/j.cell.2015.11.008
Valledor, L., Escandón, M., Meijón, M., Nukarinen, E., Cañal, M. J., & Weckwerth, W. (2014). A universal protocol for the combined isolation of metabolites, DNA, long RNAs, small RNAs, and proteins from plants and microorganisms. *The Plant Journal*, *79*(1), 173–180. https://doi.org/10.1111/tpj.12546
VanInsberghe, D., Maas, K. R., Cardenas, E., Strachan, C. R., Hallam, S. J., & Mohn, W. W. (2015). Non-symbiotic Bradyrhizobium ecotypes dominate North

American forest soils. *ISME Journal*, *9*(11), 2435–2441. https://doi.org/10.1038/ismej.2015.54
Vellai, T., Takacs-Vellai, K., Zhang, Y., Kovacs, A. L., Orosz, L., & Müller, F. (2003). Influence of TOR kinase on lifespan in C. elegans. *Nature*, *426*(6967), 620. https://doi.org/10.1038/426620a
Vighi, G., Marcucci, F., Sensi, L., Di Cara, G., & Frati, F. (2008). Allergy and the gastrointestinal system. In *Clinical and Experimental Immunology* (Vol. 153, Issue SUPPL. 1, pp. 3–6). Clin Exp Immunol. https://doi.org/10.1111/j.1365-2249.2008.03713.x
Vijg, J., & Campisi, J. (2008). Puzzles, promises and a cure for ageing. In *Nature* (Vol. 454, Issue 7208, pp. 1065–1071). Nature Publishing Group. https://doi.org/10.1038/nature07216
Virtanen, P., Gommers, R., Oliphant, T. E., Haberland, M., Reddy, T., Cournapeau, D., Burovski, E., Peterson, P., Weckesser, W., Bright, J., van der Walt, S. J., Brett, M., Wilson, J., Millman, K. J., Mayorov, N., Nelson, A. R. J., Jones, E., Kern, R., Larson, E., … Vázquez-Baeza, Y. (2020). SciPy 1.0: fundamental algorithms for scientific computing in Python. *Nature Methods*, *17*(3), 261–272. https://doi.org/10.1038/s41592-019-0686-2
Von Zychlinski, A., Williams, M., McCormick, S., & Kleffmann, T. (2014). Absolute quantification of apolipoproteins and associated proteins on human plasma lipoproteins. *Journal of Proteomics*, *106*, 181–190. https://doi.org/10.1016/j.jprot.2014.04.030
Vrtílek, M., Žák, J., Pšenička, M., & Reichard, M. (2018). Extremely rapid maturation of a wild African annual fish. In *Current Biology* (Vol. 28, Issue 15, pp. R822–R824). Cell Press. https://doi.org/10.1016/j.cub.2018.06.031
Vuong, H. E., Yano, J. M., Fung, T. C., & Hsiao, E. Y. (2017). The Microbiome and Host Behavior. *Annual Review of Neuroscience*, *40*(1), 21–49. https://doi.org/10.1146/annurev-neuro-072116-031347
Wahlström, A., Sayin, S. I., Marschall, H. U., & Bäckhed, F. (2016). Intestinal Crosstalk between Bile Acids and Microbiota and Its Impact on Host Metabolism. In *Cell Metabolism* (Vol. 24, Issue 1, pp. 41–50). Cell Press. https://doi.org/10.1016/j.cmet.2016.05.005
Wallace, K. N., Akhter, S., Smith, E. M., Lorent, K., & Pack, M. (2005). Intestinal growth and differentiation in zebrafish. *Mechanisms of Development*, *122*(2), 157–173. https://doi.org/10.1016/j.mod.2004.10.009
Wang, Q., Garrity, G. M., Tiedje, J. M., & Cole, J. R. (2007). Naïve Bayesian classifier for rapid assignment of rRNA sequences into the new bacterial taxonomy. *Applied and Environmental Microbiology*, *73*(16), 5261–5267. https://doi.org/10.1128/AEM.00062-07
Wang, X., Yuan, M., Mi, H., Suo, S., Eteer, K., Li, S., Lu, Q., Xu, J., & Hu, J. (2020). The feasibility of differentiating colorectal cancer from normal and inflammatory thickening colon wall using CT texture analysis. *Scientific Reports*, *10*(1), 1–13. https://doi.org/10.1038/s41598-020-62973-1
Wang, Y., An, Y., Ma, W., Yu, H., Lu, Y., Lu, Y., Zhang, X., Wang, Y., Liu, W., Wang, T., & Xiao, R. (2020). 27-Hydroxycholesterol contributes to cognitive deficits in APP/PS1 transgenic mice through microbiota dysbiosis and intestinal barrier dysfunction. *Journal of Neuroinflammation*, *17*(1). https://doi.org/10.1186/s12974-020-01873-7

Wang, Z., Du, J., Lam, S., Mathavan, S., Matsudaira, P., & Gong, Z. (2010). Morphological and molecular evidence for functional organization along the rostrocaudal axis of the adult zebrafish intestine. *BMC Genomics*, *11*(1), 392. https://doi.org/10.1186/1471-2164-11-392

Warskulat, U., Flögel, U., Jacoby, C., Hartwig, H.-G., Thewissen, M., Merx, M. W., Molojavyi, A., Heller-Stilb, B., Schrader, J., & Häussinger, D. (2004). Taurine transporter knockout depletes muscle taurine levels and results in severe skeletal muscle impairment but leaves cardiac function uncompromised. *The FASEB Journal*. https://doi.org/10.1096/fj.03-0496fje

Wei, J., Guo, X., Liu, H., Chen, Y., & Wang, W. (2018). The variation profile of intestinal microbiota in blunt snout bream (Megalobrama amblycephala) during feeding habit transition. *BMC Microbiology*, *18*(1), 99. https://doi.org/10.1186/s12866-018-1246-0

Westfall, S., Lomis, N., & Prakash, S. (2018). Longevity extension in Drosophila through gut-brain communication. *Scientific Reports*, *8*(1), 8362. https://doi.org/10.1038/s41598-018-25382-z

Wickham, H., Averick, M., Bryan, J., Chang, W., McGowan, L., François, R., Grolemund, G., Hayes, A., Henry, L., Hester, J., Kuhn, M., Pedersen, T., Miller, E., Bache, S., Müller, K., Ooms, J., Robinson, D., Seidel, D., Spinu, V., … Yutani, H. (2019). Welcome to the Tidyverse. *Journal of Open Source Software*, *4*(43), 1686. https://doi.org/10.21105/joss.01686

Willing, B. P., Russell, S. L., & Finlay, B. B. (2011). Shifting the balance: Antibiotic effects on host-microbiota mutualism. In *Nature Reviews Microbiology* (Vol. 9, Issue 4, pp. 233–243). Nature Publishing Group. https://doi.org/10.1038/nrmicro2536

Willinger, T. (2019). Oxysterols in intestinal immunity and inflammation. In *Journal of Internal Medicine* (Vol. 285, Issue 4, pp. 367–380). Blackwell Publishing Ltd. https://doi.org/10.1111/joim.12855

Wilmoth, J. R. (2000). Demography of longevity: Past, present, and future trends. *Experimental Gerontology*, *35*(9–10), 1111–1129. https://doi.org/10.1016/S0531-5565(00)00194-7

Wilson, J. M., & Castro, L. F. C. (2010). Morphological diversity of the gastrointestinal tract in fishes. *Fish Physiology*, *30*, 1–55. https://doi.org/10.1016/S1546-5098(10)03001-3

Wong, J. M. T., Malec, P. A., Mabrouk, O. S., Ro, J., Dus, M., & Kennedy, R. T. (2016). Benzoyl chloride derivatization with liquid chromatography-mass spectrometry for targeted metabolomics of neurochemicals in biological samples. *Journal of Chromatography A*, *1446*, 78–90. https://doi.org/10.1016/j.chroma.2016.04.006

Wourms, J. P. (1972). The developmental biology of annual fishes. III. Pre-embryonic and embryonic diapause of variable duration in the eggs of annual fishes. *Journal of Experimental Zoology*, *182*(3), 389–414. https://doi.org/10.1002/jez.1401820310

Wu, G. D., Chen, J., Hoffmann, C., Bittinger, K., Chen, Y. Y., Keilbaugh, S. A., Bewtra, M., Knights, D., Walters, W. A., Knight, R., Sinha, R., Gilroy, E., Gupta, K., Baldassano, R., Nessel, L., Li, H., Bushman, F. D., & Lewis, J. D. (2011). Linking long-term dietary patterns with gut microbial enterotypes. *Science*, *334*(6052), 105–108. https://doi.org/10.1126/science.1208344

Wu, Y. (n.d.). *idemp*. https://github.com/yhwu/idemp
Wynn, T. A. (2008). Cellular and molecular mechanisms of fibrosis. In *Journal of Pathology* (Vol. 214, Issue 2, pp. 199–210). NIH Public Access. https://doi.org/10.1002/path.2277
Xia, J., Psychogios, N., Young, N., & Wishart, D. S. (2009). MetaboAnalyst: A web server for metabolomic data analysis and interpretation. *Nucleic Acids Research*, *37*(SUPPL. 2), W652–W660. https://doi.org/10.1093/nar/gkp356
Xu, Y. J., Arneja, A. S., Tappia, P. S., & Dhalla, N. S. (2008). The potential health benefits of Taurine in cardiovascular disease. In *Experimental and Clinical Cardiology* (Vol. 13, Issue 2, pp. 57–65). Pulsus Group. /pmc/articles/PMC2586397/
Yan, W., Sun, C., Zheng, J., Wen, C., Ji, C., Zhang, D., Chen, Y., Hou, Z., & Yang, N. (2019). Efficacy of Fecal Sampling as a Gut Proxy in the Study of Chicken Gut Microbiota. *Frontiers in Microbiology*, *10*. https://doi.org/10.3389/fmicb.2019.02126
Yanagita, T., Han, S. Y., Hu, Y., Nagao, K., Kitajima, H., & Murakami, S. (2008). Taurine reduces the secretion of apolipoprotein B100 and lipids in HepG2 cells. *Lipids in Health and Disease*, *7*, 38. https://doi.org/10.1186/1476-511X-7-38
Yatsunenko, T., Rey, F. E., Manary, M. J., Trehan, I., Dominguez-Bello, M. G., Contreras, M., Magris, M., Hidalgo, G., Baldassano, R. N., Anokhin, A. P., Heath, A. C., Warner, B., Reeder, J., Kuczynski, J., Caporaso, J. G., Lozupone, C. A., Lauber, C., Clemente, J. C., Knights, D., … Gordon, J. I. (2012). Human gut microbiome viewed across age and geography. In *Nature* (Vol. 486, Issue 7402, pp. 222–227). Nature Publishing Group. https://doi.org/10.1038/nature11053
Yoshimoto, S., Loo, T. M., Atarashi, K., Kanda, H., Sato, S., Oyadomari, S., Iwakura, Y., Oshima, K., Morita, H., Hattori, M., Honda, K., Ishikawa, Y., Hara, E., & Ohtani, N. (2013). Obesity-induced gut microbial metabolite promotes liver cancer through senescence secretome. *Nature*, *499*(7456), 97–101. https://doi.org/10.1038/nature12347
Yu, Z., Zhai, G., Singmann, P., He, Y., Xu, T., Prehn, C., Römisch-Margl, W., Lattka, E., Gieger, C., Soranzo, N., Heinrich, J., Standl, M., Thiering, E., Mittelstraß, K., Wichmann, H. E., Peters, A., Suhre, K., Li, Y., Adamski, J., … Wang-Sattler, R. (2012). Human serum metabolic profiles are age dependent. *Aging Cell*, *11*(6), 960–967. https://doi.org/10.1111/j.1474-9726.2012.00865.x
Yurkovetskiy, L., Burrows, M., Khan, A. A., Graham, L., Volchkov, P., Becker, L., Antonopoulos, D., Umesaki, Y., & Chervonsky, A. V. (2013). Gender bias in autoimmunity is influenced by microbiota. *Immunity*, *39*(2), 400–412. https://doi.org/10.1016/j.immuni.2013.08.013
Žák, J., Dyková, I., & Reichard, M. (2020). Good performance of turquoise killifish (Nothobranchius furzeri) on pelleted diet as a step towards husbandry standardization. *Scientific Reports*, *10*(1), 1–11. https://doi.org/10.1038/s41598-020-65930-0
Zhang, Y., Li, X., Luo, Z., Ma, L., Zhu, S., Wang, Z., Wen, J., Cheng, S., Gu, W., Lian, Q., Zhao, X., Fan, W., Ling, Z., Ye, J., Zheng, S., Li, D., Wang, H., Liu, J., & Sun, B. (2020). ECM1 is an essential factor for the determination of M1 macrophage polarization in IBD in response to LPS stimulation. *Proceedings of the National Academy of Sciences of the United States of America*, *117*(6),

3083–3092. https://doi.org/10.1073/pnas.1912774117
Zheng, Y., Valdez, P. A., Danilenko, D. M., Hu, Y., Sa, S. M., Gong, Q., Abbas, A. R., Modrusan, Z., Ghilardi, N., De Sauvage, F. J., & Ouyang, W. (2008). Interleukin-22 mediates early host defense against attaching and effacing bacterial pathogens. *Nature Medicine*, *14*(3), 282–289. https://doi.org/10.1038/nm1720
Zi, J., Yu, X., Li, Y., Hu, X., Xu, C., Wang, X., Liu, X., & Fu, R. (2003). Coloration strategies in peacock feathers. *Proceedings of the National Academy of Sciences of the United States of America*, *100*(22), 12576–12578. https://doi.org/10.1073/pnas.2133313100
Zoetendal, E. G., Raes, J., Van Den Bogert, B., Arumugam, M., Booijink, C. C., Troost, F. J., Bork, P., Wels, M., De Vos, W. M., & Kleerebezem, M. (2012). The human small intestinal microbiota is driven by rapid uptake and conversion of simple carbohydrates. *ISME Journal*, *6*(7), 1415–1426. https://doi.org/10.1038/ismej.2011.212
Zwingenberger, A. L., Marks, S. L., Baker, T. W., & Moore, P. F. (2010). Ultrasonographic evaluation of the muscularis propria in cats with diffuse small intestinal lymphoma or inflammatory bowel disease. *Journal of Veterinary Internal Medicine*, *24*(2), 289–292. https://doi.org/10.1111/j.1939-1676.2009.0457.x

Supplementary Material

Supplementary table 1: Primers used for 16S rRNA library preparation – Step 2

Primer name	Primer Sequence 5' to 3'
P1_PCR_i5_D501_TATAGCCT	AATGATACGGCGACCACCGAGATCTACACtatagcctACACTCTTTCCCTACACGACGCTCTTCCGATCT
P1_PCR_i5_D502_ATAGAGGC	AATGATACGGCGACCACCGAGATCTACACatagaggcACACTCTTTCCCTACACGACGCTCTTCCGATCT
P1_PCR_i5_D503_CCTATCCT	AATGATACGGCGACCACCGAGATCTACACcctatcctACACTCTTTCCCTACACGACGCTCTTCCGATCT
P1_PCR_i5_D504_GGCTCTGA	AATGATACGGCGACCACCGAGATCTACACggctctgaACACTCTTTCCCTACACGACGCTCTTCCGATCT
P1_PCR_i5_D505_AGGCGAAG	AATGATACGGCGACCACCGAGATCTACACaggcgaagACACTCTTTCCCTACACGACGCTCTTCCGATCT
P1_PCR_i5_D506_TAATCTTA	AATGATACGGCGACCACCGAGATCTACACtaatcttaACACTCTTTCCCTACACGACGCTCTTCCGATCT
P1_PCR_i5_D507_CAGGACGT	AATGATACGGCGACCACCGAGATCTACACcaggacgtACACTCTTTCCCTACACGACGCTCTTCCGATCT
P1_PCR_i5_D508_GTACTGAC	AATGATACGGCGACCACCGAGATCTACACgtactgacACACTCTTTCCCTACACGACGCTCTTCCGATCT
P1_PCR_i5_D509_TTCGGATG	AATGATACGGCGACCACCGAGATCTACACttcggatgACACTCTTTCCCTACACGACGCTCTTCCGATCT
P1_PCR_i5_D510_ACTCATAA	AATGATACGGCGACCACCGAGATCTACACactcataaACACTCTTTCCCTACACGACGCTCTTCCGATCT
P1_PCR_i5_D511_GCGCCTCT	AATGATACGGCGACCACCGAGATCTACACgcgcctctACACTCTTTCCCTACACGACGCTCTTCCGATCT
P1_PCR_i5_D512_CGCGGCTA	AATGATACGGCGACCACCGAGATCTACACcgcggctaACACTCTTTCCCTACACGACGCTCTTCCGATCT
P1_PCR_i5_D513_TTATTCGT	AATGATACGGCGACCACCGAGATCTACACttattcgtACACTCTTTCCCTACACGACGCTCTTCCGATCT
P1_PCR_i5_D514_CCTACGAA	AATGATACGGCGACCACCGAGATCTACACcctacgaaACACTCTTTCCCTACACGACGCTCTTCCGATCT
P1_PCR_i5_D515_AGCAGATC	AATGATACGGCGACCACCGAGATCTACACagcagatcACACTCTTTCCCTACACGACGCTCTTCCGATCT
P1_PCR_i5_D516_GCGGAGCG	AATGATACGGCGACCACCGAGATCTACACgcggagcgACACTCTTTCCCTACACGACGCTCTTCCGATCT
P1_PCR_i5_D517_TACTTACT	AATGATACGGCGACCACCGAGATCTACACtacttactACACTCTTTCCCTACACGACGCTCTTCCGATCT
P1_PCR_i5_D518_AGGAAGTC	AATGATACGGCGACCACCGAGATCTACACaggaagtcACACTCTTTCCCTACACGACGCTCTTCCGATCT
P1_PCR_i5_D519_GGCGACGG	AATGATACGGCGACCACCGAGATCTACACggcgacggACACTCTTTCCCTACACGACGCTCTTCCGATCT
P1_PCR_i5_D520_CCTCGGAC	AATGATACGGCGACCACCGAGATCTACACcctcggacACACTCTTTCCCTACACGACGCTCTTCCGATCT
P1_PCR_i5_A001_GTCTTAGG	AATGATACGGCGACCACCGAGATCTACACgtcttaggACACTCTTTCCCTACACGACGCTCTTCCGATCT
P1_PCR_i5_A002_ACTGATCG	AATGATACGGCGACCACCGAGATCTACACactgatcgACACTCTTTCCCTACACGACGCTCTTCCGATCT
P1_PCR_i5_A003_TAGCTGCA	AATGATACGGCGACCACCGAGATCTACACtagctgcaACACTCTTTCCCTACACGACGCTCTTCCGATCT
P1_PCR_i5_A004_GACGTCGA	AATGATACGGCGACCACCGAGATCTACACgacgtcgaACACTCTTTCCCTACACGACGCTCTTCCGATCT
P1_PCR_i5_A005_GACTGCAT	AATGATACGGCGACCACCGAGATCTACACgactgcatACACTCTTTCCCTACACGACGCTCTTCCGATCT
P1_PCR_i5_A006_AACCAGTC	AATGATACGGCGACCACCGAGATCTACACaaccagtcACACTCTTTCCCTACACGACGCTCTTCCGATCT
P1_PCR_i5_A007_CCATTGAG	AATGATACGGCGACCACCGAGATCTACACccattgagACACTCTTTCCCTACACGACGCTCTTCCGATCT
P1_PCR_i5_A008_GATCTCCA	AATGATACGGCGACCACCGAGATCTACACgatctccaACACTCTTTCCCTACACGACGCTCTTCCGATCT
P1_PCR_i5_A009_TCCCATAG	AATGATACGGCGACCACCGAGATCTACACtcccatagACACTCTTTCCCTACACGACGCTCTTCCGATCT
P1_PCR_i5_A010_TCGTCAGT	AATGATACGGCGACCACCGAGATCTACACtcgtcagtACACTCTTTCCCTACACGACGCTCTTCCGATCT

P1_PCR_i5_A011_ATGTGGAC	AATGATACGGCGACCACCGAGATCTACACatgtggacACACTCTTTCCCTACACGACGCTCTTCCGATCT
P1_PCR_i5_A012_ATGACGAG	AATGATACGGCGACCACCGAGATCTACACatgacgagACACTCTTTCCCTACACGACGCTCTTCCGATCT
P1_PCR_i5_A013_TTCATCGC	AATGATACGGCGACCACCGAGATCTACACttcatcgcACACTCTTTCCCTACACGACGCTCTTCCGATCT
P1_PCR_i5_A014_GGAGACAT	AATGATACGGCGACCACCGAGATCTACACggagacatACACTCTTTCCCTACACGACGCTCTTCCGATCT
P1_PCR_i5_A015_AAAGCCTG	AATGATACGGCGACCACCGAGATCTACACaaagcctgACACTCTTTCCCTACACGACGCTCTTCCGATCT
P1_PCR_i5_A016_ACGATAGC	AATGATACGGCGACCACCGAGATCTACACacgatagcACACTCTTTCCCTACACGACGCTCTTCCGATCT
P1_PCR_i5_A017_GTAACAGC	AATGATACGGCGACCACCGAGATCTACACgtaacagcACACTCTTTCCCTACACGACGCTCTTCCGATCT
P1_PCR_i5_A018_TGTGTACG	AATGATACGGCGACCACCGAGATCTACACtgtgtacgACACTCTTTCCCTACACGACGCTCTTCCGATCT
P1_PCR_i5_A019_TAGTCACG	AATGATACGGCGACCACCGAGATCTACACtagtcacgACACTCTTTCCCTACACGACGCTCTTCCGATCT
P1_PCR_i5_A020_GCTAGCTT	AATGATACGGCGACCACCGAGATCTACACgctagcttACACTCTTTCCCTACACGACGCTCTTCCGATCT
P1_PCR_i5_A021_GATCCCAT	AATGATACGGCGACCACCGAGATCTACACgatcccatACACTCTTTCCCTACACGACGCTCTTCCGATCT
P1_PCR_i5_A022_TGGATGCT	AATGATACGGCGACCACCGAGATCTACACtggatgctACACTCTTTCCCTACACGACGCTCTTCCGATCT
P1_PCR_i5_A023_CGGATTAG	AATGATACGGCGACCACCGAGATCTACACcggattagACACTCTTTCCCTACACGACGCTCTTCCGATCT
P1_PCR_i5_A024_GGTTTCAC	AATGATACGGCGACCACCGAGATCTACACggtttcacACACTCTTTCCCTACACGACGCTCTTCCGATCT
P1_PCR_i5_A025_TATCGCAC	AATGATACGGCGACCACCGAGATCTACACtatcgcacACACTCTTTCCCTACACGACGCTCTTCCGATCT
P1_PCR_i5_A026_ACTCCGTA	AATGATACGGCGACCACCGAGATCTACACactccgtaACACTCTTTCCCTACACGACGCTCTTCCGATCT
P1_PCR_i5_A027_GCACTGAA	AATGATACGGCGACCACCGAGATCTACACgcactgaaACACTCTTTCCCTACACGACGCTCTTCCGATCT
P1_PCR_i5_A028_GTGCACTT	AATGATACGGCGACCACCGAGATCTACACgtgcacttACACTCTTTCCCTACACGACGCTCTTCCGATCT
P1_PCR_i5_A029_GTCTGGAA	AATGATACGGCGACCACCGAGATCTACACgtctggaaACACTCTTTCCCTACACGACGCTCTTCCGATCT
P1_PCR_i5_A030_AGCCTTAC	AATGATACGGCGACCACCGAGATCTACACagccttacACACTCTTTCCCTACACGACGCTCTTCCGATCT
P1_PCR_i5_A031_AGTTCAGG	AATGATACGGCGACCACCGAGATCTACACagttcaggACACTCTTTCCCTACACGACGCTCTTCCGATCT
P1_PCR_i5_A032_GCATATCC	AATGATACGGCGACCACCGAGATCTACACgcatatccACACTCTTTCCCTACACGACGCTCTTCCGATCT
P1_PCR_i5_A033_CTACAGTG	AATGATACGGCGACCACCGAGATCTACACctacagtgACACTCTTTCCCTACACGACGCTCTTCCGATCT
P1_PCR_i5_A034_ATCAGGTC	AATGATACGGCGACCACCGAGATCTACACatcaggtcACACTCTTTCCCTACACGACGCTCTTCCGATCT
P1_PCR_i5_A035_CGACTTTC	AATGATACGGCGACCACCGAGATCTACACcgactttcACACTCTTTCCCTACACGACGCTCTTCCGATCT
P1_PCR_i5_A036_AAGCGTTG	AATGATACGGCGACCACCGAGATCTACACaagcgttgACACTCTTTCCCTACACGACGCTCTTCCGATCT
P1_PCR_i5_A037_TTGACCGT	AATGATACGGCGACCACCGAGATCTACACttgaccgtACACTCTTTCCCTACACGACGCTCTTCCGATCT
P1_PCR_i5_A038_AATTCGCG	AATGATACGGCGACCACCGAGATCTACACaattcgcgACACTCTTTCCCTACACGACGCTCTTCCGATCT
P1_PCR_i5_A039_GATGAACC	AATGATACGGCGACCACCGAGATCTACACgatgaaccACACTCTTTCCCTACACGACGCTCTTCCGATCT
P1_PCR_i5_A040_GACCGTTT	AATGATACGGCGACCACCGAGATCTACACgaccgtttACACTCTTTCCCTACACGACGCTCTTCCGATCT
P1_PCR_i5_A041_CTAGTGAC	AATGATACGGCGACCACCGAGATCTACACctagtgacACACTCTTTCCCTACACGACGCTCTTCCGATCT
P1_PCR_i5_A042_CGGGATAT	AATGATACGGCGACCACCGAGATCTACACcgggatatACACTCTTTCCCTACACGACGCTCTTCCGATCT
P1_PCR_i5_A043_GATGCGAA	AATGATACGGCGACCACCGAGATCTACACgatgcgaaACACTCTTTCCCTACACGACGCTCTTCCGATCT
P1_PCR_i5_A044_GATAACGC	AATGATACGGCGACCACCGAGATCTACACgataacgcACACTCTTTCCCTACACGACGCTCTTCCGATCT
P1_PCR_i5_A045_ACTTTCGG	AATGATACGGCGACCACCGAGATCTACACactttcggACACTCTTTCCCTACACGACGCTCTTCCGATCT

P1_PCR_i5_A046_GCTCGTAA	AATGATACGGCGACCACCGAGATCTACACgctcgtaaACACTCTTTCCCTACACGACGCTCTTCCGATCT
P1_PCR_i5_A047_ATTCCCGA	AATGATACGGCGACCACCGAGATCTACACattcccgaACACTCTTTCCCTACACGACGCTCTTCCGATCT
P1_PCR_i5_A048_ACATCGTG	AATGATACGGCGACCACCGAGATCTACACacatcgtgACACTCTTTCCCTACACGACGCTCTTCCGATCT
P1_PCR_i5_A049_AAAGGTCG	AATGATACGGCGACCACCGAGATCTACACaaaggtcgACACTCTTTCCCTACACGACGCTCTTCCGATCT
P1_PCR_i5_A050_CCCTAGAA	AATGATACGGCGACCACCGAGATCTACACccctagaaACACTCTTTCCCTACACGACGCTCTTCCGATCT
P1_PCR_i5_A051_TGCCGATA	AATGATACGGCGACCACCGAGATCTACACtgccgataACACTCTTTCCCTACACGACGCTCTTCCGATCT
P1_PCR_i5_A052_AGGTGCTA	AATGATACGGCGACCACCGAGATCTACACaggtgctaACACTCTTTCCCTACACGACGCTCTTCCGATCT
P1_PCR_i5_A053_AGTGAGTC	AATGATACGGCGACCACCGAGATCTACACagtgagtcACACTCTTTCCCTACACGACGCTCTTCCGATCT
P1_PCR_i5_A054_ACGCCATT	AATGATACGGCGACCACCGAGATCTACACacgccattACACTCTTTCCCTACACGACGCTCTTCCGATCT
P1_PCR_i5_A055_ACTGGGAA	AATGATACGGCGACCACCGAGATCTACACactgggaaACACTCTTTCCCTACACGACGCTCTTCCGATCT
P1_PCR_i5_A056_AGACGTGA	AATGATACGGCGACCACCGAGATCTACACagacgtgaACACTCTTTCCCTACACGACGCTCTTCCGATCT
P1_PCR_i5_A057_AACCACGT	AATGATACGGCGACCACCGAGATCTACACaaccacgtACACTCTTTCCCTACACGACGCTCTTCCGATCT
P1_PCR_i5_A058_AACTCTGG	AATGATACGGCGACCACCGAGATCTACACaactctggACACTCTTTCCCTACACGACGCTCTTCCGATCT
P1_PCR_i5_A059_GGGACTTA	AATGATACGGCGACCACCGAGATCTACACgggacttaACACTCTTTCCCTACACGACGCTCTTCCGATCT
P1_PCR_i5_A060_GTCGAGTA	AATGATACGGCGACCACCGAGATCTACACgtcgagtaACACTCTTTCCCTACACGACGCTCTTCCGATCT
P1_PCR_i5_A061_GCTGTAGT	AATGATACGGCGACCACCGAGATCTACACgctgtagtACACTCTTTCCCTACACGACGCTCTTCCGATCT
P1_PCR_i5_A062_ACCTTGAC	AATGATACGGCGACCACCGAGATCTACACaccttgacACACTCTTTCCCTACACGACGCTCTTCCGATCT
P1_PCR_i5_A063_TGTACCTC	AATGATACGGCGACCACCGAGATCTACACtgtacctcACACTCTTTCCCTACACGACGCTCTTCCGATCT
P1_PCR_i5_A064_TCCGAATG	AATGATACGGCGACCACCGAGATCTACACtccgaatgACACTCTTTCCCTACACGACGCTCTTCCGATCT
P1_PCR_i5_A065_CTGCTTGA	AATGATACGGCGACCACCGAGATCTACACctgcttgaACACTCTTTCCCTACACGACGCTCTTCCGATCT
P1_PCR_i5_A066_GGATTCCA	AATGATACGGCGACCACCGAGATCTACACggattccaACACTCTTTCCCTACACGACGCTCTTCCGATCT
P1_PCR_i5_A067_TGATTCGC	AATGATACGGCGACCACCGAGATCTACACtgattcgcACACTCTTTCCCTACACGACGCTCTTCCGATCT
P1_PCR_i5_A068_TGTAAGCC	AATGATACGGCGACCACCGAGATCTACACtgtaagccACACTCTTTCCCTACACGACGCTCTTCCGATCT
P1_PCR_i5_A069_TTCGCAAC	AATGATACGGCGACCACCGAGATCTACACttcgcaacACACTCTTTCCCTACACGACGCTCTTCCGATCT
P1_PCR_i5_A070_TGAGAAGC	AATGATACGGCGACCACCGAGATCTACACtgagaagcACACTCTTTCCCTACACGACGCTCTTCCGATCT
P1_PCR_i5_A071_GCCATTAC	AATGATACGGCGACCACCGAGATCTACACgccattacACACTCTTTCCCTACACGACGCTCTTCCGATCT
P1_PCR_i5_A072_TTGGCTAG	AATGATACGGCGACCACCGAGATCTACACttggctagACACTCTTTCCCTACACGACGCTCTTCCGATCT
P1_PCR_i5_A073_CAAAGGCT	AATGATACGGCGACCACCGAGATCTACACcaaaggctACACTCTTTCCCTACACGACGCTCTTCCGATCT
P1_PCR_i5_A074_ACTGCCAT	AATGATACGGCGACCACCGAGATCTACACactgccatACACTCTTTCCCTACACGACGCTCTTCCGATCT
P1_PCR_i5_A075_ATATCGGC	AATGATACGGCGACCACCGAGATCTACACatatcggcACACTCTTTCCCTACACGACGCTCTTCCGATCT
P1_PCR_i5_A076_AACGTTGC	AATGATACGGCGACCACCGAGATCTACACaacgttgcACACTCTTTCCCTACACGACGCTCTTCCGATCT
P2_PCR_i7_N701_TAAGGCGA	CAAGCAGAAGACGGCATACGAGATtcgccttaGTGACTGGAGTTCAGACGTGTGC
P2_PCR_i7_N702_CGTACTAG	CAAGCAGAAGACGGCATACGAGATctagtacgGTGACTGGAGTTCAGACGTGTGC
P2_PCR_i7_N703_AGGCAGAA	CAAGCAGAAGACGGCATACGAGATttctgcctGTGACTGGAGTTCAGACGTGTGC
P2_PCR_i7_N704_TCCTGAGC	CAAGCAGAAGACGGCATACGAGATgctcaggaGTGACTGGAGTTCAGACGTGTGC

P2_PCR_i7_N705_GGACTCCT	CAAGCAGAAGACGGCATACGAGATaggagtccGTGACTGGAGTTCAGACGTGTGC
P2_PCR_i7_N706_TAGGCATG	CAAGCAGAAGACGGCATACGAGATcatgcctaGTGACTGGAGTTCAGACGTGTGC
P2_PCR_i7_N707_CTCTCTAC	CAAGCAGAAGACGGCATACGAGATgtagagagGTGACTGGAGTTCAGACGTGTGC
P2_PCR_i7_N710_CGAGGCTG	CAAGCAGAAGACGGCATACGAGATcagcctcgGTGACTGGAGTTCAGACGTGTGC
P2_PCR_i7_N711_AAGAGGCA	CAAGCAGAAGACGGCATACGAGATtgcctcttGTGACTGGAGTTCAGACGTGTGC
P2_PCR_i7_N712_GTAGAGGA	CAAGCAGAAGACGGCATACGAGATtcctctacGTGACTGGAGTTCAGACGTGTGC
P2_PCR_i7_N714_GCTCATGA	CAAGCAGAAGACGGCATACGAGATtcatgagcGTGACTGGAGTTCAGACGTGTGC
P2_PCR_i7_N715_ATCTCAGG	CAAGCAGAAGACGGCATACGAGATcctgagatGTGACTGGAGTTCAGACGTGTGC
P2_PCR_i7_N716_ACTCGCTA	CAAGCAGAAGACGGCATACGAGATtagcgagtGTGACTGGAGTTCAGACGTGTGC
P2_PCR_i7_N718_GGAGCTAC	CAAGCAGAAGACGGCATACGAGATgtagctccGTGACTGGAGTTCAGACGTGTGC
P2_PCR_i7_N719_GCGTAGTA	CAAGCAGAAGACGGCATACGAGATtactacgcGTGACTGGAGTTCAGACGTGTGC
P2_PCR_i7_N720_CGGAGCCT	CAAGCAGAAGACGGCATACGAGATaggctccgGTGACTGGAGTTCAGACGTGTGC
P2_PCR_i7_N721_TACGCTGC	CAAGCAGAAGACGGCATACGAGATgcagcgtaGTGACTGGAGTTCAGACGTGTGC
P2_PCR_i7_N722_ATGCGCAG	CAAGCAGAAGACGGCATACGAGATctgcgcatGTGACTGGAGTTCAGACGTGTGC
P2_PCR_i7_N723_TAGCGCTC	CAAGCAGAAGACGGCATACGAGATgagcgctaGTGACTGGAGTTCAGACGTGTGC
P2_PCR_i7_N724_ACTGAGCG	CAAGCAGAAGACGGCATACGAGATcgctcagtGTGACTGGAGTTCAGACGTGTGC
P2_PCR_i7_N726_CCTAAGAC	CAAGCAGAAGACGGCATACGAGATgtcttaggGTGACTGGAGTTCAGACGTGTGC
P2_PCR_i7_N727_CGATCAGT	CAAGCAGAAGACGGCATACGAGATactgatcgGTGACTGGAGTTCAGACGTGTGC
P2_PCR_i7_N728_TGCAGCTA	CAAGCAGAAGACGGCATACGAGATtagctgcaGTGACTGGAGTTCAGACGTGTGC
P2_PCR_i7_N729_TCGACGTC	CAAGCAGAAGACGGCATACGAGATgacgtcgaGTGACTGGAGTTCAGACGTGTGC
P2_PCR_i7_B001_ATGCAGTC	CAAGCAGAAGACGGCATACGAGATgactgcatGTGACTGGAGTTCAGACGTGTGC
P2_PCR_i7_B002_GACTGGTT	CAAGCAGAAGACGGCATACGAGATaaccagtcGTGACTGGAGTTCAGACGTGTGC
P2_PCR_i7_B003_CTCAATGG	CAAGCAGAAGACGGCATACGAGATccattgagGTGACTGGAGTTCAGACGTGTGC
P2_PCR_i7_B004_TGGAGATC	CAAGCAGAAGACGGCATACGAGATgatctccaGTGACTGGAGTTCAGACGTGTGC
P2_PCR_i7_B005_CTATGGGA	CAAGCAGAAGACGGCATACGAGATtcccatagGTGACTGGAGTTCAGACGTGTGC
P2_PCR_i7_B006_ACTGACGA	CAAGCAGAAGACGGCATACGAGATtcgtcagtGTGACTGGAGTTCAGACGTGTGC
P2_PCR_i7_B007_GTCCACAT	CAAGCAGAAGACGGCATACGAGATatgtggacGTGACTGGAGTTCAGACGTGTGC
P2_PCR_i7_B008_CTCGTCAT	CAAGCAGAAGACGGCATACGAGATatgacgagGTGACTGGAGTTCAGACGTGTGC
P2_PCR_i7_B009_GCGATGAA	CAAGCAGAAGACGGCATACGAGATttcatcgcGTGACTGGAGTTCAGACGTGTGC
P2_PCR_i7_B010_ATGTCTCC	CAAGCAGAAGACGGCATACGAGATggagacatGTGACTGGAGTTCAGACGTGTGC
P2_PCR_i7_B011_CAGGCTTT	CAAGCAGAAGACGGCATACGAGATaaagcctgGTGACTGGAGTTCAGACGTGTGC
P2_PCR_i7_B012_GCTATCGT	CAAGCAGAAGACGGCATACGAGATacgatagcGTGACTGGAGTTCAGACGTGTGC
P2_PCR_i7_B013_GCTGTTAC	CAAGCAGAAGACGGCATACGAGATgtaacagcGTGACTGGAGTTCAGACGTGTGC
P2_PCR_i7_B014_CGTACACA	CAAGCAGAAGACGGCATACGAGATtgtgtacgGTGACTGGAGTTCAGACGTGTGC
P2_PCR_i7_B015_CGTGACTA	CAAGCAGAAGACGGCATACGAGATtagtcacgGTGACTGGAGTTCAGACGTGTGC

P2_PCR_i7_B016_AAGCTAGC	CAAGCAGAAGACGGCATACGAGATgctagcttGTGACTGGAGTTCAGACGTGTGC
P2_PCR_i7_B017_ATGGGATC	CAAGCAGAAGACGGCATACGAGATgatcccatGTGACTGGAGTTCAGACGTGTGC
P2_PCR_i7_B018_AGCATCCA	CAAGCAGAAGACGGCATACGAGATtggatgctGTGACTGGAGTTCAGACGTGTGC
P2_PCR_i7_B019_CTAATCCG	CAAGCAGAAGACGGCATACGAGATcggattagGTGACTGGAGTTCAGACGTGTGC
P2_PCR_i7_B020_GTGAAACC	CAAGCAGAAGACGGCATACGAGATggtttcacGTGACTGGAGTTCAGACGTGTGC
P2_PCR_i7_B021_GTGCGATA	CAAGCAGAAGACGGCATACGAGATtatcgcacGTGACTGGAGTTCAGACGTGTGC
P2_PCR_i7_B022_TACGGAGT	CAAGCAGAAGACGGCATACGAGATactccgtaGTGACTGGAGTTCAGACGTGTGC
P2_PCR_i7_B023_TTCAGTGC	CAAGCAGAAGACGGCATACGAGATgcactgaaGTGACTGGAGTTCAGACGTGTGC
P2_PCR_i7_B024_AAGTGCAC	CAAGCAGAAGACGGCATACGAGATgtgcacttGTGACTGGAGTTCAGACGTGTGC
P2_PCR_i7_B025_TTCCAGAC	CAAGCAGAAGACGGCATACGAGATgtctggaaGTGACTGGAGTTCAGACGTGTGC
P2_PCR_i7_B026_GTAAGGCT	CAAGCAGAAGACGGCATACGAGATagccttacGTGACTGGAGTTCAGACGTGTGC
P2_PCR_i7_B027_CCTGAACT	CAAGCAGAAGACGGCATACGAGATagttcaggGTGACTGGAGTTCAGACGTGTGC
P2_PCR_i7_B028_GGATATGC	CAAGCAGAAGACGGCATACGAGATgcatatccGTGACTGGAGTTCAGACGTGTGC
P2_PCR_i7_B029_CACTGTAG	CAAGCAGAAGACGGCATACGAGATctacagtgGTGACTGGAGTTCAGACGTGTGC
P2_PCR_i7_B030_GACCTGAT	CAAGCAGAAGACGGCATACGAGATatcaggtcGTGACTGGAGTTCAGACGTGTGC
P2_PCR_i7_B031_GAAAGTCG	CAAGCAGAAGACGGCATACGAGATcgactttcGTGACTGGAGTTCAGACGTGTGC
P2_PCR_i7_B032_CAACGCTT	CAAGCAGAAGACGGCATACGAGATaagcgttgGTGACTGGAGTTCAGACGTGTGC
P2_PCR_i7_B033_ACGGTCAA	CAAGCAGAAGACGGCATACGAGATttgaccgtGTGACTGGAGTTCAGACGTGTGC
P2_PCR_i7_B034_CGCGAATT	CAAGCAGAAGACGGCATACGAGATaattcgcgGTGACTGGAGTTCAGACGTGTGC
P2_PCR_i7_B035_GGTTCATC	CAAGCAGAAGACGGCATACGAGATgatgaaccGTGACTGGAGTTCAGACGTGTGC
P2_PCR_i7_B036_AAACGGTC	CAAGCAGAAGACGGCATACGAGATgaccgtttGTGACTGGAGTTCAGACGTGTGC
P2_PCR_i7_B037_GTCACTAG	CAAGCAGAAGACGGCATACGAGATctagtgacGTGACTGGAGTTCAGACGTGTGC
P2_PCR_i7_B038_ATATCCCG	CAAGCAGAAGACGGCATACGAGATcgggatatGTGACTGGAGTTCAGACGTGTGC
P2_PCR_i7_B039_TTCGCATC	CAAGCAGAAGACGGCATACGAGATgatgcgaaGTGACTGGAGTTCAGACGTGTGC
P2_PCR_i7_B040_GCGTTATC	CAAGCAGAAGACGGCATACGAGATgataacgcGTGACTGGAGTTCAGACGTGTGC
P2_PCR_i7_B041_CCGAAAGT	CAAGCAGAAGACGGCATACGAGATactttcggGTGACTGGAGTTCAGACGTGTGC
P2_PCR_i7_B042_TTACGAGC	CAAGCAGAAGACGGCATACGAGATgctcgtaaGTGACTGGAGTTCAGACGTGTGC
P2_PCR_i7_B043_TCGGGAAT	CAAGCAGAAGACGGCATACGAGATattcccgaGTGACTGGAGTTCAGACGTGTGC
P2_PCR_i7_B044_CACGATGT	CAAGCAGAAGACGGCATACGAGATacatcgtgGTGACTGGAGTTCAGACGTGTGC
P2_PCR_i7_B045_CGACCTTT	CAAGCAGAAGACGGCATACGAGATaaaggtcgGTGACTGGAGTTCAGACGTGTGC
P2_PCR_i7_B046_TTCTAGGG	CAAGCAGAAGACGGCATACGAGATccctagaaGTGACTGGAGTTCAGACGTGTGC
P2_PCR_i7_B047_TATCGGCA	CAAGCAGAAGACGGCATACGAGATtgccgataGTGACTGGAGTTCAGACGTGTGC
P2_PCR_i7_B048_TAGCACCT	CAAGCAGAAGACGGCATACGAGATaggtgctaGTGACTGGAGTTCAGACGTGTGC
P2_PCR_i7_B049_GACTCACT	CAAGCAGAAGACGGCATACGAGATagtgagtcGTGACTGGAGTTCAGACGTGTGC
P2_PCR_i7_B050_AATGGCGT	CAAGCAGAAGACGGCATACGAGATacgccattGTGACTGGAGTTCAGACGTGTGC

P2_PCR_i7_B051_TTCCCAGT	CAAGCAGAAGACGGCATACGAGATactgggaaGTGACTGGAGTTCAGACGTGTGC
P2_PCR_i7_B052_TCACGTCT	CAAGCAGAAGACGGCATACGAGATagacgtgaGTGACTGGAGTTCAGACGTGTGC
P2_PCR_i7_B053_ACGTGGTT	CAAGCAGAAGACGGCATACGAGATaaccacgtGTGACTGGAGTTCAGACGTGTGC
P2_PCR_i7_B054_CCAGAGTT	CAAGCAGAAGACGGCATACGAGATaactctggGTGACTGGAGTTCAGACGTGTGC
P2_PCR_i7_B055_TAAGTCCC	CAAGCAGAAGACGGCATACGAGATgggacttaGTGACTGGAGTTCAGACGTGTGC
P2_PCR_i7_B056_TACTCGAC	CAAGCAGAAGACGGCATACGAGATgtcgagtaGTGACTGGAGTTCAGACGTGTGC
P2_PCR_i7_B057_ACTACAGC	CAAGCAGAAGACGGCATACGAGATgctgtagtGTGACTGGAGTTCAGACGTGTGC
P2_PCR_i7_B058_GTCAAGGT	CAAGCAGAAGACGGCATACGAGATaccttgacGTGACTGGAGTTCAGACGTGTGC
P2_PCR_i7_B059_GAGGTACA	CAAGCAGAAGACGGCATACGAGATtgtacctcGTGACTGGAGTTCAGACGTGTGC
P2_PCR_i7_B060_CATTCGGA	CAAGCAGAAGACGGCATACGAGATtccgaatgGTGACTGGAGTTCAGACGTGTGC
P2_PCR_i7_B061_TCAAGCAG	CAAGCAGAAGACGGCATACGAGATctgcttgaGTGACTGGAGTTCAGACGTGTGC
P2_PCR_i7_B062_TGGAATCC	CAAGCAGAAGACGGCATACGAGATggattccaGTGACTGGAGTTCAGACGTGTGC
P2_PCR_i7_B063_GCGAATCA	CAAGCAGAAGACGGCATACGAGATtgattcgcGTGACTGGAGTTCAGACGTGTGC
P2_PCR_i7_B064_GGCTTACA	CAAGCAGAAGACGGCATACGAGATtgtaagccGTGACTGGAGTTCAGACGTGTGC
P2_PCR_i7_B065_GTTGCGAA	CAAGCAGAAGACGGCATACGAGATttcgcaacGTGACTGGAGTTCAGACGTGTGC
P2_PCR_i7_B066_GCTTCTCA	CAAGCAGAAGACGGCATACGAGATtgagaagcGTGACTGGAGTTCAGACGTGTGC
P2_PCR_i7_B067_GTAATGGC	CAAGCAGAAGACGGCATACGAGATgccattacGTGACTGGAGTTCAGACGTGTGC
P2_PCR_i7_B068_CTAGCCAA	CAAGCAGAAGACGGCATACGAGATttggctagGTGACTGGAGTTCAGACGTGTGC
P2_PCR_i7_B069_AGCCTTTG	CAAGCAGAAGACGGCATACGAGATcaaaggctGTGACTGGAGTTCAGACGTGTGC
P2_PCR_i7_B070_ATGGCAGT	CAAGCAGAAGACGGCATACGAGATactgccatGTGACTGGAGTTCAGACGTGTGC
P2_PCR_i7_B071_GCCGATAT	CAAGCAGAAGACGGCATACGAGATatatcggcGTGACTGGAGTTCAGACGTGTGC
P2_PCR_i7_B072_GCAACGTT	CAAGCAGAAGACGGCATACGAGATaacgttgcGTGACTGGAGTTCAGACGTGTGC

Work contributions

I performed all experiments and analyses described in this thesis myself, except for:

The actual 16S rRNA amplicon sequencing (excluding the library preparation) was conducted at Admera Health, LLC.

Untargeted and targeted metabolomic assays and raw spectrum assignment was performed by Dr. Patrick Giavalisco at the metabolomics core facility (Max-Planck-Institute for Biology of Ageing).

The proteomics assay and the differential expression analysis was performed by Dr. Ilian Atanassov at the proteomic core facility (Max-Planck-Institute for Biology of Ageing).

My bachelor student Quinn Quesenberry performed the histology experiments under my supervision.

Sam Kean performed the Random Forest classifications on all the microbiota datasets.

Erklärung

Hiermit versichere ich an Eides statt, dass ich die vorliegende Dissertation selbstständig und ohne die Benutzung anderer als der angegebenen Hilfsmittel und Literatur angefertigt habe. Alle Stellen, die wörtlich oder sinngemäß aus veröffentlichten und nicht veröffentlichten Werken dem Wortlaut oder dem Sinn nach entnommen wurden, sind als solche kenntlich gemacht. Ich versichere an Eides statt, dass diese Dissertation noch keiner anderen Fakultät oder Universität zur Prüfung vorgelegen hat; dass sie - abgesehen von unten angegebenen Teilpublikationen und eingebundenen Artikeln und Manuskripten - noch nicht veröffentlicht worden ist sowie, dass ich eine Veröffentlichung der Dissertation vor Abschluss der Promotion nicht ohne Genehmigung des Promotionsausschusses vornehmen werde. Die Bestimmungen dieser Ordnung sind mir bekannt. Darüber hinaus erkläre ich hiermit, dass ich die Ordnung zur Sicherung guter wissenschaftlicher Praxis und zum Umgang mit wissenschaftlichem Fehlverhalten der Universität zu Köln gelesen und sie bei der Durchführung der Dissertation zugrundeliegenden Arbeiten und der schriftlich verfassten Dissertation beachtet habe und verpflichte mich hiermit, die dort genannten Vorgaben bei allen wissenschaftlichen Tätigkeiten zu beachten und umzusetzen. Ich versichere, dass die eingereichte elektronische Fassung der eingereichten Druckfassung vollständig entspricht.

Die von mir vorgelegte Dissertation ist von Dr. Dario R. Valenzano betreut worden.

Teilpublikationen:

Patrick Smith*, David Willemsen*, Miriam Popkes*, Franziska Metge, Edson Gandiwa, Martin Reichard, Dario R. Valenzano, 2017: Regulation of life span by the gut microbiota in the short-lived African turquoise killifish. ELife, 6. https://doi.org/10.7554/eLife.27014

Miriam Popkes & Dario R. Valenzano, 2020: Microbiota-host interactions shape ageing dynamics. Philosophical Transactions of the Royal Society B: Biological Sciences, *375*(1808), 20190596. https://doi.org/10.1098/rstb.2019.0596

Köln, 20.05.2021